Time Evolution and Path Integral Formulations of Langevin Equations Driven by General Shot Noise Processes

A DISSERTATION PRESENTED BY
FILIP BONJA
TO
SCHOOL OF MATHEMATICAL SCIENCES

IN PARTIAL FULFILLMENT OF THE REQUIREMENTS
FOR THE DEGREE OF
DOCTOR OF PHILOSOPHY IN MATHEMATICS

QUEEN MARY, UNIVERSITY OF LONDON
LONDON, ENGLAND
DECEMBER 2021

To my family for their utmost support, both financially and spiritually, thank you. This is my dedication to you, showing that your patience for my personal and professional growth has finally paid off, and I have finally become a doctor. Sizleri çok seviyorum, iyi ki hayatımdasınız, iyi ki varsınız.

To my supervisor, who has always been very supportive of my progression in obtaining this challenging and taxing degree. For all the good times and, naturally, the bad times together over these past 5 years, thank you for always believing in what I can achieve and pointing me to the right direction in instances where I seemed lost in (physical) translation. This thesis is also dedicated to you, where without your guidance it would just have been empty pages past this dedication page.

To my friends, who have motivated me throughout this period, whether or not we shared any common interest in mathematics, though in most if not all cases we did not, thank you for your motivating speeches over a pint or few, short-talks while awkwardly looking at my computer screen over my shoulder, and pat-on-the-backs afterwards. Thank you for letting me know that true friends only want from you to be happy.

Last but definitely not least,

To my partner, who has been in my life for only 4 years but have made me feel like a lifetime. Without your utmost support and love, I would not have finished my thesis on time. Thank you for deeply caring for me during these years. Thank you for nodding back when I felt pressured from academia and life. Thank you for *always* being by my side, in sickness and in health, in thick and thin. Thank you for showing me that life is way beyond books, articles, academics and jobs. Life only becomes life when you find the right person next to you, supporting you unconditionally in every step you take. I love you, те сакам многу љубов моја.

Thesis advisor: Dr. Adrian Baule Filip Bonja

Time Evolution and Path Integral Formulations of Langevin Equations Driven by General Shot Noise Processes

Abstract

In this thesis we analyze the properties of a broad class of non-Markovian stochastic processes driven by Generalized Shot Noise (GSN) and aim to find their transition probabilities via distinct yet fundamental approaches.

Stochastic processes are widely used mathematical tools to model uncertain behavior in a physical system. Recent studies show that the current stochastic models, which assume Markov or memoryless property, are inaccurate to model complex physical systems, from molecular dynamics in porous media to mild correlations of stock price returns in financial markets. We show that one can model these problems with a non-Markovian stochastic process X as the solution of the Generalized Langevin Equation (GLE) $\dot{X}_t = -V'(X_t) + \xi_t$, where V is the potential of the environment and ξ_t is a GSN trajectory.

We show that the non-Markovian GLE can be obtained by relaxing the Markov property with an impulse function h that creates diverse mathematical properties. Next, we show three distinct methods, each with their own rights and caveats, of finding the transition probability of X_t: first by directly from its characteristic functional, second by evaluating its time evolution equation, and third by formulating its path integral.

Subsequently, we reserved the last part of our thesis for the application of the path integral results to two separate physical systems: tracking the position of a particle in a porous biological medium, and forecasting the price trajectory of a financial instrument that shows correlations in returns.

Contents

Listing of figures

List of Abbreviations and Symbols

GSN	**G**eneralized **S**hot **N**oise
GWN	**G**aussian **W**hite **N**oise
PWN	**P**oisson **W**hite **N**oise
PDF	**P**robability **D**ensity **F**unction
PMF	**P**robability **M**ass **F**unction
CDF	**C**cumulative **D**istribution **F**unction
CF	**C**haracteristic **F**unction
CFal	**C**haracteristic **F**unctiona**l**
LE	**L**angevin **E**quation
ELE	**E**uler-**L**agrange **E**quation
EMM	**E**quivalent **M**artingale **M**easure
ME	**M**aster **E**quation
MSD	**M**ean **S**quared **D**isplacement
MCT	**M**arkov **C**onvergence **T**heorem
TNL	**T**ime **N**on-**L**ocal differential equations
SDE	**S**tochastic **D**ifferential **E**quations
SDΔE	**S**tochastic **D**ifferential-**D**ifference **E**quations
ODE	**O**rdinary **D**ifferential **E**quations
PDE	**P**artial **D**ifferential **E**quations
FPE	**F**okker-**P**lanck **E**quation
s.p.	**s**tochastic **p**rocess

$\mathbb{R}$	The set of real numbers
$\mathbb{N}$	The set of natural numbers
$\mathbb{C}$	The set of complex numbers
Ω	The sample space of probability events
$\mathcal{F}$	The event space consist of sets of σ algebras of Ω
$\mathcal{L}$	Laplace transform operator
$\mathscr{L}$	Lagrangian function
$\mathscr{C}$	Configuration space
$\mathbb{P}$	Generic symbol for probability measure, PDF of PMF
$\mathbb{Q}$	Probability measure denoting the EMM
$X = (X_t)_{t\geq 0}$	General definition of a s.p., or the position process
$L = (L_t)_{t\geq 0}$	Compound Poisson process
$N = (N_t)_{t\geq 0}$	Poisson process
$W = (W_t)_{t\geq 0}$	Wiener process
$\xi = (\xi_t)_{t\geq 0}$	GSN process
$\dot{X}$	Time derivative of a s.p. X
$\dot{f}$	Time derivative of a function f
$f^{(i)}$	i-th time derivative of a function f
$\Phi_X[g]$	CFal of a s.p. X with test function g
$\phi_{X_T}(\theta)$	CF of a s.p. X at time T
$h(t)$	Impulse function of the GSN process

The mathematical sciences particularly exhibit order, symmetry, and limitation; and these are the greatest forms of the beautiful.

Aristotle

0 Introduction

Mechanisms including biological transport and financial markets are highly complex involving multi-body system analysis. Depending on whether it is active transport of molecules in biology or determining the volatility of a financial security for risk management or fair pricing, mathematical modeling can be purely deterministic, purely stochastic or a combination of both, depending on the available data and the characteristics of the variable environment [2]. As nature is heavily controlled with stochastic factors, we specified our notion to stochastic modeling.

Stochastic modeling in systems biology offers promising results in many fields including genetics (e.g. expression of mRNAs [14], life cycle of proteins [15]), evolutionary biology (e.g. ancestral lineage behavior [17], protein sequence evolution [16]) or intermittent search strategies [18]. Furthermore, recent developments indicate that using non-Gaussian processes show even more promising results in modelling biophysical mechanisms, for example, migration of T-cells to find extreme targets [19].

As realistic systems are highly complex, to decisively model the system using discrete state and continuous-time would require some finite memory effect to take place. In fact, processes that violate the Markov property, in a physical context, is a direct causality of the past affecting the present; for example, it is experimentally shown that average waiting times between different biochemical reactions are not exponentially distributed, an indication of non-Markovianity in the system [20].

Using this scope, Kanazawa and his collaborators [3] have started to work on stochastic modelling of tracer diffusion in active suspensions. According to empirical findings, the active diffusion of the tracer experimentally exhibited the following unique features that can no longer be explained as a Brownian motion:

(i) its mean square displacement (MSD) exhibited a crossover between super-diffusion with $\sim t^{\alpha}$ $(1 < \alpha \leq 2)$ for short times and normal diffusion $(\alpha = 1)$ for long times [6 7 8 10 11 12];

(ii) the probability density function (PDF) of position displacements exhibited strong non-Gaussian features manifest as power-law tails [9 13], and the PDF eventually reverted to a Gaussian shape [12 13];

Using this scope, [3] used the following Langevin equation (LE) to model the diffusion of tracers, given by the position X_t at time t, the LE reads:

$$\begin{aligned} \Gamma \frac{\mathrm{d}X_t}{\mathrm{d}t} &= \xi_t, \\ \xi_t &= \sum_{i=1}^{N_t} h(t - T_i), \end{aligned} \tag{0.0.1}$$

where Γ is the viscous coefficient, N_t forms the Poisson process with intensity $\lambda > 0$, and $\{T_i\}$ are the arrival times of the Poisson process. Here, h is the *impulse function* that is fitted using simulation data of the force exerted on the tracer. Consequently, the force ξ_t forms the *General Shot Noise* (GSN) process with finite intensity.

Their findings show that the LE driven by the GSN ξ can be applied to a variety of scenarios where enhanced diffusion points detailed above are observed. Authors also pinpoint that additional force fields may lead to novel mechanisms to control and exploit enhanced diffusion in artificial devices.

Using the recent findings of [3], we added additional terms to their original LE and started working on analyzing the velocity of a particle using the following non-Markovian system:

$$\begin{aligned} \frac{\mathrm{d}X_t}{\mathrm{d}t} &= -V'(X_t) + \xi_t, \\ \xi_t &= \sum_{i=1}^{N_t} A_i h(t - T_i), \end{aligned} \tag{0.0.2}$$

where $X = (X_t)_{t\geq 0}$ is the position process of the particle, V corresponds to the potential of the environment, $\xi = (\xi_t)_{t\geq 0}$ is the GSN process such that $N = (N_t)_{t\geq 0}$ is the Poisson process with intensity λ, T_i are the arrival times of N, A_i are iid jump amplitudes and h is the impulse function that is assumed to be smooth on $\mathbb{R}$. We shall call this type of system given above the non-Markovian Langevin Equation.

Notice that in the Markovian case, the impulse function is simply the Dirac delta function, $h \mapsto \delta$, in which case the position process X becomes the Compound Poisson process.

0.1 Intuitive Examples

In literature, non-Markovianity in Langevin equations are generally established by inducing a non-local position process, where (e.g.[66]) the system is defined by:

$$\dot{X}_t = -\gamma f(X_t, X_{t-\tau}) + \sigma\xi_t. \tag{0.1.1}$$

Here, the function f is smooth and ξ_t is the white noise processes satisfying delta-correlation $\langle \xi_t \xi_s \rangle = \delta(t-s)$. In this realm, finding the Master Equation of X_t is not as simple due to its dependence to all the past values X_τ, where $\tau < t < 0$; instead, the Master Equation is generally given for the joint probability distribution of X. By equally partitioning the interval $[\tau, t]$ into ordered sequence of size n, $\{t_i\}_{i=1}^n$, the Master Equation for the joint PDF P_n of $(X_{t_1}, ..., X_{t_n})$ is given by the following:

$$\begin{aligned}\frac{\partial P_n}{\partial t_n}(x_n, t_n; ...; x_1, t_1) =& D\frac{\partial^2}{\partial x_n^2} P_n(x_n, t_n; ...; x_1, t_1) \\ &+ \gamma \frac{\partial}{\partial x_n} \int \mathrm{d}x' f(x_n, x') P_{n+1}(x_n, t_n; x', t'; ...; x_1, t_1).\end{aligned} \tag{0.1.2}$$

Methods to find the Master Equation for the marginal distribution of X_t include applying the simplest case of linear function $f(x, y) = y$, where (0.1.1) becomes the so-called Delayed Langevin Equation, and rewriting (0.1.1) in terms of Green's functions[67].

We next outline in next two sections some examples of multi-body systems in biology and finance, where current models involving Markov processes seem inadequate, and more "relaxed" models involving short- or long-term memory are needed to be adapted.

0.1.1 Biology

One of the most promising fields with a potential application of the non-Markovian LE is in biology, where it can be applied to various scenarios from molecular dynamics to cancer modelling and bioinformatics.

A potential application is identified in cancer immunotherapy, as in the heterogeneity of cancer cells [124] and genetic and phenotypic resistance of tumours [130] all indicate non-Markovianity in the system. Further, in the field of bioinformatics, a recent paper by Sristava & Chen (2010) [131] show that non-Markovian Langevin equations driven by GSN process ξ are used to enhance data analysis on sequencing ribonucleic acids (RNA), the building blocks of life.

One example we can focus on is in molecular biology, using the extensive article published by Łuczka in 2005 [125]. The author first shows that the activation rate of an intramolecular motion of a molecule can be much greater in the Markovian description, and non-Markovian frameworks are better suited to model this scenario. The author posits that the PDF of X (modeling the motion of the molecule) driven by the non-Markovian GLE in (0.0.2) is extremely difficult to solve unless the GSN process ξ is either Gaussian White Noise or Poisson white noise, and instead defines the following LE:

$$m\ddot{X}_t + \int_0^t \gamma(t-s)\dot{X}_s \, \mathrm{d}s + V'(X_t) = \xi_t, \tag{0.1.3}$$

where V is the potential of the system, and m is the mass of the particle in question. The integral kernel γ is defined as

$$\gamma(t) = \int_0^\infty \frac{\rho(s)}{s} \cos(st) \, \mathrm{d}s, \tag{0.1.4}$$

where

$$\rho(\omega) = \sum_k \frac{\lambda_k^2}{m_k \omega_k} \delta(\omega - \omega_k) \tag{0.1.5}$$

such that m_k, λ_k and ω_k are coefficients describing the oscillations within the intramolecular medium.

Lastly, the colored noise ξ is completely characterised by its correlation function $\langle \xi_t \xi_s \rangle = D\gamma(t-s)$ for some positive diffusion coefficient D.

The paper also asserts that the memory effects caused by the integral kernel γ play a significant role and modify the activation rate, causality that is not taken into account in the Markovian realm. Although distinct, the model itself does not have a closed-form solution of the PDF of X for general γ, where the author instead derives the PDF by explicitly defining examples of γ.

0.1.2 Finance

Due to their simplicity and analytical closed-form solutions, current research for deriving models underlying financial instruments have been widely applied to Markov processes[44,48,49,52]. However, recent empirical data show that correct implementation of financial models requires taking a look at the ensemble average of the driving process, rather than the time average, indicating non-stationarity of increments and hence a non-Markovian behavior.

Quantitative finance lacks a solid description for non-Markovian processes; characteristics such as memory effects are commonly observed in human behavior in financial markets[132,133], and non-Gaussian processes are widely used to better model the security prices (for example see[134]).

Further, an article published by[53] indicates that high-frequency trading data using liquid foreign currency pairs (e.g. Euro to Dollar exchange rate) turn out to be non-Markovian, due to self-similarity and non-stationarity of returns on investment.

Similarly, an article published by Frank in 2007[54] indicates in detail that the pricing models of financial instruments, such as bonds, should involve past time dependence. Financial trading in general is heavily influenced by events that happen in the past. Therefore, recently, time-delayed evolution equations in financial physics have been discussed that account for memory effects.

In regards, the author in[54] focuses on the following model driving the interest rate process $R =$

$(R_t)_{t\geq 0}$ as a Delayed Langevin Equation:

$$\dot{R}_t = -\gamma\left(R_t - \langle R_t\rangle\right) + \sum_{i=1}^{N} A_i\left(R_{t-T_i} - \langle R_t\rangle\right) + \sigma\dot{W}_t \tag{0.1.6}$$

where $\{A_i\}$ are jump amplitudes, $\{T_i\} \sim U(0,t)$ are iid uniformly distributed random variables, γ is the friction coefficient, σ is the volatility of the interest rate and $\dot{W}_t$ forms the Gaussian white noise (i.e. time derivative of the Wiener process), with correlation $\left\langle \dot{W}_t \dot{W}_s \right\rangle = 2D\delta(t-s)$. Here, the interest process R is a non-Markovian version of the renowned Ornstein-Uhlenbeck process. Using this Delayed Langevin Equation, authors compute the price of a bond $M(T)$ with unit coupon rate and at time of maturity T as follows:

$$M(T) = \left\langle \exp\left(-\int_0^T \mathrm{d}t\, R_t\right)\right\rangle, \tag{0.1.7}$$

and conclude that time delays can induce a *smoothening* of strong system nonlinearities, a process widely observed in price behavior of complex financial instruments. Albeit explicitly, the authors of [54] derive the PDF of the non-Markovian interest rate process R by *approximating* from the solution of the Markovian PDF (where $T_i = 0$) by means of perturbation theoretic techniques [55].

Another example of non-Markovian frameworks in financial mathematics is by directly modelling the *volatility* of the underlying noise, such as the Bergomi model [116]. The Bergomi model assumes that the price process X follows the following LE:

$$\begin{aligned} \dot{X}_t &= rX_t + \sqrt{V_t}X_t\dot{W}_t, \\ V_t &= \exp\left(\eta B_t - \frac{1}{2}\eta^2 t^{2H}\right), \end{aligned} \tag{0.1.8}$$

where r refers to the constant interest rate, V_t forms the non-Markovian stochastic process modelling the volatility of X, $\eta > 0$ is a positive constant and B_t forms the *fractional Brownian motion*

with *Hurst exponent* $H \in [0,1]$ defined by its correlation $\langle B_t B_s \rangle = 1/2 \left(t^{2H} + s^{2H} - |t-s|^{2H} \right)$, and similar to the Delayed Langevin Equation above, the noise $\dot{W}_t$ forms the Gaussian white noise (GWN) process with correlation $\left\langle \dot{W}_t \dot{W}_s \right\rangle = \delta(t-s)$. Due to the non-Markovian nature of V, the solution X of the LE has been solved numerically [116], and fully analytic representation of X has been shown by [117] by approximating V as a Markov process. In fact, as we will show in later chapters of this thesis, authors in [117] further assert that one can only fully represent any non-Markovian stochastic process by an *infinite* dimensional Markov process.

0.2 Motivation and Chapter Breakdown

As we have outlined in the previous section, current studies on non-Markovian models that are used in biology and finance either provide numerical techniques to solve the corresponding LE's, or approximate them by simpler Markovian processes to derive analytic solutions. There also has been insufficient research on combining non-Markovian models into one unified model that would encompass different behaviours on time dependence on correlations.

This thesis aims to show that the GSN process ξ as in (0.0.2) is a potential candidate to derive a unified model for non-Markovian LE's. In detail, the impulse function h of ξ plays a very important role such that it can embed different types of time-dependent correlations into ξ, which in turn defines X as a broad class of non-Markovian stochastic processes. We also show two main approaches to find the PDF of X as the solution of such general non-Markovian GLE.

The thesis is structured as follows. We first introduce the concept of stochastic processes in Chapter 1. Here, we outline some examples of Markovian stochastic processes that have been widely used in literature: the Wiener process, the Poisson process and the Compound Poisson process. We next outline the Markov property, also known as the memoryless property, of stochastic processes, which dictates that if X is a Markov process, then all the future realizations of X are independent of

their past and that X only retains the memory at its present time. We next embark on defining X as the solution of a Markovian GLE. We finalize the introductory part of the chapter by introducing the Master Equation and the path integral formulation of X, both of which would enable us to find its PDF and its transition probability.

The first chapter as a whole provides us the necessary foundation to embark on the GSN processes in Chapter 2. Here, we show that the characteristics of the impulse function h plays a very important role in determining the behavior of ξ and therefore X; for example, X is a non-Markovian process for all integrable impulse functions h unless h is a Dirac delta function, $h = \delta$. Furthermore, we assert that the GSN process has a correlation function that specifically depends on the impulse function h. We also cover in this chapter three broad types of h, left-tailed, right-tailed and $n-$hierarchy. We also show the functional correspondence between the position process X and the GSN process ξ, where the correspondence can only occur when non-Markovian GLE $\dot{X}_t = -V'(X_t) + \xi_t$ is linear, i.e. for zero or Harmonic potential $V(x) = \gamma x^2/2$ with $\gamma \geq 0$. Lastly, from the functional correspondence, we next derive the correlation function and the MSD of X, where one can then find a relationship with the impulse function h. Thus, one can get the whole characteristics of the position process X by solely referring to its MSD. We end this chapter by deriving the PDF of X from the functional correspondence of ξ and applying exemplary impulse functions to fit their resulting PDF's by Monte Carlo simulation.

In Chapter 3 we show new findings on the characteristics of the GSN process. We first start by showing the hierarchical nature of the time derivative of the GSN process. This hierarchical nature of ξ further strengthens our understanding that the joint tuple of X and the hierarchies of ξ becomes an infinite-dimensional Markov process. Conveniently, we next infer that if the impulse function of ξ is an $n-$hierarchy type, then the infinite-dimensional Markov process reduces to $(n+1)-$dimensions. We next show in this chapter two methods of finding the PDF of non-Markovian X for general potential V and impulse function h, firstly by the Markovian *Ito's approach*,

and next by the *path integral formulation*. As the name suggests, the Ito's approach helps us find the joint PDF of X and the hierarchies of ξ, where choosing a 1-hierarchy function helps us derive the joint PDF of (X, ξ) , commonly referred to as *Klein-Kramers equation*. On the other hand, the path integral formulation is more intricate as it helps us find the marginal PDF of X for any impulse function.

We next analyze the asymptotic limits of the GSN process and prove by *Markov Convergence Theorem* that if the impulse function h is integrable, then ξ asymptotically converges to the Poisson white noise (PWN) process. This is an important finding for us as it consequentially implies that any non-Markovian process driven by ξ will asymptotically converge to a Markovian process as long as the integrable condition for h holds. Next, we prove that under Gaussian Limits the CPN process converges to a general Gaussian noise process where the impulse function h continues to play an important role; we outline an example that the fractional Brownian motion as used in the Bergomi model can be defined as the generalized Gaussian process with a specific type of impulse function. We then end this chapter by showing an example of Markov Convergence Theorem by simulating the PDF's of X under zero potential by overlapping the PDF's of Markovian X driven by GSN process with that of the PWN process.

These new findings of the GSN process characteristics next lead us to Chapter 4, where we show how to find the PDF of the non-Markovian position process X by calculating its *Lagrangian* and *action*. The path integral approach has been widely used in the Markovian regime to find the *optimal path* of X by solving its *Euler-Lagrange Equations* (ELE's), also known as the *equations of motion*, of the Markovian LE. We extend this to the non-Markovian realm by showing that the resulting ELE's are *time non-local* and become hard to solve analytically. We next show that one can in fact localize the non-Markovian ELE to $(2n + 2)-$dimensional Markovian ELE if the impulse function of ξ is of an $n-$hierarchy type. We first give a simple example of unit order hierarchy (i.e. $n = 1$) and find the solutions of the localized ELE's, where one can obtain the optimal action of X and thus find its

PDF. However, by increasing the order of the hierarchy of h the resulting Markovian ELE's become highly coupled and therefore difficult to solve.

To overcome this coupling problem, we define a very useful method called the *Markov Embedding Technique* by asserting that any impulse function can be defined as a sum of K independent, unit order hierarchy, and complex-valued impulse functions. This leads us to define the complex-valued GSN process ξ, and therefore a complex-valued non-Markovian position process X via the GLE. Using this technique, we then compute the complex-valued and uncoupled system of local ELE's. This new method of calculating optimal path and action via the Markov Embedding Technique is then strengthened by using exemplary impulse functions; exponential decay (first-order hierarchy), damped oscillation (second-order hierarchy), and power-law decay (infinite-order hierarchy).

We next combine all the results we derived throughout this thesis in Chapter 5, where we applied the Markov Embedding Technique to real life scenarios. We provide two applicable scenarios where we will use the Markov Embedding Technique. We first calibrate an impulse function to the clinical data of the Mean Square Displacement of the mitochondria submersed in course-grained medium, where empirical results show the diffusion model is anomalous, suggesting non-Markovianity in nature[33]. Next, we apply the GSN process ξ to model the value of S&P500 financial index, and aim to capture its behavior during the Covid-19 pandemic.

We lastly bring this thesis to fruition in Chapter 6, where we outline the new methods we have defined and utilized so far, together with their strengths and weaknesses. We also propose future research topics that would further strengthen the GSN process as the potential candidate for unifying non-Markovian stochastic processes.

Mathematics, which most of us see as the most factual of all sciences, constitutes the most colossal metaphor imaginable, and must be judged, aesthetically as well as intellectually in terms of the success of this metaphor.

Norbert Wiener

1

Preliminaries: Stochastic processes

In this chapter, we first introduce the definition of a stochastic process from a physical point of view. We then give a few examples of stochastic processes, such as the Poisson point process, the Wiener process, and the Compound Poisson process. Next in our chapter, we outline the Markov property of s.p.'s, and categorize the noise terms as white or colored. This is a common tool in analyzing dynamical systems driven by stochastic processes.

Finally, we end this chapter by defining the Langevin equation, and showing how to construct the dynamical system using various stochastic processes, with common applications to biological systems and finance.

We assume that throughout this chapter, and by extension the thesis, the reader has basic knowledge of probability theory, such as calculating moments, defining conditional probabilities and expectations. For further details please refer to the introductory book by Ross (2014)[50].

1.1 Definition of Stochastic Processes

Stochastic processes are functions of random variables that define the statistical distribution of one- (or multi-) parameter family of events. In other words, given an index $t \in T$ (usually denoted as *time*), a stochastic process $X = (X_t)_{t\in T}$ is a sequence of random variables such that each element X_t is an event happening at time t.

Let us give a brief introduction below:

Definition 1.1.1. *Given time $t \in T$, a stochastic process $X = (X_t)_{t\in T}$ is a set of random variables defined on a* probability space $(\Omega, \mathcal{F}, \mathbb{P})$ *where Ω is the* sample space *that consists of all possible events, $\mathcal{F}$ is the* event space *that consists of all subsets of Ω* [i]*, and $\mathbb{P}$, called the* probability measure*, is the common* probability density function (pdf) *defined on $\mathbb{P} : \Omega \times T \to [0, 1]$, such that for all $t \in T$, the probability of an event X_t, called a* realization at time *t, to take place in a region $E \in \Omega$, is given by:*

$$Pr\left(X_t \in E\right) = \int_{E\in\Omega} \mathrm{d}x\, \mathbb{P}(x, t). \tag{1.1.1}$$

Furthermore, if $\mathbb{P}$ is a probability mass function, then the probability is given by the summation over

[i] Here, $\mathcal{F}$ is called the σ-algebra of Ω and contains all possible combinations of events, hence $\mathcal{F} \subseteq 2^{\Omega}$. More mathematical foundations can be extracted from [68].

the region E:

$$Pr\left(X_t \in E\right) = \sum_{E \in \Omega} \mathbb{P}(x,t). \tag{1.1.2}$$

Therefore, given a stochastic process $X = (X_t)_{t \in T}$, for each $t \in T$, the realization X_t is a random variable with probability distribution $\mathbb{P}(x,t)$.

Notice also that regarding to the above definition, we can assert that a stochastic process can be *discrete* or *continuous*. A discrete stochastic process (also known as *time series*) is simply the case where the index set T is countable, e.g. the set of natural numbers $\mathbb{N}$. On the other hand, continuous stochastic processes are the case where T is uncountable, e.g. the set of real numbers $\mathbb{R}$. In this thesis, we will focus on continuous stochastic processes with non-negative real set of indices, $T = \mathbb{R} \backslash \mathbb{R}^- = \{\forall t : \ t \geq 0\}$, i.e. the physical time.

Furthermore, we can also define herein the *expectation* of a realization X_t over its sample space Ω;

$$\langle X_t \rangle := \int_\Omega \mathrm{d}x \, x \cdot \mathbb{P}(x,t), \tag{1.1.3}$$

and, in general, the *n-th moment* of X_t is given by:

$$\langle X_t^n \rangle := \int_\Omega \mathrm{d}x \, x^n \cdot \mathbb{P}(x,t). \tag{1.1.4}$$

Lastly, using the n-th moment of any realization (i.e. random variable) X_t, one can define the *characteristic function* (CF) of X_t, denoted by ϕ_{X_t}, as follows:

$$\phi_X(\theta,t) := \left\langle e^{iX_t\theta} \right\rangle = \int_\Omega \mathrm{d}x \, e^{ix\theta} \cdot \mathbb{P}(x,t), \tag{1.1.5}$$

where i is the imaginary constant. It is important to note that any random variable has uniquely defined PDF and CF. Since stochastic processes are sequences of random variables, one can simply

extend the uniqueness property to stochastic processes[68].

Lastly, similar to the CF of a random variable, we can define the unique *characteristic functional* (CFal) of a random variable. Given a stochastic process X_t, its CFal with a test function g, is given by:

$$\Phi_X[g] := \left\langle \exp\left(i \int_0^\infty \mathrm{d}\tau \, g(\tau) X_\tau \right) \right\rangle \tag{1.1.6}$$

An important application of the CFal is for computing high order expectations of the stochastic processes. Given a stochastic process X, its cumulants of orders $n, m \in \mathbb{N}$ of the autocovariance of X can be found by computing the *variational derivatives* (refer to[21] for methodology) of its CFal:

$$\langle X_t^n X_s^m \rangle = \frac{1}{i^{n+m}} \frac{\delta^{n+m} \Phi_X[g]}{\delta^n g(t) \delta^m g(s)} \bigg|_{g=0}. \tag{1.1.7}$$

Calculating the autocovariance of X via its CFal is an important tool to study and categorize stochastic processes. In the next section, we focus on defining stochastic processes that will not only be used for categorization, but will also play a foundation to define and analyze the GSN process in subsequent chapters.

1.2 Some Examples of Stochastic Processes

As stated in Definition 1.1.1, a stochastic process can be formed by any combination of probability space $(\Omega, \mathcal{F}, \mathbb{P})$, and since $\mathbb{P}$ uniquely defines stochastic processes, one can construct an infinite class of stochastic processes.

However, we will be focusing on 3 major classes of stochastic processes: the Poisson point process, the Wiener process, and the Compound Poisson process.

1.2.1 Poisson Process

Named after French mathematician Siméon Denis Poisson, the Poisson processes are by far the simplest kind of continuous stochastic processes. Despite not having worked directly on this process before, Poisson gave a major foundation to this class of stochastic processes due to its indirect connection with the Poisson random variables [51].

The Poisson process $N = (N_t)_{t \geq 0}$ with intensity λ is a *counting process*, where

- Each realization N_t is non-negative integer-valued, and
- Each following realization is non-decreasing, i.e. for all $s > t$ we have that $N_s > N_t$.

Therefore, the Poisson process has unit increments and is, therefore, a counting process. In addition to being a counting process, each realization of the Poisson process has a Poisson distribution with mean λt, i.e. $N_t \sim Poisson(\lambda t)$ with pmf:

$$\mathbb{P}(N_t = n) := \frac{(\lambda t)^n}{n!} e^{-\lambda t}. \tag{1.2.1}$$

This is the simplest definition of the Poisson process; however, in consequence of its eclectic applications, the notation, terminology and level of mathematical rigor used to define and study the Poisson processes generally varies according to the context. In the below definition, we outline the formal and original mathematical definition of the Poisson process by defining its arrival and inter-arrival times.

Definition 1.2.1. *Let $\{X_i\}_{\in \mathbb{N}}$ be a collection of iid[ii] random variables defined on a probability space $(\Omega, \mathcal{F}, \mathbb{P})$ such that X_i have an* exponential distribution *with parameter λ, denoted by $X_i \overset{iid}{\sim} Exp(\lambda)$. Let $\{T_i\}_{i \in \mathbb{N}}$ also be a collection of random variables such that $T_0 = X_0$ and $T_i = X_i + T_{i-1}$ for all $i > 0$.*

[ii] Independent and identically distributed.

Then $N = \{N_t\}_{t\geq 0}$ is a Poisson process with intensity λ if each realization has the following cumulative distribution function (CDF):

$$\mathbb{P}(N_t \leq n) = \mathbb{P}(T_n \geq t). \tag{1.2.2}$$

In context, $\{T_i\}_{i\geq 0}$ and $\{X_i\}_{i\geq 0}$ are respectively called the *arrival times* and *inter-arrival times* of the Poisson process N. This definition showcases the importance of the probability distribution of inter-arrival times: a stochastic process is a Poisson process with intensity λ if and only if its inter-arrival times have iid exponential distribution with mean λ. Another important outcome from the construction is that since the inter-arrival times are independent, Poisson processes also hold the so-called memoryless property of Markov processes.

Lastly, as a counting process, the Poisson process is also known as a *pure jump process* or a *càdlàg* [iii] *process*, meaning that the process has right-continuity and left limits. Given the Poisson process N as above, one can hence infer that the *limit from the right* of any realization is continuous, $\lim_{s\to t^+} N_s = N_t$ and we denote the limit part as $\lim_{s\to t^-} N_t =: N_{t^-}$. The difference between the left and right limits is denoted by $\Delta N_t := N_t - N_{t^-}$. Lastly, note that for the Poisson process N, since it is a counting process, its jump sizes are of unit size. A visual representation is given in Figure 1.1.

Interestingly, the above definition of the Poisson processes is not directly linked to the Poisson distribution; it was not until 1909 when Hans W. Geiger and Ernest Rutherford developed the mathematical model for the ticking time of the Geiger counter. They found that the counter, assumed to be a random process, has probability function p_n as the solution of the following family of ODE's[47] $p_n'(t) = -\lambda p_n(t) - \lambda p_{n-1}(t)$, where $p_0'(t) = -\lambda p_0(t)$. Conveniently, the solution of this family of ODE is indeed the pmf of the Poisson distribution with mean λ, after which the random

[iii] Right-continuous with left-limits (fr. continue à droite, limites à gauche).

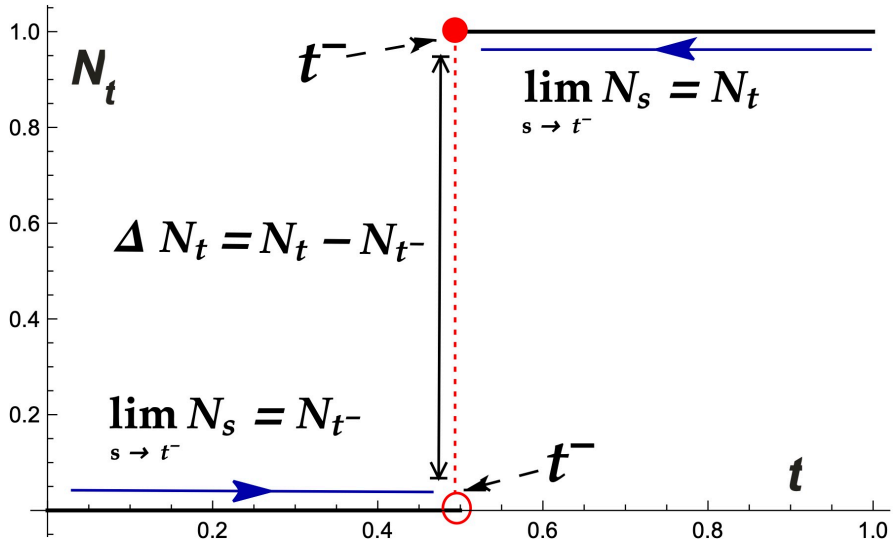

Figure 1.1: Realization of the Poisson process N with single and unit jump at time t, where one-sided limits and the jump size are visually explained. Here to time of jump t is split into continuous part, t^+, and discontinuous part t^-.

process was named.

1.2.2 Compound Poisson Process

The Compound Poisson process is very sought in the financial sector since it is used for modelling jumps of random size and random direction. As the name suggests, this process is an extension of the Poisson process defined in the previous section.

We begin with the definition of the Compound Poisson process below:

Definition 1.2.2. *Let N be a Poisson process with intensity λ and arrival times $\{T_i\}_{i\in\mathbb{N}}$, and let $\{A_i\}_{i\in\mathbb{N}}$ be a set of iid random variables. Then, the corresponding process $L = (L_t)_{t\geq 0}$ is called the* Compound Poisson process *if each realization is of the following form:*

$$L_t = \sum_{i=0}^{N_t} A_i \Theta(t - T_i), \tag{1.2.3}$$

where Θ *is the Heaviside step function. In literature, each element* A_i *is called the* jump amplitude *of the Compound Poisson process.*

Like its close relative to the Poisson process, the Compound Poisson process is also a càdlàg process. In fact, the Poisson process is the Compound Poisson process with almost surely unit jump amplitudes, i.e. $\forall i \in \mathbb{N}$, $A_i = 1$ almost surely. However, due to the inclusion of the jump amplitudes, the Compound Poisson processes are in general not counting processes.

The jump size of any realization of the Compound Poisson process L is proportional to its jump amplitudes, i.e. $\Delta L_t = A_{N_t} \Delta N_t$. This can be directly extracted in subsequent chapters when we use the same method to find the jump size of our stochastic process of interest.

The Compound Poisson process will have a variety of applications in our thesis. The first interesting property that we will assert is that, under certain limiting conditions, the Compound Poisson process converges to the Wiener process, defined in the next section.

1.2.3 Wiener Process

Similar to the Poisson process and the Compound Poisson process, the Wiener process is another widely studied stochastic process in literature. As explained in Chapter 0, Wiener processes have a variety of applications in various industries due to their easy definition, simulation, and concrete mathematical foundation.

We begin this section by the rigorous definition of the Wiener process:

Definition 1.2.3. *A stochastic process* $W = (W_t)_{t \geq 0}$ *defined on a probability space* $(\Omega, \mathcal{F}, \mathbb{P})$ *is a Wiener process, also known as Brownian motion* [iv]*, if the following conditions hold:*

(i) W has continuous paths almost surely under $\mathbb{P}$*,*

[iv] Due to their usage in literature, we use both names interchangeably in this thesis.

(ii) *The initial starting point of the path is almost surely at* 0: $\mathbb{P}(W_0 = 0) = 1$,

(iii) $\forall s, t : \ 0 \leq s \leq t$, *each increment* $W_t - W_s$ *has equal probability distribution as* W_{t-s}, *that is:* $W_t - W_s \overset{D}{=} W_{t-s}$,

(iv) $\forall u, s, t : \ 0 \leq u \leq s \leq t$, $W_t - W_s$ *is independent of* W_u,

(v) $\forall s, t : \ 0 \leq s \leq t$, *each increment* $W_t - W_s$ *has a Normal distribution with variance* $t - s$, *that is:* $W_t - W_s \sim \mathcal{N}(0, (t - s))$.

In regards to the above definitions, condition (i) asserts that the Wiener process is one of the few stochastic processes with almost surely continuous paths.

It is also a very interesting fact that the Compound Poisson process converges to the Wiener process under certain limits, which we will call the Gaussian limits.

First, we establish the Lévy continuity theorem for stochastic processes:

Lemma 1.2.1 (Lévy's Continuity Theorem). *Let* $\{X_n\}$ *be a collection of random variables with corresponding characteristic functions* ϕ_n *and let* X *be another random variable with characteristic function* ϕ. *Then, the following statements are equivalent:*

1. *The random variables* $\{X_n\}$ *converge in distribution to* X, *i.e.*

$$X_n \xrightarrow{\mathcal{D}} X.$$

2. *The sequence of characteristic functions* $\{\phi_n\}$ *converges point-wise to* ϕ, *i.e. for all* $\theta \in \mathbb{R}$,

$$\lim_{n \to \infty} \phi_n(\theta) = \phi(\theta).$$

Using Lemma 1.2.1, we next prove the following theorem for Gaussian limits:

Theorem 1.2.1. *Let $L = (L_t)_{t\geq 0}$ be a Compound Poisson process with intensity $\lambda > 0$ and iid jump amplitudes $\{A_i\}$. Furthermore, let $W = (W_t)_{t\geq 0}$ be the Wiener process.*

Then, for fixed $\lambda \left\langle A_1^2 \right\rangle$, the Compound Poisson Process converges in distribution to the Wiener process under the following limits:

$$\lim_{\substack{\lambda\to\infty \\ \langle A_1\rangle\to 0}} L_t \xrightarrow{\mathcal{D}} W_t$$

Proof. Firstly, w.l.og., let us fix $\lambda \left\langle A_1^2 \right\rangle = 1$ to one so that we can rewrite $\lambda = 1/\left\langle A_1^2 \right\rangle$. Then, using Lemma 1.2.1, the theorem can be written as follows:

$$\lim_{\substack{\lambda\to\infty \\ \langle A_1\rangle\to 0}} \phi_L(\theta, t) = \phi_W(\theta, t),$$

where the characteristic function of the Compound Poisson process is given by [v]:

$$\phi_L(\theta, t) = \exp\left[\lambda t \left(\phi_{A_1}(\theta) - 1\right)\right]$$

and that of the Wiener process by [vi]:

$$\phi_W(\theta, t) = \exp\left[-\frac{1}{2}\theta^2 t\right].$$

[v] The CF of the Compound Poisson process will be proven in Chapter 2 when we outline the CFal of the GSN process.

[vi] The CF of the Wiener process is simply the Inverse Fourier Transform of its PDF, recalling that $W_t \sim \mathcal{N}(0, t)$.

Notice that ϕ_L can be written as the Taylor expansion

$$\begin{aligned}
\phi_L(\theta,t) &= \exp\left[\frac{t}{\langle A_1^2\rangle}\left(\phi_{A_1}(\theta)-1\right)\right] \\
&= \exp\left[\frac{t}{\langle A_1^2\rangle}\left(\left\langle e^{i\theta A_1}\right\rangle - 1\right)\right] \\
&= \exp\left[\frac{t}{\langle A_i^2\rangle}\left(\left\langle 1+i\theta A_1-\frac{1}{2}\theta^2 A_1^2+\mathcal{O}(A_1^3)\right\rangle - 1\right)\right] \\
&= \exp\left[\frac{i\langle A_1\rangle}{\langle A_1^2\rangle}t\theta-\frac{1}{2}t\theta^2+\frac{\mathcal{O}\left(\langle A_1^3\rangle\right)}{\langle A_1^2\rangle}\right]
\end{aligned} \tag{1.2.4}$$

Furthermore, when $\langle A_1\rangle$ approaches to zero, the expectation $\langle A_1^n\rangle$ vanishes faster than $\langle A_1\rangle$ for $n > 2$. Hence, the $\mathcal{O}(\langle A_1^3\rangle)$ vanishes as $\langle A_1\rangle$ approaches zero. Furthermore, also notice that the term $\lambda\langle A_1\rangle = \langle A_1\rangle / \langle A_1^2\rangle \to 0$ as $\langle A_1\rangle \to 0$.

Therefore, we get that

$$\lim_{\substack{\lambda\to\infty \\ \langle A_1\rangle\to 0}} \phi_L(\theta,t) = \exp\left[-\frac{1}{2}t\theta^2\right] = \phi_W(\theta,t). \tag{1.2.5}$$

This point-wise converge of characteristic functions completes our proof. □

Furthermore, condition (iv) is also highly important as it asserts that the Wiener process has independent increments. This will be very useful to define the Markov property of stochastic processes.

1.3 Markov Property

The Markov property is a very extensive tool for studying characteristics of stochastic processes, where some future predictions about stochastic processes is independent of the past, given the

present state of the process. If a stochastic process holds the Markov property, then one can assert simple predictions about its future states at any given time.

As the name suggests, a stochastic process $X = (X_t)_{t\geq 0}$ defined on the probability space $(\Omega, \mathcal{F}, \mathbb{P})$ is a Markov process if the conditional probability of finding the realization X_t in a region $E \in \Omega$ given all the past realizations up to time $s < t$ is equal to the conditional probability of finding X_t in $E \in \Omega$ given the realization X_s, i.e.:

$$\mathbb{P}\left(X_t \in E \,|\, \mathcal{F}_s\right) = \mathbb{P}\left(X_t \in E \,|\, X_s\right). \tag{1.3.1}$$

Here, $\mathcal{F}_s$ is called the *filtration* of the event space $\mathcal{F}$ such that it contains all the combinations of events up to time $s < t$.

This property empirically shows that future realizations of X are independent of their past and that the s.p. has memory only at the current time s. This nature of behavior is why the Markov processes are also known as *stochastic processes with one step memory*[69].

To test whether a stochastic process holds the Markov property, we first have to outline the definition of a *white noise* process:

Definition 1.3.1. *A stochastic process X is called a* white noise process *if its covariance is delta-correlated, i.e. for all $s, t > 0$ and some constant $K \in \mathbb{R}$:*

$$\langle X_t X_s \rangle = K\delta(t - s), \tag{1.3.2}$$

where δ is the Dirac delta function.

One thing to note is that one can rewrite Definition 1.3.1 in Fourier space by taking into account the *spectral density* of a stochastic process.

Definition 1.3.2. *Let X be a s.p. with defined* correlation function $R_X(\tau) := \langle X_t X_{t+\tau} \rangle$. *Then, the*

spectral density *S of a s.p. X is the Fourier transform of its correlation function:*

$$S_X(\omega) := \mathcal{F}\{R_X(\tau)\}(\omega) = \frac{1}{\sqrt{2\pi}} \int_{\mathbb{R}} \mathrm{d}\tau \, e^{i\omega\tau} \langle X_t X_{t+\tau} \rangle \, . \tag{1.3.3}$$

Therefore, we can reiterate Definition 1.3.1 using the spectral density function: a stochastic process ξ is a white noise process if it has constant spectral density, i.e.:

$$S_\xi(\omega) = \frac{1}{\sqrt{2\pi}} \int_{\mathbb{R}} \mathrm{d}\tau \, e^{i\omega\tau} \delta(\tau) = \frac{1}{\sqrt{2\pi}}. \tag{1.3.4}$$

The white noise processes have been applied to various sectors since the early 1900's; the assumption of the rate of return for stock investments to be white noise have been widely used to describe various asset pricing models[45].

We next introduce Van Kampen's Lemma[46], which states that there is a direct correspondence between Markov processes and white noise processes:

Theorem 1.3.1 (Van Kampen's Lemma)**.** *Let $X = (X_t)_{t\geq 0}$ and $\xi = (\xi_t)_{t\geq 0}$ be two stochastic processes connected by the following SDE: $\dot{X}_t = f(X_t) + \xi_t$, where f is any smooth function. Then, X is a Markov process if ξ is a white noise process.*

Conversely, X is not a Markov process if ξ is not a white noise process.

In layman's terms, what Theorem 1.3.1 tells us is that any s.p. X that is the solution of such SDE is completely characterized by the random force ξ. If ξ is a white noise process, then integrating $\dot{X}$ out will yield a one-step memory, i.e. Markov, process X[125] [127].

We will next be using this important characterization to classify stochastic processes into Markovian and non-Markovian processes.

In detail, all the three exemplary stochastic processes we have previously defined in this chapter are in fact Markov processes. Let us show briefly in the following remarks:

Remark 1.3.1. *The Wiener process $W = (W_t)_{t\geq 0}$ is a Markov process.*

Proof. We will use Theorem 1.3.1 to show that the Wiener process holds the Markov property. First of all, the covariance function of W is widely known[68] to be given by the minimum function: $\langle W_t W_s \rangle = \min(t,s) = (t-s)\,\Theta(t-s)$. Next, we find the covariance function of its derivatives:

$$\begin{aligned}\left\langle \frac{\mathrm{d}W_t}{\mathrm{d}t}\frac{\mathrm{d}W_s}{\mathrm{d}s}\right\rangle &= \frac{\mathrm{d}^2}{\mathrm{d}t\,\mathrm{d}s}\left[(t-s)\,\Theta(t-s)\right]\\ &= \frac{\mathrm{d}}{\mathrm{d}s}\left[\Theta(t-s)+(t-s)\delta(t-s)\right]\\ &= -\delta(t-s)+\delta(t-s)-(t-s)\delta'(t-s)\\ &= \delta(t-s),\end{aligned} \tag{1.3.5}$$

where in last step we used the property of the Dirac delta function $-x\delta'(x) = \delta(x)$. Therefore, since $\dot{W}$ is delta-correlated, it is a white noise process, which implies that by choosing $f(x) = 0$ in Theorem 1.3.1, W is a Markov process. □

Note that there are a variety of ways to prove this remark. Instead of differentiating the covariance function of W, we can instead directly find the covariance of $\dot{W}$ via its CFal[27]:

$$\Phi_{\dot{W}}[g] = \left\langle \exp i\int_0^\infty \mathrm{d}t\, g(t)\,\dot{W}_t\right\rangle = \exp\left(-\frac{1}{2}\int_0^\infty \mathrm{d}t\, g(t)^2\right). \tag{1.3.6}$$

Therefore, using Equation 1.1.7, we indeed get delta correlation:

$$\begin{aligned}&\frac{\delta\Phi_{\dot{W}}[g]}{\delta g(t_1)} = -\frac{1}{2}\int_0^\infty \mathrm{d}t\, 2g(t)\delta(t-t_1)\Phi_{\dot{W}}[g],\\ \implies &\frac{\delta^2\Phi_{\dot{W}}[g]}{\delta g(t_1)\delta g(t_2)} = -\int_0^\infty \mathrm{d}t\,\delta(t-t_2)\delta(t-t_1)\Phi_{\dot{W}}[g] + \frac{\delta\Phi_{\dot{W}}[g]}{\delta g(t_2)}\frac{\delta\Phi_{\dot{W}}[g]}{\delta g(t_1)},\\ \implies &\langle W_{t_1} W_{t_2}\rangle = \int_0^\infty \mathrm{d}t\,\delta(t-t_1)\delta(t-t_2) = \delta(t_1-t_2).\end{aligned} \tag{1.3.7}$$

In Figure 1.2 we have plotted the simulation of the Wiener process together with its derivative, the GWN process in the inset.

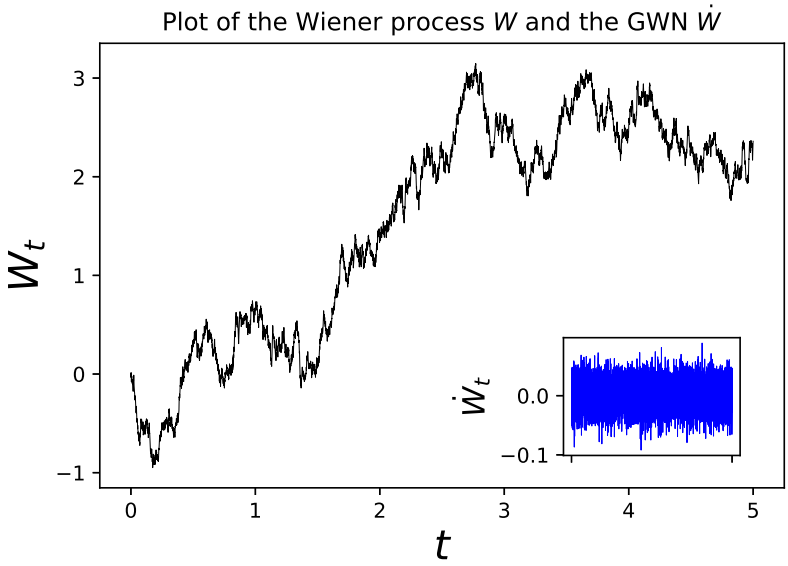

Figure 1.2: Simulation of a realization of the Wiener process W together with the GWN $\dot{W}$ realization as shown in the inset.

We next look into the Poisson process.

Remark 1.3.2. *The Poisson process $N = (N_t)_{t\geq 0}$ with intensity λ is a Markov process.*

Proof. In this example, inr order to infer the Markov property of the Poisson process, we will first find the CFal of the Poisson process N and calculate its covariance using Equation (1.1.7).

The CFal can be found by the following double expectation:

$$\Phi_N[g] = \left\langle \exp i \int_0^\infty \mathrm{d}\tau\, g(\tau) N_\tau \right\rangle = \lim_{t\to\infty} \left\langle \left\langle \exp i \int_0^t \mathrm{d}\tau\, g(\tau) N_\tau \,\middle|\, \int_0^t \mathrm{d}\tau\, N_\tau \right\rangle \,\middle|\, \int_0^t \mathrm{d}\tau\, N_\tau \right\rangle . \tag{1.3.8}$$

The expectation conditioned on the event $\int_0^t \mathrm{d}\tau\, N_\tau = n$ is therefore given by:

$$\left\langle \exp i \int_0^t \mathrm{d}\tau\, g(\tau) N_\tau \;\middle|\; \int_0^t \mathrm{d}\tau\, N_\tau = n \right\rangle = \left(\exp i \int_\tau^t \mathrm{d}s\, g(s) \right)^n . \tag{1.3.9}$$

Notice that by the additive nature of the Poisson process, we have that $\int_0^t \mathrm{d}\tau\, N_\tau = N_{\int_0^t \mathrm{d}\tau} \sim$ *Poisson* $\left(\lambda \int_0^t \mathrm{d}\tau\right)$ and therefore, the total expectation by:

$$\begin{aligned}
\Phi_N[g] &= \left\langle \exp i \int_0^\infty \mathrm{d}\tau\, g(\tau) N_\tau \right\rangle = \lim_{t\to\infty} \left\langle \left(\exp i \int_\tau^t \mathrm{d}s\, g(s) \right)^{\int_0^t \mathrm{d}\tau\, N_\tau} \right\rangle \\
&= \lim_{t\to\infty} \sum_{n=0}^{\infty} \left(\exp i \int_\tau^t \mathrm{d}s\, g(s) \right)^n \frac{\exp\left(-\lambda \int_0^t \mathrm{d}\tau\right) \left(\lambda \int_0^t \mathrm{d}\tau\right)^n}{n!} \\
&= \lim_{t\to\infty} \exp\left(-\lambda \int_0^t \mathrm{d}\tau \right) \cdot \exp\left(\lambda \int_0^t \mathrm{d}\tau\, \exp i \int_\tau^t \mathrm{d}s\, g(s) \right) \\
&= \lim_{t\to\infty} \exp\left[\lambda \int_0^t \mathrm{d}\tau \left(e^{i \int_\tau^t \mathrm{d}s\, g(s)} - 1 \right) \right] \\
&= \exp\left[\lambda \int_0^\infty \mathrm{d}\tau \left(e^{i \int_\tau^\infty \mathrm{d}s\, g(s)} - 1 \right) \right] .
\end{aligned} \tag{1.3.10}$$

Therefore, the covariance of N can be computed by taking the second functional derivative of $\Phi_N[g]$ as in Equation (1.1.7). Let's take the functional derivative of $\Phi_N[g]$ with respect to test functions

$g(t_1)$ and $g(t_2)$:

$$\begin{aligned}
\frac{\delta^2 \Phi_N[g]}{\delta g(t_1)\,\delta g(t_2)} &= \frac{\delta}{\delta g(t_1)} \left\{ \frac{\delta}{\delta g(t_2)} \exp\left[\lambda \int_0^\infty \mathrm{d}\tau \left(e^{i\int_\tau^\infty \mathrm{d}s\, g(s)} - 1 \right) \right] \right\} \\
&= \frac{\delta}{\delta g(t_1)} \left\{ \lambda \int_0^\infty \mathrm{d}\tau \left[i \int_\tau^\infty \mathrm{d}s \left(\delta(s - t_1) e^{i\int_\tau^\infty \mathrm{d}s\, g(s)} \right) \right] \Phi_N[g] \right\} \\
&= \frac{\delta}{\delta g(t_1)} \left\{ \lambda \int_0^\infty \mathrm{d}\tau \left[i\Theta(t_1 - \tau) e^{i\int_\tau^\infty \mathrm{d}s\, g(s)} \right] \Phi_N[g] \right\} \\
&= \lambda^2 \int_0^\infty \mathrm{d}\tau \left[(i)^2 \Theta(t_1 - \tau) \int_\tau^\infty \mathrm{d}s\, \delta(s - t_2) e^{i\int_\tau^\infty \mathrm{d}s\, g(s)} \right] \Phi_N[g] \\
&+ (i)^2 \frac{\delta \Phi_N[g]}{\delta g(t_1)} \cdot \frac{\delta \Phi_N[g]}{\delta g(t_2)} \\
&= \lambda \int_0^\infty \mathrm{d}\tau \left[(i)^2 \Theta(t_1 - \tau)\Theta(t_2 - \tau) e^{i\int_\tau^\infty \mathrm{d}s\, g(s)} \right] \Phi_N[g] + (i)^2 \frac{\delta \Phi_N[g]}{\delta g(t_1)} \cdot \frac{\delta \Phi_N[g]}{\delta g(t_2)}.
\end{aligned} \tag{1.3.11}$$

Therefore, the covariance function of the Poisson process is given by dividing both sides by $(i)^2$ and letting $g = 0$:

$$\langle N_{t_1} N_{t_2} \rangle = \lambda \int_0^\infty \mathrm{d}\tau\, \Theta(t_1 - \tau)\Theta(t_2 - \tau), \tag{1.3.12}$$

where due to the definition of the Poisson process the latter plus terms vanish: $\langle N_{t_1} \rangle = \langle N_{t_2} \rangle = 0$. Lastly, in order to find that N is Markovian, we will compute the covariance of its derivatives, like in the case of the Wiener process:

$$\left\langle \dot{N}_{t_1} \dot{N}_{t_2} \right\rangle = \frac{\mathrm{d}^2}{\mathrm{d}t_1\, \mathrm{d}t_2} \langle N_{t_1} N_{t_2} \rangle = \lambda \int_0^\infty \mathrm{d}\tau\, \delta(t_1 - \tau)\delta(t_2 - \tau) = \lambda \delta(t_1 - t_2), \tag{1.3.13}$$

which implies that $\dot{N}$ is indeed white noise. Thus, by letting $f(x) = 0$ in Theorem 1.3.1 again, the Poisson process N is a Markov process. □

In Figure 1.3 we have plotted the simulation of the Poisson process N together with its derivative $\dot{N}$, i.e. the PWN with unit jump amplitudes, in the inset. Lastly, a very similar case for the Com-

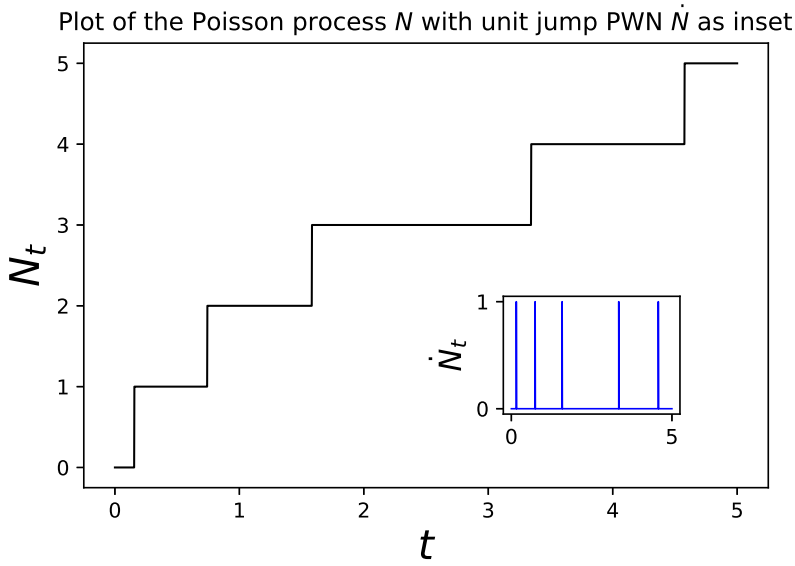

Figure 1.3: Simulation of the Poisson process N together with the unit jump PWN $\dot{N}$ as shown in the inset. Notice that $\dot{N}$ is simply the PWN with almost surely unit jump amplitudes, i.e. $\forall i \in \mathbb{N}$, $A_i = 1$ almost surely. We used $\lambda = 1.2$ for our simulation.

pound Poisson process can be extracted from Remark 1.3.2. We have detailed this case in the following remark.

Remark 1.3.3. *Given the Compound Poisson process $L = (L_t)_{t\geq 0}$ with intensity λ and iid jump amplitudes $\{A_i\}_{i\in\mathbb{N}}$, the time derivative of L is indeed white noise and the covariance is given by: $\langle \dot{L}_t \dot{L}_s \rangle = \lambda \langle A_1^2 \rangle \delta(t-s)$. Therefore, the Compound Poisson process L is also a Markov process.*

Proof. This is the very same method of deriving the CFal of the Poisson process N with the addition of the jump amplitudes. The CFal of L is given by:

$$\begin{aligned}\Phi_L[g] &= \left\langle \exp i \int_0^\infty \mathrm{d}\tau\, g(\tau) L_\tau \right\rangle \\ &= \lim_{t\to\infty} \left\langle \left\langle \exp i \int_0^t \mathrm{d}\tau\, g(\tau) \sum_{i=1}^{N_\tau} A_i \Theta(\tau - T_i) \,\middle|\, \int_0^t \mathrm{d}\tau\, N_\tau \right\rangle \,\middle|\, \int_0^t \mathrm{d}\tau\, N_\tau \right\rangle .\end{aligned} \tag{1.3.14}$$

The inner expectation conditioned on the event $\int_0^t \mathrm{d}\tau\, N_\tau = n$ is given by:

$$\begin{aligned}\left\langle \exp i \int_0^t \mathrm{d}\tau\, g(\tau) \sum_{i=1}^{N_\tau} A_i \Theta(\tau - T_i) \;\middle|\; \int_0^t \mathrm{d}\tau\, N_\tau = n \right\rangle &= \left\langle \exp i \int_\tau^t \mathrm{d}s\, g(s) \sum_{i=1}^{n} A_i \Theta(s-\tau) \right\rangle, \\ &= \left\langle \left(\exp i \int_\tau^t \mathrm{d}s\, g(s) A_1 \right)^n \right\rangle,\end{aligned} \tag{1.3.15}$$

where $\Theta(s-\tau) = 1$ and the summation term simplifies due to the iid nature of the jump amplitudes. Therefore, taking the expectation with respect to the Poisson random variable as before, the CFal of L is given by:

$$\begin{aligned}\Phi_L[g] = \lim_{t\to\infty} \left\langle \left(\exp i \int_\tau^t \mathrm{d}s\, g(s) A_1 \right)^{\int_0^t \mathrm{d}\tau\, N_\tau} \right\rangle &= \lim_{t\to\infty} \exp\left[\lambda \int_0^t \mathrm{d}\tau \left(e^{iA_1 \int_\tau^t \mathrm{d}s\, g(s)} - 1 \right) \right] \\ &= \exp\left[\lambda \int_0^\infty \mathrm{d}\tau \left(\phi_{A_1} \left(\int_\tau^\infty \mathrm{d}s\, g(s) \right) - 1 \right) \right],\end{aligned} \tag{1.3.16}$$

where we defined ϕ_{A_1} to be the CF of the jump amplitudes for easier writing. Like in the case of Poisson process, differentiating the CFal twice yields:

$$\frac{\partial^2 \Phi_L[g]}{\partial g(t_1)\, \partial g(t_2)} = \lambda \int_0^\infty \mathrm{d}\tau \left[(i)^2 \phi''_{A_1} \left(\int_\tau^\infty \mathrm{d}s\, g(s) \right) \Theta(t_1 - \tau)\Theta(t_2 - \tau) \right] \Phi_L[g] + (i)^2 \frac{\partial \Phi_L[g]}{\partial g(t_1)} \cdot \frac{\partial \Phi_L[g]}{\partial g(t_2)}. \tag{1.3.17}$$

Therefore, the covariance is given by dividing both sides by $(i)^2$ and letting $g = 0$:

$$\langle L_{t_1} L_{t_2} \rangle = \lambda \left\langle A_1^2 \right\rangle \int_0^\infty \mathrm{d}\tau\, \Theta(t_1 - \tau)\Theta(t_2 - \tau), \tag{1.3.18}$$

which implies that the covariance of their derivatives is indeed delta-correlated:

$$\left\langle \dot{L}_{t_1} \dot{L}_{t_2} \right\rangle = \lambda \left\langle A_1^2 \right\rangle \int_0^\infty \mathrm{d}\tau \, \delta(t_1 - \tau)\delta(t_2 - \tau) = \lambda \left\langle A_1^2 \right\rangle \delta(t_1 - t_2), \tag{1.3.19}$$

which finishes our proof. □

In Figure 1.4 we have plotted the simulation of the Compound Poisson process L together with its derivative, the PWN process $\dot{L}$, in the inset.

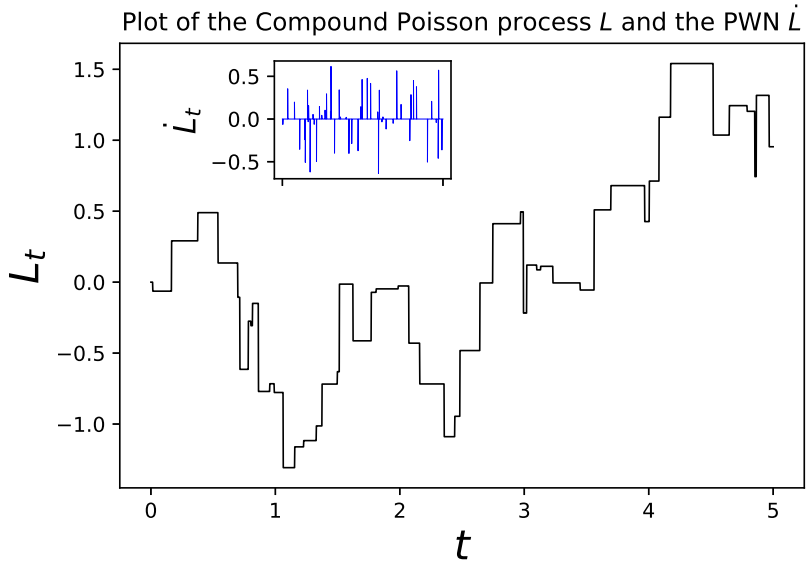

Figure 1.4: Simulation of the Compound Poisson process L together with the PWN $\dot{L}$ as shown in the inset. We used $\lambda = 1.2$ and $A_i \sim \mathcal{N}\left(0, \lambda^{-1}\right)$ for our simulation.

Now that we have given a foundation for our upcoming chapters dealing with the GSN process, we will finish this chapter by going briefly through the Langevin equations.

1.4 Introduction to Langevin Equations

The Langevin equation (LE) is an SDE that describes the time evolution of a stochastic process. It is generally given by the following equation:

$$\dot{X}_t = -V'(X_t) + \xi_t, \tag{1.4.1}$$

where X_t forms the stochastic process $X = (X_t)_{t\geq 0}$ that is generally called the *position process* in physical terminology, ξ_t forms the stochastic noise process $\xi = (\xi_t)_{t\geq 0}$ that induces randomness to X, and V is called the potential of the system.

In many simple LE's, the noise term ξ is generally assumed to be white noise, i.e. $\langle \xi_t \xi_s \rangle = K\delta(t-s)$ for some constant K. In fact, this is what van Kampen laid out in Theorem 1.3.1: given a LE as in Equation 1.4.1, if the noise ξ is white, then X is Markovian; if the noise ξ is colored, then X is non-Markovian.

As we established in the previous sections of this chapter, traditionally used white noise processes as the derivative of the Wiener process, $\dot{W}$, which is distinctively called the *Gaussian* White Noise (GWN). For example, letting $V = \gamma x^2/2$, $\gamma \in \mathbb{R}$ to be a harmonic potential yields the famous Ornstein-Uhlenbeck (OU) process, which we will focus on in the next section below.

1.4.1 Ornstein-Uhlenbeck Process

The OU process is the solution to one of the simplest Langevin equations, where the potential is harmonic, $V(x) = \gamma x^2/2$, and the random noise ξ driving the process X is the GWN:

$$\dot{X}_t = -\gamma X_t + \sigma \dot{W}_t, \tag{1.4.2}$$

where $\gamma, \sigma > 0$ are constants. In literature, the LE is usually written in differential form by multiplying both sides by $\mathrm{d}t$:

$$\frac{\mathrm{d}X_t}{\mathrm{d}t} = -\gamma X_t + \sigma \frac{\mathrm{d}W_t}{\mathrm{d}t} \iff \mathrm{d}X_t = -\gamma X_t \,\mathrm{d}t + \sigma \,\mathrm{d}W_t. \tag{1.4.3}$$

The OU process X has very interesting properties. First and foremost, by Theorem 1.3.1, it is a Markov process. Second of all, the OU process is a *mean-reverting* s.p., where it tends to fluctuate around its *long-term mean*, $X_t = 0$, which is the global minimum of the harmonic potential V [vii]. A simulation of the OU process is given in Figure 1.5 using 3 different initial conditions: $X_0 = \{-5, -2, 3\}$. We can see that the process X tends to say around the long-term limit (red dashed line) regardless of its initial conditions. Furthermore, the OU process corrects its path back towards its long-term limit from fluctuations caused by $\dot{W}$. Further to the mean-reverting stage, the role of γ is also very important. Here, γ corresponds to *the rate* of which the OU process X fixes its paths along the long-term limit. The larger the γ, the faster X will revert to its long-term mean. In Figure 1.6 such property of γ can be visualized.

Furthermore, one can also define *Generalized* Ornstein-Uhlenbeck (GenOU) processes using white noises other than the GWN. The most famous one is using the derivative of the Compound Poisson process, $\dot{L}$, which is generally called the *Poisson* White Noise (PWN), where the GenOU process X will now be the solution of $\dot{X}_t = -\gamma X_t + \dot{\sigma} L_t$.

The GenOU process is also widely used in literature, especially those related to financial applications. The "traditional" OU process X driven by the GWN is a Gaussian process, where each realiza-

[vii] That being said, the potential can be defined in a non-symmetric way as $V(x) = (x - a)^2/2$ for some $a \in \mathbb{R}$. In this case, the long-term limit of the corresponding OU process will be at $X_t = a$. This type of OU process with non-symmetric potential is widely used in the finance industry. For example, one usually seeks the OU process to model interest rates $R = (R_t)_{t \geq 0}$ that conventionally requires to be sticky around a non-zero market reference point $R_t = a$ [28].

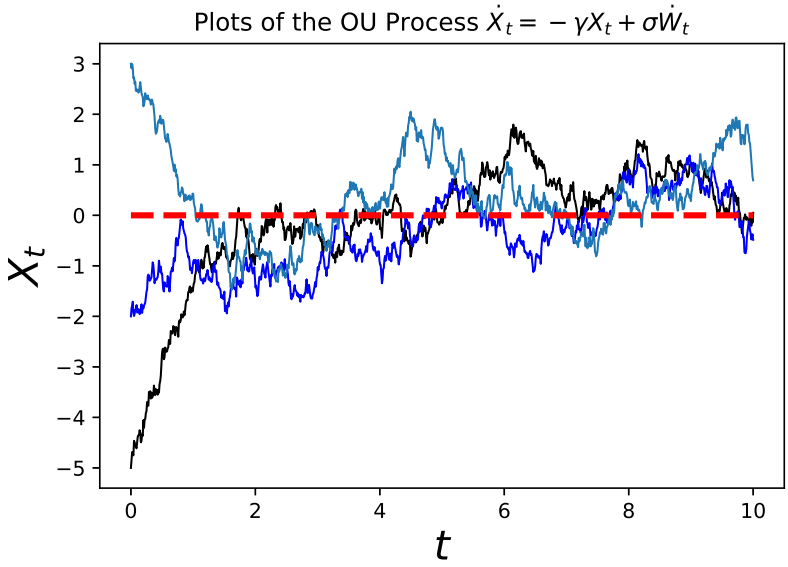

Figure 1.5: Realizations of the OU process X using 3 different initial conditions. Notice that regardless of where it starts from, or the resulting random fluctuations due to the GWN $\dot{W}$, the OU process always tends to stick around $X_t = 0$ (red dashed line), i.e. the global minimum of the harmonic potential $V(x) = \gamma x^2/2$. We used $\gamma = 2$ and $\sigma = 1$.

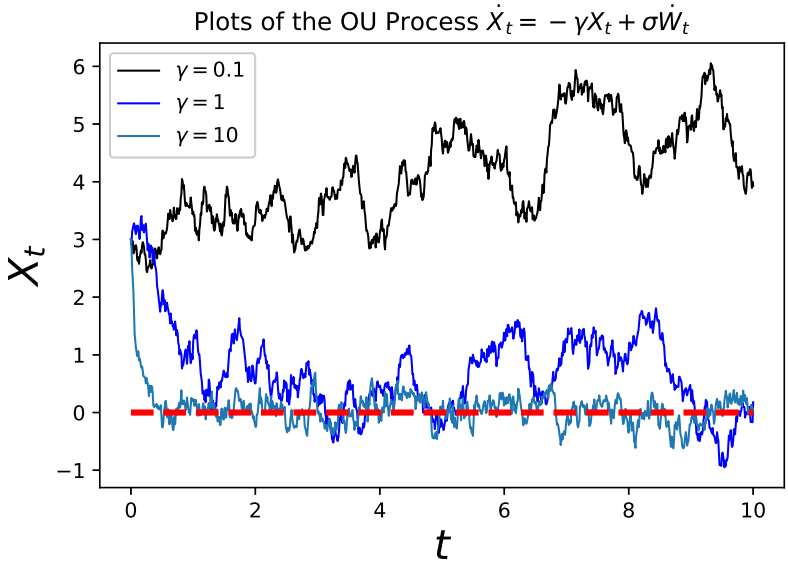

Figure 1.6: Realizations of the OU process X using 3 different values of γ. Here, we can clearly distinguish that the larger the value of γ, the faster the OU process X converges to its long-term mean (red dashed line), i.e. the global minimum of the harmonic potential $V(x) = \gamma x^2/2$. We used the initial condition $X_0 = 3$ and $\sigma = 1$.

tion X_t has a Gaussian/Normal distribution [viii] [28] [29]. Preference over the GenOU is widely sought in instances where the probability distribution of X is empirically known not to be Gaussian, i.e. the process X has discontinuous jumps.

For visualization purposes, simulations of the GenOU process are given in Figure 1.7 for the same set of initial conditions as in the case of the GWN. Last but definitely not least, the OU pro-

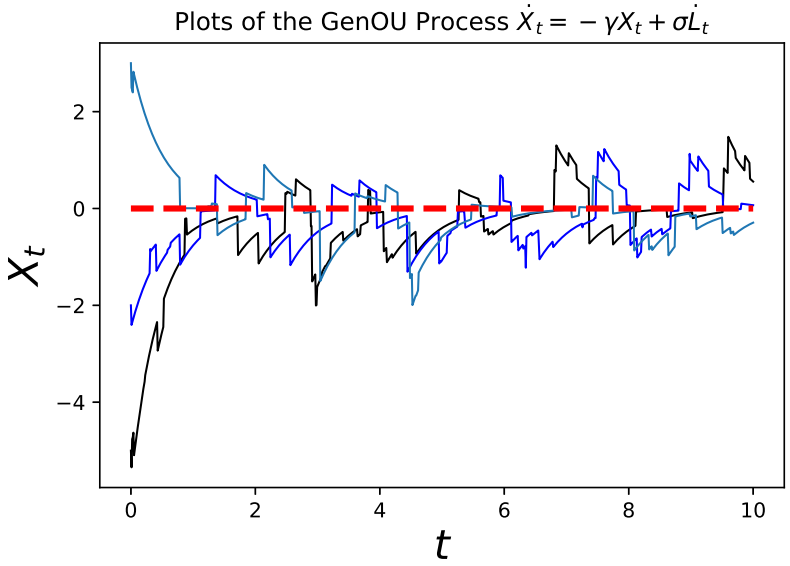

Figure 1.7: 3 realizations of the OU process X using different initial conditions. Again in the same case of the OU process, regardless of where it starts from, or the resulting random non-Gaussian fluctuations due to the PWN $\dot{L}$, the GenOU process always tends to stay around $X_t = 0$ (red dashed line), which is the global minimum of the harmonic potential $V(x) = \gamma x^2/2$. The PWN is simulated with intensity $\lambda = 5$ and Normally-distributed jump amplitudes $A_i \sim \mathcal{N}\left(0, \lambda^{-1}\right)$. We also used $\gamma = 2$ for the Harmonic potential.

cess driven by the GWN X has the following covariance function [30]:

$$\langle X_{t_1} X_{t_2} \rangle = \frac{\sigma^2}{2\gamma} \left(e^{-\gamma|t_1 - t_2|} - e^{-\gamma(t_1 + t_2)} \right). \tag{1.4.4}$$

Furthermore, for the case of GenOU process, the coefficient σ simply becomes $\lambda \left\langle A_1^2 \right\rangle$ where λ and

[viii] The proof is relatively simple by finding the unique solution of Equation (1.4.2) via Ito's lemma in Lemma 1.5.2 and applying additive properties of the Normal distribution.

A_1 are respectively the intensity and iid jump amplitudes of the Compound Poisson process; this directly coincides with our Gaussian Limits property as proven in Theorem 1.2.1.

Lastly, we will prove in upcoming chapters that the GSN noise process with a specific memory kernel is in fact the GenOU process.

1.5 Introduction to Master Equations

Now that we grasped the generic idea behind s.p.'s and how to derive the LE's, we now focus on finding the PDE governing the PDF of a s.p. X driven by a LE.

The Master Equation (ME) of a stochastic process X defined over the probability space $(\Omega, \mathcal{F}, \mathbb{P})$ is a PDE describing the time evolution of the PDF of X, $\mathbb{P}(x,t)$. The ME, in its broadest definition, has the following form:

$$\frac{\partial \mathbb{P}}{\partial t} = \mathcal{A}\mathbb{P}(x,t), \tag{1.5.1}$$

where $\mathcal{A}$ is the differential operator that contains the spatial derivatives of $\mathbb{P}$.

The most famous, if not the sole, way to derive the ME of X driven by the generic LE in Equation 1.4.1 is via the generalized Ito's lemma[84 68]:

Lemma 1.5.1 (Generalized Ito's lemma)**.** *Let X be a s.p. driven by $\dot{X} = -V'(X_t) + \xi_t$, where ξ is any noise process. Then, given a* smooth *function $f : \mathbb{R} \to \mathbb{R}$, one has the following SDΔE for $f(X_t)$:*

$$\mathrm{d}f(X_t) - \Delta f(X_t) = \sum_{m=1}^{2} \frac{1}{m!} \frac{\mathrm{d}^m f}{\mathrm{d}x^m} (\mathrm{d}X_t)^m - \sum_{m=1}^{2} \frac{1}{m!} \frac{\mathrm{d}^m f}{\mathrm{d}x^m} (\Delta X_t)^m , \tag{1.5.2}$$

where Δf and ΔX_t are respectively the jump sizes of $f(X_t)$ and X_t.

The proof of Lemma 1.5.1 can be simply outlined by applying Taylor's expansion on $f(x)$ with

infinitesimal increment $\mathrm{d}x$:

$$f(x+\mathrm{d}x) = f(x) + \frac{\mathrm{d}f}{\mathrm{d}x}\,\mathrm{d}x + \frac{1}{2}\frac{\mathrm{d}^2 f}{\mathrm{d}x^2}\,(\mathrm{d}x)^2 + \cdots + \frac{1}{m!}\frac{\mathrm{d}^m f}{\mathrm{d}x^m}\,(\mathrm{d}x)^m + \ldots, \tag{1.5.3}$$

where $\mathrm{d}f(x+\mathrm{d}x) - f(x) = \mathrm{d}f(x)$. This is followed by correcting Taylor's expansion by splitting X into purely continuous and purely discontinuous parts, noting that the summations stop at the second derivative since the purely continuous part of $\mathrm{d}X_t$ will vanish for powers higher than 2[68]. Lastly, Δf will contain infinite order derivatives if the noise process ξ contains jumps.

Although solving the SDE in Lemma 1.5.1 w.r.t f is not relatively straightforward, there are multiple instances where Ito's formula reduces to a finite order SDE, which is much easier to analyze.

For example, Ito's formula for X driven by the GWN process reduces to a much simpler form below:

Lemma 1.5.2. *Let X be a s.p. driven by the LE: $\dot{X} = V'(X_t) + \sigma\dot{W}_t$, where $\sigma > 0$ is a constant and $\dot{W}$ is the GWN process such that for all $s, t > 0$, $\left\langle \dot{W}_t \dot{W}_s \right\rangle = \delta(t-s)$. Then, for any twice-differentiable function $f : \mathbb{R} \to \mathbb{R}$, the following SDE for $f(X_t)$ holds:*

$$\mathrm{d}f(X_t) = \frac{\partial f}{\partial x}\,\mathrm{d}X_t + \frac{\sigma^2}{2}\frac{\partial^2 f}{\partial x^2}\,\mathrm{d}t. \tag{1.5.4}$$

Proof. Referring to the generic formula in Lemma 1.5.1, notice first that the jump terms vanish: By rewriting the LE in differential form, $\mathrm{d}X_t = -V'(X_t)\,\mathrm{d}t + \sigma\,\mathrm{d}W_t$, we can then write the jump discontinuities as $\Delta X_t = -V'(X_t)\Delta t + \sigma\Delta W_t$. Since time is continuous, it is trivial that $\Delta t = 0$. Furthermore, referring to Definition 1.2.3, the Wiener process W is a continuous-time s.p. and therefore we have that $\Delta W_t = 0$ almost surely.

Next, we square the differential form to yield the following:

$$(\mathrm{d}X_t)^2 = V'(X_t)^2\,(\mathrm{d}t)^2 + \sigma^2\,(\mathrm{d}W_t)^2 + 2\sigma V'(X_t)\,\mathrm{d}t\,\mathrm{d}W_t. \tag{1.5.5}$$

Regarding to the squared form, it is trivial that $(\mathrm{d}t)^2 = 0$. Furthermore, again by[68], we have that the *quadratic variation* of W_t converges to $\mathrm{d}t$ under mean-square convergence, i.e. $(\mathrm{d}W_t)^2 \xrightarrow{m.s.} \mathrm{d}t$, and that $\mathrm{d}t \cdot \mathrm{d}W_t \xrightarrow{m.s.} 0$. From the extension of the properties mentioned herein, we can also infer that the higher orders of m for $(\mathrm{d}X_t)^m$ simply converge to 0 in mean-square, yielding the desired SDE. □

The reason why Ito's lemma is important is that one can find the differential operator $\mathcal{A}$ directly from the solution of f. In fact, the linear operator applied to f is the *adjoint* [ix] of the linear operator in the ME:

$$\langle f, \mathcal{A}\mathbb{P}\rangle = \langle \mathcal{A}^* f, \mathbb{P}\rangle\,, \tag{1.5.6}$$

where the notation $\langle\cdot,\cdot\rangle$ refers to the inner product [x]. In most contexts, the adjoint operator $\mathcal{A}^*$ is called the *infinitesimal generator* of the s.p. X (e.g. Chapter 37 of[93]).

Let us now find the ME of X via the SDE for f derived in Lemma 1.5.2. Rewrite the SDE of f in

[ix] An adjoint of a linear operator $\mathcal{A}$, denoted by $\mathcal{A}^*$, is any linear operator that satisfies the condition $\mathcal{A}^*\mathcal{A} = 1$.

[x] In detail, it is the inner product in Euclidean space. For any two functions $f, g : \mathbb{R} \to \mathbb{R}$, their inner product is given by:

$$\langle f, g\rangle = \int_{\mathbb{R}} \mathrm{d}x\, f(x) g(x). \tag{1.5.7}$$

dot notation by dividing both sides by $\mathrm{d}t$, followed by taking their average yields the following:

$$\begin{aligned}\left\langle \frac{\mathrm{d}f(X_t)}{\mathrm{d}t} \right\rangle &= \left\langle \frac{\partial f}{\partial x}\dot{X} \right\rangle + \frac{\sigma^2}{2}\left\langle \frac{\partial^2 f}{\partial x^2} \right\rangle \\ &= \left\langle \frac{\partial f}{\partial x}\left(-V'(X_t) + \xi_t\right) \right\rangle + \frac{\sigma^2}{2}\left\langle \frac{\partial^2 f}{\partial x^2} \right\rangle \\ &= -\left\langle \frac{\partial f}{\partial x}V'(X_t) \right\rangle + \left\langle \frac{\partial f}{\partial x}\xi_t \right\rangle + \frac{\sigma^2}{2}\left\langle \frac{\partial^2 f}{\partial x^2} \right\rangle .\end{aligned} \tag{1.5.8}$$

Notice that due to the iid nature of the GWN, we have that $\left\langle \frac{\partial f}{\partial x}\xi_t \right\rangle = \langle \xi_t \rangle \left\langle \frac{\partial f}{\partial x} \right\rangle = 0$. Furthermore, given the PDF of X as $\mathbb{P}$, we can apply integration by parts to the following expectation:

$$\left\langle \frac{\partial f}{\partial x}V'(X_t) \right\rangle = \int_{\mathbb{R}} \mathrm{d}x \, \frac{\partial f(x)}{\partial x}V'(x)\mathbb{P}(x,t) = -\int_{\mathbb{R}} \mathrm{d}x f(x)\frac{\partial}{\partial x}\left[V'(x)\mathbb{P}(x,t)\right]. \tag{1.5.9}$$

Similarly, we can apply integration by parts twice to the following,

$$\left\langle \frac{\partial^2 f}{\partial x^2} \right\rangle = \int_{\mathbb{R}} \mathrm{d}x \, \frac{\partial^2 f(x)}{\partial x^2}\mathbb{P}(x,t) = \int_{\mathbb{R}} \mathrm{d}x f(x)\frac{\partial^2 \mathbb{P}}{\partial x^2}. \tag{1.5.10}$$

Rewriting the expectations as integrals w.r.t. f yields the following:

$$\int_{\mathbb{R}} \mathrm{d}x f(x)\frac{\partial \mathbb{P}}{\partial t} = \int_{\mathbb{R}} \mathrm{d}x f(x)\left(\frac{\partial}{\partial x}\left[V'(x)\mathbb{P}(x,t)\right] + \frac{\sigma^2}{2}\frac{\partial^2 \mathbb{P}}{\partial x^2}\right). \tag{1.5.11}$$

Disregarding the integration and f yields the ME for a GWN driven general s.p. X:

$$\frac{\partial \mathbb{P}}{\partial t} = \frac{\partial}{\partial x}\left[V'(x)\mathbb{P}(x,t)\right] + \frac{\sigma^2}{2}\frac{\partial^2 \mathbb{P}}{\partial x^2}. \tag{1.5.12}$$

Notice that the linear operator of the ME in Equation (1.5.12) is simply the following spatial differentials:

$$\mathcal{A} = V''(x) + V'(x)\frac{\partial}{\partial x} + \frac{\sigma^2}{2}\frac{\partial^2}{\partial x^2}, \tag{1.5.13}$$

and its adjoint $\mathcal{A}^*$ can simply be referred from Equation (1.5.8) to be:

$$\mathcal{A}^* = -V'(x)\frac{\partial}{\partial x} + \frac{\sigma^2}{2}\frac{\partial^2}{\partial x^2}. \tag{1.5.14}$$

It is important to note that the Master Equation given in Equation 1.5.12 is a second-order PDE solely due to the Gaussian nature of the noise process ξ. In fact, Master Equations of GWN-driven Langevin Equations are an extensively studied class of second-order PDE's that are exclusively called the *Fokker-Planck Equations*[57]. For non-Gaussian processes, the Master Equation will instead be an infinite order PDE [xi].

We finally finish this section, and subsequently this chapter, by further extending generalized Ito's lemma in Lemma 1.5.1 to bivariate functions:

Lemma 1.5.3 (Generalized Multivariate Ito's Lemma). *Let $\vec{X} = \left(X^1, X^2, \ldots, X^n\right)$ be a collection stochastic processes that need not be independent. Then, given a smooth function $f : \mathbb{R}^n \to \mathbb{R}$, one has the following SDΔE:*

$$\begin{aligned}
&\mathrm{d}f(\vec{X}_t) - \Delta f(\vec{X}_t) \\
&= \sum_{m_1=1}^{2}\sum_{m_2=1}^{2}\cdots\sum_{m_n=1}^{2} \frac{1}{m_1!m_2!\ldots m_n!}\frac{\partial^{m_1+m_2+\cdots+m_n}f}{\partial x_1^{m_1}\partial x_2^{m_2}\ldots\partial x_n^{m_n}}\left(\mathrm{d}X_t^1\right)^{m_1}\left(\mathrm{d}X_t^2\right)^{m_2}\ldots\left(\mathrm{d}X_t^n\right)^{m_n} \\
&\quad - \sum_{m_1=1}^{2}\sum_{m_2=1}^{2}\cdots\sum_{m_n=1}^{2} \frac{1}{m_1!m_2!\ldots m_n!}\frac{\partial^{m_1+m_2+\cdots+m_n}f}{\partial x_1^{m_1}\partial x_2^{m_2}\ldots\partial x_n^{m_n}}\left(\Delta X_t^1\right)^{m_1}\left(\Delta X_t^2\right)^{m_2}\ldots\left(\Delta X_t^n\right)^{m_n}
\end{aligned} \tag{1.5.15}$$

Much like its univariate counterpart, the multivariate Ito's lemma mentioned in Lemma 1.5.3 for the two dimensional s.p. (X, ξ) can be used to find the joint PDF of the tuple (X_t, ξ_t). This will be very useful in later chapters when we introduce the GSN noise process ξ, where the resulting

[xi] Nonetheless, in most physical contexts, such Master Equations that are driven by non-Gaussian noises are called *Higher-Order Fokker Planck Equations*[94] [123].

position process X will be marginally non-Markovian, but the collection of X together with ξ and its derivatives, $(X, \xi, \dot{\xi}, \ddot{\xi}, \dots)$, will be a Markov process.

1.6 Chapter Review

In this chapter, we have briefly undergone the broad definition of what a stochastic process means, with some detailed examples of the Poisson process, the Compound Poisson process, and the Wiener process. We have also discussed how to find the CF and the CFal of such processes, which are very useful in calculating their moments and the covariance functions. We next entailed the Markov property of stochastic processes that is a very useful tool for classifying stochastic processes into memoryless processes and processes with memory. In this section we have also gone through the time derivative of Markov processes that are white noise, and shown that the time derivatives of the Wiener process, Poisson process and Compound Poisson processes are white noise processes. Later in this chapter, we defined a broad classification of Langevin equations with some examples widely used in literature. Finally, we gave a broad outline of how to derive Master Equations for LE's driven by Gaussian White Noise process, where in this particular case the Master Equation is usually called the *Fokker-Planck Equation*.

Next chapter, we focus on our Colored Poisson process, which shares similar characteristics as to other noise processes but violates the Markov property.

Truth is ever to be found in the simplicity, and not in the multiplicity and confusion of things.

Sir Isaac Newton

2

Introduction to the Generalized Shot Noise Process

Throughout the previous chapter, we focused on defining stochastic processes that obey the Markov property. As outlined in Theorem 1.3.1, asserting whether a s.p. either obeys or violates the Markov property is directly linked by its underlying noise: given the s.p. X as the solution of the LE $\dot{X} = -V'(X_t) + \xi_t$, we have that X is a Markov process if ξ is a white noise process. However, what hap-

pens if ξ is not white, but *colored*?

In this chapter, we aim to connect the previous definitions, namely the Wiener process, the Poisson process and the Compound Poisson process, as well as the Markov property, in order to properly define the GSN process such that it is not a white noise process. Later in this chapter, we classify the GSN processes with respect to their innate definitions, the most widely studied example is the *Colored Poisson* noise process. We then finish this chapter by focusing on how to construct the CF of GSN processes, which can be used to find their PDF via Inverse Fourier Transform (IFT).

2.1 Definition of the GSN Process

The GSN process is a very interesting stochastic process that has in fact been used to formulate non-Markovian LE's in theory since the 1920's, starting with the Campbell noise[99], and further extended in the early 1950's[101 109]. Due to its limitations to finding the PDF and solving the time evolution equations, the GSN processes have not been widely used in practice.

We disclose the broad definition of the GSN process below:

Definition 2.1.1. *Let $N = (N_t)_{t\geq 0}$ be the Poisson process with intensity λ, jump amplitudes $\{A_i\}_{i\in\mathbb{N}}$ and arrival times $\{T_i\}_{i\in\mathbb{N}}$. Let $h : \mathbb{R} \to \mathbb{R}$ be a smooth function. Then, the* GSN process *$\xi = (\xi_t)_{t\geq 0}$ is formed by the following realization:*

$$\xi_t = \sum_{i=1}^{N_t} A_i h(t - T_i). \tag{2.1.1}$$

Throughout this thesis, the function h will be called the impulse function *of the GSN process.*

Notice the similarity of the GSN process ξ to that of the Compound Poisson process, as given in Definition 1.2.2. In fact, the Compound Poisson process is a special type of GSN process where the impulse function is the Heaviside step function, i.e. $h = \Theta$. An even more interesting property

is that the PWN, which is the time derivative of the Compound Poisson process, is also another special type of GSN process where the impulse function is the Dirac delta function, i.e. $h = \delta$. The proof of this relation will be given in Section 3.1 of the next chapter, when we identify the time derivative of the GSN process ξ.

2.2 Visual Representation of Impulse Functions

An important outcome that we can draw from the two examples of the impulse function $h = \delta$ and $h = \Theta$ is that h plays a very important role in categorizing the GSN process ξ. Given the case for $h = \Theta$, the process ξ becomes a colored noise process; whereas for $h = \delta$, the process ξ becomes a Poisson White Noise (PWN) process [i].

The conditions for such behavior of ξ can be visualized in Figures 2.1 and 2.2. In the case of Dirac delta impulse function, the s.p. ξ becomes a Poisson white noise, as there is zero step involved with the impulse size; whereas in the case of Heaviside function, the impulses have a unit step size, which creates a Markovian (i.e. unit step memory) process ξ. In latter Figure 2.2, the grey points are where the intersection of different impulses we also can witness where memory is formed.

Now that we have defined the simplest impulse function functions, we can focus on something more advanced. Let the impulse function instead be a rectangular function, defined as follows:

$$h(t) := \operatorname{rect}(t; a, b) = \begin{cases} 0 & t < a, \\ \frac{1}{b-a} & a \leq t \leq b, \\ 1 & t > b. \end{cases} \tag{2.2.1}$$

We have plotted the impulses regarding the rectangular function in Figure 2.3. Notice that this

[i] Recall from Theorem 1.2.1 that under certain limitations, collectively called *Gaussian limits*, the PWN will converge to Gaussian White Noise (GWN) process.

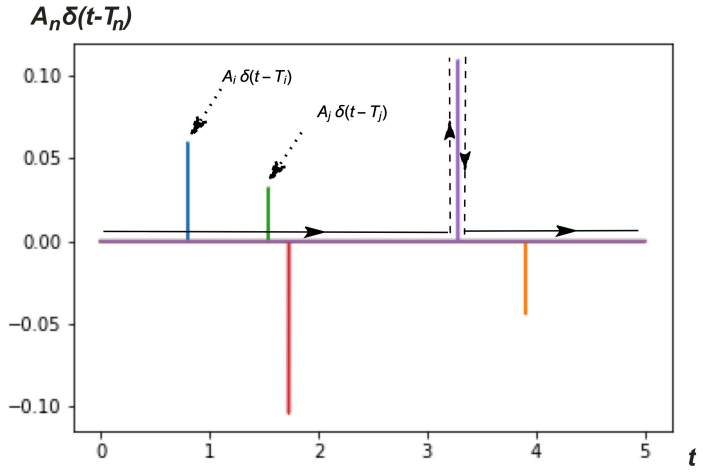

Figure 2.1: Impulse response $A_n\delta(t - T_n)$ with Dirac delta impulse function. Notice that the impulses i and j are unit impulses with zero steps, indicating PWN nature of ξ. For this plot we used jump amplitudes $A_i \sim \mathcal{N}(0, \lambda^{-1})$ with $\lambda = 10$. Throughout this thesis, we use statistically independent (iid) jump amplitudes A_i for our simulations. Finally, the arrival times T_i are derived from the Poisson process with intensity λt. A sample impulse response trajectory is shown in directional arrows, where dashed parts are discontinuous jumps.

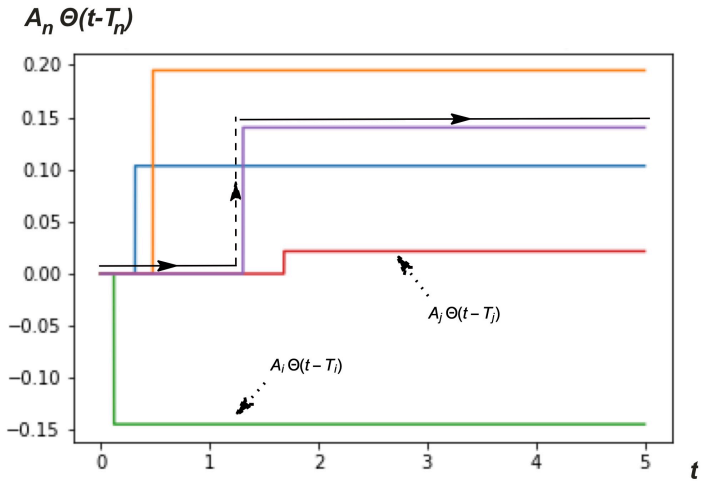

Figure 2.2: Impulse response $A_n\Theta(t - T_n; a = 1/2, b = 1/2)$ with Heaviside impulse function. Notice that the impulses i and j are unit impulses with one step, indicating that the s.p. ξ a one-step memory, i.e. Markov, process. We used jump amplitudes $A_i \sim \mathcal{N}(0, \lambda^{-1})$ with $\lambda = 10$, and the arrival times T_i are derived from the Poisson process with intensity λt. A sample impulse response trajectory is shown in directional arrows, where dashed parts are discontinuous jumps.

time the impulse function has two steps, where it is indicated by continuous straight lines. This results in a colored noise process again. Let us advance further into the impulse functions by defin-

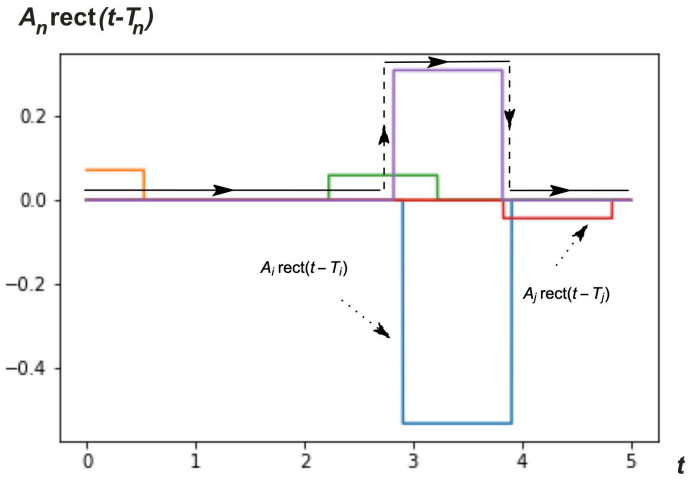

Figure 2.3: Impulse response $A_n\text{rect}(t - T_n; a = -1/2, b = 1/2)$ with Rectangular impulse function. Notice that the impulses i and j are unit impulses with two steps, indicating that the s.p. ξ a colored noise process. We used jump amplitudes $A_i \sim \mathcal{N}(0, \lambda^{-1})$ with $\lambda = 10$, and the arrival times T_i are derived from the Poisson process with intensity λt. A sample impulse response trajectory is shown in directional arrows, where dashed parts are discontinuous jumps.

ing *continuous* cases. Let the impulse function now be an exponentially decaying function, i.e. $h(x) = \alpha e^{-\alpha x}$, where $\alpha > 0$ determines the rate of decay. The GSN process with exponentially decaying impulse function is commonly known in literature as the CP process[74 101 109].

The impulse responses using this function is given in Figure 2.4, where one can see that the impulse function will promote infinite steps to the noise process. In the following Figure 2.5 one can see the impulse trajectories for the exponentially decaying impulse function. Another example that we can give herein is the damped and oscillating impulse function. This type of impulse function is similar to exponential decay; however, it includes an additional sinusoid oscillating term that is useful to extend the memory condition as we will observe in later chapters of our thesis.

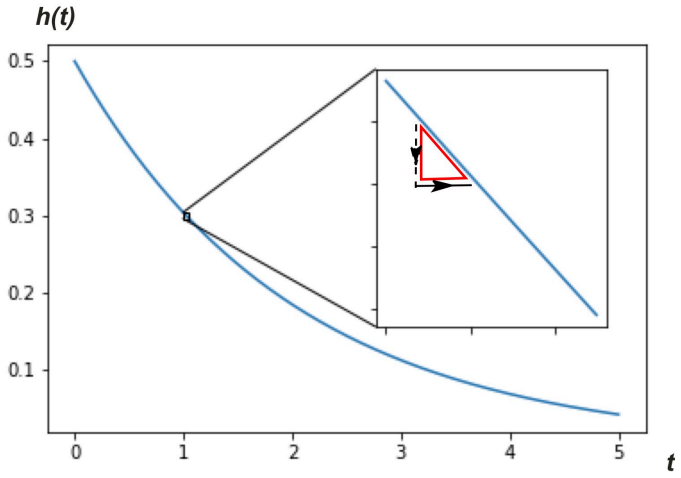

Figure 2.4: Plot of the exponentially decaying impulse function $h(t) = \alpha e^{-\alpha t}$. Notice that the steps in this impulse function is infinite; upon zooming to a small region of h, the impulse function gain an additional step along the infinitesimally small right triangle. Here we used $\alpha = 1/2$ for better visualization.

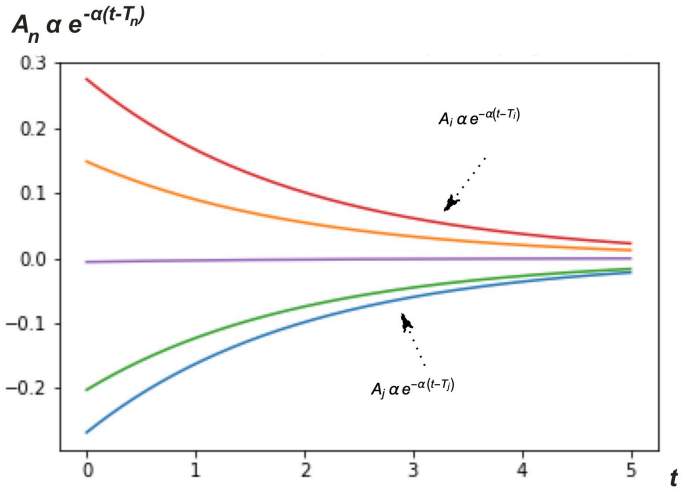

Figure 2.5: Impulse response $A_n \alpha e^{-\alpha(t-T_n)}$ with exponentially decaying impulse function. Notice that the impulses i and j are unit impulses with infinite steps, indicating that the s.p. ξ is a colored noise process. We used the decay rate $\alpha = 1/2$, and the jump amplitudes $A_i \sim \mathcal{N}(0, \lambda^{-1})$ with $\lambda = 10$, where the arrival times T_i are derived from the Poisson process with intensity λt.

A damped and oscillatory impulse function is generally defined to be of the following form:

$$h(t) := \frac{\alpha^2 + \beta^2}{\alpha + \beta} e^{-\alpha t} \left(\sin \beta t + \cos \beta t\right),$$

where $\alpha, \beta > 0$ are constants.

Regarding to this particular impulse function the impulse response can be visualized in Figure 2.6.

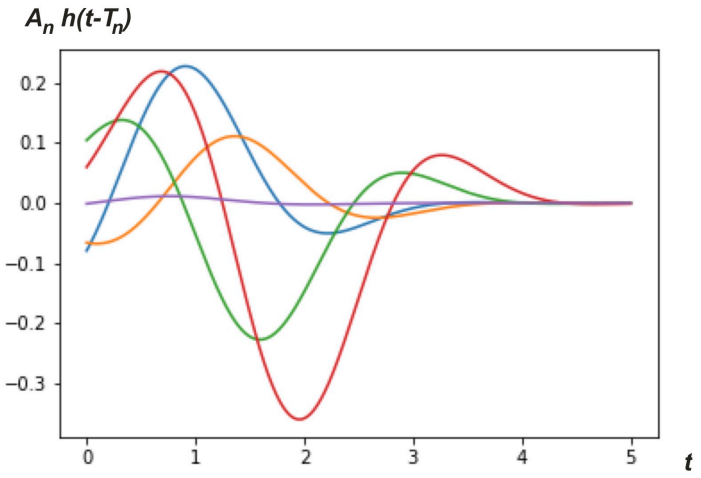

Figure 2.6: Impulse response for jump sizes $A_n h(t - T_n; \alpha = 1, \beta = 2)$ with damped and oscillating impulse function. Notice that the impulses have infinite steps, indicating that the s.p. ξ again a colored process. We used jump amplitudes $A_i \sim \mathcal{N}(0, \lambda^{-1})$ with $\lambda = 10$, and the arrival times T_i are derived from the Poisson process with intensity λt.

The last example of a impulse function we would like to introduce is the sigmoid function. It is in general defined as:

$$h(t; \alpha) = \frac{e^{\alpha t}}{1 + e^{\alpha t}}, \tag{2.2.2}$$

where α is the steepness coefficient. The reason behind using the Sigmoid kernel is due to its resemblance to the Heaviside step function. In fact, the coefficient α decides the rate of saturation to $\lim_{t \to \infty} h(t) = 1$, where simple analysis shows that for large α the sigmoid function converges to

the Heaviside step function:

$$\lim_{\alpha\to\infty} \frac{e^{\alpha t}}{1+e^{\alpha t}} = \Theta(t). \tag{2.2.3}$$

This *relaxed* version of the sigmoid function is highly used in various mathematical applications where continuous version of the Heaviside step function is needed to be used[95]. The impulse response regarding to this impulse function is given in Figure 2.7.

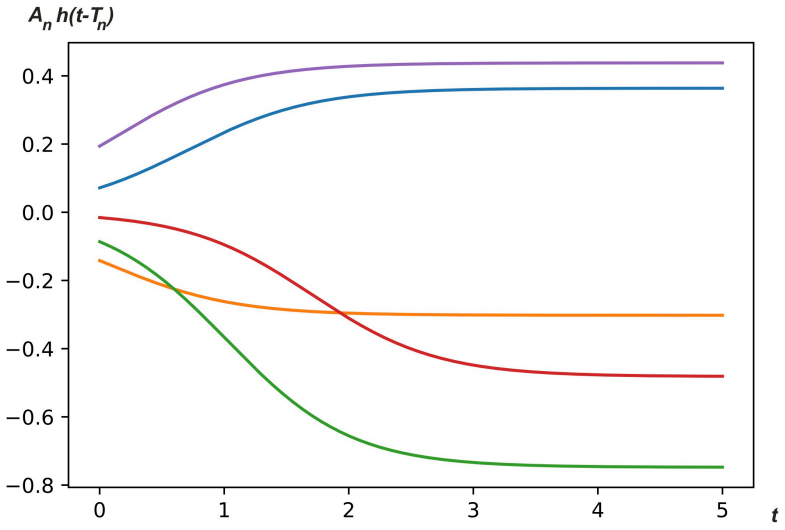

Figure 2.7: Impulse response for jump sizes $A_n h(t;\alpha = 2)$ with sigmoid impulse function. Notice that the impulses have infinite steps, indicating that the s.p. ξ again a colored process. We used jump amplitudes $A_i \sim \mathcal{N}(0, \lambda^{-1})$ with $\lambda = 10$, and the arrival times T_i are derived from the Poisson process with intensity λt.

So where does the term *colored noise* come into play? In general, *any* noise where the impulse function itself is not Dirac delta is a *colored* noise process, meaning that the noise does not have zero-step memory. Given the step size n in the impulse function, one can summarize this property as follows:

- If $n = 0$, then the noise becomes a white noise process; and
- If $n > 0$, then the noise becomes a *colored* noise process.

Now that we have grasped the visual representation of impulse functions and their classifications to white or colored noise, let's prove their existence by computing their autocovariances via their CFal.

2.3 Finding the Characteristic Function of the GSN process

We now find the CFal of the noise process ξ. This will be useful in not only classifying ξ, but also to find the CFal of X obeying the Langevin equation (0.0.2) using the method from Caceres & Budini's paper published 1997 (ref. [99]).

We first reproduce the paper's result for Campbell noise and apply the same technique to our GSN process ξ, then use the functional correspondence technique to find the CFal of X.

Next, we apply some candidate impulse functions to the CFals of ξ and X in order to deduce similarities between known Lévy processes, e.g. Compound Poisson process and Wiener process.

2.3.1 Reproducing the Result with Campbell Noise

Note that Campbell et al. used the following noise in deriving their LE [Equation (2.6) of[99]]:

$$\xi_t = \sum_{i=1}^{S} \psi(t - T_i), \tag{2.3.1}$$

where T_i are iid random variables with density $\mathrm{d}q$ with support on $[0, \infty[$, and $S \sim \mathit{Poisson}(\lambda = 1)$ is a Poisson-distributed random variable with unit intensity. From here, one can get the CFal of ξ,

$$\Phi_\xi[g] = \left\langle \exp i \int_0^\infty g(t)\xi_t \,\mathrm{d}t \right\rangle = \left\langle \exp i \int_0^\infty g(t) \sum_{i=1}^{S} \psi(t - T_i) \,\mathrm{d}t \right\rangle, \tag{2.3.2}$$

by conditioning on $S = s$:

$$\begin{aligned}\left\langle \exp i \int_0^\infty g(t) \sum_{i=1}^{S} \psi(t - T_i)\, \mathrm{d}t \,\middle|\, S = s \right\rangle &= \left\langle \exp i \int_0^\infty g(t) \sum_{i=1}^{s} \psi(t - T_i)\, \mathrm{d}t \right\rangle \\ &= \int_0^\infty \left(\exp \left[is \int_0^\infty \psi(t - \tau)\, \mathrm{d}t \right] \right) q(\tau)\, \mathrm{d}\tau.\end{aligned} \tag{2.3.3}$$

Hence, we simply get Φ_ξ by averaging over S:

$$\begin{aligned}\Phi_\xi[g] &= \left\langle \int_0^\infty \left(\exp \left[iS \int_0^\infty \psi(t - \tau)\, \mathrm{d}t \right] \right) q(\tau)\, \mathrm{d}\tau \right\rangle \\ &= \sum_{s=0}^{\infty} \int_0^\infty \left(\exp \left[is \int_0^\infty \psi(t - \tau)\, \mathrm{d}t \right] \right) q(\tau)\, \mathrm{d}\tau \frac{e^{-1}}{s!} \\ &= \int_0^\infty e^{-1} \left(\sum_{s=0}^{\infty} \frac{\left(\exp \left[i \int_0^\infty \psi(t - \tau)\, \mathrm{d}t \right] \right)^s}{s!} \right) q(\tau)\, \mathrm{d}\tau \\ &= \int_0^\infty \left(\exp \left[\left(\exp i \int_0^\infty \psi(t - \tau) g(t)\, \mathrm{d}t \right) \right] - 1 \right) q(\tau)\, \mathrm{d}\tau.\end{aligned} \tag{2.3.4}$$

However, our GSN process is not the Campbell noise: by far the most important difference is that Campbell noise assumes a Poisson-distributed random variable S over the summation; whereas we assume a Poisson process $(N_t)_{t \geq 0}$.

2.3.2 Characteristic Functional of the GSN process

Note that using the definition of the CFal, we first compute the following double expectation, as in cases for the Poisson and Compound Poisson processes:

$$\begin{aligned}\Phi_\xi[g] &= \left\langle \exp i \int_0^\infty \mathrm{d}\tau\, g(\tau) \xi_\tau \right\rangle = \left\langle \exp i \int_0^\infty \mathrm{d}\tau\, g(\tau) \sum_{i=1}^{N_\tau} A_i h(\tau - T_i) \right\rangle \\ &= \lim_{t \to \infty} \left\langle \left\langle \exp i \int_0^t \mathrm{d}\tau\, g(\tau) \sum_{i=1}^{N_\tau} A_i h(\tau - T_i) \,\middle|\, \int_0^t \mathrm{d}\tau\, N_\tau \right\rangle \,\middle|\, \int_0^t \mathrm{d}\tau\, N_\tau \right\rangle\end{aligned} \tag{2.3.5}$$

Due to the iid nature of A_i, the inner expectation conditioned on the event $\int_0^t \mathrm{d}\tau\, N_\tau = n$ is given by:

$$\begin{aligned}&\left\langle \exp i \int_0^t \mathrm{d}\tau\, g(\tau) \sum_{i=1}^{N_\tau} A_i h(\tau - T_i) \middle| \int_0^t \mathrm{d}\tau\, N_\tau = n \right\rangle \\ &= \left\langle \exp i \int_\tau^t \mathrm{d}s\, g(s) \sum_{i=1}^{n} A_i h(s-\tau) \right\rangle = \left\langle \left(\exp iA_1 \int_\tau^t \mathrm{d}s\, g(s) h(s-\tau) \right)^n \right\rangle .\end{aligned} \tag{2.3.6}$$

Therefore, we get the characteristic functional by the total expectation as follows:

$$\begin{aligned}\Phi_\xi[g] &= \lim_{t\to\infty} \left\langle \left(\exp iA_1 \int_\tau^t \mathrm{d}s\, g(s) h(s-\tau) \right)^{\int_0^t \mathrm{d}\tau\, N_\tau} \right\rangle \\ &= \lim_{t\to\infty} \sum_{n=0}^{\infty} e^{-\lambda \int_0^t \mathrm{d}\tau} \frac{1}{n!} \left(\exp iA_1 \int_\tau^t \mathrm{d}s\, g(s) h(s-\tau) \right)^n \\ &= \lim_{t\to\infty} \exp\left[\lambda \int_0^t \mathrm{d}\tau \left(\phi_{A_1} \left(\int_\tau^t \mathrm{d}s\, g(s) h(s-\tau) \right) - 1 \right) \right] \\ &= \exp\left[\lambda \int_0^\infty \mathrm{d}\tau \left(\phi_{A_1} \left(\int_\tau^\infty \mathrm{d}s\, g(s) h(s-\tau) \right) - 1 \right) \right] .\end{aligned} \tag{2.3.7}$$

First and foremost, we confirm in below Lemma that the condition for ξ to be a white noise process solely depends on the impulse function h:

Lemma 2.3.1. *Let ξ be the GSN process as given in Definition 2.1.1. Then, ξ is not a white noise process unless the impulse function h is a Dirac delta function.*

Proof. The proof is relatively simple, as we only require to find whether the covariance function of ξ is delta-correlated. In order to do that, let's find the two functional derivatives of $\Phi_\xi[g]$ w.r.t. test

functions $g(t_1)$ and $g(t_2)$:

$$
\begin{aligned}
&\frac{\delta^2 \Phi_\xi[g]}{\delta g(t_1)\delta g(t_2)} = \frac{\delta}{\delta g(t_1)} \left\{ \frac{\delta}{\delta g(t_2)} \exp\left[\lambda \int_0^\infty \mathrm{d}\tau \left(\phi_{A_1} \left(\int_\tau^\infty \mathrm{d}s\, g(s) h(s-\tau) \right) - 1 \right) \right] \right\} \\
=&\frac{\delta}{\delta g(t_1)} \left[\lambda \int_0^\infty \mathrm{d}\tau \left(\int_\tau^\infty \mathrm{d}s\, \delta(s-t_1) h(s-\tau) \cdot \phi'_{A_1} \left(\int_\tau^\infty \mathrm{d}s\, g(s) h(s-\tau) \right) \right) \Phi_\xi[g] \right] \\
=&\frac{\delta}{\delta g(t_1)} \left[\lambda \int_0^\infty \mathrm{d}\tau \left(\Theta(t_1-\tau) h(t_1-\tau) \phi'_{A_1} \left(\int_\tau^\infty \mathrm{d}s\, g(s) h(s-\tau) \right) \right) \Phi_\xi[g] \right] \\
=&\lambda \int_0^\infty \mathrm{d}\tau \left(\Theta(t_1-\tau) h(t_1-\tau) \int_\tau^\infty \mathrm{d}s\, \delta(s-t_2) h(s-\tau) \cdot \phi''_{A_1} \left(\int_\tau^\infty \mathrm{d}s\, g(s) h(s-\tau) \right) \right) \Phi_\xi[g] \\
&+ \frac{\delta \Phi_\xi[g]}{\delta g(t_1)} \frac{\delta \Phi_\xi[g]}{\delta g(t_2)} \\
=&\lambda \int_0^\infty \mathrm{d}\tau \left(\Theta(t_1-\tau) h(t_1-\tau) \Theta(t_2-\tau) h(t_2-\tau) \cdot \phi''_{A_1} \left(\int_\tau^\infty \mathrm{d}s\, g(s) h(s-\tau) \right) \right) \Phi_\xi[g] \\
&+ \frac{\delta \Phi_\xi[g]}{\delta g(t_1)} \frac{\delta \Phi_\xi[g]}{\delta g(t_2)}.
\end{aligned}
\tag{2.3.8}
$$

Then the covariance of the GSN process is simply given by letting dividing both sides by i^2 and letting $g = 0$, noting that by construction of the GSN process as in Definition 2.1.1, $\langle \xi_t \rangle = 0$ for all $t \geq 0$:

$$
\left\langle \xi_{t_1} \xi_{t_2} \right\rangle = \lambda \left\langle A_1^2 \right\rangle \int_0^\infty \mathrm{d}\tau\, \Theta(t_1-\tau) h(t_1-\tau) \cdot \Theta(t_2-\tau) h(t_2-\tau). \tag{2.3.9}
$$

Since Θ are only Heaviside step functions, the only case where Equation (2.3.9) above is delta-correlated is the case where $h = \delta$, which concludes our proof. □

2.4 Correlation Functions of GSN processes driven by the Exemplary Impulse Functions

Now that we have the covariance of the GSN process ξ, we can now confirm that the below-defined impulse functions are indeed classified into white and colored noise processes.

2.4.1 Heaviside Impulse Function

By defining $h(t) = \Theta(t)$, the covariance of ξ simply becomes

$$\begin{aligned}\left\langle \xi_{t_1} \xi_{t_2} \right\rangle &= \lambda \left\langle A_1^2 \right\rangle \int_0^\infty \mathrm{d}\tau\, \Theta(t_1 - \tau)\Theta(t_1 - \tau) \cdot \Theta(t_2 - \tau)\Theta(t_2 - \tau) \\ &= \lambda \left\langle A_1^2 \right\rangle \int_0^\infty \mathrm{d}\tau\, \Theta(t_1 - \tau)\Theta(t_2 - \tau) \\ &= \lambda \left\langle A_1^2 \right\rangle \min\{t_1, t_2\}.\end{aligned} \tag{2.4.1}$$

As we established, this is indeed a Markovian noise process; in fact, it is the Compound Poisson process. This can also be visualized in the simulation in Figure 2.8 below. Furthermore, applying Lemma 1.3.1, we get that the covariance of the derivative of ξ is delta-correlated as expected:

$$\begin{aligned}\left\langle \dot{\xi}_{t_1} \dot{\xi}_{t_2} \right\rangle &= \lambda \left\langle A_1^2 \right\rangle \int_0^\infty \frac{\mathrm{d}\Theta(t_1 - \tau)}{\mathrm{d}t_1} \cdot \frac{\mathrm{d}\Theta(t_2 - \tau)}{\mathrm{d}t_2} \\ &= \lambda \left\langle A_1^2 \right\rangle \int_0^\infty \mathrm{d}\tau\, \delta(t_1 - \tau)\delta(t_2 - \tau) \\ &= \lambda \left\langle A_1^2 \right\rangle \delta(t_1 - t_2).\end{aligned} \tag{2.4.2}$$

2.4.2 Rectangular Impulse Function

For more mathematical rigour, note that one can rewrite the rectangular function $\mathrm{rect}(t; a, b)$ in terms of Heaviside functions as $\mathrm{rect}(t; a, b) = (b - a)^{-1} \left(\Theta(t - a) - \Theta(t - b)\right)$. Then, upon applying this definition to the covariance of ξ, we can see that ξ is indeed not delta correlated, i.e. not

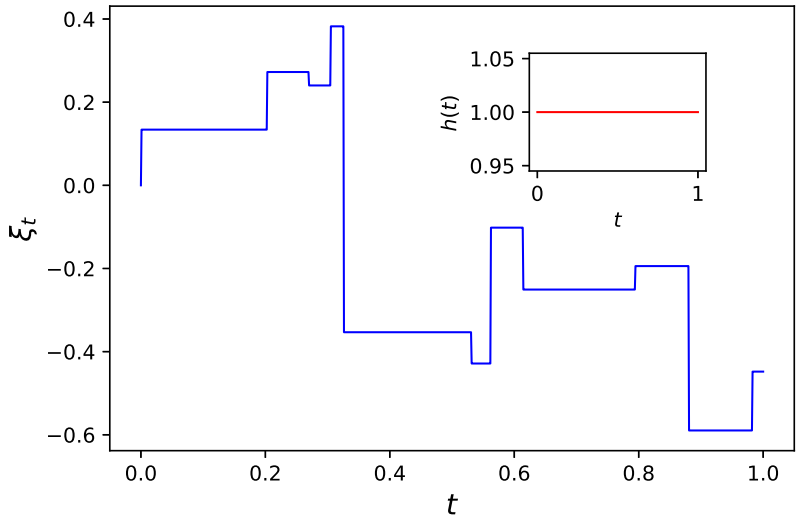

Figure 2.8: Simulating the GSN process with Heaviside impulse function $h(t) = \Theta(t)$, i.e. the Compound Poisson process. The inset is the plot of the impulse function. We used $\lambda = 10$ and $A_i \sim \mathcal{N}(0, \lambda^{-1})$ for our simulation.

white:

$$\begin{aligned}\left\langle \xi_{t_1} \xi_{t_2} \right\rangle = &\frac{\lambda \left\langle A_1^2 \right\rangle}{b-a} \int_0^\infty \mathrm{d}\tau \, \Theta(t_1 - \tau)\Theta(t_2 - \tau) \cdot \\ &\cdot \left(\Theta(t_1 - \tau - a) - \Theta(t_1 - \tau - b)\right) \left(\Theta(t_2 - \tau - a) - \Theta(t_2 - \tau - b)\right), \end{aligned} \tag{2.4.3}$$

Interestingly, the covariance function of ξ resembles that of the Compound Poisson process as in Equation (1.3.18); however, the time delay by coefficients a and b contribute to the colored and non-Markovian nature of ξ. This can also be visualized in Figure 2.9, where we simulated the GSN process ξ with $\mathrm{rect}(t; a = -1/2, b = 1/2)$ as impulse function.

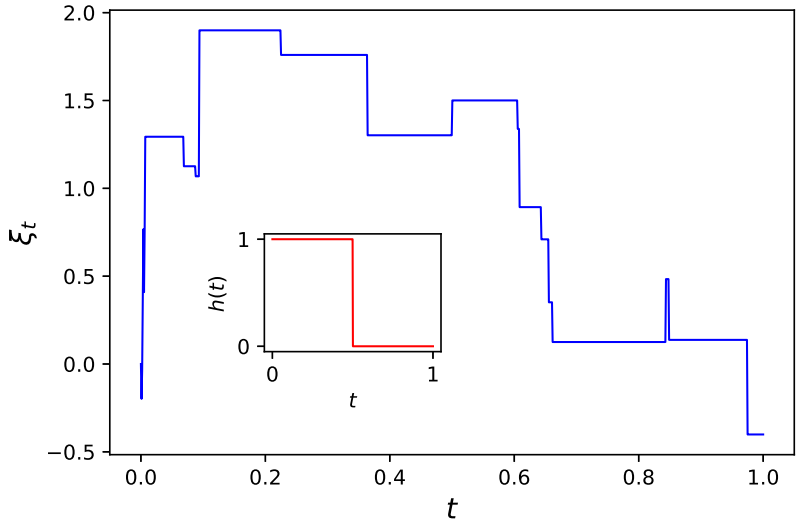

Figure 2.9: Simulating the GSN process with Rectangular impulse function $h(t) = \text{rect}(t; a = -1/2, b = 1/2)$. Notice its close resemblance to the Compound Poisson (Markov) process as in Figure 2.8. The inset is the plot of the impulse function. We used $\lambda = 10$ and $A_i \sim \mathcal{N}(0, \lambda^{-1})$ for our simulation.

2.4.3 Exponentially Decaying Impulse Function

Recall that the exponentially decaying impulse function is defined by $h(t) = \alpha e^{-\alpha t}$, where $\alpha > 0$ is the rate of decay. The covariance of ξ is given by:

$$\begin{aligned}
\left\langle \xi_{t_1} \xi_{t_2} \right\rangle &= \lambda \left\langle A_1^2 \right\rangle \int_0^\infty \mathrm{d}\tau \, \Theta(t_1 - \tau)\Theta(t_2 - \tau)\alpha^2 e^{-\alpha(t_1-\tau)} e^{-\alpha(t_2-\tau)} \\
&= \lambda \left\langle A_1^2 \right\rangle \alpha^2 e^{-\alpha(t_1+t_2)} \int_0^\infty \mathrm{d}\tau \, \Theta(t_1 - \tau)\Theta(t_2 - \tau) e^{2\alpha\tau} \\
&= \lambda \left\langle A_1^2 \right\rangle \alpha^2 e^{-\alpha(t_1+t_2)} \int_0^{t_1 \wedge t_2} \mathrm{d}\tau \, e^{2\alpha\tau} \\
&= \lambda \left\langle A_1^2 \right\rangle \alpha^2 e^{-\alpha(t_1+t_2)} \frac{e^{2\alpha(t_1 \wedge t_2)} - 1}{2\alpha} \\
&= \lambda \left\langle A_1^2 \right\rangle \frac{\alpha}{2} \left(e^{-\alpha|t_1 - t_2|} - e^{-\alpha(t_1+t_2)} \right).
\end{aligned} \tag{2.4.4}$$

Notice that the covariance of the GSN process ξ in this case is exactly the covariance of the GenOU process X defined in Equation (1.4.2): $\dot{X}_t = -\alpha X_t + \alpha \dot{L}_t$, where in this instance the constants are $\gamma = \sigma = \alpha$. This is the fundamental outcome of the exponentially decaying impulse function. Due to fact that the GenOU process is very well defined, there is extensive research on colored noises driven by this particular impulse function[75 87 97]. In more detail, this correspondence is due to the hierarchical nature of the GSN process ξ *per se*, on which we will focus extensively in later chapters. For visualization, we have given a simulation of the GSN process in Figure 2.10 below.

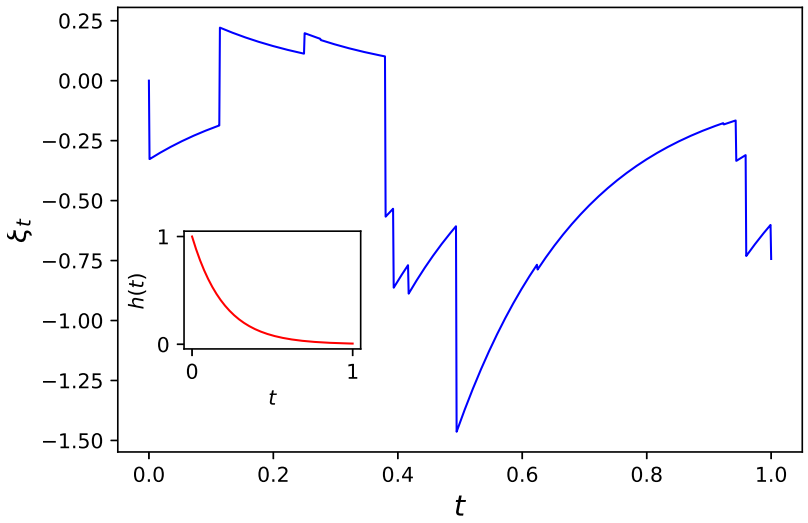

Figure 2.10: Realization of the GSN process ξ with exponentially decaying impulse function $h(t) = \alpha e^{-\alpha t}$. The inset is the plot of the impulse function. We used $\alpha = 2, \lambda = 10$ and $A_i \sim \mathcal{N}(0, \lambda^{-1})$ for simulating the realization.

2.4.4 Damped and Oscillating Impulse Function

As explained in previous section, one can relax the strictly decaying condition of the impulse function by introducing oscillation. Recalling our damped oscillating impulse function

$$h(t) = \frac{\alpha^2+\beta^2}{\alpha+\beta} e^{-\alpha t} \left(\sin \beta t + \cos \beta t\right), \tag{2.4.5}$$

where $\alpha, \beta > 0$. Therefore, the covariance function of ξ driven by this impulse function is given by:

$$\begin{aligned}
&\left\langle \xi_{t_1} \xi_{t_2} \right\rangle \\
&= \left(\frac{\alpha^2+\beta^2}{\alpha+\beta}\right)^2 e^{-\alpha(t_1+t_2)} \int_0^\infty \mathrm{d}\tau\, \Theta(t_1-\tau)\Theta(t_2-\tau) e^{2\alpha\tau} \left[\sin\beta\left(t_1-\tau\right) + \cos\beta\left(t_1-\tau\right)\right] \cdot \\
&\qquad\qquad \cdot \left[\sin\beta\left(t_2-\tau\right) + \cos\beta\left(t_2-\tau\right)\right] \\
&= \left(\frac{\alpha^2+\beta^2}{\alpha+\beta}\right)^2 e^{-\alpha(t_1+t_2)} \int_0^{t_1\wedge t_2} \mathrm{d}\tau\, e^{2\alpha\tau} \left[\sin\beta\left(t_1-\tau\right) + \cos\beta\left(t_1-\tau\right)\right] \left[\sin\beta\left(t_2-\tau\right) + \cos\beta\left(t_2-\tau\right)\right] \\
&= \frac{\alpha^2+\beta^2}{2\alpha\left(\alpha+\beta\right)^2} \Bigg[\left(\alpha^2+\beta^2\right)\left(e^{-\alpha|t_1-t_2|} - e^{\alpha(t_1+t_2)}\right)\cos\beta\left|t_1-t_2\right| - \alpha\left(\beta\cos\beta\left(t_1+t_2\right) + \alpha\sin\beta\left(t_1+t_2\right)\right) \\
&\qquad\qquad + \alpha e^{-\alpha|t_1-t_2|}\left(\beta\cos\beta\left|t_1-t_2\right| + \alpha\sin\beta\left|t_1-t_2\right|\right) \Bigg]
\end{aligned} \tag{2.4.6}$$

By directly checking their covariance, we can be certain that the noise process ξ is indeed colored, with simulation given in Figure 2.11 below.

Our last example will be to define another smooth yet non-decaying impulse function: the sigmoid kernel.

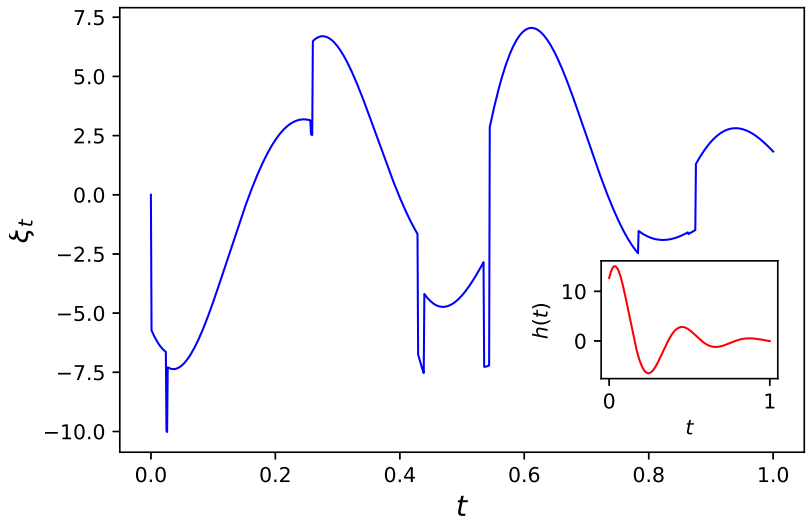

Figure 2.11: Realization of the GSN process ξ with damped and oscillating impulse function $h(t) = \left(\alpha^2 + \beta^2\right) / (\alpha + \beta)\, e^{-\alpha t} (\sin \beta t + \cos \beta t)$. The inset is the plot of the impulse function, where we chose a large β to promote oscillation within this time range. We used $\alpha = 4, \beta = 15, \lambda = 10$ and $A_i \sim \mathcal{N}(0, \lambda^{-1})$ for simulating the realization.

2.4.5 Sigmoid Impulse Function

The sigmoid function is defined by:

$$h(t) = \frac{e^{\alpha t}}{1 + e^{\alpha t}}. \tag{2.4.7}$$

As detailed in Section 2.2, the sigmoid function is an important tool to approximate the Heaviside step function in continuous form. Let's see how the covariance of ξ behaves with this impulse function:

$$\begin{aligned}
\left\langle \xi_{t_1} \xi_{t_2} \right\rangle &= e^{\alpha(t_1+t_2)} \int_0^\infty \mathrm{d}\tau\, \Theta(t_1 - \tau)\Theta(t_2 - \tau) \frac{e^{-2\alpha\tau}}{\left(1 + e^{\alpha(t_1-\tau)}\right)\left(1 + e^{\alpha(t_2-\tau)}\right)} \\
&= e^{\alpha(t_1+t_2)} \int_0^{t_1 \wedge t_2} \mathrm{d}\tau\, \frac{e^{-2\alpha\tau}}{\left(1 + e^{\alpha(t_1-\tau)}\right)\left(1 + e^{\alpha(t_2-\tau)}\right)} \\
&= \frac{1}{\alpha\left(e^{\alpha t_1} - e^{\alpha t_2}\right)} \Big[- e^{\alpha t_2} \left(\ln\left(1 + e^{\alpha t_1}\right) - \ln\left(e^{\alpha t_1} + e^{\alpha(t_1 \wedge t_2)}\right) + \alpha\left(t_1 \wedge t_2\right) \right) \\
&\qquad + e^{\alpha t_1} \left(\ln\left(1 + e^{\alpha t_2}\right) - \ln\left(e^{\alpha t_2} + e^{\alpha(t_1 \wedge t_2)}\right) + \alpha\left(t_1 \wedge t_2\right) \right) \Big]
\end{aligned} \tag{2.4.8}$$

The resulting covariance is clearly not delta-correlated, hence ξ is indeed a colored noise. The simulation of ξ together with the impulse function embedded is given in Figure 2.12.

Next, we will outline 3 broad classifications of impulse functions that will be useful in further analyzing the GSN process in Chapter 3 and finding the solutions for the optimal paths of the position process X in Chapter 4.

2.5 Classification of Impulse Functions

Throughout this chapter, we have deeply analyzed how the impulse function directly changes the behavior of the GSN process. In this section, we will categorize the impulse functions into 3 major groups: left-tailed, right-tailed and hierarchical.

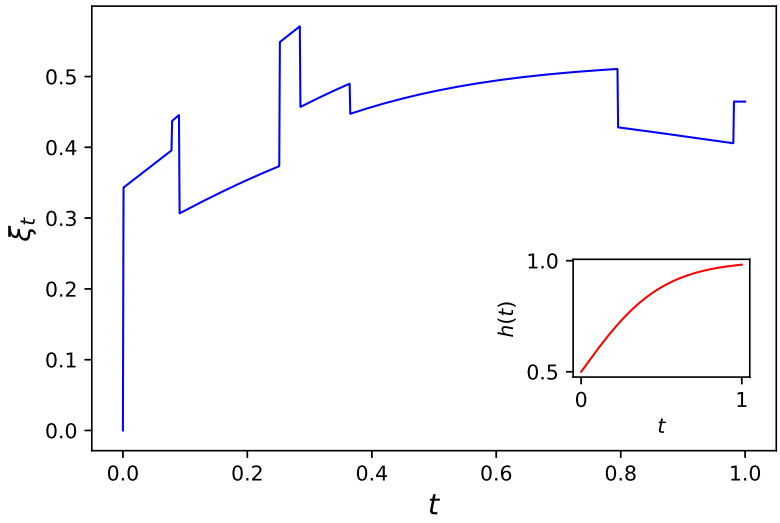

Figure 2.12: Realization of the GSN process ξ with sigmoid impulse function $h(t) = e^{\alpha t} / (1 + e^{\alpha t})$. The inset is the plot of the impulse function. We used $\alpha = 4$, $\lambda = 10$ and $A_i \sim \mathcal{N}(0, \lambda^{-1})$ for our simulating the realization.

2.5.1 Left-Tailed Impulse Functions

The *left tailed impulse functions* are, as the name suggests, asymptotically zero from their left tails. In more mathematical rigor, a impulse function h is left-tailed if $\lim_{t \to 0} h(t) = 0$. From our candidate impulse functions, the Heaviside step function and the sigmoid function are examples of left-tailed kernels.

2.5.2 Right-Tailed Impulse Functions

The *right-tailed impulse functions* are, on contrast, asymptotically zero from their right tails, i.e. $\lim_{t \to \infty} h(t) = 0$. In this case, candidate impulse functions such as the exponential decay function and the damped and oscillating function are examples of right-tailed impulse functions.

As we haven't categorized any asymptotics on their right tail, left-tailed impulse functions are not integrable through time; examples include the Heaviside step function and the sigmoid function,

where both of their integrals diverge at infinity.

On the contrary, right-tailed impulse functions can be globally integrable through time if they are bounded everywhere on $[0, \infty[$. Therefore, both exponential decay function and the damped and oscillating function are integrable impulse functions; a counterexample could be a power law decay impulse function, $h(t) = t^{-a}$ for $a > 0$, where it is a right-tailed but not integrable on $[0, \infty[$ due to singularity at $t = 0$.

Both globally integrable and globally not integrable impulse functions give rise to very interesting asymptotic properties of the GSN process. We will go through them in detail in Chapter 3.

Lastly, we identify the third and highly important class of impulse functions.

2.5.3 n-th Hierarchy Impulse Functions

This third class of impulse functions can be simply defined as *any* impulse function h that obeys a *linear* and *homogeneous* n-th order ODE; i.e., with suitable initial conditions, any function h that is a unique solution of the IVP:

$$\sum_{i=0}^{n} c_i h^{(i)}(t) = 0, \quad h^{(i)}(0) = a_i \tag{2.5.1}$$

is an n-th hierarchy impulse function, where $h^{(i)}$ is the $i-$th time derivative of h, $c_i \in \mathbb{R}$ are constant coefficients and $a_i \in \mathbb{R}$ are suitable initial conditions.

For example, from our candidate impulse functions, the exponentially decaying function, $h(x) = \alpha e^{-\alpha x}$ is a first hierarchy impulse function, as it is the solution of the first order linear homogeneous ODE: $\dot{h}(t) + \alpha h(t) = 0$ with initial condition $h(0) = \alpha$.

Furthermore, the damped oscillating function,

$$h(t) = \frac{\alpha^2 + \beta^2}{\alpha + \beta} e^{-\alpha t} \left(\sin \beta t + \cos \beta t\right), \tag{2.5.2}$$

is a 2nd hierarchy impulse function. By the unique solution, the characteristic roots of the ODE are $r = \alpha \pm \beta i$. This implies that the characteristic equation of the ODE is of the form:

$$(r - \alpha - \beta i)(r - \alpha + \beta i) = (r - \alpha)^2 + \beta^2 = r^2 - 2\alpha r + \alpha^2 + \beta^2 = 0. \tag{2.5.3}$$

Therefore the resulting linear homogeneous initial value problem becomes:

$$h''(t) - 2\alpha h'(t) + \left(\alpha^2 + \beta^2\right) h(t) = 0, \quad h(0) = 1,\ h'(0) = \beta - \alpha. \tag{2.5.4}$$

The n-th hierarchy impulse functions will be highly useful to find the Markovian correspondence of the Langevin equations due to the hierarchical nature of the corresponding GSN processes ξ.

Now that we showed how the impulse function affects the color of the noise process ξ, we can now focus on finding the characteristics of the position process X driven by the LE as in Equation (1.4.1).

2.6 Characteristics of the Position Process Driven by the Langevin Equation

In this section, we now apply our knowledge of the GSN process to the LE as in Equation (1.4.1).

First and foremost, the potential V plays an important role in finding the CFal of X from ξ. In detail, if we were to assume the LE is, in fact, an ordinary differential equation, i.e. $\dot{x}(t) = -V'(x(t)) + f(t)$ for some function f, then we observe that the resulting ODE for $\dot{x}$ is nonlinear unless the function V is parabolic, where it can be solved easily under suitable initial condition.

This is exactly the case for an interesting article by Caceres & Budini in 1997[99]. In their paper, the authors postulate that the CFal relationship between X and ξ can only be found in closed form solution if the potential V is harmonic, i.e. $V(x) = \gamma x^2/2$ for some positive γ. Under this condi-

tion, the authors have proven in Equation (2.3) of their paper[99] that given the LE with harmonic potential, i.e. $\dot{X}_t = -\gamma X_t + \xi_t$, the following relationship exists between the CFals of X and ξ:

$$\Phi_X[g] = \Phi_\xi \left[e^{\gamma t} \int_t^\infty \mathrm{d}s\, g(s) e^{-\gamma s} \right]. \tag{2.6.1}$$

Due to its similarity in the definition of the [Markovian] OU process, we will call the solution of the LE $\dot{X}_t = -\gamma X_t + \xi_t$ with GSN ξ the *Non-Markovian Ornstein-Uhlenbeck Process*.

Therefore, plugging the inner test function of Φ_ξ in Equation (2.6.1) to its definition in Equation (2.3.7) yields the CFal of X for any impulse function h under harmonic potential:

$$\Phi_X[g] = \exp\left[\lambda \int_0^\infty \mathrm{d}\tau \left(\phi_{A_1} \left(\int_\tau^\infty \mathrm{d}t\, h(t-\tau) e^{\gamma t} \int_t^\infty \mathrm{d}s\, e^{-\gamma s} g(s) \right) - 1 \right) \right]. \tag{2.6.2}$$

From Equation (2.6.2), one can retrieve the autocovariances of X by taking the variational derivative twice:

$$\begin{aligned}
\frac{\delta^2 \Phi_X[g]}{\delta g(t_1)\delta g(t_2)} &= \frac{\delta}{\delta g(t_2)} \left\{ \lambda \int_0^\infty \mathrm{d}\tau \int_\tau^\infty \mathrm{d}t\, h(t-\tau) e^{\gamma t} \int_\tau^\infty \mathrm{d}s\, e^{-\gamma s} \delta(s-t_1) \cdot \right. \\
&\qquad \left. \cdot \phi'_{A_1} \left(\int_\tau^\infty \mathrm{d}t\, h(t-\tau) e^{\gamma t} \int_t^\infty \mathrm{d}s\, e^{-\gamma s} g(s) \right) \Phi_X[g] \right\} \\
&= e^{-\gamma t_1} \frac{\delta}{\delta g(t_2)} \left\{ \lambda \int_0^\infty \mathrm{d}\tau\, \Theta(t_1-\tau) \int_\tau^{t_1} \mathrm{d}t\, h(t-\tau) e^{\gamma t} \cdot \right. \\
&\qquad \left. \cdot \phi'_{A_1} \left(\int_\tau^\infty \mathrm{d}t\, h(t-\tau) e^{\gamma t} \int_t^\infty \mathrm{d}s\, e^{-\gamma s} g(s) \right) \Phi_X[g] \right\} \\
&= e^{-\gamma(t_1+t_2)} \left\{ \lambda \int_0^\infty \mathrm{d}\tau\, \Theta(t_1-\tau)\Theta(t_2-\tau) \left(\int_\tau^{t_1} \mathrm{d}t\, h(t-\tau) e^{\gamma t} \right) \left(\int_\tau^{t_2} \mathrm{d}t\, h(t-\tau) e^{\gamma t} \right) \right. \\
&\qquad \left. \cdot \phi''_{A_1} \left(\int_\tau^\infty \mathrm{d}t\, h(t-\tau) e^{\gamma t} \int_t^\infty \mathrm{d}s\, e^{-\gamma s} g(s) \right) \Phi_X[g] \right\} + \frac{\partial \Phi_X[g]}{\partial g(t_1)} \frac{\partial \Phi_X[g]}{\partial g(t_2)},
\end{aligned} \tag{2.6.3}$$

Therefore, by Equation (1.1.7) the autocovariance of X is given by:

$$\langle X_{t_1} X_{t_2} \rangle = \lambda \left\langle A_1^2 \right\rangle e^{-\gamma(t_1+t_2)} \int_0^\infty \mathrm{d}\tau\, \Theta(t_1-\tau)\Theta(t_2-\tau) \left(\int_\tau^{t_1} \mathrm{d}t\, h(t-\tau) e^{\gamma t} \right) \left(\int_\tau^{t_2} \mathrm{d}t\, h(t-\tau) e^{\gamma t} \right). \tag{2.6.4}$$

Evidently, defining $g(t) = \theta\delta(T-t)$ and plugging in to the CFal of X in Equation (2.6.2) will yield $\phi_X(\theta, T)$, the CF of X at time T:

$$\begin{aligned}
\phi_X(\theta, T) &= \exp\left[\lambda \int_0^\infty \mathrm{d}\tau \left(\phi_{A_1} \left(\theta \int_\tau^\infty \mathrm{d}t\, h(t-\tau) e^{\gamma t} \int_t^\infty \mathrm{d}s\, \delta(T-s) e^{-\gamma s} \right) - 1 \right) \right] \\
&= \exp\left[\lambda \int_0^\infty \mathrm{d}\tau \left(\phi_{A_1} \left(\theta \int_\tau^\infty \mathrm{d}t\, h(t-\tau) e^{\gamma t} \Theta(T-t) e^{-\gamma T} \right) - 1 \right) \right] \\
&= \exp\left[\lambda \int_0^\infty \mathrm{d}\tau \left(\phi_{A_1} \left(\theta\, \Theta(T-\tau) \int_\tau^T \mathrm{d}t\, h(t-\tau) e^{\gamma(t-T)} \right) - 1 \right) \right] \\
&= \exp\left[\lambda \int_0^T \mathrm{d}\tau\, \phi_{A_1} \left(\theta \int_\tau^T \mathrm{d}t\, h(t-\tau) e^{\gamma(t-T)} \right) - \lambda T \right].
\end{aligned} \tag{2.6.5}$$

Lastly, one can take the Inverse Fourier Transform (IFT) of ϕ_X to get the PDF of the position process, denoted by $\mathbb{P}_X$, either analytically or numerically, depending on the selected impulse function h as well as distribution of iid jump amplitudes A_1:

$$\mathbb{P}_X(x, T) = \frac{1}{2\pi} \int_{-\infty}^\infty \mathrm{d}\omega\, e^{-i\omega x} \phi_X(\omega, T). \tag{2.6.6}$$

Now that the PDF of X can be found via its CF, we now simulate the LE of X via harmonic potential, where various candidate impulse functions for the GSN process ξ will be used.

The simulation results for 4 candidate impulse functions for the GSN process ξ driving the harmonic LE $\dot{X}_t = -\gamma X_t + \xi_t$:

1. Dirac Delta: $h(t) = \delta(t)$;

2. Exponential decay: $h(t) = \alpha e^{-\alpha t}$;

3. Damped oscillator: $h(t) = \left(\alpha^2 + \beta^2\right) / \left(\alpha + \beta\right) e^{-\alpha t} \left(\sin \beta t + \cos \beta t\right)$;

4. Sigmoid: $h(t) = e^{\alpha t} / \left(1 + e^{\alpha t}\right)$.

The first function is used as a control, as the resulting position process X is the GenOU process which is Markovian and widely analyzed. The second and third functions are respectively classified as first and second hierarchy and right-tailed impulse functions, as detailed in Section 2.5. The first candidate is a left-tailed non-integrable impulse function. The numerical solution of PDF derived by the IFT of the CF of X as given in Equation (2.6.5) is plotted against the simulations obtained by Monte Carlo in Figure 2.13 and Figure 2.14 in logarithmic scale. The results indicate some inter-

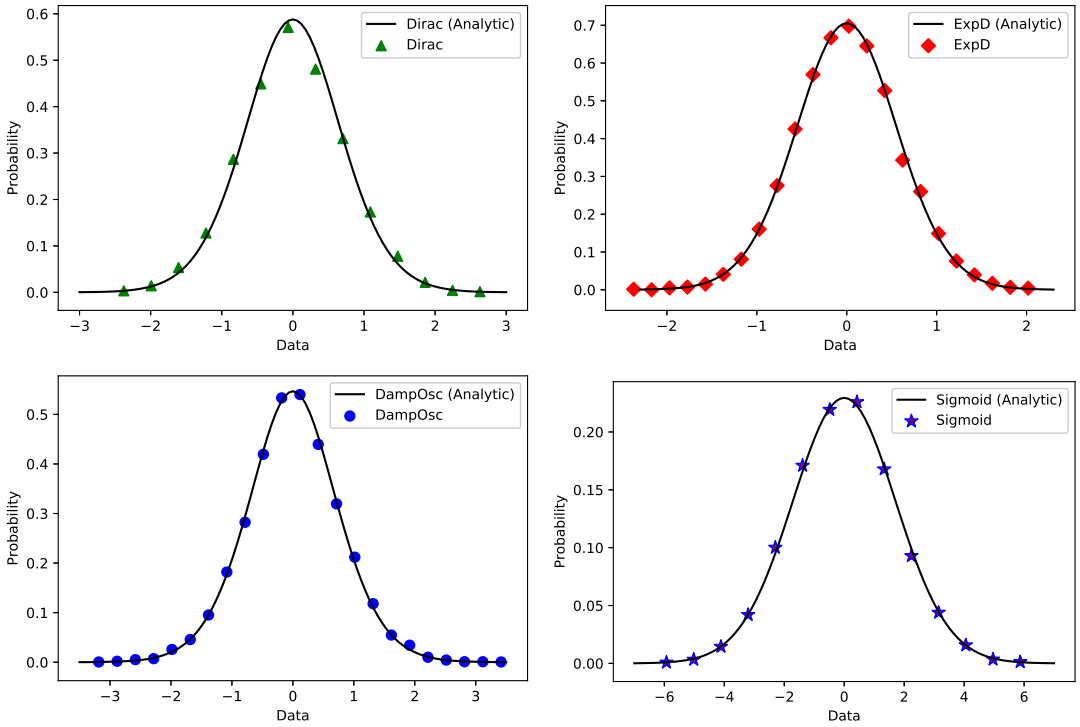

Figure 2.13: Plots of the PDF of X_t at $t = 5$. Scatter plots are simulations obtained by Monte Carlo method with 7,000 iterations and the resulting histogram is split into 23 equal bins. Lines are results obtained numerically via IFT of the CF with Dirac Delta (Delta) (where X becomes the GenOU process), exponentially decaying (ExpD), damped oscillatory (DampOsc) and Sigmoid impulse functions. We used $\alpha = 2, \beta = 5, \lambda = 10, A_i \sim \mathcal{N}(0, \lambda^{-1})$ and $\gamma = 1$ for calculating the PDF's.

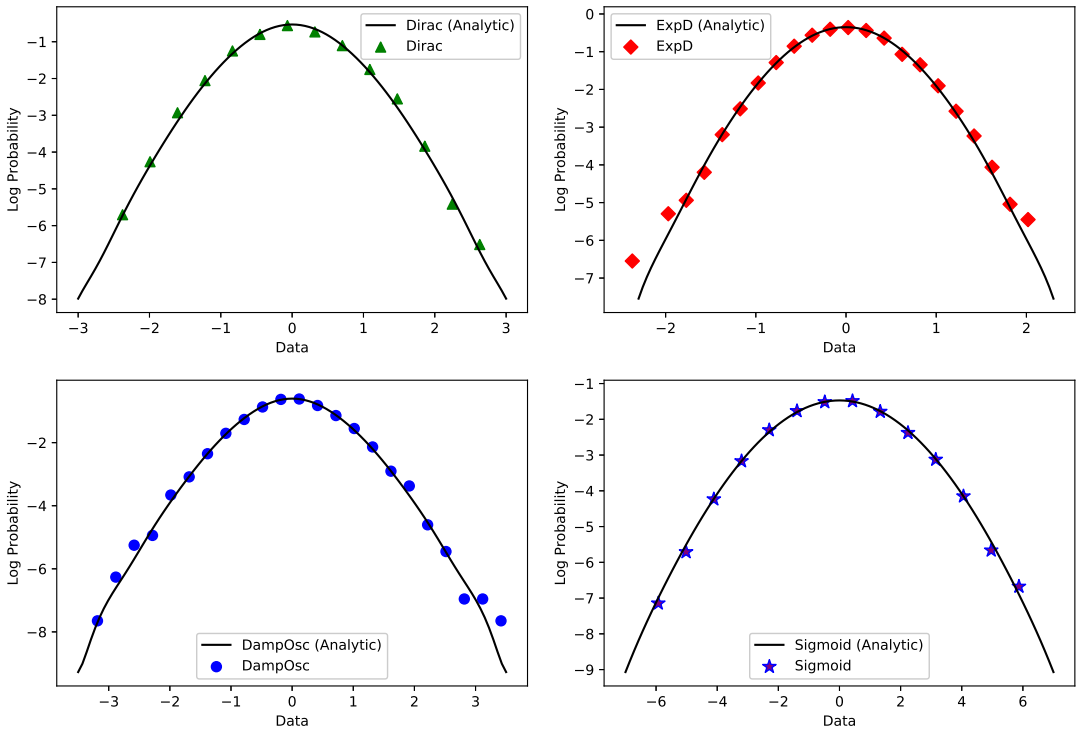

Figure 2.14: Plots of the log-scale PDF of X_t at $t = 5$. Scatter plots are simulations obtained by Monte Carlo method with 7,000 iterations and the resulting histogram is split into 23 equal bins. Lines are analytic results obtained numerically via IFT of the CF with Dirac Delta (Delta) (where X becomes the GenOU process), exponentially decaying (ExpD), damped oscillatory (DampOsc) and Sigmoid impulse functions. We used $\alpha = 2, \beta = 5, \lambda = 10, A_i \sim \mathcal{N}(0, \lambda^{-1})$ and $\gamma = 1$ for calculating the PDF's.

esting behaviors of the position process X. First and foremost, the rate of diffusion varies greatly for different impulse functions and their coefficients. We observe that the GenOU has faster diffusion than both ExpD and DampOsc cases; however, the Sigmoid function greatly took over the diffusion rate, where we observe a larger sample space of probabilities.

Although the diffusion rates can be compromised between the ExpD, DampOsc and GenOU cases by perturbing their coefficients, it is evident that the left-tailed impulse functions have a higher span of diffusion.

We can further witness this diffusive behavior by taking a look at their Mean Squared Displacements (MSD). The MSD of a s.p. X is simply given by its autocovariance in Equation (2.6.4):

$$\begin{aligned} MSD(t) &= \left\langle X_t^2 \right\rangle = \langle X_{t_1} X_{t_2} \rangle \mid_{t_1=t_2=t} \\ &= \lambda \left\langle A_1^2 \right\rangle e^{-2\gamma t} \int_0^t \mathrm{d}\tau \left(\int_\tau^t \mathrm{d}s \, h(s-\tau) e^{\gamma s} \right)^2 \end{aligned} \tag{2.6.7}$$

By computing its MSD, a s.p. X is said to be:

- sub-diffusive if $MSD(t) \propto t^a$ for $0 < a < 1$.
- diffusive if $MSD(t) \propto t$
- superdiffusive if $MSD(t) \propto t^a$ for $a > 1$.

The GenOU process is widely known to be sub-diffusive; this can be easily verified by its autocovariance in Equation (1.4.4) (also subsequently in Equation (2.4.4)). Again using the GenOU process as control, we observe that the resulting MSD's of X driven by colored noise show an interchange between different diffusive behaviors. The position process X under ExpD and DampOsc impulse functions start off as super-diffusive, but later switch to sub-diffusion. On the other hand, the position process X under Sigmoid impulse function starts off as super-diffusive, then later switches

to normal diffusion. This change of behaviors can be visualized in Figure 2.15, where we split the figure into 2 plots to better see the change in diffusion behavior.

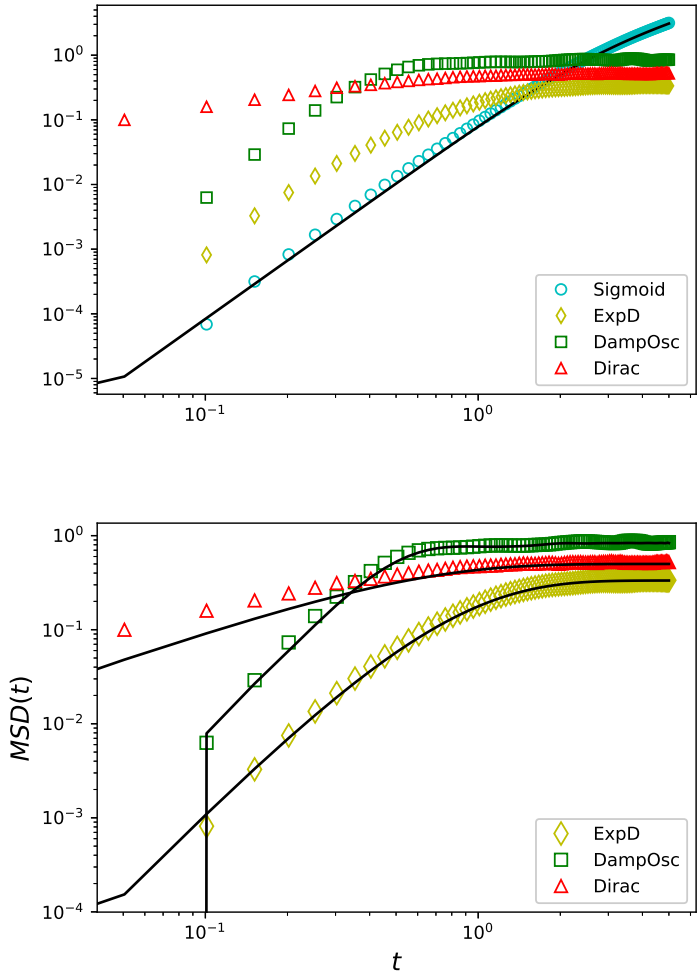

Figure 2.15: Logarithmic plot of the MSD simulations of the position process X as the solution of $\dot{X}_t = -\gamma X_t + \xi_t$, where ξ is the GSN process with Dirac Delta (Delta) (where X becomes the GenOU process), exponentially decaying (ExpD), damped oscillatory (DampOsc) and Sigmoid impulse functions. The black curves in the bottom plot are analytic solutions of the MSD's via Equation (2.6.4) that fit the simulations. We used $\alpha = 2, \beta = 5, \lambda = 10, A_t \sim \mathcal{N}(0, \lambda^{-1})$ and $\gamma = 1$ for the simulations.

2.7 Chapter Review

In this chapter, we have defined the GSN process in detail, where we focused on how the impulse function generates memory *per se* and yields either white or colored noise processes. We also established that different candidate functions cause a wide range of interesting behaviors, such as the change in diffusion behavior for the position process X

We note that due to the non-linear nature governing the LE, any potential V other than the harmonic potential is next to impossible to solve via this CFal correspondence approach. The linear correspondence between X and ξ is necessary to obtain the CFal of X (hence V has to be quadratic), from which the PDF can be extracted via IFT. Higher-order V's are currently impossible to solve analytically; in order to find the CFal of X under, say, double-well potential (hence V is a polynomial of order 4), one first has to analytically solve Abel's equation of the first kind to find the CFal relationship. Although there are extensive attempts to solve Abel's equation of the first kind (cf.[98]), this is still one of the most prominent open questions in mathematics.

However, there are some other intricate methods to find the PDF of the position process X: via the Master Equation or the Path Integral approach.

Particularly in the next chapter, we would like to point out one of our most important outcomes, where we will use two methods to find the Master Equation of the LE. The first outcome will be the somewhat standardized method to find Master Equations, the Ito's approach[68]. The second one will be the non-Markovian way to find Master Equations provided by Hanggi[74].

What is mathematics? It is only a systematic effort of solving puzzles posed by nature.

Shakuntala Devi

3

Further Results on the GSN process

This chapter of our thesis will consist of our new findings on the GSN process, where we will use the definitions and properties mentioned in the previous chapters of our thesis to establish the recursive nature of the GSN process with respect to its time derivative, which is colored depending on the nature of h as outlined in Section 2.5. This property of the GSN process will be a very useful tool to find the optimal path and action of the position processes.

Next, we will derive the time evolution equation (aka Master Equation (ME)) of the position process X driven via the LE entailed in Equation (0.0.2). As defined in our Chapter 1 of our thesis, the Master Equation is another useful method of finding the PDF of X,the other being the CFal method as detailed in Chapter 2.

We will then end this chapter by deriving the asymptotic and limiting distributions of the GSN process and show that under certain conditions, the GSN process converges to either white noise processes, non-Markovian Gaussian processes, or general Markov processes. This convergence to a wide array of classes of stochastic processes shows the fundamental and relaxed properties and vast potential applications of the GSN process.

3.1 Time Derivative and Hierarchical Nature of the GSN Process

Recall from Equation (0.0.2) that we have trying to solve the following dynamical system:

$$\begin{aligned} \frac{\mathrm{d}X_t}{\mathrm{d}t} &= -V'(X_t) + \xi_t, \\ \xi_t &:= \sum_{i=1}^{N_t} A_i h(t - T_i), \end{aligned} \tag{3.1.1}$$

with potential V and impulse function h. Depending on the class of impulse functions, the GSN process ξ exhibits a mixture of continuous and discontinuous processes.

We will aim to show this using the time derivative of ξ_t [i]. In general sense, the time derivative of ξ

[i] Although the time derivative of stochastic processes is not well-defined[62], we will instead outline it using Itō's framework, where for any s.p. X where $X_0 = 0$ a.s., one can write the following integral representation of its time derivative:

$$X_t = \int_0^t \mathrm{d}X_\tau = \int_0^t \mathrm{d}\tau \, \frac{\mathrm{d}X_\tau}{\mathrm{d}\tau} = \int_0^t \mathrm{d}\tau \, \dot{X}_\tau \tag{3.1.2}$$

forms another s.p. $\dot{\xi}$, where each of its realizations $\dot{\xi}_t$ is defined by:

$$\dot{\xi}_t := \lim_{s \to 0} \frac{1}{s} \left(\xi_{t+s} - \xi_t \right). \tag{3.1.3}$$

By the $\mathbb{P}$-additivity of the Poisson process, we can indeed find the sole form solution as follows:

$$\begin{aligned}
\dot{\xi}_t = \frac{\mathrm{d}\xi_t}{\mathrm{d}t} &= \lim_{s \to 0} \left(\sum_{i=1}^{N_t-} A_i \frac{h(t+s-T_i) - h(t-T_i)}{s} + \frac{1}{s} \sum_{i=N_t-+1}^{N_{t+s}} A_i h(t+s-T_i) \right) \\
&= \sum_{i=1}^{N_t-} A_i \dot{h}\left(t - T_i\right) + \lim_{s \to 0} \frac{1}{s} \sum_{i=1}^{N_{t+s}-N_t-} A_{i+N_t-} h\left(t+s-T_{i+N_t-}\right) \\
&= \sum_{i=1}^{N_t-} A_i \dot{h}\left(t - T_i\right) + A_{N_t-} h\left(t - T_{N_t-}\right) \frac{\mathrm{d}N_t}{\mathrm{d}t} \\
&= \sum_{i=1}^{N_t-} A_i \dot{h}\left(t - T_i\right) + A_{N_t-} h\left(0\right) \frac{\mathrm{d}N_t}{\mathrm{d}t},
\end{aligned} \tag{3.1.4}$$

as in the last step, since $\{T_i\}$ are arrival times, which are *ordered* collection of random variables, we have that $t = T_{N_t}$ almost surely. This results in $h\left(t - T_{N_t}\right) = h(0)$ almost surely.

We can also rewrite $\dot{\xi}_t$ in SDE form by multiplying both sides by $\mathrm{d}t$,

$$\mathrm{d}\xi_t = \sum_{i=1}^{N_t-} A_i \dot{h}(t - T_i)\, \mathrm{d}t + A_{N_t-} h\left(0\right) \mathrm{d}N_t. \tag{3.1.5}$$

If h is not differentiable, then the SDE of ξ will instead be of the following form:

$$\mathrm{d}\xi_t = \sum_{i=1}^{N_t-} A_i\, \mathrm{d}h(t - T_i) + A_{N_t-} h\left(0\right) \mathrm{d}N_t. \tag{3.1.6}$$

The differentiability of h plays a key role in defining the jump size of ξ_t. For general kernel function

h with discontinuities, the jump size is defined by:

$$\Delta\xi_t = \sum_{i=1}^{N_{t-}} A_i \Delta h(t - T_i) + A_{N_{t-}} h(0)\, \Delta N_t. \tag{3.1.7}$$

Notice that the summation term containing Δh vanishes if h is differentiable, yielding $\Delta\xi_t = A_{N_{t-}} h(0)\, \Delta N_t$, the jump size of the Compound Poisson process as in Definition 1.2.2 multiplied by $h(0)$.

Therefore, we can draw two conclusions on the behavior of ξ_t: if h is differentiable at least once, then

1. The SDE governing ξ_t as in (3.1.5) will have a purely continuous drift term, and a càdlàg [ii] jump term;
2. The jump size of the GSN process $\Delta\xi_t$ depends only on the [Markovian] Compound Poisson jump size $A_{N_{t-}}\, \Delta N_t$ and is independent from the path of ξ_t.

Throughout this thesis, we will assume that the impulse function h is differentiable, or in its broadest term, its *distributional derivative* exists [iii].

Notice further that the SDE of ξ_t in Equation (3.1.5) can be categorized into two main processes, a dependent GSN process, ${}^{(1)}\xi$, and an independent Compound Poisson process Y:

$$\mathrm{d}\xi_t = \underbrace{\sum_{i=1}^{N_{t-}} A_i \dot{h}(t - T_i)\, \mathrm{d}t}_{{}^{(1)}\xi_t} + h(0) \underbrace{A_{N_{t-}}\, \mathrm{d}N_t}_{\mathrm{d}Y_t}. \tag{3.1.8}$$

[ii] Recalling from Chapter 1, a càdlàg process is a stochastic process where right-limits are continuous and left limits are discontinuous (fr. continue à droite, limites à gauche). Refer to Figure 1.1 for visualization.

[iii] A simple example is the Dirac delta function, which is the distributional derivative of the Heaviside step function,

$$\frac{\mathrm{d}\Theta(x)}{\mathrm{d}x} = \delta(x).$$

More mathematical rigour on calculus for distributions can be inferred from [63].

Now, one can iterate the differentiation steps in Equation (3.1.4) to get the SDE for ${}^{(1)}\xi_t$:

$$\mathrm{d}^{(1)}\xi_t = \sum_{i=1}^{N_{t-}} A_i \,\mathrm{d}\dot{h}(t - T_i) + A_{N_{t-}} \dot{h}\,(0)\,\mathrm{d}N_t. \tag{3.1.9}$$

If h is twice differentiable, then we get $\mathrm{d}\dot{h}(t - T_i) = \ddot{h}(t - T_i)\,\mathrm{d}t$. Interestingly, for the SDE of ${}^{(1)}\xi_t$ we get another GSN process, ${}^{(2)}\xi$ and the same Compound Poisson process Y:

$$\mathrm{d}^{(1)}\xi_t = \underbrace{\sum_{i=1}^{N_{t-}} A_i \ddot{h}(t - T_i)\,\mathrm{d}t}_{{}^{(2)}\xi_t} + \dot{h}\,(0)\,\underbrace{A_{N_{t-}}\,\mathrm{d}N_t}_{\mathrm{d}Y_t}. \tag{3.1.10}$$

Therefore, rewriting the original GSN process $\xi = {}^{(0)}\xi$ for easier writing, given a smooth impulse function h over $\mathbb{R}$, we get a infinite order hierarchical system of SDE's for the GSN process ξ:

$$\begin{aligned}
\mathrm{d}^{(0)}\xi_t &= {}^{(1)}\xi_t\,\mathrm{d}t + h\,(0)\,\mathrm{d}Y_t \\
\mathrm{d}^{(1)}\xi_t &= {}^{(2)}\xi_t\,\mathrm{d}t + \dot{h}\,(0)\,\mathrm{d}Y_t \\
\mathrm{d}^{(2)}\xi_t &= {}^{(3)}\xi_t\,\mathrm{d}t + \ddot{h}\,(0)\,\mathrm{d}Y_t \\
&\vdots \\
\mathrm{d}^{(n-1)}\xi_t &= {}^{(n)}\xi_t\,\mathrm{d}t + h^{(n-1)}\,(0)\,\mathrm{d}Y_t, \\
&\vdots
\end{aligned} \tag{3.1.11}$$

where each GSN process ${}^{(n)}\xi$ is defined by the following realization:

$${}^{(n)}\xi_t = \sum_{i=1}^{N_t} A_i h^{(n)}(t - T_i). \tag{3.1.12}$$

Notice that given a general LE for $X, \dot{X}_t = -V'(X_t) + \xi_t$, where ξ_t is defined by the hierarchy in

Equation (3.1.11) (in LE form) with smooth function h:

$$\begin{aligned}
\dot{X}_t &= -V'(X_t) + {}^{(0)}\dot{\xi}_t \\
{}^{(0)}\dot{\xi}_t &= {}^{(1)}\xi_t + h(0)\,\dot{Y}_t \\
{}^{(1)}\dot{\xi}_t &= {}^{(2)}\xi_t + \dot{h}(0)\,\dot{Y}_t \\
{}^{(2)}\dot{\xi}_t &= {}^{(3)}\xi_t + \ddot{h}(0)\,\dot{Y}_t \\
&\vdots \\
{}^{(n-1)}\dot{\xi}_t &= {}^{(n)}\xi_t + h^{(n-1)}(0)\,\dot{Y}_t, \\
&\vdots
\end{aligned} \tag{3.1.13}$$

the joint tuple $\left(X, {}^{(0)}\dot{\xi}, {}^{(1)}\xi, {}^{(2)}\xi, \ldots, {}^{(n)}\xi, \ldots\right)$ forms an infinite dimensional Markov process. This means that if we define an infinite dimensional stochastic process $\vec{Z}$ with realization $\vec{Z}_t = \left(X_t, {}^{(0)}\dot{\xi}_t, {}^{(1)}\xi_t, {}^{(2)}\xi_t, \ldots, {}^{(n)}\xi_t, \ldots\right)$, then, by extension of Theorem 1.3.1, $\vec{Z}$ is a Markov process if and only if its realization is a solution of the Langevin Equation $\dot{\vec{Z}}_t = \vec{F}\left(\vec{Z}_t\right) + \dot{\vec{Y}}_t$, where $\vec{F}$ is an infinite dimensional smooth function and $\dot{\vec{Y}}_t$ is an infinite dimensional vector of white noise processes.

One can write the LE in Equation (3.1.13) in matrix form by defining infinite dimensional vectors $\vec{\Xi}_t = \left({}^{(0)}\xi_t, {}^{(1)}\xi_t, {}^{(2)}\xi_t, \ldots, {}^{(n-1)}\xi_t, \ldots\right)^\top$ and $\vec{\eta} = \left(h(0), \dot{h}(0), \ddot{h}(0), \ldots, h^{(n-1)}(0), \ldots\right)^\top$. Then, the LE can be rewritten as follows,

$$\begin{aligned}
\dot{X}_t &= -V'(X_t) + {}^{(0)}\dot{\xi}_t \\
\dot{\vec{\Xi}}_t &= \mathbf{A}\vec{\Xi}_t + \vec{\eta}\dot{L}_t,
\end{aligned} \tag{3.1.14}$$

where $\mathbf{A}$, the *coefficient matrix*, is an infinite dimensional matrix given by:

$$\mathbf{A} = \begin{pmatrix} 0 & 1 & 0 & 0 & \dots & 0 & 0 & \dots \\ 0 & 0 & 1 & 0 & \dots & 0 & 0 & \dots \\ 0 & 0 & 0 & 1 & \dots & 0 & 0 & \dots \\ \vdots & \vdots & \vdots & \vdots & \ddots & \vdots & \vdots & \ddots \\ 0 & 0 & 0 & 0 & \dots & 1 & 0 & \dots \\ 0 & 0 & 0 & 0 & \dots & 0 & 1 & \dots \\ \vdots & \vdots & \vdots & \vdots & \ddots & \vdots & \vdots & \ddots \end{pmatrix}. \tag{3.1.15}$$

Furthermore, we can define the vectors $\vec{Z}_t := \left(X_t, \vec{\Xi}_t\right)^\top$ and $\vec{Y}_t := (0, \vec{\eta})^\top Y_t$. Then, given an infinite dimensional function $\vec{F}$:

$$\vec{F} : \mathbb{R}^\infty \to \mathbb{R}^\infty, \tag{3.1.16}$$

we can define $\vec{F}\left(\vec{Z}_t\right) := \left(-V'(X_t) + \xi_t, \mathbf{A}\vec{\Xi}_t\right)^\top$ and rewrite the LE in vector form $\vec{Z}$ as follows:

$$\dot{\vec{Z}}_t = \vec{F}\left(\vec{Z}_t\right) + \dot{\vec{Y}}_t, \tag{3.1.17}$$

where $\dot{\vec{Y}}$ is now the PWN process multiplied by coefficient vector $\vec{\eta}$. Therefore, by Theorem 1.3.1, Equation (3.1.17) is an infinite dimensional Markov process with Markovian tuple $Z = \left(X, \xi, {}^{(1)}\xi, \dots, {}^{(n)}\xi, \dots\right)$.

One way of reducing the dimension of the Markovian tuple is by specifically defining the impulse function h. Recall in to our classification in Section 2.5 that given an $n-$th hierarchy impulse function h as the solution of the linear IVP:

$$\sum_{i=0}^{n} c_i h^{(i)}(t) = 0, \quad h^{(i)}(0) = a_i \tag{3.1.18}$$

where $c_i,\ a_i \in \mathbb{R}$ are constant coefficients. Then, rewriting the largest order of h independently, we get that $h^{(n)}(t) = \left(\sum_{i=0}^{n-1} c_i h^{(i)}(t)\right)/c_n$. For simpler writing, we can assume without loss of generality that $c_n = -1$. Therefore, one can rewrite the realization of ${}^{(n)}\xi$ as follows:

$$\begin{aligned}
{}^{(n)}\xi_t &= \sum_{i=1}^{N_t} A_i h^{(n)}\left(t - T_i\right) = \sum_{i=1}^{N_t} A_i \sum_{j=0}^{n-1} c_j h^{(j)}\left(t - T_i\right) \\
&= \sum_{j=0}^{n-1} c_j \sum_{i=1}^{N_t} A_i h^{(j)}\left(t - T_i\right) \\
&= \sum_{j=0}^{n-1} c_j \cdot {}^{(j)}\xi_t.
\end{aligned} \tag{3.1.19}$$

Therefore, the hierarchical SDE of ξ will be reduced to a finite order:

$$\begin{aligned}
\mathrm{d}^{(0)}\xi_t &= {}^{(1)}\xi_t\,\mathrm{d}t + h\left(0\right)\mathrm{d}Y_t \\
\mathrm{d}^{(1)}\xi_t &= {}^{(2)}\xi_t\,\mathrm{d}t + \dot{h}\left(0\right)\mathrm{d}Y_t \\
\mathrm{d}^{(2)}\xi_t &= {}^{(3)}\xi_t\,\mathrm{d}t + \ddot{h}\left(0\right)\mathrm{d}Y_t \\
&\vdots \\
\mathrm{d}^{(n-1)}\xi_t &= \left(\sum_{j=0}^{n-1} c_j \cdot {}^{(j)}\xi_t\right)\mathrm{d}t + h^{(n-1)}\left(0\right)\mathrm{d}Y_t.
\end{aligned} \tag{3.1.20}$$

In this case, the LE can be rewritten as follows,

$$\begin{aligned}
\dot{X}_t &= -V'(X_t) + {}^{(0)}\dot{\xi}_t \\
\dot{\vec{\Xi}}_t &= \mathbf{A}\vec{\Xi}_t + \vec{\eta}\dot{L}_t,
\end{aligned} \tag{3.1.21}$$

where the coefficient matrix $\mathbf{A}$ is now of size $n \times n$:

$$\mathbf{A} = \begin{pmatrix} 0 & 1 & 0 & 0 & \dots & 0 & 0 \\ 0 & 0 & 1 & 0 & \dots & 0 & 0 \\ 0 & 0 & 0 & 1 & \dots & 0 & 0 \\ \vdots & \vdots & \vdots & \vdots & \ddots & \vdots & \vdots \\ 0 & 0 & 0 & 0 & \dots & 1 & 0 \\ 0 & 0 & 0 & 0 & \dots & 0 & 1 \\ c_0 & c_1 & c_2 & c_3 & \dots & c_{n-2} & c_{n-1} \end{pmatrix}. \tag{3.1.22}$$

Lastly, given the multivariable function $\vec{F} : \mathbb{R}^{n+1} \to \mathbb{R}^{n+1}$, we can define $\vec{F}\left(\vec{Z}_t\right) := \left(-V'(X_t) + {}^{(0)}\xi_t, \mathbf{A}\vec{\Xi}_t\right)^\top$ as before and rewrite the LE in $(n+1)-$dimensional vector form $\vec{Z}$ as follows:

$$\dot{\vec{Z}}_t = \vec{F}\left(\vec{Z}_t\right) + \dot{\vec{Y}}_t, \tag{3.1.23}$$

Thus, if the GSN ξ has $n-$hierarchy impulse function, then the resulting Markovian tuple $\left(X, {}^{(0)}\xi, {}^{(1)}\xi, \dots, {}^{(n-1)}\xi\right)$ becomes an $(n+1)-$dimensional Markov process.

3.1.1 Examples of Impulse Functions on Hierarchy Reduction

Now, we give some examples of n-th hierarchical impulse functions and observe how the rank reduces in the Markovian tuple.

The first and trivial candidate of impulse functions is the exponential decay, $h(x) = \alpha^{-\alpha x}$. Recall that h is the solution of the IVP $\dot{h}(t) = -\alpha h(t),\ h(0) = \alpha$. Therefore, the LE for the Markovian

tuple $\vec{Z}$ is simply given by the following:

$$\begin{aligned} \dot{X}_t &= -V'(X_t) + \xi_t \\ \dot{\xi}_t &= -\alpha \xi_t \, \mathrm{d}t + \alpha \dot{L}_t, \end{aligned} \tag{3.1.24}$$

where we have the scalar reduction $\mathbf{A} = \vec{\eta} = \alpha$. Due to its simplicity and numerical efficacy, this type of GSN process has been widely analyzed in literature, such as in finding the closed-form ME of X[74] as well as calculating its optimal escape probabilities under Gaussian Limits[87 97].

Another example that one can give is the damped oscillating impulse function,

$$h(t) = \frac{\alpha^2 + \beta^2}{\alpha + \beta} e^{-\alpha t} \left(\sin \beta t + \cos \beta t \right), \tag{3.1.25}$$

which is the solution of the IVP

$$\ddot{h}(t) - 2\alpha \dot{h}(t) + \left(\alpha^2 + \beta^2 \right) h(t) = 0, \quad h(0) = 1, \; \dot{h}(0) = \beta - \alpha. \tag{3.1.26}$$

In this instance, the LE for $\vec{Z}$ is given by the following:

$$\begin{aligned} \dot{X}_t &= -V'(X_t) + \xi_t \\ \dot{\xi}_t &= {}^{(1)}\xi_t + \dot{L}_t \\ {}^{(1)}\dot{\xi}_t &= 2\alpha \, {}^{(1)}\xi_t - \left(\alpha^2 + \beta^2 \right) \xi_t + (\beta - \alpha) \dot{L}_t, \end{aligned} \tag{3.1.27}$$

where we obtain the coefficient vector $\vec{\eta} = (1, \beta - \alpha)^\top$ and the 2×2 coefficient matrix $\mathbf{A}$ as

$$\mathbf{A} = \begin{pmatrix} 0 & 1 \\ -(\alpha^2 + \beta^2) & 2\alpha \end{pmatrix}. \tag{3.1.28}$$

3.2 Master Equation of the GSN Process

In this section, we propose two methods of finding the ME of the GSN process ξ and the position process X driven by the LE in Equation (0.0.2). The first method is by standard Itō's approach, where it is widely used in finding time evolution equations for Markovian processes[68]. We show here that due to the non-Markovian nature of ξ, one cannot simply find the ME for the PDF of X, where instead a joint distribution has to be derived via Multivariate Itō's Lemma as we discussed in Lemma 1.5.3.

Next, we show Hänggi's method which, by using the CFal approach, relaxes the Markov assumption in solving the ME.

3.2.1 Finding the Master Equation via Itō's Approach

Recalling the generalized Itō's lemma in Lemma 1.5.2, given a smooth function $f : \mathbb{R} \to \mathbb{R}$, the SDE of $f(X_t)$ driven by the LE in differential form $\mathrm{d}X_t = -V'(X_t) + \xi_t \,\mathrm{d}t$ is given by:

$$\begin{aligned} \mathrm{d}f - \Delta f &= f'\left(X_{t^-}\right)\mathrm{d}X_t + \frac{1}{2}f''\left(X_{t^-}\right)\left(\mathrm{d}X_t\right)^2 - f'\left(X_{t^-}\right)\Delta X_t - \frac{1}{2}f''\left(X_{t^-}\right)\left(\Delta X_t\right)^2 \\ \implies \mathrm{d}f &= f'\left(X_t\right)\left(-V'(X_t) + \xi_t\right)\mathrm{d}t + \frac{1}{2}f''\left(X_t\right)\left(\left(-V'(X_t) + \xi_t\right)\mathrm{d}t\right)^2 \\ &= f'\left(X_t\right)\left(-V'(X_t) + \xi_t\right)\mathrm{d}t, \end{aligned} \tag{3.2.1}$$

where since X is continuous in time, the jump terms Δf and ΔX_t vanish, and we have that $(\mathrm{d}t)^2 = 0$. Denoting the PDF of X by $\mathbb{P}_X$, if we attempt to find the infinitesimal generator $\mathcal{A}^*$ as in Equation (1.5.6) we get the following:

$$\frac{\mathrm{d}}{\mathrm{d}t}\langle f\rangle = -\left\langle f'\left(X_t\right)V'(X_t)\right\rangle + \left\langle f'\left(X_t\right)\xi_t\right\rangle. \tag{3.2.2}$$

Unlike the white noise case as in Equation (1.5.8), the colored nature of ξ indicates that the realizations X_t and ξ_t are not necessarily independent for any given t, i.e. $\langle f'(X_t)\,\xi_t\rangle \neq \langle f'(X_t)\rangle\,\langle \xi_t\rangle$. Therefore, one has to find the *joint PDF* of the tuple (X, ξ).

This time, let the function $f : \mathbb{R}\times\mathbb{R} \to \mathbb{R}$ be a smooth bivariate function. Then, assuming the impulse function h to be differentiable at least once, we obtain the SDE for $f(X_t, \xi_t)$ by applying generalized multivariate Itō's lemma as in Lemma 1.5.3:

$$
\begin{aligned}
&\mathrm{d}f - \Delta f \\
=&\frac{\partial f}{\partial x}\,\mathrm{d}X_t + \frac{\partial f}{\partial y}\,\mathrm{d}\xi_t + \frac{1}{2}\left(\frac{\partial^2 f}{\partial y^2}\,(\mathrm{d}X_t)^2 + \frac{\partial^2 f}{\partial x\partial y}\,\mathrm{d}X_t\,\mathrm{d}\xi_t + \frac{\partial^2 f}{\partial y^2}\,(\mathrm{d}\xi_t)^2\right) \\
&- \frac{\partial f}{\partial x}\Delta X_t - \frac{\partial f}{\partial y}\Delta\xi_t - \frac{1}{2}\left(\frac{\partial^2 f}{\partial x^2}\,(\Delta X_t)^2 + \frac{\partial^2 f}{\partial x\partial y}\Delta X_t\Delta\xi_t + \frac{\partial^2 f}{\partial y^2}\,(\Delta\xi_t)^2\right) \\
=&\frac{\partial f}{\partial x}\left(-V'(X_t) + \xi_t\right)\mathrm{d}t + \frac{\partial f}{\partial y}\left(\sum_{i=1}^{N_t-} A_i\dot{h}(t-T_i)\,\mathrm{d}t + A_{N_t}h(0)\,\mathrm{d}N_t\right) + \frac{1}{2}\frac{\partial^2 f}{\partial y^2}A_{N_t}^2 h(0)^2\,\mathrm{d}N_t \\
&- \frac{\partial f}{\partial y}A_{N_t}h(0)\Delta N_t - \frac{1}{2}A_{N_t}^2 h(0)^2\Delta N_t \\
=&\left[\frac{\partial f}{\partial x}\left(-V'(X_t) + \xi_t\right) + \frac{\partial f}{\partial y}\sum_{i=1}^{N_t-} A_i\dot{h}(t-T_i)\right]\mathrm{d}t + \left[\frac{\partial f}{\partial y}A_{N_t}h(0) + \frac{1}{2}\frac{\partial^2 f}{\partial y^2}A_{N_t}^2 h(0)^2\right]\Delta N_t,
\end{aligned}
\tag{3.2.3}
$$

where we reduced in last step the fact that N is a purely discontinuous process so $\mathrm{d}N_t = 0$ almost surely. We can retrieve the ME for the tuple (X, ξ) by applying the infinitesimal generator approach:

$$
\begin{aligned}
\frac{\mathrm{d}}{\mathrm{d}t}\langle f\rangle = &\left\langle \frac{\partial f}{\partial x}\left(-V'(X_t) + \xi_t\right) + \frac{\partial f}{\partial y}\sum_{i=1}^{N_t-} A_i\dot{h}(t-T_i)\right\rangle \\
&+ \langle\Delta f\rangle + \left\langle \frac{\partial f}{\partial y}A_{N_t}h(0) + \frac{1}{2}\frac{\partial^2 f}{\partial y^2}A_{N_t}^2 h(0)^2\right\rangle\langle\Delta N_t\rangle\,.
\end{aligned}
\tag{3.2.4}
$$

Notice first that that due to Poissonian nature of ξ, we have that $\Delta f(X_t, \xi_t) \neq 0$. In fact, one can further analyze this jump size by taking its Taylor expansion:

$$\begin{aligned} f(x,y) &= \sum_{m=0}^{\infty}\sum_{n=0}^{\infty} \frac{x^m y^n}{m!n!} \frac{\partial^{m+n} f}{\partial^m x \partial^n y} \\ \implies \Delta f(X_t, \xi_t) &= \sum_{m=0}^{\infty}\sum_{n=1}^{\infty} \frac{X_t^m \Delta\left(\xi_t^n\right)}{m!n!} \frac{\partial^{m+n} f}{\partial^m x \partial^n y}\left(X_t, \xi_{t^-}\right), \end{aligned} \tag{3.2.5}$$

where we can further expand the jump term $\Delta\left(\xi_t^n\right)$ as follows:

$$\begin{aligned} \Delta\left(\xi_t^n\right) &= \Delta\xi_t \sum_{i=0}^{n-1} \xi_t^i \xi_{t^-}^{n-1-i} = \Delta\xi_t \sum_{i=0}^{n-1} \left(\xi_{t^-} + \Delta\xi_t\right)^i \xi_{t^-}^{n-1-i} = \Delta\xi_t \sum_{i=0}^{n-1}\sum_{j=0}^{i} \binom{i}{j} \xi_{t^-}^j \left(\Delta\xi_t\right)^{i-j} \xi_{t^-}^{n-1-i} \\ &= \sum_{i=0}^{n-1}\sum_{j=0}^{i} \binom{i}{j} \xi_{t^-}^{n-1-i+j} \left(\Delta\xi_t\right)^{i-j+1}. \end{aligned} \tag{3.2.6}$$

Therefore,

$$\begin{aligned} \langle \Delta f \rangle &= \sum_{m=0}^{\infty}\sum_{n=1}^{\infty}\sum_{i=0}^{n-1}\sum_{j=0}^{i} \binom{i}{j} \frac{1}{m!n!} \left\langle \left(\Delta\xi_t\right)^{i-j+1} \right\rangle \left\langle X_t^m \xi_t^{n-1-i+j} \frac{\partial^{m+n} f}{\partial^m x \partial^n y} \right\rangle \\ &= \sum_{m=0}^{\infty}\sum_{n=1}^{\infty}\sum_{i=0}^{n-1}\sum_{j=0}^{i} \binom{i}{j} \frac{1}{m!n!} \left\langle A_{N_t}^{i-j+1} \right\rangle h^{i-j+1}(0) \left\langle X_t^m \xi_t^{n-1-i+j} \frac{\partial^{m+n} f}{\partial^m x \partial^n y} \right\rangle \langle \Delta N_t \rangle. \end{aligned} \tag{3.2.7}$$

By denoting the joint PDF of (X, ξ) by $\mathbb{P}$, we obtain the following ME:

$$\begin{aligned}
&\iint \mathrm{d}x\,\mathrm{d}y \frac{\partial \mathbb{P}}{\partial t} f(x,y) \\
&= \iint \mathrm{d}x\,\mathrm{d}y \Bigg\{ \frac{\partial}{\partial x}\left[\left(V'(x)-y\right)\mathbb{P}\right] - \lambda \left\langle A_1 \right\rangle h(0) \frac{\partial \mathbb{P}}{\partial y} + \frac{1}{2}\lambda \left\langle A_1^2 \right\rangle h(0)^2 \frac{\partial^2 \mathbb{P}}{\partial y^2} \\
&\quad + \lambda \sum_{m=0}^{\infty} \sum_{n=1}^{\infty} \sum_{i=0}^{n-1} \sum_{j=0}^{i} \binom{i}{j} \frac{(-1)^{m+n}}{m!n!} \left\langle A_1^{i-j+1} \right\rangle h^{i-j+1}(0) \frac{\partial^{m+n}}{\partial x^m \partial y^n} \left[x^m y^{n-1-i+j} \mathbb{P}\right] \Bigg\} f(x,y) \\
&\quad + \left\langle \frac{\partial f}{\partial y} \sum_{i=1}^{N_t-} A_i \dot{h}(t-T_i) \right\rangle .
\end{aligned} \tag{3.2.8}$$

Notice that the ME is almost complete except the last expectation, where it contains the first hierarchy of the GSN process, ${}^{(1)}\xi$ as in Equation (3.1.11). Therefore, similar to our assertion in the beginning on this chapter, one now needs to find the joint PDF of the tuple $\left(X, \xi, {}^{(1)}\xi\right)$. Using the trivariate Itō's lemma in Lemma 1.5.3 and finding the infinitesimal generator of this system, we would then end up with the expectation containing the second hierarchy of the GSN process, ${}^{(2)}\xi$. This induction coincides with our results in the beginning of this chapter, where due to the hierarchical nature of ξ, one needs to find the joint PDF of the infinite tuple $\left(X, \xi, {}^{(1)}\xi, {}^{(2)}\xi, \ldots, {}^{(n)}\xi, \ldots\right)$.

As expected, if we choose the exponential decay impulse function $h(x) = \alpha e^{-\alpha x}$, then the last expectation would simplify to the following:

$$\left\langle \frac{\partial f}{\partial y} \sum_{i=1}^{N_t-} A_i \dot{h}(t-T_i) \right\rangle = -\alpha \left\langle \frac{\partial f}{\partial y} \sum_{i=1}^{N_t} A_i h(t-T_i) \right\rangle = -\alpha \left\langle \frac{\partial f}{\partial y} \xi_t \right\rangle , \tag{3.2.9}$$

which can be inserted back into Equation (3.2.8) and complete the ME of the Markovian tuple

(X, ξ) under exponentially decaying impulse function:

$$\begin{aligned}\frac{\partial \mathbb{P}}{\partial t} = \frac{\partial}{\partial x}\left[\left(V'(x) - y\right)\mathbb{P}\right] + \alpha\frac{\partial}{\partial y}\left[y\,\mathbb{P}\right] - \lambda\left\langle A_1\right\rangle h(0)\frac{\partial \mathbb{P}}{\partial y} + \frac{1}{2}\lambda\left\langle A_1^2\right\rangle h(0)^2\frac{\partial^2 \mathbb{P}}{\partial y^2} \\ + \lambda\sum_{m=0}^{\infty}\sum_{n=1}^{\infty}\sum_{i=0}^{n-1}\sum_{j=0}^{i}\binom{i}{j}\frac{(-1)^{m+n}}{m!n!}\left\langle A_1^{i-j+1}\right\rangle h^{i-j+1}(0)\frac{\partial^{m+n}}{\partial x^m \partial y^n}\left[x^m y^{n-1-i+j}\mathbb{P}\right].\end{aligned} \tag{3.2.10}$$

We will go through this in detail in the following section. For now, we next apply Gaussian Limits to our ME to retrieve the FPE as we introduced in Chapter 1.

3.2.2 Obtaining the Fokker-Planck Equation under Gaussian Limits

Notice that under the Gaussian Limits the summation terms in the incomplete ME in Equation (3.2.8) will be reduced to cases for $n = 2$, $i = 1$ and $j = 0$, in which case we obtain the following:

$$\begin{aligned}\iint \mathrm{d}x\,\mathrm{d}y\frac{\partial \mathbb{P}}{\partial t}f(x,y) = \iint \mathrm{d}x\,\mathrm{d}y\Bigg\{\frac{\partial}{\partial x}\left[\left(V'(x) - y\right)\mathbb{P}\right] + \frac{\sigma^2}{2}h(0)^2\frac{\partial^2 \mathbb{P}}{\partial y^2} \\ + \frac{\sigma^2}{2}h(0)^2\frac{\partial^2}{\partial y^2}\left[\sum_{m=0}^{\infty}\frac{1}{m!}\left(-\frac{\partial}{\partial x}\right)^m\left[x^m\mathbb{P}\right]\right]\Bigg\}f(x,y) \\ + \lim_{GL}\left\langle\frac{\partial f}{\partial y}\sum_{i=1}^{N_t-}A_i\dot{h}(t - T_i)\right\rangle,\end{aligned} \tag{3.2.11}$$

where the limit term $\lim_{GL}$ refers to the Gaussian Limits. Notice also that the summation term in Equation (3.2.11) converges to the PDF $\mathbb{P}$. We will prove this in the following theorem:

Theorem 3.2.1. *Given any smooth function f on $\mathbb{R} \times [0, \infty[$, the following condition always holds:*

$$\sum_{m=0}^{\infty}\frac{1}{m!}\left(-\frac{\partial}{\partial x}\right)^m\left[x^m \cdot f(x,t)\right] = f(x,t). \tag{3.2.12}$$

Proof. Applying higher-order chain rule to the summation yields the following:

$$\begin{aligned}\sum_{m=0}^{\infty}\frac{1}{m!}\left(-\frac{\partial}{\partial x}\right)^{m}[x^{m}\cdot f(x,t)] &= \sum_{m=0}^{\infty}\frac{(-1)^{m}}{m!}\sum_{k=0}^{m}\binom{m}{k}\frac{\partial^{m-k}}{\partial x^{m-k}}x^{m}\cdot\frac{\partial^{k}f(x,t)}{\partial x^{k}}\\ &= \sum_{m=0}^{\infty}\frac{(-1)^{m}}{m!}\sum_{k=0}^{m}\binom{m}{k}(k+1)_{m-k}\,x^{k}\frac{\partial^{k}f(x,t)}{\partial x^{k}},\end{aligned} \tag{3.2.13}$$

where $(k+1)_{m-k}$ is the rising factorial (aka Pochhammer symbol), which is equivalent to $m!/k!$. Substituting this back into the equation and writing the partial differential separately yields the following:

$$\begin{aligned}\sum_{m=0}^{\infty}\frac{(-1)^{m}}{m!}\sum_{k=0}^{m}\binom{m}{k}(k+1)_{m-k}\,x^{k}\frac{\partial^{k}f(x,t)}{\partial x^{k}} &= f(x,t)\sum_{m=0}^{\infty}(-1)^{m}\sum_{k=0}^{m}\binom{m}{k}\frac{1}{k!}\left(x\frac{\partial}{\partial x}\right)^{k}\\ &= f(x,t)\sum_{m=0}^{\infty}(-1)^{m}\cdot{}_1F_1\left(-m;1;-x\frac{\partial}{\partial x}\right),\end{aligned} \tag{3.2.14}$$

where now the function ${}_1F_1$ is the confluent hypergeometric function (CHF) that is derived from the inner summation[96]. The CHF ${}_1F_1(a;b;c)$ is defined as the solution w of the following ODE:

$$c\frac{\mathrm{d}^2w}{\mathrm{d}c^2}+(b-c)\frac{\mathrm{d}w}{\mathrm{d}c}-aw=0. \tag{3.2.15}$$

Notice that as $c = -x\frac{\partial}{\partial x}$, which is algebraically independent of w, the only solution of the above ODE is when $w = 0$. Therefore, we have that ${}_1F_1(-m;1;,-x\frac{\partial}{\partial x}) = 0$ and hence the series con-

verges:

$$\begin{aligned} f(x,t)\sum_{m=0}^{\infty}(-1)^m\cdot\ {}_1F_1\left(-m;1;-x\frac{\partial}{\partial x}\right) &= f(x,t)\sum_{m=0}^{\infty}(-1)^m\cdot 0 \equiv f(x,t)\lim_{B\to\infty}\sum_{m=0}^{\infty}\left(\frac{-1}{B}\right)^m \\ &= f(x,t)\lim_{B\to\infty}\frac{B}{B+1} \\ &= f(x,t), \end{aligned} \tag{3.2.16}$$

which completes our proof.

□

Thus, we can rewrite our incomplete FPE for non-Markovian yet Gaussian s.p. X as follows:

$$\begin{aligned} \iint \mathrm{d}x\,\mathrm{d}y\frac{\partial\mathbb{P}}{\partial t}f(x,y) = \iint \mathrm{d}x\,\mathrm{d}y\left\{\frac{\partial}{\partial x}\left[\left(V'(x)-y\right)\mathbb{P}\right]+\sigma^2 h(0)^2\frac{\partial^2\mathbb{P}}{\partial y^2}\right\}f(x,y) \\ +\lim_{GL}\left\langle\frac{\partial f}{\partial y}\sum_{i=1}^{N_{t^-}}A_i\dot{h}(t-T_i)\right\rangle. \end{aligned} \tag{3.2.17}$$

As we established in non-Gaussian regime, we can simplify the FPE even further by introducing the exponential decay impulse function, $h(x)=\alpha e^{-\alpha x}$. Hence,

$$\lim_{GL}\left\langle\frac{\partial f}{\partial y}\sum_{i=1}^{N_{t^-}}A_i\dot{h}(t-T_i)\right\rangle = \left\langle-\alpha\frac{\partial f}{\partial y}\xi_t\right\rangle = \alpha\iint\mathrm{d}x\,\mathrm{d}y\frac{\partial}{\partial y}\left[y\mathbb{P}\right]. \tag{3.2.18}$$

Thus we can retrieve the complete FPE for (X,ξ) that is commonly known as the Klein–Kramers

equation [125]:

$$\begin{aligned}\iint \mathrm{d}x\,\mathrm{d}y \frac{\partial \mathbb{P}}{\partial t} f(x,y) &= \iint \mathrm{d}x\,\mathrm{d}y \left\{ \frac{\partial}{\partial x}\left[\left(V'(x)-y\right)\mathbb{P}\right] + \alpha \frac{\partial}{\partial y}\left[y\mathbb{P}\right] + \sigma^2 h(0)^2 \frac{\partial^2 \mathbb{P}}{\partial y^2} \right\} f(x,y) \\ \implies \frac{\partial \mathbb{P}}{\partial t} &= \frac{\partial}{\partial x}\left[\left(V'(x)-y\right)\mathbb{P}\right] + \alpha \frac{\partial}{\partial y}\left[y\mathbb{P}\right] + \sigma^2 \alpha^2 \frac{\partial^2 \mathbb{P}}{\partial y^2}.\end{aligned} \tag{3.2.19}$$

We would like to iterate from Chapter 1 that under the Gaussian Limits and exponential decay impulse function h, the LE is given by the following:

$$\begin{aligned}\dot{X}_t &= -V'(X_t) + \xi_t \\ \dot{\xi}_t &= -\alpha \xi_t + \alpha \dot{W}_t,\end{aligned} \tag{3.2.20}$$

where $\dot{W}_t$ forms the GWN process, and hence ξ is the OU process as in Equation (1.4.2). The FPE of such system where the non-Markovian position process X is driven by the Markovian OU noise process ξ is commonly known as the Kramer's equation [56], where the FPE can be solved by separation of variables followed by inverse Laplace transform [58]. Once the joint PDF is found, the marginal PDF of the position process X, p_X, can be retrieved by integrating $\mathbb{P}$ over the sample space of ξ, i.e. $p_X(x,t) = \int_{-\infty}^{\infty} \mathrm{d}y\, \mathbb{P}(x,y,t)$.

Thus, we have shown that Itō's approach plays an important role in finding the ME of the position process X. However, this method only works in Markovian realm. Due to the hierarchical nature of the GSN process ξ, the ME can be computed for an infinite tuple of X and the hierarchies of ξ unless we choose an $n-$hierarchical impulse function h that reduces to the size of the tuple to $n+1$.

Next, we analyze another method of finding the ME of X in the non-Markovian realm by finding the path integral of X. Although we will in detail explain it, we expect the reader in the following

section to have basic knowledge of calculus of variations [iv].

3.2.3 Finding the Master Equation via Path Integral Approach

We have shown in previous section in detail that Itō's approach yields the ME for infinite order Markovian tuple $\left(X, \xi, {}^{(1)}\xi, {}^{(2)}\xi, \dots, {}^{(n)}\xi, \dots\right)$, unless we assume some properties for the impulse function h. Here, we show that the path integral approach works in the non-Markovian regime, where one can find the ME solely for X regardless of the behaviour of the impulse function. In detail, using the CFal's of both X and ξ as we have derived in Chapter 2, we find the ME of X using the Kramers-Moyal expansion method conducted by Hänggi[74].

Given the s.p. X with pdf $p(x,t)$, its general ME is given by

$$\frac{\partial p}{\partial t} = \sum_{n=1}^{\infty} \frac{(-1)^n}{n!} \frac{\partial^n}{\partial x^n} \left[\alpha_n(x) p(x,t)\right], \tag{3.2.21}$$

where

$$\alpha_n(x) = \int_{\mathbb{R}} (x' - x)^n \mathbb{P}(x'|x)\, \mathrm{d}x' \tag{3.2.22}$$

are the cumulants and $\mathbb{P}(x'|x)$ is the transition probability.

Hänggi's important proposition is to rewrite the CFal of a s.p. X

$$\Phi_X[g] = \left\langle \exp\left[i \int \mathrm{d}s\, g(s) X_s \right] \right\rangle \tag{3.2.23}$$

using the *functional Taylor Expansion*,

$$\Phi_X[g] = \sum_{n=0}^{\infty} \frac{i^n}{n!} \int \prod_{i=1}^{n} \mathrm{d}t_i\, g(t_i) \left\langle \prod_{i=1}^{n} X_{t_i} \right\rangle, \tag{3.2.24}$$

[iv] Where need be, the reader is encouraged to read [21] for detailed explanation.

where by definition

$$\left\langle \prod_{i=1}^{n} X_{t_i} \right\rangle = i^{-n} \frac{\delta^n}{\prod_{i=1}^{n} \delta g(t_i)} \Phi_X[g]\Big|_{g=0}. \tag{3.2.25}$$

One can also apply the functional Taylor expansion in terms of the *cumulant generating functional* (CGFal) $\Psi_X[g] \equiv \ln \Phi_X[g]$:

$$\Psi[g] = \sum_{n=1}^{\infty} \frac{i^n}{n!} \int \prod_{i=1}^{n} \mathrm{d}t_i \, g(t_i) K(t_1, ..., t_n), \tag{3.2.26}$$

where K is the *cumulant function*:

$$K(t_1, ..., t_n) = i^{-n} \frac{\delta^n}{\prod_{i=1}^{n} \delta g(t_i)} \Psi_X[g]\Big|_{g=0}. \tag{3.2.27}$$

Furthermore, Hänggi also looked at the general correlation function of the form $\langle X_t G[X] \rangle$, where G is an arbitrary functional. Defining another functional Σ_t as:

$$\Sigma_t[g] \equiv \frac{1}{ig(t)} \frac{\partial}{\partial t} \Psi_{X;t}[g], \tag{3.2.28}$$

where $\Psi_{X;t}$ is the "trimmed" CGFal,

$$\Psi_{X;t}[g] = \ln \Phi_{X;t}[g] = \ln \left\langle \exp \left[i \int_0^t \mathrm{d}s \, g(s) X_s \right] \right\rangle, \tag{3.2.29}$$

Hänngi found that the general correlation function can be defined as follows:

$$\langle X_t G[X] \rangle = \left\langle \Sigma_t \left[\frac{\delta}{i \delta X} \right] G[X] \right\rangle. \tag{3.2.30}$$

The next proposal of Hänngi is to find the ME of a LE of the following:

$$\dot{X}_t = \alpha(t)X_t + \beta(X_t, t)\int_0^t \mathrm{d}s\,\gamma(t,s)X_s + b(X_t,t)\,Z_t, \tag{3.2.31}$$

where Z_t forms another s.p. $Z = (Z_t)_{t\geq 0}$ that need not be independent of X.

Defining the pdf of X by $p(x,t)$, one can rewrite the pdf in terms of the average of the Dirac delta function:

$$p(x,t) = \langle \delta(X_t - x)\rangle\,. \tag{3.2.32}$$

Thus, taking the time derivative of the p yields the following:

$$\begin{aligned}
\frac{\partial}{\partial t}p(x,t) &= \frac{\partial}{\partial t}\left\langle \delta\left(X_t - x\right)\right\rangle = \left\langle \dot{X}_t\delta'\left(X_t - x\right)\right\rangle \\
&= \left\langle \left(\alpha(t)X_t + \beta(X_t,t)\cdot\int_0^t \mathrm{d}s\,\gamma(t,s)X_s + b(X_t,t)Z_t\right)\delta'\left(X_t - x\right)\right\rangle \\
&= \left\langle \alpha(t)X_t\delta'\left(X_t - x\right)\right\rangle + \left\langle \beta(X_t,t)\int_0^t \mathrm{d}s\,\gamma(t,s)X_s\delta'\left(X_t - x\right)\right\rangle + \left\langle b(X_t,t)Z_t\delta'\left(X_t - x\right)\right\rangle,
\end{aligned} \tag{3.2.33}$$

where, using the identities $-x\delta'(x) = \delta(x)$, $\delta(-x) = \delta(x)$ and $\delta'(-x) = -\delta'(x)$, we get the following expectations,

$$\begin{aligned}
\left\langle \alpha(t)X_t\delta'\left(X_t - x\right)\right\rangle &= \left\langle \alpha(t)(X_t - z)\delta'\left(X_t - x\right) + \alpha(t)x\delta'\left(X_t - x\right)\right\rangle \\
&= -\alpha(t)\left\langle \delta(x - X_t) + x\delta'(x - X_t)\right\rangle \\
&= -\alpha(t)\left\langle \frac{\partial}{\partial x}\left(x\delta\left(x - X_t\right)\right)\right\rangle \\
&= -\alpha(t)\frac{\partial}{\partial x}(x\,p(x,t)),
\end{aligned} \tag{3.2.34}$$

$$
\begin{aligned}
&\left\langle \beta(X_t,t)\int_0^t \mathrm{d}s\,\gamma(t,s)X_s\delta'\left(X_t-x\right)\right\rangle \\
&=\left\langle \left(\beta(X_t,t)-\beta(x,t)\right)\int_0^t \mathrm{d}s\,\gamma(t,s)X_s\delta'\left(X_t-x\right)\right\rangle + \left\langle \beta(x,t)\int_0^t \mathrm{d}s\,\gamma(t,s)X_s\delta'\left(X_t-x\right)\right\rangle \\
&=-\left\langle \frac{\beta(X_t,t)-\beta(x,t)}{X_t-x}\int_0^t \mathrm{d}s\,\gamma(t,s)X_s\delta\left(X_t-x\right)\right\rangle + \left\langle \beta(x,t)\int_0^t \mathrm{d}s\,\gamma(t,s)X_s\delta'\left(X_t-x\right)\right\rangle \\
&=-\left\langle \int_0^t \mathrm{d}s\,\gamma(t,s)X_s\left(\frac{\beta(x,t)-\beta(X_t,t)}{x-X_t}\delta\left(x-X_t\right)+\beta(x,t)\delta'(x-X_t)\right)\right\rangle \\
&=-\left\langle \int_0^t \mathrm{d}s\,\gamma(t,s)X_s\frac{\partial}{\partial x}(\beta(x,t)\delta\left(x-X_t\right)\right\rangle \\
&=-\frac{\partial}{\partial x}\beta(x,t)\left\langle \int_0^t \mathrm{d}s\,\gamma(t,s)X_s\delta\left(X_t-x\right)\right\rangle,
\end{aligned}
\tag{3.2.35}
$$

and similarly,

$$
\left\langle b(X_t,t)Z_t\delta'\left(X_t-x\right)\right\rangle = -\frac{\partial}{\partial x}b(x,t)\left\langle Z_t\delta\left(X_t-x\right)\right\rangle. \tag{3.2.36}
$$

Furthermore, as Z can be dependent to X, we can rewrite the last expectation as

$$
\left\langle b(X_t,t)Z_t\delta'\left(X_t-x\right)\right\rangle = -\frac{\partial}{\partial x}b(x,t)\left\langle Z_t\delta(X_t-t)\right\rangle = -\frac{\partial}{\partial x}b(x,t)\left\langle \Sigma_t\left[\frac{\delta}{i\delta Z}\right]\delta\left(X_t-x\right)\right\rangle. \tag{3.2.37}
$$

Hence, the ME governing the LE in Equation (3.2.31) is given by:

$$
\begin{aligned}
\frac{\partial}{\partial t}p(x,t) = -\alpha(t)\frac{\partial}{\partial x}(x\,p(x,t)) &- \frac{\partial}{\partial x}\beta(x,t)\left\langle \int_0^t \mathrm{d}s\,\gamma(t,s)X_s\delta\left(X_t-x\right)\right\rangle \\
&- \frac{\partial}{\partial x}b(x,t)\left\langle \Sigma_t\left[\frac{\delta}{i\delta Z}\right]\delta\left(X_t-x\right)\right\rangle.
\end{aligned}
\tag{3.2.38}
$$

Now that we have the foundation for building the non-Markovian ME, let's focus on applying it

to X driven by our LE.

3.2.4 Application of the Path Integral Approach to the Langevin Equation

We now apply the path integral approach to the following LE in Equation (0.0.2):

$$\begin{aligned} \dot{X}_t &= -V'(X_t) + \xi_t, \\ \xi_t &= \sum_{i=1}^{N_t} A_i h(t - T_i). \end{aligned} \tag{3.2.39}$$

Denoting the PDF of X by $\mathbb{P}$, we get the following:

$$\begin{aligned} \frac{\partial \mathbb{P}}{\partial t} &= \frac{\partial}{\partial t} \langle \delta(X_t - x) \rangle = \left\langle \dot{X}_t \delta'(X_t - x) \right\rangle \\ &= \left\langle \left(-V'(X_t) + \xi_t \right) \delta'(X_t - x) \right\rangle \\ &= -\left\langle \left(V'(X_t) - V'(x) \right) \delta'\left(X_t - x\right) + V'(x)\delta'\left(X_t - x\right) \right\rangle + \left\langle \xi_t \delta'\left(X_t - x\right) \right\rangle \\ &= -\left\langle -V''(x)\delta\left(X_t - x\right) + V'(x)\delta'\left(X_t - x\right) \right\rangle + \left\langle \xi_t \delta'\left(X_t - x\right) \right\rangle \\ &= -\frac{\partial}{\partial x} \left\langle V'(x)\delta\left(X_t - x\right) \right\rangle - \frac{\partial}{\partial x} \left\langle \xi_t \delta\left(X_t - x\right) \right\rangle \\ &= \frac{\partial}{\partial x} \left[V'(x)\mathbb{P}(x,t) \right] - \frac{\partial}{\partial x} \left\langle \xi_t \delta(X_t - x) \right\rangle . \end{aligned} \tag{3.2.40}$$

Notice that one can find the expectation above by plugging it into the general correlation function in Equation (3.2.30):

$$\langle \xi_t \delta(X_t - x) \rangle = \left\langle \Omega_t \left[\frac{\delta}{i\delta\xi} \right] \delta\left(X_t - x\right) \right\rangle , \tag{3.2.41}$$

where Ω_t is the auxiliary functional defined by

$$\Omega_t[g] := \frac{1}{i} \frac{\delta}{\delta g(t)} \ln \Phi_{\xi,t}[g], \tag{3.2.42}$$

and $\Phi_{\xi;t}$ is the CFal of ξ in Equation (2.3.7) trimmed at time t:

$$\Phi_{\xi;t}[g] = \exp\left[\lambda \int_0^t \mathrm{d}\tau \left(\phi_{A_1}\left(\int_\tau^t \mathrm{d}s\, g(s)h(s-\tau)\right) - 1\right)\right]. \tag{3.2.43}$$

Notice also that as Ω_t is linear, we can directly obtain the following for some time s

$$\frac{\delta}{\delta\xi_s}\delta\left(X_t - x\right) = -\left(\frac{\delta X_t}{\delta \xi_s}\right)\frac{\partial}{\partial x}\delta\left(X_t - x\right). \tag{3.2.44}$$

For any s and t the functional derivative within the parentheses simply equals to one due to the additive nature of the GSN ξ [61]. Therefore, the expectation simplifies to the following:

$$\left\langle \xi_t \delta\left(X_t - x\right)\right\rangle = \left\langle \Omega_t\left[i\frac{\partial}{\partial x}\right]\delta(X_t - x)\right\rangle = \Omega_t\left[i\frac{\partial}{\partial x}\right]\mathbb{P}(x,t). \tag{3.2.45}$$

One can also write Ω_t as the first functional derivative of the trimmed CFal $\Phi_{\xi;t}[g]$ (which we derived in prior equations leading to Equation (2.3.7)):

$$\begin{aligned}
\Omega_t[g] &= \frac{\lambda}{i}\int_0^t \mathrm{d}\tau\, h(t-\tau)\phi'_{A_1}\left(\int_\tau^t \mathrm{d}s\, g(s)h(s-\tau)\right) \\
&= \frac{\lambda}{i}\int_0^t \mathrm{d}\tau\, h(t-\tau)\left\langle iA_1 \exp\left[iA_1\int_\tau^t \mathrm{d}s\, g(s)h(s-\tau)\right]\right\rangle \\
&= \lambda\int_0^t \mathrm{d}\tau\, h(t-\tau)\left\langle A_1\sum_{n=0}^{\infty}\frac{A_1^n}{n!}\left(i\int_\tau^t \mathrm{d}s\, g(s)h(s-\tau)\right)^n\right\rangle \\
&= \lambda\int_0^t \mathrm{d}\tau\, h(t-\tau)\sum_{n=0}^{\infty}\frac{\left\langle A_1^{n+1}\right\rangle}{n!}\left(i\int_\tau^t \mathrm{d}s\, g(s)h(s-\tau)\right)^n \\
&= \sum_{n=0}^{\infty}\frac{\lambda\left\langle A_1^{n+1}\right\rangle}{n!}\int_0^t \mathrm{d}\tau\, h(t-\tau)\left(i\int_\tau^t \mathrm{d}s\, g(s)h(s-\tau)\right)^n
\end{aligned} \tag{3.2.46}$$

where we used the fact that $\phi_{A_1}(\theta) = \left\langle e^{i\theta A_1} \right\rangle \Rightarrow \phi'_{A_1}(\theta) = \left\langle iA_1 e^{i\theta A_1} \right\rangle$ and we applied Taylor expansion on the exponent. Hence we have the following equation for the auxiliary functional:

$$\begin{aligned}
\Omega_t \left[i\frac{\partial}{\partial x} \right] &= \sum_{n=0}^{\infty} \frac{\lambda \left\langle A_1^{n+1} \right\rangle}{n!} \int_0^t \mathrm{d}\tau\, h(t-\tau) \left(\int_\tau^t \mathrm{d}s \left(-\frac{\partial}{\partial x} \right) h(s-\tau) \right)^n \\
&= \sum_{n=0}^{\infty} \frac{\lambda \left\langle A_1^{n+1} \right\rangle}{n!} \int_0^t \mathrm{d}\tau\, h(t-\tau) \left(\int_\tau^t \mathrm{d}s \left(-\frac{\partial}{\partial x} \right) h(s-\tau) \right)^n \\
&= \sum_{n=0}^{\infty} \frac{\lambda \left\langle A_1^{n+1} \right\rangle}{n!} \int_0^t \mathrm{d}\tau\, h(t-\tau) \left(\int_\tau^t \mathrm{d}s\, h(s-\tau) \right)^n \left(-\frac{\partial}{\partial x} \right)^n .
\end{aligned} \tag{3.2.47}$$

Plugging Equations (3.2.47) and (3.2.45) to Equation (3.2.40) yields the non-Markovian ME that solely depends on X:

$$\begin{aligned}
\frac{\partial \mathbb{P}}{\partial t} = &\frac{\partial}{\partial x} \left[V'(x) \mathbb{P}(x,t) \right] \\
&- \frac{\partial}{\partial x} \left[\sum_{n=0}^{\infty} \frac{\lambda \left\langle A_1^{n+1} \right\rangle}{n!} \int_0^t \mathrm{d}\tau\, h(t-\tau) \left(\int_\tau^t \mathrm{d}s\, h(s-\tau) \right)^n \left(-\frac{\partial}{\partial x} \right)^n \right] \mathbb{P}(x,t).
\end{aligned} \tag{3.2.48}$$

Lastly, one can also apply the Gaussian Limits to get the non-Markovian Fokker-Planck Equation (FPE) of X:

$$\frac{\partial \mathbb{P}}{\partial t} = \frac{\partial}{\partial x} \left[V'(x) \mathbb{P}(x,t) \right] + \sigma^2 \int_0^t \mathrm{d}\tau\, h(t-\tau) \int_\tau^t \mathrm{d}s\, h(s-\tau) \frac{\partial^2 \mathbb{P}}{\partial x^2}. \tag{3.2.49}$$

We note that the resulting FPE's obtained by the Itō's approach and path integral approach show some similarities as well as distinct features. We can observe this by plugging the exponential decay impulse function $h(x) = \alpha e^{-\alpha x}$ to the non-Markovian FPE for X obtained in Equation (3.2.49) and

compare it with the Markovian FPE for (X, ξ) in Equation (3.2.19):

$$\begin{aligned}\frac{\partial \mathbb{P}}{\partial t} &= \frac{\partial}{\partial x}\left[V'(x)\mathbb{P}(x,t)\right] + \sigma^2 \int_0^t \mathrm{d}\tau\, h(t-\tau) \int_\tau^t \mathrm{d}s\, h(s-\tau) \frac{\partial^2 \mathbb{P}}{\partial x^2} \\ &= \frac{\partial}{\partial x}\left[V'(x)\mathbb{P}(x,t)\right] + \sigma^2\alpha^2 \int_0^t \mathrm{d}\tau\, e^{-\alpha(t-\tau)} \int_\tau^t \mathrm{d}s\, e^{-\alpha(s-\tau)} \frac{\partial^2 \mathbb{P}}{\partial x^2} \\ &= \frac{\partial}{\partial x}\left[V'(x)\mathbb{P}(x,t)\right] + \sigma^2 \left(1 - e^{-\alpha t} - \frac{1 - e^{-2\alpha t}}{2}\right) \frac{\partial^2 \mathbb{P}}{\partial x^2}.\end{aligned} \tag{3.2.50}$$

Furthermore, letting $\alpha \to \infty$ (thereby ξ becomes GWN) yields:

$$\lim_{\alpha \to \infty} \left(1 - e^{-\alpha t} - \frac{1 - e^{-2\alpha t}}{2}\right) = \frac{1}{2}. \tag{3.2.51}$$

As expected, by choosing harmonic potential $V(x) = \gamma x^2/2$ we obtain the FPE for the Ornstein-Uhlenbeck process that we derived in Equation (1.5.12):

$$\frac{\partial \mathbb{P}}{\partial t} = \gamma \frac{\partial}{\partial x}\left[x\mathbb{P}(x,t)\right] + \frac{\sigma^2}{2} \frac{\partial^2 \mathbb{P}}{\partial x^2}. \tag{3.2.52}$$

One may compare the Klein-Kramers Equation of the joint Markovian PDF of (X, ξ), $\mathbb{P}$, in Equation (3.2.19) with the marginal non-Markovian PDF of X, $\mathbb{P}_X$, in Equation (3.2.50) by plugging the marginalization $\mathbb{P}_X(x,t) = \int_{\mathbb{R}} \mathrm{d}y\, \mathbb{P}(x,y,t)$ into Equation (3.2.19). Once we do so, we can retrieve the first differential of Equation (3.2.50) containing the term with the potential V:

$$\begin{aligned}\frac{\partial \mathbb{P}_X}{\partial t} &= \frac{\partial}{\partial t} \int_{\mathbb{R}} \mathrm{d}y\, \mathbb{P}(x,y,t) = \int \mathrm{d}y\, \frac{\partial \mathbb{P}}{\partial t} \\ &= \int_{\mathbb{R}} \mathrm{d}y \left[\frac{\partial}{\partial x}\left[\left(V'(x) - y\right)\mathbb{P}\right] + \alpha \frac{\partial}{\partial y}\left[y\mathbb{P}\right] + \sigma^2\alpha^2 \frac{\partial^2 \mathbb{P}}{\partial y^2}\right] \\ &= \frac{\partial}{\partial x}\left[V'(x)\mathbb{P}_X(x,t)\right] + \int_{\mathbb{R}} \mathrm{d}y \left[\left(-\frac{\partial}{\partial x} + \alpha \frac{\partial}{\partial y}\right)\left[y\mathbb{P}\right] + \sigma^2\alpha^2 \frac{\partial^2 \mathbb{P}}{\partial y^2}\right].\end{aligned} \tag{3.2.53}$$

The second term above containing the integration with respect to dy is not straightforward to solve.

This is due to the fact that as X and ξ are dependent stochastic processes, their joint PDF $\mathbb{P}$ cannot be written as the product of their marginal PDF's; therefore, one cannot use traditional methods such as separation of variables by assuming solution of the form $\mathbb{P}(x,y,t) = X(x)Y(y)T(t)$. However, the generalized form of this approach, called the *functional* separation of variables, can be used to integrate the ξ-factor out of the joint PDF $\mathbb{P}$ (cf. [31] for more information).

In this thesis we instead outline 2 *ansatzes* that will transform the joint Markovian FPE in Equation (3.2.19) to the non-Markovian FPE in Equation (3.2.50). If we frist provide the following ansatz regarding to the relationship between the joint PDF $\mathbb{P}$ and marginal PDF $\mathbb{P}_X$;

$$\int_{\mathbb{R}} \mathrm{d}y \, \frac{\partial \mathbb{P}}{\partial y} = \left(\int_0^t \mathrm{d}\tau \, e^{-\alpha\tau} \right) \frac{\partial \mathbb{P}_X}{\partial x} \implies \int_{\mathbb{R}} \mathrm{d}y \, \frac{\partial^2 \mathbb{P}}{\partial y^2} = \left(\int_0^t \mathrm{d}\tau \, e^{-\alpha\tau} \int_0^\tau \mathrm{d}s \, e^{-\alpha s} \right) \frac{\partial^2 \mathbb{P}_X}{\partial x^2}, \tag{3.2.54}$$

then we can obtain the second order partial derivative of $\mathbb{P}_X$ as in Equation (3.2.50):

$$\sigma^2\alpha^2 \int_{\mathbb{R}} \mathrm{d}y \, \frac{\partial^2 \mathbb{P}}{\partial y^2} = \sigma^2\alpha^2 \left(\int_0^t \mathrm{d}\tau \, e^{-\alpha\tau} \int_0^\tau \mathrm{d}s \, e^{-\alpha s} \right) \frac{\partial^2 \mathbb{P}_X}{\partial x^2} = \sigma^2 \left(1 - e^{-\alpha t} - \frac{1 - e^{-2\alpha t}}{2} \right) \frac{\partial^2 \mathbb{P}_X}{\partial x^2}. \tag{3.2.55}$$

Notice that we have $\int_{\mathbb{R}} \mathrm{d}y \, \partial\mathbb{P}/\partial y = [\mathbb{P}(x,y,t)]_{y\in\mathbb{R}} = C(x,t)$, where $C(x,t)$ arises due to the partial integration of $\mathbb{P}$ with respect to y. Furthermore, this ansatz works for the white noise case. If we let the impulse function to be the Dirac delta function, $h \to \delta$, which holds for $\alpha \to \infty$, then the PDF relationship in Equation (3.2.54) becomes zero, $\int \mathrm{d}y \, \partial\mathbb{P}/\partial y = 0$. Moreover, if ξ is a white noise process, then the processes X and ξ will be independent and we can write the joint PDF $\mathbb{P}$ and sum of the marginal PDF's of X and ξ, $\mathbb{P}(x,y,t) = \mathbb{P}_X(x,t) + \mathbb{P}_\xi(y,t)$. Thus, we indeed get that $\int \mathrm{d}y \, \partial\mathbb{P}/\partial y = \int \mathrm{d}y \, \partial \left(\mathbb{P}_X + \mathbb{P}_\xi \right) / \partial y = [\mathbb{P}_\xi(y,t)]_{y\in\mathbb{R}} = 0$.

Subsequently, we infer the second ansatz as follows:

$$\int \mathrm{d}y \left[\left(-\frac{\partial}{\partial x} + \alpha \frac{\partial}{\partial y} \right) [y\mathbb{P}] \right] = 0. \tag{3.2.56}$$

Similar to the first ansatz, this equation can be solved using functional separation of variables. Furthermore, notice that the partial differential with respect to X is proportional to the partial differential with respect to ξ with coefficient α that directly arises from the 1-hierarchy impulse function $h(t) = \alpha e^{-\alpha t}$. This suggests that functional analytic methods such as *Fujikawa method*[78] to transform the probability spaces of (X, ξ) into that of X can also be used to integrate the joint FPE. An exemplary approach for this method is outlined in Appendix A where we used it to derive the path integral of X as part of Chapter 4.

Lastly, plugging these two ansatzes into Equation (3.2.53) results in direct correspondence between Equations (3.2.19) for joint Markovian FPE and (3.2.50) for marginal non-Markovian FPE.

We next take a look at the asymptotic properties of the GSN process ξ and show that the impulse function h of ξ plays an important role in characterizing whether ξ is asymptotically a white noise process.

3.3 Limiting and Asymptotic Theorems for the GSN Process

In this section, we show that if the impulse function h is integrable over $[0, \infty[$, then under long-time limit $t \to \infty$, the GSN ξ becomes a white-noise process and hence X becomes Markov process. Before we proceed to prove our statement as a theorem, let us show that our statement under certain examples:

3.3.1 Example For Exponential Decay Impulse Function

Let $h(t) = \alpha e^{-\alpha t}$ be the exponential decay impulse function. Applying it to the Master Equation in (3.2.48) we get,

$$\begin{aligned}\frac{\partial \mathbb{P}}{\partial t} = &\frac{\partial}{\partial x}\left[V'(x)\mathbb{P}(x,t)\right] \\ &+ \frac{\partial}{\partial x}\left[\sum_{n=0}^{\infty} \frac{\lambda \left\langle A_1^{n+1}\right\rangle}{n!}\alpha^{n+1}\int_0^t \mathrm{d}\tau\, e^{-\alpha(t-\tau)}\left(\int_\tau^t \mathrm{d}s\, e^{-\alpha(s-\tau)}\right)^n\left(-\frac{\partial}{\partial x}\right)^n\right]\mathbb{P}(x,t).\end{aligned} \tag{3.3.1}$$

Applying long-time limit yields

$$\begin{aligned}\int_0^t \mathrm{d}\tau\, e^{-\alpha(t-\tau)}\left(\int_\tau^t \mathrm{d}s\, e^{-\alpha(s-\tau)}\right)^n &= \alpha^{-n}\int_0^t \mathrm{d}\tau\, e^{-\alpha(t-\tau)}\left(1-e^{-\alpha(t-\tau)}\right)^n = \frac{\left(1-e^{-\alpha t}\right)^{n+1}}{(n+1)\,\alpha^{n+1}} \\ &\xrightarrow{t\to\infty} \frac{1}{(n+1)\alpha^{n+1}}.\end{aligned} \tag{3.3.2}$$

Therefore our ME simply reduces to the ME of GenOU process:

$$\begin{aligned}\frac{\partial \mathbb{P}}{\partial t} &= \frac{\partial}{\partial x}\left[V'(x)\mathbb{P}(x,t)\right] - \frac{\partial}{\partial x}\left[\sum_{n=0}^{\infty}\frac{\lambda\left\langle A_1^{n+1}\right\rangle}{n!}\frac{1}{n+1}\left(-\frac{\partial}{\partial x}\right)^n\right]\mathbb{P}(x,t) \\ &= \frac{\partial}{\partial x}\left[V'(x)\mathbb{P}(x,t)\right] + \sum_{n=1}^{\infty}\frac{\lambda\left\langle A_1^{n}\right\rangle}{n!}\left(-\frac{\partial}{\partial x}\right)^n\mathbb{P}(x,t).\end{aligned} \tag{3.3.3}$$

Lastly, one can easily witness that further applying Gaussian Limits will yield the Fokker Planck Equation of the OU process X.

3.3.2 Example for Power Law Impulse Function

Now, we let the impulse function be a power law decay: $h(x) = \frac{\alpha-1}{(-c)^{1-\alpha}}(x-c)^{-\alpha}$, where $\alpha, c > 0$ are positive coefficients. As one can establish, this type of impulse function does not belong to the $n-$th hierarchy classification of ξ. Therefore, applying a new impulse function will help us better understand the characteristic of our GSN ξ and hence create an ansatz to prove our long-time limit statement for general impulse function h.

For this case, we have defined variables α, c to be strictly positive in order to circumvent any singularities. Accordingly, the term $\frac{\alpha-1}{(-c)^{1-\alpha}}$ is the normalizing constant satisfying our condition [v]:

$$\int_0^\infty \mathrm{d}x\, h(x,c) = 1. \tag{3.3.4}$$

Therefore, we can solve the following integral,

$$\begin{aligned}\int_0^t \mathrm{d}\tau\, h(t-\tau)\left(\int_\tau^t \mathrm{d}s\, h(s-\tau)\right)^n &= \left(\frac{\alpha-1}{(-c)^{1-\alpha}}\right)^{n+1}\int_0^t \mathrm{d}\tau\,(t-\tau-c)^{-\alpha}\left(\int_\tau^t \mathrm{d}s\,(s-\tau-c)^{-\alpha}\right)^n \\ &= \left(\frac{\alpha-1}{(-c)^{1-\alpha}}\right)^{n+1}\frac{1}{(1-\alpha)^n}\cdot \\ &\quad\cdot\int_0^t \mathrm{d}\tau\,(t-\tau-c)^{-\alpha}\left((t-\tau-c)^{1-\alpha}-(-c)^{1-\alpha}\right)^n\end{aligned} \tag{3.3.5}$$

[v] As the impulse function h must be integrable over $[0,\infty[$, we introduced the normalization term to h such that $h(x) \to 0$ as $\alpha \to 1$. Without the normalization term the integral $\int_0^\infty \mathrm{d}x\, h(x)$ diverges as $\alpha \to 1$.

Setting $\alpha = 2$ yields the following limit:

$$\begin{aligned}
&(-c)^{n+1}(-1)^n \int_0^t \mathrm{d}\tau\,(t-\tau-c)^{-2}\left((t-\tau-c)^{-1}-(-c)^{-1}\right)^n \\
&= -c^{n+1}\frac{1}{c(n+1)}\frac{t}{c-t}\left(\frac{1}{c}+\frac{1}{c-t}\right)^n \\
&\xrightarrow{t\to\infty} \frac{1}{(n+1)},
\end{aligned} \tag{3.3.6}$$

yielding again the Master Equation of GenOU process as in Equation (3.3.3).

3.3.3 Limiting Theorem

Witnessing what we have achieved in previous examples of impulse functions, we deduce the following corollary as the Markov Convergence Theorem (MCT):

Theorem 3.3.1 (Markov Convergence Theorem). *Let X be the position process defined by the following generalized LE:*

$$\begin{aligned}
\frac{\mathrm{d}X_t}{\mathrm{d}t} &= -V'(X_t) + \xi_{t^-}, \\
\xi_t &= \sum_{i=1}^{N_t} A_i h(t-T_i),
\end{aligned} \tag{3.3.7}$$

where N_t forms the Poisson process with intensity $\lambda > 0$, A_i are iid random variables with well-defined moments, and T_i are arrival times.

For any integrable impulse function h satisfying the following condition,

$$\int_0^\infty \mathrm{d}x\, h(x) = 1, \tag{3.3.8}$$

the position process X converges in time to a Markov process driven by PWN.

In other words, we have that

$$\xi_t \xrightarrow{t\to\infty} \xi_t^{PWN}, \tag{3.3.9}$$

where ξ_t^{PWN} *is the PWN process satisfying the correlation* $\left\langle \xi_t^{PWN}\xi_s^{PWN}\right\rangle = \lambda \left\langle A_1^2\right\rangle \delta(t-s)$.

Proof. Let $\mathbb{P}$ be the pdf of X. As probability functions uniquely define the stochastic processes, we can confirm the time convergence of X using its Master Equation, as we have found in (3.2.48).

Furthermore notice that, as we have established in 2 previous examples, it is sufficient to prove the following

$$\int_0^t \mathrm{d}\tau\, h(t-\tau)\left(\int_\tau^t \mathrm{d}s\, h(s-\tau)\right)^n = \frac{1}{n+1}. \tag{3.3.10}$$

Using the substitution $u = \int_\tau^t \mathrm{d}s\, h(s-\tau)$, hence $\mathrm{d}u = -h(t-\tau)\,\mathrm{d}\tau$, we have that,

$$\int_0^{\int_0^t \mathrm{d}s\, h(s-\tau)} \mathrm{d}u\, u^n = \left[\frac{u^{n+1}}{n+1}\right]_0^{\int_0^t \mathrm{d}s\, h(s-\tau)} = \frac{1}{n+1}\left(\int_0^t \mathrm{d}s\, h(s-\tau)\right)^{n+1} \xrightarrow{t\to\infty} \frac{1}{n+1}, \tag{3.3.11}$$

where we have used our necessary condition of h in last step. □

The MCT is a very useful tool to identify the asymptotic behavior of X. The theorem simply states that for any globally integrable impulse function h, *regardless* of its classification, the GSN process ξ converges asymptotically to the PWN process.

3.3.4 Formulating a Relationship between the Impulse Function and the Diffusion Coefficient of the Position Process

Recall from Equation (3.2.49) that under Gaussian Limits we get the following FPE for X:

$$\frac{\partial \mathbb{P}}{\partial t} = \frac{\partial}{\partial x}\left[V'(x)\mathbb{P}(x,t)\right] + \sigma^2 \int_0^t \mathrm{d}\tau\, h(t-\tau)\int_\tau^t \mathrm{d}s\, h(s-\tau)\frac{\partial^2 \mathbb{P}}{\partial x^2}. \tag{3.3.12}$$

Here, we aim to show that a specific impulse function h would yield a super- (sub)-diffusive particle, i.e. $\langle X_t^2 \rangle \sim t^\beta$, for any $\beta > 1\ (< 1)$. This can be obtained by finding an impulse function satisfying the following integral equation of the diffusion coefficient:

$$\int_0^t \mathrm{d}\tau\, h(t-\tau) \int_\tau^t \mathrm{d}s\, h(s-\tau) = t^\beta. \tag{3.3.13}$$

As before, we can use change of variables $u = \int^t \mathrm{d}s\, h(s-\tau)$ to obtain the following:

$$\int_0^{\int_0^t \mathrm{d}\tau\, h(t-\tau)} \mathrm{d}u\, u = t^\beta, \tag{3.3.14}$$

yielding the following Volterra convolution equation:

$$\frac{\left(\int_0^t \mathrm{d}\tau\, h(t-\tau)\right)^2}{2} = t^\beta \Longrightarrow \int_0^t \mathrm{d}\tau\, h(t-\tau) = \sqrt{2}\, t^{\frac{\beta}{2}}. \tag{3.3.15}$$

The above integral can be solved in Laplacian space; namely, given $\mathcal{L}$ and $\mathcal{L}^{-1}$ respective the Laplace and inverse Laplace transform operators, denoting $\hat{h}(s)$ the Laplace transform of the impulse function $h(t)$ we obtain the following:

$$\mathcal{L}\left\{\int_0^t \mathrm{d}\tau\, h(t-\tau)\right\}(s) = \hat{h}(s) \cdot \frac{1}{s} = \sqrt{2}\mathcal{L}\{t^{\frac{\beta}{2}}\}(s), \tag{3.3.16}$$

where we used the convolution property. Rearranging the terms and noting that $\mathcal{L}^{-1}\{s\} = \delta'(t)$, we have the following:

$$\begin{aligned}\hat{h}(s) =& \sqrt{2}\,\mathcal{L}\left\{t^{\frac{\beta}{2}}\right\}\cdot s = \sqrt{2}\,\mathcal{L}\left\{t^{\frac{\beta}{2}}\right\}\cdot\mathcal{L}\left\{\delta'(t)\right\}\\ =& \sqrt{2}\,\mathcal{L}\left\{\int_0^t \mathrm{d}s\, s^{\frac{\beta}{2}}\delta'(t-s)\right\}\\ =& \sqrt{2}\,\mathcal{L}\left\{\int_0^t \mathrm{d}s\, \frac{\beta}{2}s^{\frac{\beta}{2}-1}\delta(t-s)\right\}\\ =& \frac{\sqrt{2}}{2}\beta\mathcal{L}\{t^{\frac{\beta}{2}-1}\Theta(t)\},\end{aligned} \tag{3.3.17}$$

yielding the desired impulse function by applying inverse Laplace transform,

$$h(t) = \frac{\sqrt{2}}{2}\beta t^{\frac{\beta}{2}-1}\Theta(t). \tag{3.3.18}$$

Notice that we can indeed generalize this approach *for any* diffusion coefficient. Given the Fokker Planck Equation (FPE) of X under Harmonic potential and Gaussian limits as,

$$\frac{\partial\mathbb{P}}{\partial t} = \gamma\frac{\partial}{\partial x}\left[x\mathbb{P}(x,t)\right] + \sigma^2 m(t)\frac{\partial^2\mathbb{P}}{\partial x^2}, \tag{3.3.19}$$

where $m(t)$ is the differentiable diffusion coefficient, the impulse function h associated with the GSN ξ must be of the form:

$$h(t) = \frac{\sqrt{2}}{2}\frac{m'(t)}{\sqrt{m(t)}}\Theta(t). \tag{3.3.20}$$

Or, in better formulation, the FPE of X under Gaussian Limits is of the following form,

$$\frac{\partial\mathbb{P}}{\partial t} = \frac{\partial}{\partial x}\left[V'(x)\mathbb{P}(x,t)\right] + \sigma^2\frac{m^2(t)}{2}\frac{\partial^2\mathbb{P}}{\partial x^2} \tag{3.3.21}$$

if and only if the impulse function is given by $h(t) = m'(t)\Theta(t)$. This is a very important outcome

of our thesis, where one can model the trajectory of any particle by assigning it a suitable impulse function h calculated from the diffusion coefficient $m(t)$ with respect to time.

3.3.5 Convergence of the GSN process to the Generalized Gaussian Process

Next, we will use the same limiting cases to our GSN in order to get a generalized Gaussian process with a well-defined correlation function. We have formally given in our Theorem below, with proof as follows:

Theorem 3.3.2. *Let ξ be the GSN process. Then, for fixed $\lambda \left\langle A_i^2 \right\rangle = \sigma^2$, our GSN process converges in distribution to a general Gaussian process G:*

$$\lim_{\substack{\lambda \to \infty \\ \langle A_i \rangle \to 0}} \xi_t \xrightarrow{\mathcal{D}} \sigma G_t, \tag{3.3.22}$$

where it is defined by the following correlation function:

$$\langle G_t G_s \rangle = \int_0^{t \wedge s} \mathrm{d}\tau \, h(t-\tau) h(s-\tau). \tag{3.3.23}$$

Proof. We apply the same concept as in the previous lemma. We will also show here that we can indeed apply the distributional converge to CFals.

Therefore,

$$\begin{aligned}
\Phi_{\xi}[g] &= \exp\left[\lambda \int_0^\infty \mathrm{d}\tau \left(\phi_{A_1}\left(\int_\tau^\infty g(t)h(t-\tau)\right) - 1\right)\right] \\
&= \exp\left[\lambda \int_0^\infty \mathrm{d}\tau \left(\left\langle \exp\left(iA_1 \int_\tau^\infty \mathrm{d}t\, g(t)h(t-\tau)\right)\right\rangle - 1\right)\right] \\
&= \exp\left[\lambda \int_0^\infty \mathrm{d}\tau \left(\left\langle 1 + iA_1 \int_\tau^\infty \mathrm{d}t\, g(t)h(t-\tau)\right.\right.\right. \\
&\qquad\qquad \left.\left.\left. - \frac{1}{2}A_1^2 \left(\int_\tau^\infty \mathrm{d}t\, g(t)h(t-\tau)\right)^2 + \mathcal{O}\left(A_1^3\right)\right\rangle - 1\right)\right] \\
\longrightarrow \exp&\left[-\frac{\sigma^2}{2}\int_0^\infty \mathrm{d}\tau \left(\int_\tau^\infty \mathrm{d}t\, g(t)h(t-\tau)\right)^2\right] =: \Phi_G[g],
\end{aligned} \tag{3.3.24}$$

where we applied the Gaussian Limits in last step.

Notice that this is indeed the CFal of the generalized Gaussian process $\sigma\left(G_t\right)_{t\geq 0}$, as its increment is defined by the Normal distribution;

$$G_t \sim \mathcal{N}\left(0, \int_0^t \mathrm{d}\tau\, h^2(t-\tau)\right), \tag{3.3.25}$$

Hence, by Lévy's Continuity Theorem, we have that the limit is indeed a generalized Gaussian process:

$$\lim_{\substack{\lambda\to\infty \\ \langle A_1\rangle \to 0 \\ \lambda\langle A_1^2\rangle = \sigma^2}} \xi_t \xrightarrow{\mathcal{D}} \sigma G_t. \tag{3.3.26}$$

Lastly, in order to prove the correlation, we simply apply two functional derivatives on $\Phi_G[g]$:

$$\begin{aligned}\frac{\partial \Phi_G[g]}{\partial g(t_1)} &= \sigma^2 \int_0^\infty \mathrm{d}\tau \int_\tau^\infty \mathrm{d}t\, g(t) h(t-\tau) \cdot \int_\tau^\infty \mathrm{d}t\, \delta(t-t_1) h(t-\tau) \Phi_G[g], \\ \frac{\partial^2 \Phi_G[g]}{\partial g(t_1) \partial g(t_2)} &= \sigma^2 \int_0^\infty \mathrm{d}\tau \int_\tau^\infty \mathrm{d}t\, \delta(t-t_1) h(t-\tau) \cdot \left(\int_\tau^\infty \mathrm{d}t\, \delta(t-t_1) h(t-\tau) \Phi_G[g] \right. \\ &\qquad \left. + \int_\tau^\infty \mathrm{d}t\, g(t) h(t-\tau) \frac{\partial \Phi_G[g]}{\partial g(t_2)} \right),\end{aligned} \tag{3.3.27}$$

where this yields the correlation function:

$$\langle G_{t_1} G_{t_2} \rangle = \int_0^{t_1 \wedge t_2} \mathrm{d}\tau\, h(t_1-\tau) h(t_2-\tau), \tag{3.3.28}$$

which completes the proof. □

Interestingly, this type of s.p. G with correlation given in Equation (3.3.23) forms by far the broadest class of Gaussian processes. For an example, the *fractal Brownian motion* (fBm) B, which is defined as the generalization of the Gaussian processes, is uniquely defined by its correlation function [106] $\langle B_{t_1} B_{t_2} \rangle = (t_1 \wedge t_2)^{2H}$, where $H \in [0,1]$ is called the Hurst parameter that determines the characteristics of the fBm, noting that $H = 1/2$ yields the Wiener process. Letting $t_1 = t_2 = t$ and equating the correlation function of fBm to that of Equation (3.3.23) in Laplace space, as we did in

Section 3.3.4, yields two impulse functions that satisfy this correlation:

$$\begin{aligned}
\mathcal{L}\left\{\int_0^t \mathrm{d}\tau\, h(t-\tau)^2\right\}(s) &= \mathcal{L}\left\{t^{2H}\right\}(s) \\
\implies \mathcal{L}\left\{h(t)^2\right\}(s) &= \mathcal{L}\left\{\int_0^t \mathrm{d}\tau\, \tau^{2H}\partial'(t-\tau)\right\}(s) \\
&= 2H\,\mathcal{L}\left\{\int_0^t \mathrm{d}\tau\, \tau^{2H-1}\partial(t-\tau)\right\}(s) \\
&= 2H\,\mathcal{L}\left\{t^{2H-1}\Theta(t)\right\}(s) \\
\implies h(t) &= \pm\sqrt{2H}\,t^{H-1/2}\Theta(t).
\end{aligned} \tag{3.3.29}$$

One can easily check that for $H = 1/2$, the impulse function above simply becomes the Heaviside step function, $h(t) = \Theta(t)$ and thus, by Theorem 1.2.1 the process ξ indeed converges to the Wiener process under Gaussian Limits. Furthermore, recalling from Section 2.5, this impulse function is left-handed (due to $\Theta(t)$) and can also be right-handed if $H < 1/2$. Also, for any $H \in [0,1]$ the impulse function is not globally integrable. We can observe this behavior in Figure 3.1 where we plotted the impulse function for various Hurst parameters H.

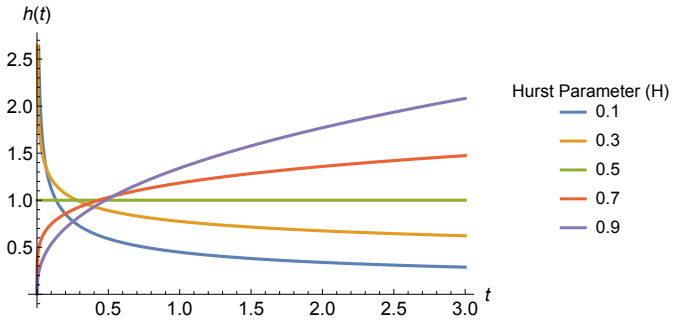

Figure 3.1: Plot of the impulse function h of the fractional Brownian motion for different Hurst parameters H.

This Gaussian distribution property of the GSN process directly indicates that one can find all the characteristics of Gaussian processes directly from the GSN process we have extensively analyzed throughout Chapters 2-3.

We now move forward to simulate our findings on the MCT, where we will show convergence in distribution of the GSN process to the PWN process using the solution of the LE in (0.0.2) with different candidate potentials V.

3.4 Simulation Results on Markov Convergence Theorem

Here, we numerically show that the asymptotic limits we have proven in this chapter are correct. For simplicity in our numerical integration, we opted to simulate the LE in Equation (0.0.2) using Gaussian jump amplitudes with CF $\phi_{A_1}(\theta) = \exp\left(-\theta^2/2\right)$, unit jump intensity $\lambda = 1$, and exponentially decaying impulse function $h(x) = \alpha e^{-\alpha x}$. We aim to numerically obtain the results of the MCT by simulating the realizations of the position process X driven by the zero-potential LE $\dot{X} = \xi$, where ξ is the GSN process.

Recalling Theorem 3.3.1, if the conditions in MCT holds, then the GSN process ξ_t converges asymptotically to the Poisson White Noise process. Therefore, X, which is formed by the time integrals of ξ, should converge to the time-integral of the PWN, i.e. the Compound Poisson process. For simulations, we chose the exponential decay impulse function where it holds the MCT conditions. Indeed, in Figure 3.2, we can observe convergence in distribution at around $t = 50$.

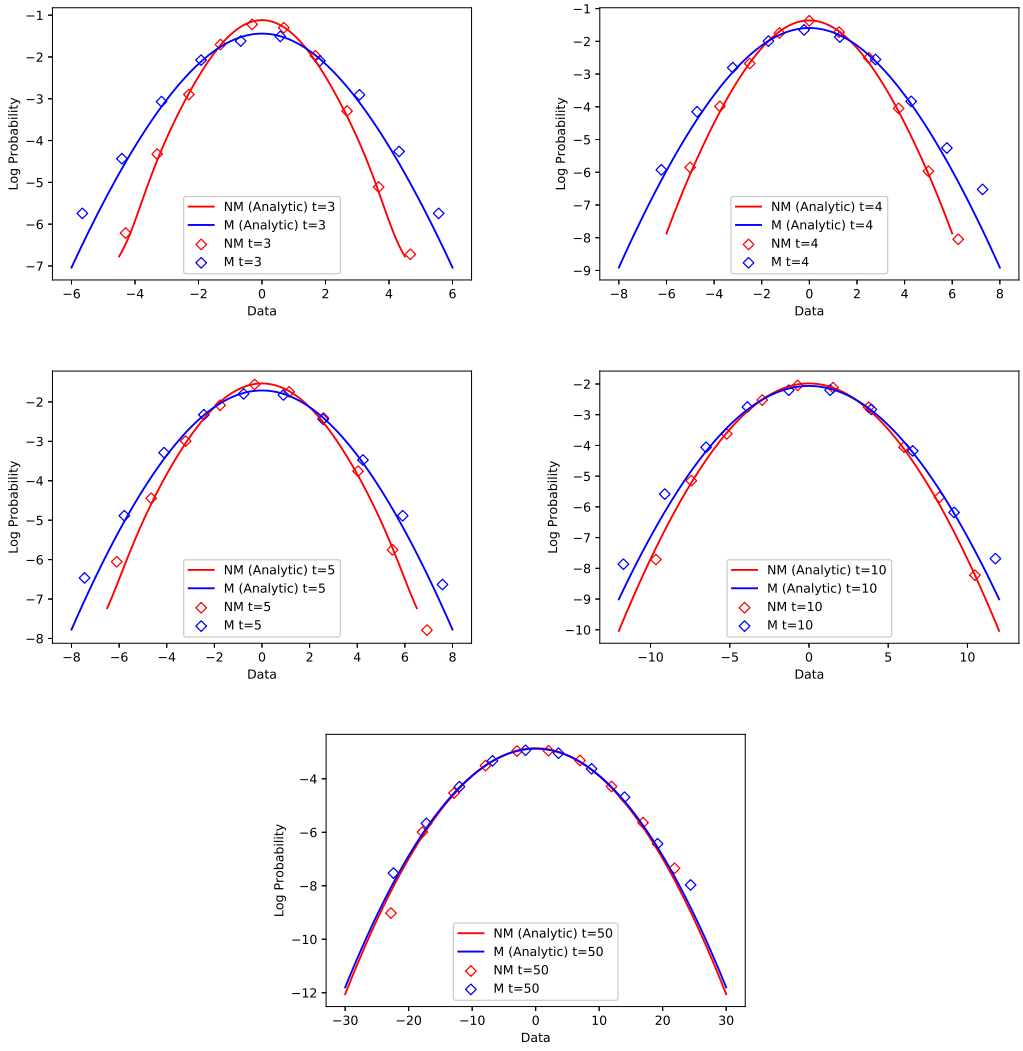

Figure 3.2: Probability distribution (log-scale) of X_t as solution of the LE $\dot{X}_t = \xi_t$. Graphs colored in red are cases where ξ is the GSN (hence X is Non-Markovian (NM)); whereas those in blue are cases where ξ the PWN (hence X is Markovian (M)). Scatter plots are simulations obtained by Monte Carlo method with 5,000 iterations, and line plots are analytic solutions of the PDF's obtained by Inverse Fourier Transform of the characteristic functions. As we increase time t, we can visualize convergence in distribution. For simulating the realizations of ξ we chose the $\alpha = 1, \lambda = 5$, and $A_i \sim \mathcal{N}(0, \lambda^{-1})$.

3.5 Chapter Review

In this chapter, we provided new results of the GSN process ξ with interesting properties. We first showed that the time derivative of ξ is recursive and depends on the time derivative of the impulse function h. The infinite recursive nature of ξ can be truncated to a finite value n if there exists an n-th order linear ODE for h.

We next derived the ME of the position process X driven by ξ, where we used both Itō's approach in Chapter 1 and Hänggi's approach that is designed especially for non-Markovian s.p.'s. Both these methods are useful tools to find the PDF of X. The Itō's method yields Markovian ME with respect to the tuple of the position process and the hierarchies of the GSN, $\left(X, \xi, {}^{(1)}\xi, \dots\right)$ as in Equation (3.2.8); whereas the Hänggi's method yields the non-Markovian ME in Equation (3.2.48) that solely governs X. Although we provided ansatzes to provide a heuristic relationship between the Markovian Master Equation of (X, ξ) via Itō's approach and the non-Markovian ME of X via Hänggi's approach, finding a analytic transformation between these two Master Equations is currently an open question, and could be further investigated in future research, such as using the functional separation of variables technique[31], or obtaining the *Jacobian* functional from transforming the joint PDF $\mathbb{P}$ to marginal PDF of X, $\mathbb{P}_X$, via *Fujikawa method*[78], outline of which can be inferred from Appendix A. Besides finding analytic correspondence, one can also apply numeric techniques, such as *method of lines*[32], to partially integrate the joint PDF $\mathbb{P}$.

Moreover, finding analytic solutions of these ME's is close to impossible unless we assume special cases for h or consider asymptotic limits of ξ. This asymptotic behavior of ξ is encompassed within the following section, where our analysis shows that the GSN process converges to the Poisson White Noise for $h \to \delta$, and further to a generalized Gaussian process under Gaussian limits. Indeed, we showed that by Markov Convergence Theorem (MCT), the GSN process ξ asymptotically converges in distribution to the PWN for any globally integrable impulse function h. We then

backed our analytical results of the MCT by numerical simulation, where we observe that the non-Markovian process converges in distribution to the Markov process (Figure 3.2).

In the next chapter, we show another method of finding the PDF of X driven by ξ via *path integral* approach, where we apply our results obtained throughout the previous chapters. We will also investigate the *escape problem* of X, which arises directly from computing its path integral.

Mathematics are the result of mysterious powers which no one understands, and which the unconscious recognition of beauty must play an important part. Out of an infinity of designs a mathematician chooses one pattern for beauty's sake and pulls it down to earth.

Marston Morse

4

Stationary Action Principle for Non-Markovian Processes

4.1 Introduction

This chapter focuses on deriving the stationary action principle using the non-Markovian process X driven by the Langevin Equation $\dot{X}_t = -V'(X_t) + \xi_t$, recalling that V is the potential of the system

and ξ_t forms the GSN process with impulse function h as in Equation 0.0.2.

We begin this chapter by introducing the basic concepts of Lagrangian mechanics, namely the concepts of the *Lagrangian*, *stationary action principle*, *Euler-Lagrange equations* and *equations of motion*. Next, we introduce the *optimal escape problem*, which is the stationary action principle of X under potential V that has more than one stable state (e.g. double-well potential).

These definitions will then be used to derive the path integral formulation, proposed by Richard Feynman & Albert Hibbs in 1965 [85], where it is found by the functional integral of the Lagrangian of stochastic processes. The path integral formulation will help us derive the probability amplitude of X, from where we can ultimately achieve the main goal of this thesis by calculating its PDF.

Path integral formulation is a very important tool used for not only finding the PDF of X for any potential V and impulse function h, but to also for helping us better understand the behavior of X, most importantly its time-non-local (TNL) property, which makes finding its PDF extremely difficult. Nonetheless, we show that if h is an $n-$hierarchy impulse function (cf. Definition 2.5.3), then the TNL property of X vanishes and we can find Lagrangian and $(2n+2)-$dimensional equations of motion of X, both of which is local in time. This property fundamentally agrees with our understanding of the hierarchical nature of ξ, as we analyzed extensively in Chapters 2,3.

We then move on to final section of this chapter by introducing the *Markov Embedding* technique in order to simplify the equations of motion of X. By approximating *any* impulse function h as a sum of exponential decay functions in the complex plane, the resulting equations of motion of X, and therefore its Lagrangian and hence its PDF, will be much more easier to calculate numerically.

Before we begin this chapter, we expect the reader to have preliminary knowledge of functional calculus, especially functional integration, as well as a basic understanding of Lagrangian mechanics. We will, albeit briefly, touchdown the Lagrangian mechanics throughout this introductory section; however for further remarks, we encourage the reader to refer to a wide-scope book published by Gi-

aquinta & Hildebrandt[21] for the mathematics of Lagrangian mechanics and functional integration, as well as[22] for further physical aspects of both concepts.

4.1.1 Path Integral Formulation

Path integral formulation was first introduced by Feynman & Hibbs to bring forth a *global* formalism of quantum mechanics[86]. The formalism is defined to predict the possible path of a particle from point A to point B by taking into account all possible paths it can take between those two points. The formulation works by integrating over the *functional space of paths* of the particle and assigning a complex-valued function π called the *probability amplitude*. One can then derive the PDF $\mathbb{P}$ of the particle by taking the squared modulus of its probability amplitude: $\mathbb{P} = |\pi|^2$.

Path integrals are widely used in scopes outside of quantum mechanics. For example, it is used in biophysics to model the transition between two different states of DNA during transcription phases[23] or modeling the evolutionary process of species[24].

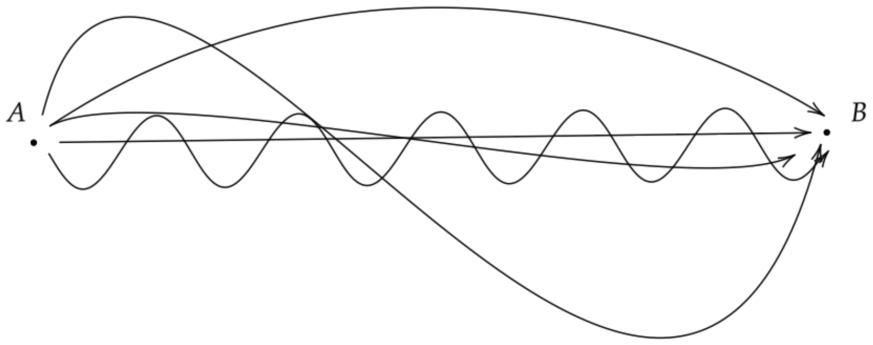

Figure 4.1: Depiction of 5 out of infinitely possible paths from point A to point B. Path integral works by integrating over all possible trajectories of the particle from A to B and output the probability amplitude π of the particle between this range.

Feynman & Hibbs showed in[85] that the probability amplitude of a particle between the time

range $[t_a, t_b]$ and end-points $x(t_a) \equiv x_a$ and $x(t_b) \equiv x_b$, is given by the following functional integration:

$$\pi(x_b, t_b | x_a, t_a) = \int_{\mathscr{C}} \mathcal{D}[x] \; \exp\left(i \int_{t_a}^{t_b} \mathrm{d}t \, \mathscr{L}\left(x(t), \dot{x}(t), \ddot{x}(t), \dots\right)\right), \tag{4.1.1}$$

where $\mathscr{C} = [x_a, x_b]$ is the *configuration space* of all paths of the particle between times t_a and t_b, and function $\mathscr{L}$ is the *Lagrangian* of the particle that depends on the particle's position function $x(t)$ all its derivatives. The tuple $(\mathscr{C}, \mathscr{L})$ together form the *Lagrangian system* of the particle [22].

In most physical contexts including formulation by Feynman & Hibbs, the integration of the Lagrangian is normally defined as the *action* functional S:

$$S[x, \dot{x}, \ddot{x}, \dots] = \int_{t_a}^{t_b} \mathrm{d}t \, \mathscr{L}\left(x(t), \dot{x}(t), \ddot{x}(t), \dots\right); \tag{4.1.2}$$

in fact, rewriting Equation (4.1.1) in terms of the action functional is the most common way to define the probability amplitude in literature:

$$\pi(x_b, t_b | x_a, t_a) = \int_{\mathscr{C}} \mathcal{D}[x] \; \exp\left(i \, S[x, \dot{x}, \ddot{x}, \dots]\right). \tag{4.1.3}$$

Here, the Lagrangian $\mathscr{L}$ of a particle is the difference between its *kinetic* energy (energy of the particle itself) and *potential* energy (energy of interaction between the particle and the external forces such as gravity, friction, etc.). Furthermore, the action S is a functional that assigns a numerical value to the Lagrangian system by integrating the Lagrangian over $[t_a, t_b]$. In fact, the action functional is used to find the *stationary action principle* by minimizing the Lagrangian.

The stationary action principle dictates that out of infinitely possible paths between points x_a and x_b, the particle travels the path that has the stationary action [22]. Such path is defined as the *optimal path* of the particle and is usually denoted with an asterisk x^*. We can explain this phenomenon in Figure 4.1, where under no external forces (i.e. zero potential energy) that can affect the system,

the optimal path of the particle that travels from point A to point B would be a straight line, as it will intuitively use the least energy. We will validate this mathematically in the next section, where by minimizing the Lagrangian we obtain an ODE called the *Euler-Lagrange Equations*, also known in physical contexts as *equation of motion*.

4.1.2 Optimal Path Calculation

As we explained in the previous section, the optimal path of a particle is found by finding its stationary action. Let $(\mathscr{C}, \mathscr{L})$ be the Lagrangian system of the particle whose position in time is defined by $x(t)$, and let S be its associated action. Then, the infinitesimal change in S is found by applying the total functional derivatives[25]:

$$\begin{aligned} S = \int_{t_a}^{t_b} \delta S &= \int_{t_a}^{t_b} \mathrm{d}t \left(\frac{\partial S}{\partial x}\delta x + \frac{\partial S}{\partial \dot{x}}\delta \dot{x} + \frac{\partial S}{\partial \ddot{x}}\delta \ddot{x} + \dots \right) \\ &= \int_{t_a}^{t_b} \mathrm{d}t \left(\frac{\partial S}{\partial x}\delta x - \frac{\mathrm{d}}{\mathrm{d}t}\frac{\partial S}{\partial \dot{x}}\delta x + \left(\frac{\mathrm{d}}{\mathrm{d}t}\right)^2 \frac{\partial S}{\partial \ddot{x}}\delta x + \dots \right) \\ &= \int_{t_a}^{t_b} \mathrm{d}t \left(\delta x \sum_{j=0}^{\infty} \left(-\frac{\mathrm{d}}{\mathrm{d}t}\right)^j \frac{\partial S}{\partial x^{(j)}} \right), \end{aligned} \tag{4.1.4}$$

where $x^{(j)}$ refers to jth time derivative of x and in the third equation we applied integration by parts j times on each $\delta x^{(j)}$. We can then find the stationary action by letting $\delta S = 0$ in Equation (4.1.4):

$$\begin{aligned} \delta S = 0 \iff \mathrm{d}t \left(\delta x \sum_{j=0}^{\infty} \left(-\frac{\mathrm{d}}{\mathrm{d}t}\right)^j \frac{\partial S}{\partial x^{(j)}} \right) = 0 \\ \implies \sum_{j=0}^{\infty} \left(-\frac{\mathrm{d}}{\mathrm{d}t}\right)^j \frac{\partial S}{\partial x^{(j)}} = 0. \end{aligned} \tag{4.1.5}$$

Instead of writing Equation (4.1.5) in terms of S, we can use its definition on Equation (4.1.2) to rewrite it in terms of the partial derivatives of the Lagrangian $\mathscr{L}$, which yields the Euler-Lagrange

Equation (ELE):

$$\sum_{j=0}^{\infty} \left(-\frac{\mathrm{d}}{\mathrm{d}t}\right)^{j} \frac{\partial \mathscr{L}}{\partial x^{(j)}} = 0. \tag{4.1.6}$$

Solving this ELE ultimately yields the optimal path $x^*(t)$ for the Lagrangian system.

Now that we have shown how this formulation is derived, we can now give some basic examples. Let us consider a particle with mass $m > 0$ defined by the Lagrangian system $(\mathscr{C}, \mathscr{L})$. Let us also first assume that the particle has zero potential energy. Defining its position in time by $x(t)$, the particle's kinetic energy and thus its Lagrangian is given by $\mathscr{L} = m\left(\dot{x}\right)^2/2$, where we can observe that it solely depends on $\dot{x}$. We then plug this into the ELE:

$$\sum_{j=0}^{\infty} \left(-\frac{\mathrm{d}}{\mathrm{d}t}\right)^{j} \frac{\partial \mathscr{L}}{\partial x^{(j)}} = -\frac{\mathrm{d}}{\mathrm{d}t}\frac{\partial \mathscr{L}}{\partial \dot{x}} = -m\frac{\mathrm{d}\dot{x}}{\mathrm{d}t} = 0. \tag{4.1.7}$$

Notice that the ELE simply becomes $m\ddot{x} = 0$, where its solution (i.e. the optimal path) is given by a straight line $x(t) = c_1 t + c_2 = x^*(t)$ with integral coefficients c_1 and c_2. This agrees with our intuitive understanding that without any potential energy, the optimal path between two points, regardless of its mass m, is always a straight line.

Let us introduce potential energy to the Lagrangian system. Defining V to be the potential function, the Lagrangian is then given by $\mathscr{L} = m\left(\dot{x}\right)^2/2 - V(x)$, where it now depends on both x and $\dot{x}$. Plugging this to the ELE yields the following:

$$\begin{aligned} \frac{\partial \mathscr{L}}{\partial x} - \frac{\mathrm{d}}{\mathrm{d}t}\frac{\partial \mathscr{L}}{\partial \dot{x}} &= 0 \\ \implies -V'(x) - m\ddot{x} &= 0. \end{aligned} \tag{4.1.8}$$

This is a classical result of *Newton's Second Law of Motion* where external force acting on a particle is equal to is its mass times its acceleration.

From the optimal path we can further obtain the stationary action of such particle. By inte-

grating the equation of motion w.r.t. over $[t_a, t]$ yields $m\dot{x} = m\dot{x}_a - \int_{t_a}^{t} \mathrm{d}\tau\, V'(x(\tau))$, where $\dot{x}_a \equiv \dot{x}(t)|_{t=t_a}$. Thus, the stationary action of the particle over the region $[t_a, t_b]$ is given by

$$S[x^*, \dot{x}^*] = \int_{t_a}^{t_b} \mathrm{d}t\, \mathscr{L}\left(x^*(t), \dot{x}^*(t)\right) = \int_{t_a}^{t_b} \mathrm{d}t \left(\frac{1}{2m} \left(m\dot{x}_a^* - \int_{t_a}^{t} \mathrm{d}\tau\, V'(x^*(\tau)) \right)^2 - V(x^*(t)) \right), \tag{4.1.9}$$

where x^*, the optimal path, is the solution of Equation (4.1.8).

We finally close this introductory section by defining the *optimal escape problem*, which is widely used for calculating stationary actions for Lagrangian systems with potentials containing local minima and maxima.

4.1.3 Optimal Escape Problem

The optimal escape problem seeks to find the rate of *escape* of a particle to *irreversibly* change its position from one stable point to a different (stable or unstable) point[76]. As given in Figure 4.2 below, the optimal escape problem calculates the stationary action (commonly referred to as the *optimal escape rate* in this instance) of a particle under the potential V with more than one stable point. Therefore, if the potential V is of this form, then the stationary action of a free particle given in Equation (4.1.9) is called its optimal escape rate.

Calculating the escape rates of physical systems has been widely used in statistical physics, where a particle located in a potential well can escape to another stable state with smaller potential energy, thereby allowing favorable conditions for the particle. Furthermore, quantum mechanics posits the true nature of *quantum tunneling*, where a particle can randomly escape a potential barrier to another stable state[77]. Stochastic processes are also commonly used in building optimal escape problems; it has been shown that particles within a local potential well that require the existence of an external force (e.g. friction) appear to show random fluctuations in motion, where stochastic processes would be employed to model the position of such particle[82].

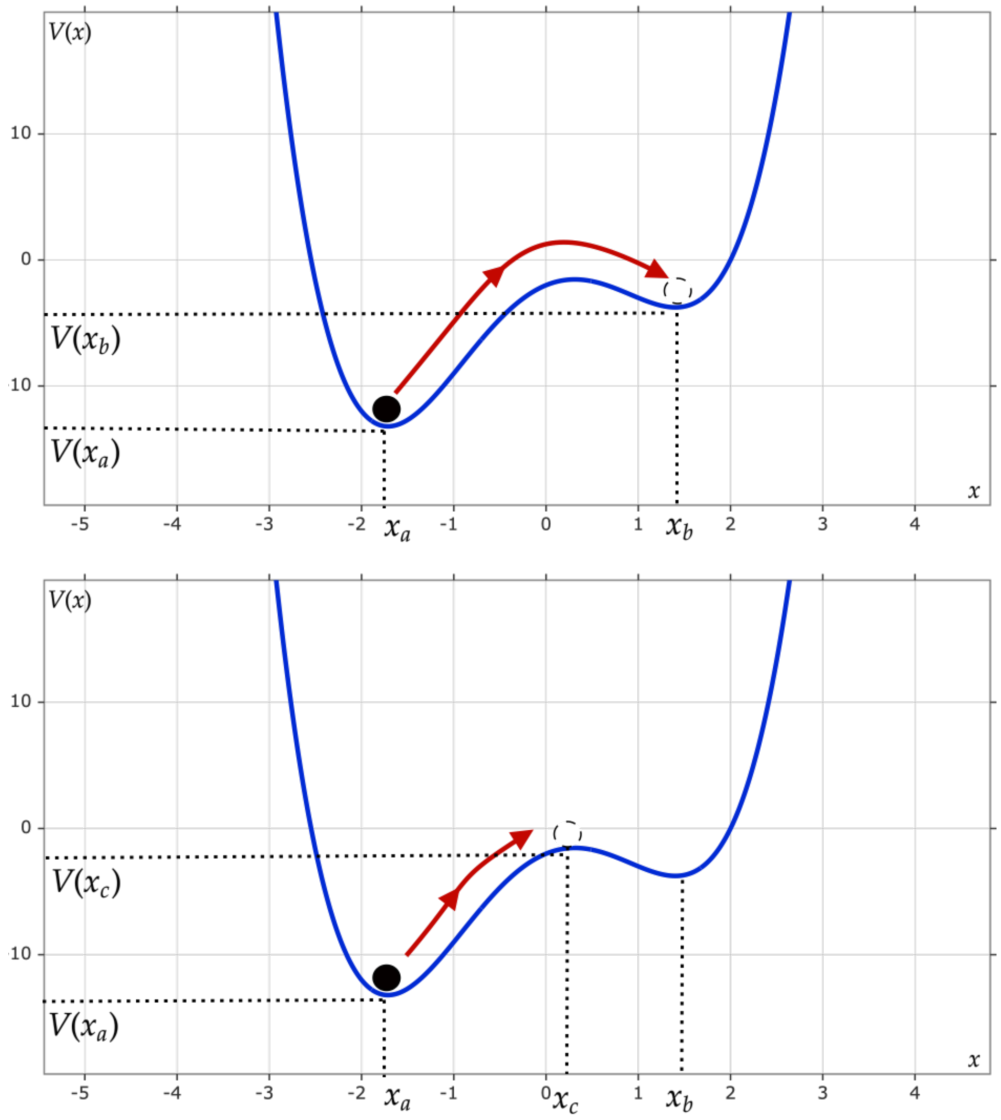

Figure 4.2: Depiction of a double-well potential $V(x) = x^4 - 5x^2 + 3x - 2$ with stable state, $x_a = x(t_a)$, metastable state $x_b = x(t_b)$ and an unstable state $x_c = x(t_c)$. Top figure: Optimal escape problem calculates the stationary action of a particle from the stable state x_a to the metastable state x_b under this potential. Bottom figure: One can also calculate the escape rate from the stable state x_a to the unstable state x_c with lowest potential.

Therefore, instead of confining within the boundaries of deterministic systems for solving the optimal escape problem, one can also define the Lagrangian system for stochastic processes. However, the resulting Lagrangian is not as straightforward to find as in the deterministic cases mentioned in the above examples. If the position of a particle is modeled by a stochastic process, we must first define it as a Langevin equation and then construct the Lagrangian from there. One method to do so is to deduce the Lagrangian straight from the LE itself, as conducted by[26], or by the CFal of the position process, as done by Hanggi in 1989[75]. Both methods work for LE's driven by white noise processes as well as GSN processes.

Due to its simplicity and more extensive analysis, we opted to use the method provided by[75] in finding the solution of our LE $\dot{X}_t = -V'(X_t) + \xi_t$ via path integral approach, where ξ_t forms the GSN process that we extensively defined in Chapter 2. Remarkably, this method also works for any potential V, which we showed to be a great caveat for finding the PDF of X via CFal approach as conducted in Chapter 3.

4.2 Finding the Probability Amplitude and the Euler-Lagrange Equations of the Position Process driven by the GSN

Let X be the position process defined by the Langevin equation $\dot{X} = -V'(X_t) + \xi_t$, where V is the potential, and $\xi_t = \sum_{i=1}^{N_t} A_i h(t - T_i)$ is the GSN as in Definition 2.1.1. As we aim to model the path of a particle between time-frames $[t_a, t_b]$, we constrain the GSN $(\xi_t)_{t\in[t_a,t_b]}$.

Then, by[75], the *probability amplitude* of X between times $[t_a, t_b]$, defined by $\pi(x_b, t_b|x_a, t_a)$, is

given by:

$$\begin{aligned}
&\pi(x_b, t_b | x_a, t_a) \\
&\quad = \int_{\mathscr{C}_X} \mathcal{D}[X] \int_{\mathscr{C}_g} \mathcal{D}\left[\frac{g}{2\pi}\right] \Phi_\xi[g] \, \exp\left(i \int_{t_a}^{t_b} \mathrm{d}t \, g(t) \left(\dot{X}_t + V'(X_t) \right) \right) \, \exp\left(\frac{1}{2} \int_{t_a}^{t_b} \mathrm{d}t \, V''(X_t) \right),
\end{aligned} \tag{4.2.1}$$

where $\mathscr{C}_X$ and $\mathscr{C}_g$ are respectively the functional space of all possible paths X and test functions g, both constrained on $[t_a, t_b]$, and $\Phi_\xi[g]$ is the CFal of the constrained GSN process ξ as in Equation (2.3.7):

$$\Phi_\xi[g] = \exp\left[\lambda \int_{t_a}^{t_b} \mathrm{d}t \left(\phi_{A_1} \left(\int_t^{t_b} \mathrm{d}s \, h(s-t) g(s) \right) - 1 \right) \right], \tag{4.2.2}$$

recalling from Definition 2.1.1 that $\lambda > 0$ is the intensity of ξ. The last exponential term containing $V''(X_t)$, commonly referred to as the Jacobian, naturally arises from discretizing the path integral in order to obtain the probablity amplitude π[83], followed by the change of functional space of the path integral term, as we show in Appendix A.

Notice further that we can gather all the exponentials in the integrands and rewrite the probability amplitude in terms of the action functional S,

$$\pi(x_b, t_b | x_a, t_a) = \int_{\mathscr{C}_X} \mathcal{D}[X] \int_{\mathscr{C}_g} \mathcal{D}\left[\frac{g}{2\pi}\right] \, \exp\left(-S[X, g] \right), \tag{4.2.3}$$

where S is given by the integral of the Lagrangian $\mathscr{L}$ of $X, \dot{X}$ and g:

$$\begin{aligned}
S[X, g] &= \int_{t_a}^{t_b} \mathscr{L}\left(X_t, \dot{X}_t, g(t) \right) \\
&= \int_{t_a}^{t_b} \mathrm{d}t \left(\lambda - \lambda \phi_{A_1} \left(\int_t^{t_b} \mathrm{d}s \, h(s-t) g(s) \right) - i g(t) \left(\dot{X}_t + V'(X_t) \right) + \frac{1}{2} V''(X_t) \right).
\end{aligned} \tag{4.2.4}$$

The optimal path (X^*, g^*) is then found by solving each component's respective ELE. This can be easily shown by extending the expansion of S in Equation (4.1.4) with respect to X and g (ref. [110]):

$$\begin{aligned} S[X,g] &= \int_{t_a}^{t_b} \delta S[X,g] = \int_{t_a}^{t_b} \mathrm{d}t \left(\frac{\partial S}{\partial X}\delta X + \frac{\partial S}{\partial g}\delta g + \frac{\partial S}{\partial \dot{X}}\delta \dot{X} + \frac{\partial S}{\partial \dot{g}}\delta \dot{g} + \frac{\partial S}{\partial \ddot{X}}\delta \ddot{X} + \frac{\partial S}{\partial \ddot{g}}\delta \ddot{g} + \dots \right) \\ &= \int_{t_a}^{t_b} \mathrm{d}t \left(\frac{\partial S}{\partial X}\delta X - \frac{\mathrm{d}}{\mathrm{d}t}\frac{\partial S}{\partial \dot{X}}\delta X + \left(\frac{\mathrm{d}}{\mathrm{d}t}\right)^2 \frac{\partial S}{\partial \ddot{X}}\delta X + \frac{\partial S}{\partial g}\delta g - \frac{\mathrm{d}}{\mathrm{d}t}\frac{\partial S}{\partial \dot{g}}\delta g + \left(\frac{\mathrm{d}}{\mathrm{d}t}\right)^2 \frac{\partial S}{\partial \ddot{g}}\delta g + \dots \right) \\ &= \int_{t_a}^{t_b} \mathrm{d}t \left(\delta X \sum_{j=0}^{\infty} \left(-\frac{\mathrm{d}}{\mathrm{d}t}\right)^j \frac{\partial S}{\partial X^{(j)}} + \delta g \sum_{j=0}^{\infty} \left(-\frac{\mathrm{d}}{\mathrm{d}t}\right)^j \frac{\partial S}{\partial g^{(j)}} \right). \end{aligned} \tag{4.2.5}$$

By letting $\delta S = 0$ the resulting ELE's will be two dimensional system of ODE's with respect to the Lagrangian $\mathscr{L}\left(X_t, \dot{X}_t, g(t)\right)$ as we initiated in the beginning of this chapter.

However, notice that one cannot explicitly define the partial derivative $\partial\mathscr{L}/\partial\dot{X}$ due to the impulse function h causing time non-locality in g. These types of ELE's that contain impulse functions are called *Time Non-Local ELE's* (TNL ELE's), as coined by [25]. Instead, one has to refer to the action functional itself to compute the TNL ELE's:

$$\begin{aligned} \frac{\partial S}{\partial X} - \frac{\mathrm{d}}{\mathrm{d}t}\frac{\partial S}{\partial \dot{X}} &= 0, \\ \frac{\partial S}{\partial g} &= 0. \end{aligned} \tag{4.2.6}$$

As it is local in t, the first equation simply becomes $\dot{g}(t) = V''(X_t)g(t) + i/2V'''(X_t)$. The second

equation, which contains the time non-local term of g, is found as follows:

$$\begin{aligned}
&\frac{\delta S}{\delta g(t)} = 0 \\
\implies &-\lambda \int_{t_a}^{t_b} \mathrm{d}\tau \int_{\tau}^{t_b} \mathrm{d}s\, h(s-\tau)\delta(s-t)\phi'_{A_1}\left(\int_{\tau}^{t_b} \mathrm{d}s\, h(s-\tau)g(s)\right) \\
&\qquad\qquad - i\int_{t_a}^{t_b} \mathrm{d}\tau\, \delta(t-\tau)\left(\dot{X}_t + V'(X_t)\right) = 0 \qquad (4.2.7)\\
\implies &-\lambda \int_{t_a}^{t_b} \mathrm{d}\tau\, h(t-\tau)\Theta(t-\tau)\phi'_{A_1}\left(\int_{\tau}^{t_b} \mathrm{d}s\, h(s-\tau)g(s)\right) - i\left(\dot{X}_t + V'(X_t)\right) = 0 \\
\implies &-\lambda \int_{t_a}^{t} \mathrm{d}\tau\, h(t-\tau)\phi'_{A_1}\left(\int_{\tau}^{t_b} \mathrm{d}s\, h(s-\tau)g(s)\right) - i\left(\dot{X}_t + V'(X_t)\right) = 0.
\end{aligned}$$

Therefore, putting them together, the TNL ELE's are given by the following system of ODE's;

$$\begin{aligned}
\dot{X}_t &= -V'(X_t) + i\lambda \int_{t_a}^{t} \mathrm{d}\tau\, h(t-\tau)\phi'_{A_1}\left(\int_{\tau}^{t_b} \mathrm{d}s\, h(s-\tau)g(s)\right) \\
\dot{g}(t) &= V''(X_t)g(t) + \frac{i}{2}V'''(X_t).
\end{aligned} \qquad (4.2.8)$$

We can also further simplify the TNL ELE's by rescaling the GSN ξ with ε, such that for sufficiently small ε (i.e. under the weak noise limit), the Lagrangian $\mathscr{L}$ can be written only in terms of g. This can be established by referring to the Baule & Sollich 2018 paper [113], where one can redefine the GSN ξ with new jump intensity $\lambda \to \lambda/\varepsilon$ and jump amplitudes $A_1 \to A_1\,\varepsilon$. In this case, the CFal of ξ is given by:

$$\Phi_{\xi}[g] = \exp\left[\frac{\lambda}{\varepsilon}\int_{t_a}^{t_b} \mathrm{d}t\left(\left\langle e^{iA_1\varepsilon\int_t^{t_b}\mathrm{d}s\, h(s-t)g(s)}\right\rangle - 1\right)\right]. \qquad (4.2.9)$$

Thus, in this regime, the probability amplitude of X is given by:

$$\pi(x_b,t_b|x_a,t_a)=\int_{\mathscr{C}_X}\mathcal{D}[X]\int_{\mathscr{C}_g}\mathcal{D}\left[\frac{g}{2\pi}\right]\exp\left[\frac{\lambda}{\varepsilon}\int_{t_a}^{t_b}\mathrm{d}t\left(\left\langle e^{i\mathcal{A}_1\varepsilon\int_t^{t_b}\mathrm{d}s\,h(s-t)g(s)}\right\rangle-1\right)\right]$$
$$\cdot\exp\left(i\int_{t_a}^{t_b}\mathrm{d}t\,g(t)\left(\dot{X}_t+V'(X_t)\right)\right)\exp\left(\frac{1}{2}\int_{t_a}^{t_b}\mathrm{d}t\,V''(X_t)\right),\tag{4.2.10}$$

where upon further rescaling $g\to g/\varepsilon$, we can rewrite the probability amplitude in terms of its action functional S and Lagrangian $\mathscr{L}$:

$$\pi(x_b,t_b|x_a,t_a)=\int_{\mathscr{C}_X}\mathcal{D}[X]\int_{\mathscr{C}_g}\mathcal{D}\left[\frac{g}{2\pi\varepsilon}\right]\exp\left[-\frac{S[X,g]}{\varepsilon}\right],\tag{4.2.11}$$

where the rescaled action is given by

$$\begin{aligned}S[X,g]&=\int_{t_a}^{t_b}\mathrm{d}t\,\mathscr{L}(X_t,\dot{X}_t,g(t)))\\&=\int_{t_a}^{t_b}\mathrm{d}t\left(\lambda\left(1-\phi_{\mathcal{A}_1}\left(\int_t^{t_b}\mathrm{d}s\,h(s-t)g(s)\right)\right)-ig(t)\left(\dot{X}_t+V'(X_t)\right)-\frac{\varepsilon}{2}V''(X_t)\right).\end{aligned}\tag{4.2.12}$$

Plugging the rescaled action above to the TNL ELE in (4.2.6) and applying the weak noise limit $\varepsilon\to 0$, we get the following coupled ODE's from which we can obtain optimal solutions (X^*,g^*):

$$\begin{aligned}&[1]\qquad\dot{g}=V''(X_t)g(t)\\&[2]\qquad\dot{X}=-V'(X_t)+i\lambda\int_{t_a}^{t}\mathrm{d}\tau\,h(t-\tau)\phi'_{\mathcal{A}_1}\left(\int_\tau^{t_b}\mathrm{d}s\,h(s-t)g(s)\right).\end{aligned}\tag{4.2.13}$$

Notice that under weak noise limit, $\varepsilon\to 0$, the Lagrangian can be rewritten by g only: by plugging

[2] to the Lagrangian we get the following,

$$\begin{aligned}\mathscr{L}(X_t, g(t)) &= \lambda\left(1-\phi_{A_1}\left(\int_t^{t_b} \mathrm{d}s\, h(s-t)g(s)\right)\right)\\ &\quad -ig(t)\left(-V'(X_t)+i\lambda\int_{t_a}^{t}\mathrm{d}\tau\, h(t-\tau)\phi'_{A_1}\left(\int_\tau^{t_b}\mathrm{d}s\, h(s-t)g(s)\right)+V'(X_t)\right)\\ &= \lambda\left(1-\phi_{A_1}\left(\int_t^{t_b} \mathrm{d}s\, h(s-t)g(s)\right)\right)+\lambda g(t)\int_{t_a}^{t}\mathrm{d}\tau\, h(t-\tau)\phi'_{A_1}\left(\int_\tau^{t_b}\mathrm{d}s\, h(s-t)g(s)\right)\\ &= \mathscr{L}\left(g^*(t)\right).\end{aligned} \tag{4.2.14}$$

Therefore, the stationary action $S[g^*(t)]$ can be found by by integrating the Lagrangian. However, notice that the solution g^* of the ELE must be purely complex in order to get a purely real solution for X^*. Thus, by re-defining $g^*(t) \equiv ik(t)$, we get the stationary action as follows:

$$\begin{aligned}S[g^*(t)] &= \int_0^t \mathrm{d}\tau\, \mathscr{L}\left(ik(\tau)\right)\\ &= \lambda\int_0^t \mathrm{d}\tau\Bigg[1-\bar{\phi}_{A_1}\left(\int_\tau^{t_b}\mathrm{d}s\, h(s-\tau)k(s)\right)\\ &\qquad\qquad +ik(\tau)\int_{t_a}^{\tau}\mathrm{d}s\, h(\tau-s)\bar{\phi}'_{A_1}\left(\int_s^{t_b}\mathrm{d}u\, h(u-s)k(u)\right)\Bigg],\end{aligned} \tag{4.2.15}$$

where $\bar{\phi}_{A_1}\left(k(t)\right) = \phi_{A_1}\left(g(t)\right)$ with Wick-rotated derivatives: $\frac{\partial}{\partial g}\phi_{A_1}\left(g(t)\right) \to i\frac{\partial}{\partial k}\bar{\phi}_{A_1}\left(k(t)\right)$.

Even though g is an arbitrary test function, due to the integration factor over $[\tau, t_b]$ in $\dot{X}_t$, which causes TNL problem, one has to know in prior the function g over $[t_a, t_b]$. We will explain methods to convert the TNL ELE to higher-order local ELE in Section 4.5.

But before this, in the next two sections we describe ways to analytically solve the TNL ELE for different types of potentials V; zero potential $V(x) = 0$ and Harmonic potential $V(x) = \gamma x^2/2$.

4.3 Optimal Path and Stationary Action for Zero and Harmonic Potentials

4.3.1 Markovian Ornstein-Uhlenbeck Process

Recall from Chapter 1 that OU process is the solution of the LE $\dot{X}_t = -V'(X_t) + \xi_t$ where ξ is the GWN and $V(x) = \gamma x^2/2$ is Harmonic potential.

Let's first rewrite the original (i.e. not k-transformed) ELE's of g^* and X^* under Harmonic potential:

$$\begin{aligned} \dot{g} &= \gamma g(t), \\ \dot{X} &= -\gamma X_t + i\lambda \int_{t_a}^{t} \mathrm{d}\tau\, h(t-\tau)\phi'_{A_1}\left(\int_{\tau}^{t_b} \mathrm{d}s\, h(s-t)g(s)\right). \end{aligned} \tag{4.3.1}$$

Then, since ξ is the GWN process, we have the memory-less property $h(x) = \delta(x)$ and the following characteristic function of the jump amplitude under Gaussian limits $\phi_{A_1}(\theta) = -\frac{1}{2}\left\langle A_1^2 \right\rangle \theta^2 + 1$ such that $\phi'_{A_1}(\theta) = -\left\langle A_1^2 \right\rangle \theta$. Hence, after integrating out the Dirac delta functions, the ELE of X^* reduces to

$$\begin{aligned} \dot{X} &= -\gamma X_t + i\lambda \int_{t_a}^{t} \mathrm{d}\tau\, \delta(t-\tau)\phi'_{A_1}\left(\int_{\tau}^{t_b} \mathrm{d}s\, \delta(s-t)g(s)\right) \\ &= -\gamma X_t + i\Theta(t_b - t)\lambda\phi'_{A_1}(g(t)) \\ &= -\gamma X_t - i\Theta(t_b - t)\lambda\left\langle A_1^2 \right\rangle g(t). \end{aligned} \tag{4.3.2}$$

Defining $\sigma^2 = \lambda\left\langle A_1^2 \right\rangle$ under Gaussian limit and noting due to the boundary value that $\Theta(t_b - t) = 1$, we get the following simplified ELE's:

$$\begin{aligned} \dot{g} &= \gamma g(t), \\ \dot{X} &= -\gamma X_t - i\sigma^2 g(t). \end{aligned} \tag{4.3.3}$$

Note that with boundary condition $g(0) = g(t_a)$ first ELE has general solution $g^*(t) = g(0)e^{\gamma(t-t_a)}$. Hence, the ELE for X^* is given by $\dot{X} = -\gamma X_t - ig(0)\sigma^2 e^{\gamma(t-t_a)}$. It is important to actually fix $g(0) = g_0$ as a function of space and time, i.e. $g_0 = g_0(x_b, t_b|x_a, t_a)$, where it can be fully derived from solving the ELEs with initial conditions of trajectory points from (x_a, t_a) to (x_b, t_b).

In detail, the solution of the second ELE $\dot{X} = -\gamma X_t - ig_0\sigma^2 e^{\gamma(t-t_a)}$ under the boundary condition $X_{t_b} = x_b$ is given by:

$$X_t^* = \frac{e^{-\gamma(t+t_a)}}{\gamma}\left(\gamma x_b e^{\gamma(t_a+t_b)} - \frac{1}{2}ig_0\sigma^2\left(e^{2\gamma t} - e^{2\gamma t_b}\right)\right), \tag{4.3.4}$$

where under the second boundary condition $X_{t_a}^* = x_a$ we can find the function g_0:

$$\begin{aligned} x_a &= \frac{e^{-2\gamma t_a}}{\gamma}\left(\gamma x_b e^{\gamma(t_a+t_b)} - \frac{1}{2}ig_0\sigma^2\left(e^{2\gamma t_a} - e^{2\gamma t_b}\right)\right) \\ \implies g_0 &= \frac{2i\gamma e^{\gamma t_a}\left(x_a e^{\gamma t_a} - x_b e^{\gamma t_b}\right)}{\sigma^2\left(e^{2\gamma t_a} - e^{2\gamma t_b}\right)}. \end{aligned} \tag{4.3.5}$$

Plugging this to our X^* equation and re-arranging the terms yields the closed form solution of the optimal path of the OU-process:

$$X_t^* = \frac{e^{\gamma t}}{e^{2\gamma t_a} - e^{2\gamma t_b}}\left(\left(e^{\gamma(2t+t_a)} - e^{\gamma(2t_b+t_a)}\right)x_a - \left(e^{\gamma(2t+t_b)} - e^{\gamma(2t_a+t_b)}\right)x_b\right). \tag{4.3.6}$$

Remark 4.3.1. *An interesting yet also obvious case is that upon applying $\gamma \to 0$ limit, in which case X becomes Brownian motion, the optimal path is given by a straight line,*

$$\lim_{\gamma\to 0} X_t^* = \frac{(t-t_b)x_a - (t-t_a)x_b}{t_a - t_b}. \tag{4.3.7}$$

This agrees with the consensus that the shortest path between two points, under no external or internal force present, *is a straight line.*

Now that we have found the optimal path, let's rewrite the stationary action in case for the OU process. For simplicity, we can insert the ELE for X given above to the action functional $S[X, g]$ given in Equation (4.2.12):

$$\begin{aligned}
S[X,g] &= \int_{t_a}^{t_b} \mathrm{d}\tau \left[\lambda \left(1 - \phi_{A_1} \left(\int_{\tau}^{t_b} \mathrm{d}s\, h(s-\tau) g(s) \right) \right) - i g(\tau) \left(\dot{X}_\tau + V'(X_\tau) \right) \right] \\
&= \int_{t_a}^{t_b} \mathrm{d}\tau \left[\lambda \left(1 + \frac{1}{2} \left\langle A_1^2 \right\rangle \left(-\Theta(\tau_b - \tau)^2 \right) g(\tau)^2 - 1 - i g(\tau) \left(-i\lambda \left\langle A_1^2 \right\rangle g(\tau) \right) \right] \right. \\
&= -\frac{1}{2}\sigma^2 \int_{t_a}^{t_b} \mathrm{d}\tau\, g(\tau)^2 \\
\implies S(x_b, t_b | x_a, t_a) &= -\frac{1}{2}\sigma^2 g_0^2 \int_{t_a}^{t_b} \mathrm{d}\tau\, e^{2\gamma(\tau - t_a)} = -\frac{1}{2} \left(\frac{2i\gamma e^{\gamma t_a} \left(x_a e^{\gamma t_a} - x_b e^{\gamma t_b} \right)}{\sigma^2 \left(e^{2\gamma t_a} - e^{2\gamma t_b} \right)} \right)^2 \sigma^2 \frac{e^{2\gamma(t_b - t_a)} - 1}{2\gamma} \\
&= \frac{\gamma}{\sigma^2} \frac{\left(x_b e^{\gamma t_b} - x_a e^{\gamma t_a} \right)^2}{e^{2\gamma t_b} - e^{2\gamma t_a}}.
\end{aligned} \tag{4.3.8}$$

The stationary action for OU case is interesting because for large enough time, the action simply depends on the current state of X. We have explained this in a bit more detail in the following remark.

Remark 4.3.2. *Given the following stationary action for the OU process,*

$$S(x_b, t_b | x_a, t_a) = \frac{\gamma}{\sigma^2} \frac{\left(x_b e^{\gamma t_b} - x_a e^{\gamma t_a} \right)^2}{e^{2\gamma t_b} - e^{2\gamma t_a}}, \tag{4.3.9}$$

where recalling that t_a is time observed for the event $X_{t_a} = x_a$ such that $t_a < t_b$. Then, the stationary action will be independent from initial state x_a if one waits for a sufficiently long time; i.e. we have that,

$$\lim_{t_b \to \infty} S(x_b, t_b | x_a, t_a) = \frac{\gamma}{\sigma^2} x_b^2. \tag{4.3.10}$$

Note also that by simply letting $\gamma = 0$ (i.e. zero potential energy) we will retrieve the optimal path X^* and action $S(x_b, t_b | x_a, t_a)$ for Wiener process. Under zero potential, the ELE for X reads

$\dot{X} = -i\sigma^2 g(t)$ with solution given by:

$$X_t^* = \frac{(t - t_b)x_a - (t - t_a)x_b}{t_a - t_b} \tag{4.3.11}$$

and the stationary action simply becomes

$$S(x_b, t_b | x_a, t_a) = \frac{(x_b - x_a)^2}{2\sigma^2(t_b - t_a)}. \tag{4.3.12}$$

Now that we have analyzed the optimal escape problem for Gaussian white noise, we will expand this functional technique for Poisson white noise (i.e. X becomes the GenOU process) then establish the novel foundation for the case for GSN ξ.

Let us refer to the original set of ELE's for X and g under Harmonic potential:

$$\begin{aligned} \dot{g} &= \gamma g(t), \\ \dot{X} &= -\gamma X_t + i\lambda \int_{t_a}^{t} \mathrm{d}\tau \, h(t - \tau) \phi'_{A_1} \left(\int_{\tau}^{t_b} \mathrm{d}s \, h(s - t) g(s) \right). \end{aligned} \tag{4.3.13}$$

As in previous attempt for OU process, we will let the impulse function to Dirac delta $h \to \delta$, however relax the condition for Gaussian limits. Solving for δ yields the ELEs for Generalized OU process:

$$\begin{aligned} \dot{g} &= \gamma g(t), \\ \dot{X} &= -\gamma X_t + i\lambda \phi'_{A_1}(g(t)), \end{aligned} \tag{4.3.14}$$

where $g(t) = g_0 \exp(\gamma(t - t_a))$. As we will establish in the next section considering GSN ξ, we have an implicit equation for g_0 and therefore finding g_0 can only be achieved by directly defining ϕ'_{A_1} or by numeric techniques. For its similarity to the following results, we leave the solutions for optimal path X^* and action S for the next section.

4.3.2 Non-Markovian Ornstein-Uhlenbeck Process

Recall in Chapter 2 that the Non-Markovian OU Process is defined as the solution of the LE $\dot{X}_t = -V'(X_t) + \xi_t$, where the potential is harmonic $V(x) = \gamma x^2/2$ and the noise ξ is the GSN with Gaussian Limits. Therefore, the CF simplifies to $\phi_{A_1}(\theta) = -\frac{1}{2}\left\langle A_1^2 \right\rangle \theta^2 + 1$. Fixing $\sigma^2 = \lambda \left\langle A_1^2 \right\rangle$ and get the following ELE's:

$$\begin{aligned} \dot{g} &= \gamma g(t), \\ \dot{X} &= -\gamma X_t - i\sigma^2 \int_{t_a}^{t} \mathrm{d}\tau\, h(t-\tau) \int_{\tau}^{t_b} \mathrm{d}s\, h(s-\tau) g(s). \end{aligned} \tag{4.3.15}$$

Under the initial condition $g(0) = g_0$ we get that $g(t) = g_0 \exp\left(\gamma(t - t_a)\right)$ and hence get the following ODE: $\dot{X} = -\gamma X_t - i\sigma^2 g_0 e^{-\gamma t_a} \int_{t_a}^{t} \mathrm{d}\tau\, h(t-\tau) \int_{\tau}^{t_b} \mathrm{d}s\, h(s-\tau) e^{\gamma s}$. Applying the second boundary condition $X_{t_b} = x_b$ yields the general solution for X^*:

$$X_t^* = e^{-\gamma t}\left(x_b e^{\gamma t_b} + i\sigma^2 g_0 \int_{t}^{t_b} \mathrm{d}s\, e^{\gamma s} \int_{t_a}^{s} \mathrm{d}\tau\, h(s-\tau) \int_{\tau}^{t_b} \mathrm{d}u\, h(u-\tau) e^{\gamma(u-t_a)} \right). \tag{4.3.16}$$

Notice that from above we can explicitly express g_0. By letting the first boundary condition $X_{t_a} = x_a$, we get:

$$\begin{aligned} x_a &= e^{-\gamma t_a}\left(x_b e^{\gamma t_b} + i\sigma^2 g_0 \int_{t_a}^{t_b} \mathrm{d}s\, e^{\gamma s} \int_{t_a}^{s} \mathrm{d}\tau\, h(s-\tau) \int_{\tau}^{t_b} \mathrm{d}u\, h(u-\tau) e^{\gamma(u-t_a)} \right) \\ \implies g_0 &= \frac{i}{\sigma^2}\left(x_b e^{\gamma t_b} - x_a e^{\gamma t_a}\right) \left(x_b e^{\gamma t_b} + i\sigma^2 g_0 \int_{t_a}^{t_b} \mathrm{d}s\, e^{\gamma s} \int_{t_a}^{s} \mathrm{d}\tau\, h(s-\tau) \int_{\tau}^{t_b} \mathrm{d}u\, h(u-\tau) e^{\gamma(u-t_a)} \right)^{-1}. \end{aligned} \tag{4.3.17}$$

As in the Markovian counterpart, one can explicitly define the initial condition g_0 from the TNL ELE's for the Non-Markovian OU process. However, it is close to impossible to do so without the Gaussian Limits.

Let us know show below the case for Non-Markovian GenOU process X, where the TNL ELE is now given by:

$$\begin{aligned} \dot{g} &= \gamma g(t), \\ \dot{X} &= -\gamma X_t + i\lambda \int_{t_a}^{t} \mathrm{d}\tau\, h(t-\tau)\phi'_{A_1}\left(\int_{\tau}^{t_b} \mathrm{d}s\, h(s-t)g(s)\right). \end{aligned} \tag{4.3.18}$$

As before, we next aim to find the coefficient under the boundary condition $g(0) = g(t_a) = g_0(x_b, t_b|x_a, t_a)$ using solution of the first ELE $g^*(t) = g_0 \exp\left(\gamma(t-t_a)\right)$. Plugging this back into the second ELE and solving it under the boundary condition $X_{t_b} = x_b$ yields:

$$\begin{aligned} \dot{X} &= -\gamma X_t + i\lambda \int_{t_a}^{t} \mathrm{d}\tau\, h(t-\tau)\phi'_{A_1}\left(\int_{\tau}^{t_b} \mathrm{d}s\, h(s-t)g(s)\right) \\ \implies X_t^* &= e^{-\gamma t}\left(x_b e^{\gamma t_b} - i\lambda \int_{t}^{t_b} \mathrm{d}s\, e^{\gamma s} \int_{t_a}^{s} \mathrm{d}\tau\, h(s-\tau)\phi'_{A_1}\left(g_0 \int_{\tau}^{t_b} \mathrm{d}u\, h(u-\tau)e^{\gamma(u-t_a)}\right)\right). \end{aligned} \tag{4.3.19}$$

In order to find g_0, we need to plug into the X^* solution the next boundary condition $X_{t_a} = x_a$:

$$x_b e^{\gamma t_b} - x_a e^{\gamma t_a} = i\lambda \int_{t_a}^{t_b} \mathrm{d}s\, e^{\gamma s} \int_{t_a}^{s} \mathrm{d}\tau\, h(s-\tau)\phi'_{A_1}\left(g_0 \int_{\tau}^{t_b} \mathrm{d}u\, h(u-\tau)e^{\gamma(u-t_a)}\right). \tag{4.3.20}$$

The above equation will almost surely be implicit for g_0 due to characteristic function ϕ_{A_1}. However, we can still get a better understanding of the behavior of g_0 by taking *Double Laplace transform* with respect to t_a and t_b as detailed by Debnath L. in 2016[120]; or by defining the LHS as $f(t_a, t_b)$ and RHS by $K(t_a, t_b, s) := e^{\gamma s}\int_{t_a}^{s} \mathrm{d}\tau\, h(s-\tau)$ and obtain the *two-dimensional Volterra Integral equation*:

$$f(t_a, t_b) = \int_{t_a}^{t_b} \mathrm{d}s\, K(t_a, t_b, s)\phi'_{A_1}\left(g_0 \int_{\tau}^{t_b} \mathrm{d}u\, h(u-\tau)e^{\gamma(u-t_a)}\right), \tag{4.3.21}$$

where we can then numerically solve it for ϕ'_{A_1} using kernel separation method published by Fazli et

al. 2016[121].

Now that we have expressed the foundation to retrieve the coefficient g_0, let's observe the behavior of the optimal path and stationary action by applying the simplest impulse function, the exponential decay $h(x) = \alpha e^{-\alpha x}$, where the resulting noise ξ will be the CP noise process.

Plugging the impulse function to the second ELE in Equation (4.3.19) and solving the integrals yields the ELE for X:

$$\dot{X} = -\gamma X_t + i\alpha\lambda \int_{t_a}^{t} \mathrm{d}\tau\, e^{-\alpha(t-\tau)} \phi'_{A_1}\left(\frac{\alpha g_0}{\alpha-\gamma} e^{-\gamma t_a + \alpha\tau}\left(e^{-(\alpha-\gamma)\tau} - e^{-(\alpha-\gamma)t_b}\right)\right) \tag{4.3.22}$$

Furthermore, the stationary action S that solely depends on X^* will also be given by plugging the solutions of $\dot{g}$ and $\dot{X}$ above to the action functional in Equation (4.2.12), given by:

$$\begin{aligned}
&S[X^*, g^*] \\
&= \int_{t_a}^{t_b} \mathrm{d}\tau \left[\lambda\left(1 - \phi_{A_1}\left(\int_{\tau}^{t_b} \mathrm{d}s\, h(s-\tau) g(s)\right)\right) - ig(\tau)\left(\dot{X}_\tau + V'(X_\tau)\right)\right] \\
&= \int_{t_a}^{t_b} \mathrm{d}\tau \Bigg[\lambda\left(1 - \phi_{A_1}\left(\frac{\alpha g_0}{\alpha-\gamma} e^{-\gamma t_a + \alpha\tau}\left(e^{-(\alpha-\gamma)\tau} - e^{-(\alpha-\gamma)t_b}\right)\right)\right) \\
&\qquad - ig_0 e^{\gamma(\tau - t_a)}\Bigg(-\gamma X_\tau + i\alpha\lambda \int_{t_a}^{\tau} \mathrm{d}s\, e^{-\alpha(\tau-s)} \phi'_{A_1}\left(\frac{\alpha g_0}{\alpha-\gamma} e^{-\gamma t_a + \alpha s}\left(e^{-(\alpha-\gamma)s} - e^{-(\alpha-\gamma)t_b}\right)\right) \\
&\qquad\qquad + V'(X_\tau)\Bigg)\Bigg] \\
&= S[X^*]
\end{aligned} \tag{4.3.23}$$

From the optimal path and action, we can also find the case for the free particle (i.e. without

potential energy) by letting $\gamma = 0$:

$$\dot{X}_t = i\alpha\lambda \int_{t_a}^{t} \mathrm{d}\tau\, e^{-\alpha(t-\tau)} \phi'_{A_1}\left(g_0\left(1 - e^{\alpha(\tau - t_b)}\right)\right), \tag{4.3.24}$$

where from here we can also obtain the stationary action of the free particle:

$$\begin{aligned} &S[X^*] \\ &= \int_{t_a}^{t_b} \mathrm{d}\tau \left[\lambda\left(1 - \phi_{A_1}\left(g_0\left(1 - e^{\alpha(\tau - t_b)}\right)\right)\right) - ig_0\left(i\alpha\lambda \int_{t_a}^{\tau} \mathrm{d}u\, e^{-\alpha(\tau-u)} \phi'_{A_1}\left(g_0\left(1 - e^{\alpha(u - t_b)}\right)\right)\right)\right] \end{aligned} \tag{4.3.25}$$

We now established that although one can find optimal path and stationary action for the Harmonic potential easily, one cannot fully analytically describe them due to the initial condition g_0 being embedded within the CF of the jump amplitude, ϕ_{A_1}.

4.4 Optimal Path and Stationary Action for General Potential

Let the potential V in this case be an undefined potential. We will separately analyze for different noise cases, first starting with Poisson white noise to compare our results with Baule & Sollich 2015 [113] and lastly with our GSN process ξ.

4.4.1 Poisson White Noise Process

In this case, under k-transformation as in Equation (4.2.15), we have the following set of TNL ELE's,

$$\begin{aligned} \dot{k} &= V''(X_t)k(t), \\ \dot{X} &= -V'(X_t) - \lambda\phi'_{A_1}(k(t)). \end{aligned} \tag{4.4.1}$$

As can be visualized, the above set of ODE can only be solvable for specific cases of potential V; the harmonic potential is a trivial case as we have established in the previous section. However, as we assign higher leading order to V, we step into the realm of non-linear ODEs, where one usually finds numerical solutions. Nonetheless, there are some analytic approaches, and we will briefly explain them in the next section considering the GSN.

Finally, one can also numerically integrate the stationary action S given in Equation (4.2.15) under Poisson white noise, *i.e.* $h \to \delta$:

$$S(x_b, t_b | x_a, t_a) = \lambda \int_{t_a}^{t_b} \mathrm{d}\tau \left[1 - \bar{\phi}_{A_1}(k(\tau)) + k(\tau) \bar{\phi}'_{A_1}(k(\tau)) \right], \tag{4.4.2}$$

which we can find by directly integrating k^*.

4.4.2 GSN Process

In the case of the GSN process we now have the following TNL ELE's for the system:

$$\begin{aligned} \dot{g} &= V''(X_t) g(t), \\ \dot{X} &= -V'(X_t) + i\lambda \int_{t_a}^{t} \mathrm{d}\tau \, h(t-\tau) \phi'_{A_1} \left(\int_{\tau}^{t_b} \mathrm{d}s \, h(s-\tau) g(s) \right). \end{aligned} \tag{4.4.3}$$

As you may recall, we now have coupled, nonlinear and non-local systems of ODE's. There are some techniques to simplify these equations, such as the Dirichlet expansion [114] or advanced Lie symmetry techniques [115]. Numerical solutions of these ODE's can also be found by the Forward Euler's scheme as given in Chapter 16 Section 5.1.3.1 of [119]. However, all these schemes assign specific potential V to numerically approximate the solutions of the ODE's.

In summary, when dealing with non-Markovian processes of any potential $V(x)$ with leading order x^n, $n > 1$ (i.e. any potential that is neither constant nor Harmonic): one has to know the

entire function g prior to solving the optimal escape problem. We can directly observe this from the general TNL ELE in Equation (4.2.8) where the equation of motion for X has integration of the impulse function h over $[t, t_b]$ such that t_b is the end of our time constraint.

This may also seem empirically sensible, as due to the impulse function h, the position process can hold all prior information of X generated since its inception. Therefore, even numerically computing the solution of both g and X requires non-standard techniques that are beyond the scope of this thesis.

In the next section, we instead show that if the impulse function is an $n-$hierarchy function, then one can overcome knowing the entire function g to solve the equations of motion, and thus obtain a *localized* ELE from the TNL ELE.

4.5 Localizing the Euler Lagrange Equations using $n-$Hierarchy Impulse Functions

We postulate that the integration of entire function g is *solely* related to the impulse function h, specifically the behaviour of its differentials. Recall from Equation (3.1.8) and that for any general kernel h, the time derivative of our GSN ξ is given by:

$$\dot{\xi}_t = \sum_{i=1}^{N_t} A_i \dot{h}(t - T_i) + h(0)\dot{L}_t, \tag{4.5.1}$$

where the first variable on the RHS forms another GSN process ${}^{(1)}\xi$ with impulse function $\dot{h}$, and the second variable $\dot{L}_t$ forms the PWN.

Further differentiation of ${}^{(1)}\xi_t$ as explained in Chapter 3 yields the following recursion:

$${}^{(n-1)}\dot{\xi}_t = {}^{(n)}\xi_t + h^{(n-1)}(0)\dot{L}_t, \tag{4.5.2}$$

where ${}^{(n)}\xi_t$ forms the GSN process with impulse function $h^{(n)}(t)$. Furthermore, recalling the $n-$hierarchical impulse function defined by in Equation (2.5.1): $\sum_{i=0}^{n} c_i h^{(i)}(t) = 0,\ h^{(i)}(0) = a_i$, one can simplify the 2 dimensional TNL ELE's into $(n+1)$-dimensional *localized* ELE's if h is an $n-$hierarchical function, as the LE reduces to $(n+1)$ dimensions:

$$\begin{aligned}
\dot{X}_t &= -V'(X_t) + \xi_t \\
\dot{\xi}_t &= {}^{(1)}\xi_t + h(0)\dot{L}_t \\
{}^{(1)}\dot{\xi}_t &= {}^{(2)}\xi_t + \dot{h}(0)\dot{L}_t \\
&\vdots \\
{}^{(n-1)}\dot{\xi}_t &= \left(\sum_{j=0}^{n-1} c_j \cdot {}^{(j)}\xi_t\right) + h^{(n-1)}(0)\,\dot{L}_t,
\end{aligned} \tag{4.5.3}$$

Notice also that by taking the n-th derivative of X, we can plug in all the ODEs above into the first ODE involving X, after which we can derive the desired probability amplitude, action and equations of motion.

Remark 4.5.1. *From the above relation of periodicity, we understand that the behaviour of* ξ must be well-defined *in order to solve Euler-Lagrange equations involving non-Markovian behaviours under any potential V. In fact, if the impulse function h is not an $n-$hierarchy function, then we have to know the entire function g as given in Equation (4.2.13).*

In the following two sections, we outlined some hierarchical impulse functions (see Section 2.5.3 for review) in first and fourth-order derivatives. This indeed circumvents the non-local problem and reduces the dimension of the LE to a point where it is much easier to solve numerically.

4.5.1 Example 1: Exponentially Decaying Impulse Function

In this example, we define the simplest impulse function $h(x) = \alpha e^{-\alpha x}$ where the resulting GSN ξ is the CP noise process. From here, we simply get the following Langevin equation[60]:

$$\begin{aligned} \dot{X}_t &= -V'(X_t) + \xi_t \\ \dot{\xi}_t &= -\alpha \xi_t + \alpha \dot{L}_t, \end{aligned} \tag{4.5.4}$$

where $\dot{L}_t$ forms the PWN process.

By taking $h \to \delta$ in the general Lagrangian of the GSN process, one obtains the Lagrangian of the PWN as: $\mathscr{L} = \lambda \left[1 - \phi_{A_1}(g(t))\right] - ig(t)\dot{L}_t$[113]. From here, we can find an ODE relationship between $\dot{L}$ and X directly by combining the ξ terms together. This is done by taking the time derivative of $\dot{X}$ above and equating it to the LE for ξ: $\ddot{X}_t + V''(X_t)\dot{X}_t = -\alpha\xi_t + \alpha\dot{L}_t$. Hence, we can write this equation in terms of $\dot{L}_t$:

$$\dot{L}_t = \frac{\ddot{X}_t + V''(X_t)\dot{X}_t + \alpha\left(\dot{X}_t + V'(X_t)\right)}{\alpha}. \tag{4.5.5}$$

Plugging this to the Lagrangian of the Poisson white noise, we get the general Lagrangian that depends on the first two derivatives of X and g:

$$\mathscr{L}\left(X_t, \dot{X}_t, \ddot{X}_t, g(t)\right) = \lambda\left[1 - \phi_{A_1}(g(t))\right] - ig(t)\left(\frac{\ddot{X}_t + V''(X_t)\dot{X}_t + \alpha\left(\dot{X}_t + V'(X_t)\right)}{\alpha}\right). \tag{4.5.6}$$

Notice how the Lagrangian is now localized without integration over g. Therefore, the correspond-

ing ELE for X and g can be solved directly by its Lagrangian:

$$\begin{aligned} \frac{\mathrm{d}^2}{\mathrm{d}t^2}\left(\frac{\partial \mathscr{L}}{\partial \ddot{X}}\right) - \frac{\mathrm{d}}{\mathrm{d}t}\left(\frac{\partial \mathscr{L}}{\partial \dot{X}}\right) + \frac{\partial \mathscr{L}}{\partial X} &= 0, \\ \frac{\partial \mathscr{L}}{\partial g} &= 0. \end{aligned} \tag{4.5.7}$$

The first ODE is given as follows,

$$\frac{\mathrm{d}^2}{\mathrm{d}t^2}\left[\frac{-ig(t)}{\alpha}\right] - \frac{\mathrm{d}}{\mathrm{d}t}\left[\frac{-ig(t)}{\alpha}\left(V''(X_t)+\alpha\right)\right] - \frac{ig(t)}{\alpha}\left(V'''(X_t)\dot{X}_t + \alpha V''(X_t)\right) = 0 \tag{4.5.8}$$

The second ODE is simply given by:

$$\ddot{X} + \left(V''(X_t)+\alpha\right)\dot{X} + \alpha V'(X_t) = i\alpha\lambda\phi'_{A_1}\left(g(t)\right). \tag{4.5.9}$$

Notice that the resulting ODE is now localized, two-dimensional and second-order, and can be solved numerically. In subsection simulations sector of this chapter we plotted the optimal trajectory of X and g where we used the same potential V and conditions x_a, x_b, t_a, t_b as in [113].

4.5.2 Example 2: Damped and Oscillating Impulse Function

Similarly, here we expand the above impulse function by introducing an oscillatory term;

$$h(t;\alpha) = \alpha e^{-\alpha t}\left(\cos\alpha t + \sin\alpha t\right), \tag{4.5.10}$$

where $\alpha > 0$ is the parameter that contributes to range of memory. This is the special case of the broader Damped and Oscillating impulse function that we defined in Chapter 1 with $\alpha = \beta$.

Therefore, the impulse function is periodic in its fourth derivative, i.e. $\mathrm{d}^4h/\,\mathrm{d}t^4 = -4h(t)$, and

we can rewrite the LE as five dimensional LE:

$$\begin{aligned}
\dot{X}_t &= -V'(X_t) + \xi_t \\
\dot{\xi}_t &= {}^{(1)}\xi_t + h(0)\dot{L}_t \\
{}^{(1)}\dot{\xi}_t &= {}^{(2)}\xi_t + \dot{h}(0)\dot{L}_t \\
{}^{(2)}\dot{\xi}_t &= {}^{(3)}\xi_t + \ddot{h}(0)\dot{L}_t \\
{}^{(3)}\dot{\xi}_t &= -4\xi_t + \dddot{h}(0)\dot{L}_t.
\end{aligned} \tag{4.5.11}$$

From here, we outline two approaches to solve the resulting ELE: first by differentiating X, and second by solving the Matrix ODE resulting from the 4−hierarchy nature of h.

Via Differentiating the Position Process Taking the fifth derivative of X and combining the rest of the ODE's in Equation (4.5.11) yields the following ODE for X:

$$\begin{aligned}
&\ddddot{X} = -V^{(5)}(X)\dot{X}^4 - 6V^{(4)}(X)\dot{X}^2\ddot{X} - 3V'''(X)\ddot{X}^2 - 4V'''(X)\dot{X}\dddot{X} - V''(X)\ddddot{X} - 4(\dot{X} + V'(X)) + \dddot{h}(0)\dot{L}_t. \\
&\implies \dot{L}_t = \frac{\ddddot{X} + V^{(5)}(X)\dot{X}^4 + 6V^{(4)}(X)\dot{X}^2\ddot{X} + 3V'''(X)\ddot{X}^2 + 4V'''(X)\dot{X}\dddot{X} + V''(X)\ddddot{X} + 4(\dot{X} + V'(X))}{\dddot{h}(0)}
\end{aligned} \tag{4.5.12}$$

As before, $\dot{L}_t$ forms PWN process with Lagrangian $\mathscr{L}(g(t)) = \lambda\left[1 - \phi_{A_1}(g(t))\right] - ig(t)\dot{L}_t$. Once we plug the equation for $\dot{L}_t$ above to its Lagrangian, we now obtain the Lagrangian that depends up

to 5 derivatives of X and on g:

$$\begin{aligned}
&\mathscr{L}\left(X_t, \dot{X}_t, \ddot{X}_t, \dddot{X}_t, \ddddot{X}_t, \dddddot{X}_t, g(t)\right) \\
=&\lambda\left[1-\phi_{A_1}\left(g(t)\right)\right] \\
&-ig(t)\frac{\dddddot{X}+V^{(5)}(X)\dot{X}^4+6V^{(4)}(X)\dot{X}^2\ddot{X}+3V'''(X)\ddot{X}^2+4V'''(X)\dot{X}\dddot{X}+V''(X)\ddddot{X}+4(\dot{X}+V'(X))}{\dddot{b}(0)}.
\end{aligned} \tag{4.5.13}$$

And lastly, the equations of motion is given by the localized ELE's for the above Lagrangian g:

$$\begin{aligned}
&-\frac{\mathrm{d}^5}{\mathrm{d}t^5}\left(\frac{\partial\mathscr{L}}{\partial\dddddot{X}}\right)+\frac{\mathrm{d}^4}{\mathrm{d}t^4}\left(\frac{\partial\mathscr{L}}{\partial\ddddot{X}}\right)-\frac{\mathrm{d}^3}{\mathrm{d}t^3}\left(\frac{\partial\mathscr{L}}{\partial\dddot{X}}\right)+\frac{\mathrm{d}^2}{\mathrm{d}t^2}\left(\frac{\partial\mathscr{L}}{\partial\ddot{X}}\right)-\frac{\mathrm{d}}{\mathrm{d}t}\left(\frac{\partial\mathscr{L}}{\partial\dot{X}}\right)+\frac{\partial\mathscr{L}}{\partial X}=0 \\
&\frac{\partial\mathscr{L}}{\partial g}=0
\end{aligned} \tag{4.5.14}$$

We can observe from the ELE above that is it now localized, yet we now have a highly coupled and nonlinear systems of ODE's with respect to X and g.

Next, we show the second method by solving the LE as a matrix equation.

Via Solving the Matrix ODE Notice that one can rewrite Equation (4.5.11) in matrix form:

$$\begin{aligned}
\dot{X}_t &= -V'(X_t)+\xi_t \\
\frac{\mathrm{d}}{\mathrm{d}t}\begin{pmatrix}\xi_t\\ \tilde{\xi}_t^{(1)}\\ \tilde{\xi}_t^{(2)}\\ \tilde{\xi}_t^{(3)}\end{pmatrix} &= \begin{pmatrix}0&1&0&0\\0&0&1&0\\0&0&0&1\\-4&0&0&0\end{pmatrix}\begin{pmatrix}\xi_t\\ \tilde{\xi}_t^{(1)}\\ \tilde{\xi}_t^{(2)}\\ \tilde{\xi}_t^{(3)}\end{pmatrix}+\begin{pmatrix}h(0)\\ \dot{h}(0)\\ \ddot{h}(0)\\ \dddot{h}(0)\end{pmatrix}\dot{L}_t,
\end{aligned} \tag{4.5.15}$$

where one can define $\vec{\Xi}_t := \left(\xi_t, \tilde{\xi}_t^{(1)}, \tilde{\xi}_t^{(2)}, \tilde{\xi}_t^{(3)}\right)^\top$, the coefficient matrix as $\mathbf{A}$ and

$$\vec{\eta}(t) := \dot{L}_t \left(h(0), \dot{h}(0), \ddot{h}(0), \dddot{h}(0)\right)^\top$$

to get the four dimensional first order linear ODE $\dot{\vec{\Xi}}_t = \mathbf{A}\vec{\Xi}_t + \vec{\eta}(t)$. This is indeed solvable and one can obtain the solution for ξ_t. However, one problem that naturally occurs is that the solution of ξ_t will contain stochastic time integrals in form $\int \mathrm{d}\tau\, \dot{L}_\tau$, which would be hard to derive its Lagrangian.

We have shown now that both methods (by taking derivatives of X and by solving the Matrix ODE) result in nonlinear or stochastic integral terms that can only be solved numerically.

In the next section, we will apply the beautiful hierarchic nature of the GSN and derive interesting and new results on Lagrangian and equations of motion.

4.6 Finding the Localized ELE for General $n-$Hierarchy Impulse Function

Here, we show that one can extend solving the Matrix ODE for the damped and oscillating impulse function case for a more general, $n-$hierarchical case.

Let $h(x)$ be the impulse function of the GSN ξ satisfying the LE $\dot{X}_t = -V'(X_t) + \xi_t$, such that h is the solution of the general n-th order linear IVP:

$$\sum_{i=0}^{n} c_i h^{(i)}(t) = 0, \quad h^{(i)}(0) = a_i, \tag{4.6.1}$$

where $a_i,\ c_i \in \mathbb{R}$ are scalars. Therefore, we showed in Equation (2.5.1) that the LE for ξ becomes hierarchical as follows:

$$\begin{aligned}
\dot{X}_t &= -V'(X_t) + \xi_t \\
\dot{\xi}_t &= {}^{(1)}\xi_t + h(0)\dot{L}_t \\
{}^{(1)}\dot{\xi}_t &= {}^{(2)}\xi_t + \dot{h}(0)\dot{L}_t \\
&\vdots \\
{}^{(n-1)}\dot{\xi}_t &= \left(\sum_{j=0}^{n-1} c_j \cdot {}^{(j)}\xi_t\right) + h^{(n-1)}(0)\,\dot{L}_t,
\end{aligned} \tag{4.6.2}$$

Defining $\vec{\Xi}_t := \left(\xi_t, {}^{(1)}\xi_t, {}^{(2)}\xi, \cdots, {}^{(n-1)}\xi\right)^\top$ and $\vec{\eta} := \left(h(0), \dot{h}(0), \ddot{h}(0), \cdots, h^{(n-1)}(0)\right)^\top$ yields

the matrix ODE as follows:

$$\dot{\vec{\Xi}}_t = \begin{pmatrix} 0 & 1 & 0 & 0 & \dots & 0 & 0 \\ 0 & 0 & 1 & 0 & \dots & 0 & 0 \\ 0 & 0 & 0 & 1 & \dots & 0 & 0 \\ \vdots & \vdots & \vdots & \vdots & \ddots & \vdots & \vdots \\ 0 & 0 & 0 & 0 & \dots & 1 & 0 \\ 0 & 0 & 0 & 0 & \dots & 0 & 1 \\ c_0 & c_1 & c_2 & c_3 & \dots & c_{n-2} & c_{n-1} \end{pmatrix} \vec{\Xi}_t + \vec{\eta}\,\dot{L}_t = \mathbf{A}\vec{\Xi}_t + \vec{\eta}\,\dot{L}_t. \tag{4.6.3}$$

Furthermore, we can go one step further and find the action of the system. By defining the vectors as $\vec{Z}_t := \left(X_t, \vec{\Xi}_t\right)^\top, \vec{F}\left(\vec{Z}_t\right) := \left(-V'(X_t) + \xi_t, \mathbf{A}\vec{\Xi}_t\right)^\top$ and $\vec{Y}_t := (0, \vec{\eta})^\top\, Y_t = \vec{u}\, Y_t$, one can write the Markovian LE for $\vec{Z}$ as:

$$\dot{\vec{Z}}_t = \vec{F}\left(\vec{Z}_t\right) + \dot{\vec{Y}}_t, \tag{4.6.4}$$

where $\dot{\vec{Y}}$ is the vector of Poisson white noise processes. Therefore, as in the case of Bray & McKane 1989, one can find the Lagrangian of $\vec{Z}_t$ by first finding the CFal of $\dot{\vec{Y}}_t$, which is given by

$$\Phi_{\vec{Y}}[\vec{k}(t)] = \left\langle \exp i \int \mathrm{d}t\, \vec{k}(t) \vec{Y}_t \right\rangle = \left\langle \exp i \int \mathrm{d}t\, \left(\vec{k}\cdot\vec{u}\right) \dot{L}_t \right\rangle = \exp\left[\lambda \int \mathrm{d}t \left(1 - \phi_{A_1}\left(\vec{k}\cdot\vec{u}\right)\right)\right]. \tag{4.6.5}$$

Therefore, the Lagrangian of $\vec{Z}$ is given by the following:

$$\mathscr{L} = \lambda\left[1 - \phi_{A_1}\left(\vec{k}\cdot\vec{u}\right)\right] - i\vec{k}\left(\dot{\vec{Z}} - \vec{F}\left(\vec{Z}\right)\right), \tag{4.6.6}$$

where $\vec{k} = (k(t), \vec{g}(t))^\top$ is a vector with auxiliary test function k, such that one can rewrite the

Lagrangian as follows:

$$\mathscr{L} = -ik(t)\left(\dot{X} + V'(X_t) - \left\langle \vec{I}, \vec{\Xi}_t \right\rangle\right) + \lambda\left[1 - \phi_{A_1}\left(\vec{g}\cdot\vec{\eta}\right)\right] - i\vec{g}\left(\dot{\vec{\Xi}}_t - \mathbf{A}\vec{\Xi}_t\right) \tag{4.6.7}$$

with $\vec{I} = (1, 0, 0, ..., 0)^\top$. Notice that we now have a localized Lagrangian that depends on $X_t, \dot{X}_t, \vec{g}(t)$, $k(t), \vec{\Xi}_t$ and $\dot{\vec{\Xi}}_t$. In order to get the optimal path, we minimize $\mathscr{L}$ w.r.t. these variables, resulting the following localized ELE's:

$$\begin{aligned} -\frac{\mathrm{d}}{\mathrm{d}t}\frac{\partial\mathscr{L}}{\partial\dot{X}} + \frac{\partial\mathscr{L}}{\partial X} &= 0, \\ \frac{\partial\mathscr{L}}{\partial\vec{g}} &= 0, \\ \frac{\partial\mathscr{L}}{\partial k} &= 0, \\ -\frac{\mathrm{d}}{\mathrm{d}t}\frac{\partial\mathscr{L}}{\partial\dot{\vec{\Xi}}} + \frac{\partial\mathscr{L}}{\partial\vec{\Xi}} &= 0. \end{aligned} \tag{4.6.8}$$

Solving this yields the following $(2n+2)-$dimensional systems of ODE's:

$$\begin{aligned} \dot{k}(t) &= V''(X_t)k(t) \\ \dot{\vec{\Xi}}_t &= \mathbf{A}\vec{\Xi}_t + i\lambda\vec{\eta}\phi'_{A_1}\left(\vec{g}\cdot\vec{\eta}\right) \\ \dot{X}_t &= -V'(X_t) + \left\langle \vec{I}, \vec{\Xi}_t \right\rangle \\ \dot{\vec{g}}(t) &= \mathbf{A}^\top\vec{g}(t) - \vec{I}k(t). \end{aligned} \tag{4.6.9}$$

4.6.1 Application to Literature: CP Noise Process under Gaussian Limits

Now that we have the general foundation of building a time local ELE, we now apply this to the results obtained by Bray & McKane 1989[112], where the GSN is the OU process, i.e. its impulse function is exponential decay, $b(x) = \alpha e^{-\alpha x}$ and is under Gaussian Limits.

Therefore, we have the following reduced LE's:

$$\begin{aligned}\dot{X}_t &= -V'(X_t) + \xi_t \\ \dot{\xi}_t &= -\alpha\xi_t + \alpha\dot{W}_t.\end{aligned} \tag{4.6.10}$$

We can rewrite this in vector form $\dot{\vec{Z}}_t = \vec{F}\left(\vec{Z}_t\right) + \vec{u}\,\dot{Y}_t$ as in the previous section, which yields the following:

$$\frac{\mathrm{d}}{\mathrm{d}t}\begin{pmatrix} X_t \\ \xi_t \end{pmatrix} = \begin{pmatrix} -V'(X_t) + \xi_t \\ -\alpha\xi_t \end{pmatrix} + \begin{pmatrix} 0 \\ \alpha \end{pmatrix}\dot{W}_t. \tag{4.6.11}$$

Next, we apply it to the Lagrangian, noting that applying Gaussian Limits to the general model we get the following CF of our Gaussian white noise process: $\Phi_{\dot{\vec{W}}}[\vec{k(t)}] = \exp\left(-D/2\left(\vec{k}\cdot\vec{u}\right)^2\right)$, where $\vec{k}(t) = (k(t), g(t))^\top$ as before.

Note that the diffusion coefficient D and the imaginary number i can be removed w.l.o.g. by rewriting $\vec{u} \to -i\vec{u}/D$ and $\vec{k} \to -i\vec{k}/D$. Thus, it remains to find the Lagrangian of the system:

$$\begin{aligned}\mathscr{L} &= \frac{1}{2}\left(\vec{k}\cdot\vec{u}\right)^2 + \vec{k}\cdot\left(\dot{\vec{Z}} - \vec{F}\left(\vec{Z}\right)\right) \\ &= k(t)\left(\dot{X}_t + V'(X_t) - \xi_t\right) + \frac{1}{2}g(t)^2 + g(t)\left(\dot{\xi}_t + \alpha\xi_t\right).\end{aligned} \tag{4.6.12}$$

It remains to apply the localized ELE's as in Equation (4.6.8):

$$\begin{aligned}\dot{k}(t) &= V''(X_t)k(t) \\ \dot{\xi}_t &= -\alpha\xi_t + g(t) \\ \dot{X}_t &= -V'(X_t) + \xi_t \\ \dot{g}(t) &= \alpha g(t) - k(t).\end{aligned} \tag{4.6.13}$$

Notice that our ELE in Equation (4.6.8) is localized and four dimensional; the non-local and one

dimensional ELE found by Bray & McKane is:

$$-\ddot{X}+V'V''+\alpha^{-2}\left(\dddot{X}+3\dot{X}\ddot{X}V'''+\dot{X}^3V''''-\dot{X}^2V''V'''-\ddot{X}V''^2\right)=0. \tag{4.6.14}$$

We can prove that Bray&McKane's non-local ELE and our localized higher dimensional ELE are the same. Notice that from our ELE one can rewrite the instantons $g=\dot{\xi}+\alpha\xi$ and $k=\alpha^2\xi-\ddot{\xi}$. Then, we take the fourth order derivative of X:

$$\begin{aligned}
&\dot{X}=-V'+\xi\\
\implies &\ddot{X}=-\dot{X}V''+\dot{\xi}=-\dot{X}V''-\alpha\xi+g\\
\implies &\dddot{X}=-\dot{X}^2V'''-\ddot{X}V''-\alpha\dot{\xi}+\dot{g}\\
&\quad=-\dot{X}^2V'''-\ddot{X}V''-\alpha\left(-\alpha\xi+g\right)+\alpha g-k\\
&\quad=-\dot{X}^2V'''-\ddot{X}V''+\alpha^2\xi-k\\
\implies &\ddddot{X}=-\dot{X}^3V''''-3\dot{X}\ddot{X}V'''-\dot{\dddot{X}}V''+\alpha^2\dot{\xi}-\dot{k}\\
&\quad=-\dot{X}^3V''''-3\dot{X}\ddot{X}V'''-\dot{\dddot{X}}V''+\alpha^2\left(-\alpha\xi+g\right)-kV''\\
&\quad=-\dot{X}^3V''''-3\dot{X}\ddot{X}V'''-\dot{\dddot{X}}V''-\alpha^3\xi+\alpha^2g-kV''\\
&\quad=-\dot{X}^3V''''-3\dot{X}\ddot{X}V'''-\dot{\dddot{X}}V''-\alpha^3\xi+\alpha^2\left(\dot{\xi}+\alpha\xi\right)-\left(\alpha^2\xi-\ddot{\xi}\right)V''\\
&\quad=-\dot{X}^3V''''-3\dot{X}\ddot{X}V'''-\dot{\dddot{X}}V''+\alpha^2\dot{\xi}-\left(\alpha^2\xi-\ddot{\xi}\right)V'',
\end{aligned} \tag{4.6.15}$$

where the derivatives of ξ can now be retrieved from the LE: $\dot{\xi}=\ddot{X}+\dot{X}V''$ and $\ddot{\xi}=\dddot{X}+\dot{X}^2V'''+$

$\ddot{X}V''$. Therefore, plugging these back to the fourth order derivative of X yields:

$$\begin{aligned}\dddot{X} &= -\dot{X}^3 V'''' - 3\dot{X}\ddot{X}V''' - \dddot{X}V'' + \alpha^2\dot{\xi} - \left(\alpha^2\xi - \ddot{\xi}\right)V'' \\ &= -\dot{X}^3 V'''' - 3\dot{X}\ddot{X}V''' - \dddot{X}V'' + \alpha^2\left(\ddot{X} + \dot{X}V''\right) - \left(\alpha^2\left(\dot{X} + V'\right) - \dddot{X} - \dot{X}^2 V''' - \ddot{X}V''\right)V'' \\ &= -\dot{X}^3 V'''' - 3\dot{X}\ddot{X}V''' + \dot{X}^2 V''V''' + \ddot{X}V''^2 + \alpha^2\left(\ddot{X} - V'V''\right).\end{aligned} \tag{4.6.16}$$

Moving all the variables to the LHS and dividing the equation with α^2 yields the desired non-local ELE in Equation (4.6.14).

One can numerically solve the ELE in Equation (4.6.8) via Mathematica; however in order to progress on that one needs to find the boundary conditions for the tuple $(X_t, \xi_t, g(t), k(t))$. The first two are relatively trivial. As we are aiming to find the instanton of X_t within some boundary $[t_a, t_b]$, we can decide on the boundary conditions for X as $X_{t_a} = x_a$ and $X_{t_b} = x_b$. As for our CP process ξ, we can choose an initial condition $\xi_{t_a} = 0$ without loss of generality.

As for the latter two in the tuple, choosing the initial conditions $g_{t_a} = g_0$ and $k_{t_a} = k_0$ is not relatively straightforward.

First, notice that our ELE yields explicit solution for $g(t)$ given g_0: $g(t) = g_0 e^{\alpha(t-t_a)}$. Plugging this to the ODE for ξ yields: $\dot{\xi}_t = -\alpha\xi_t - iDg_0 e^{\alpha(t-t_a)}$, where, given the initial condition $\xi_{t_a} = 0$ has explicit solution

$$\xi_t = \frac{-iDg_0 e^{-\alpha t}\left(-1 + e^{2\alpha t}\right)}{2\alpha}. \tag{4.6.17}$$

In order to explicitly solve for g_0, one needs to assign additional boundary condition $\xi_{t_b} = s_b$ to get:

$$s_b = \frac{-iDg_0 e^{-\alpha t_b}\left(-1 + e^{2\alpha t_b}\right)}{2\alpha} \implies g_0 = \frac{2i\alpha s_b e^{\alpha t_b}}{D\left(-1 + e^{2\alpha t_b}\right)}. \tag{4.6.18}$$

The initial condition for $k(t)$ is even trickier to solve. Directly from the first ELE we obtain $k(t) =$

$k_0 e^{\int_{t_a}^{t} \mathrm{d}\tau\, V''(X_\tau)}$. In order to find an equation for k_0, one needs to fix a boundary for k, e.g. $k_{t_b} = k_b$ to get

$$k_0 = k_b e^{-\int_{t_a}^{t_b} \mathrm{d}\tau\, V''(X_\tau)}, \tag{4.6.19}$$

where this is now solvable if one knows the [optimal] values of X_t on $t \in [t_a, t_b]$.

These assumptions are similarly required in the Bray & McKane paper, where they focus on finding the ELE solely w.r.t X. Given the Lagrangian,

$$\mathscr{L}_{bray} = \left(\dot{X}_t + V'(X_t)\right)^2 + \frac{1}{\alpha^2}\left(\ddot{X}_t + V''(X_t)\dot{X}_t\right)^2, \tag{4.6.20}$$

the corresponding ELE for X_t is of fourth order and requires multiple boundary conditions to solve the ODE. The authors choose asymptotic boundary conditions to be the two global minima of the double well potential of the form: $V(x) = -v_1 x^2/2 + v_2 x^4/4$, where $v_1, v_2 > 0$. In below figure, the potential that we used in our numerical calculation is given. The authors here used the points a and b as the two asymptotic boundary conditions of the ELE, i.e. $\lim_{t\to-\infty} X_t = -\sqrt{v_1/v_2} = a$, and $\lim_{t\to+\infty} X_t = b$. They also proposed to choose a point d that is between these two extreme boundary conditions as their third initial condition. Instead of solving the ODE of X at the fourth order, the authors instead integrated the Lagrangian w.r.t to time and multiplied the integration by $\dot{X}$ to reduce their ELE to third order. Furthermore, in their subsequent article published in Bray, McKane & Newman in 1990[59], the authors further reduce the order of their ELE by introducing $y(x) = \dot{x}$ and rewriting the ELE in terms of y. They next propose 2 boundary conditions $y(a) = y(b) = 0$, where $x = a$ and $x = b$ are bottom and top of the symmetric wells as given in Figure 4.3.

However, instead of transforming our localized ELE to that of Bray & McKane's, we instead proposed to revert the boundary conditions of the transformed, second-order non-local ELE: $0 = y(a) = \dot{X}_0 = \dot{X}_T = y(b)$, where we set $t_a = 0$ and $t_b = T$ for some $T > 0$. Together with the desired boundary conditions of moving from the bottom of the hill towards the top, we choose the

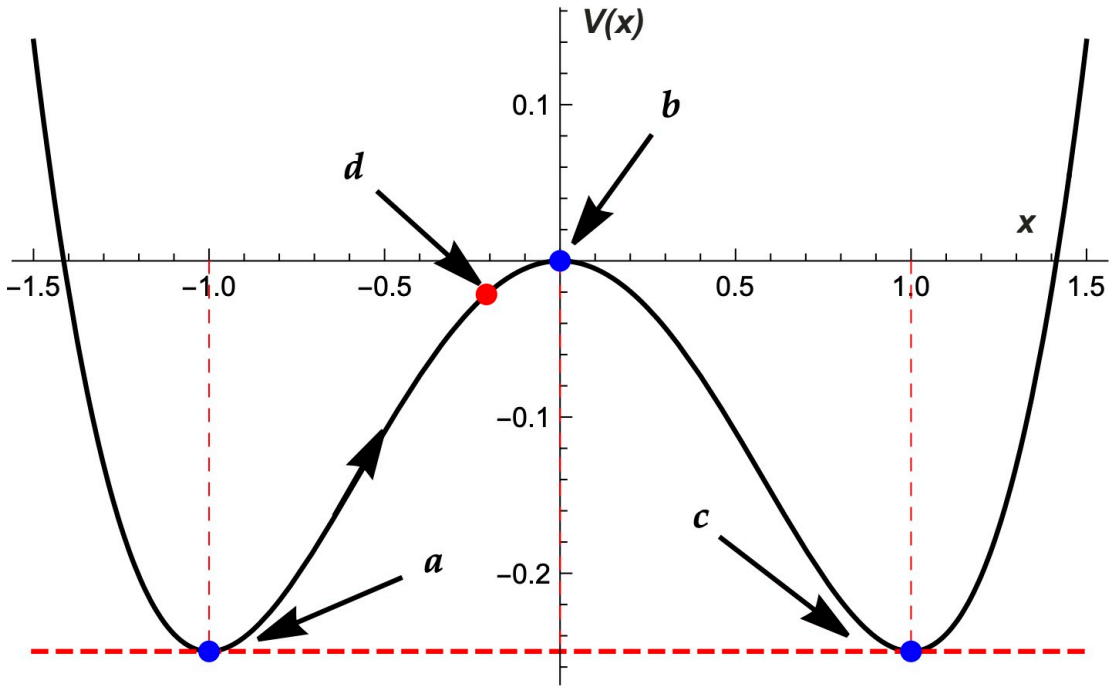

Figure 4.3: General graph of the potential $V(x) = -x^2/2 + x^4/4$ with suggested points a, b, c and d to be used in our numerical calculations.

free variable $d = (a+b)/2$ (which is the midpoint of the potential V) and apply 2 more boundary conditions on X: $X_0 = a$, and $X_T = b$. Now, we have 4 boundary conditions for X, and one can instead numerically solve the Bray & McKane's un-transformed fourth-order ELE as in Equation (4.6.14).

Before applying the initial conditions (IC's) obtained by Bray & McKane to our system of ODE's, notice that they solely depend on X, and that one can derive the IC for ξ by applying $\dot{X}_0 = -V'(X_0) + \xi_0 \implies \xi_0 = V'(X_0)$. Likewise, $\dot{X}_T = 0 \implies \xi_T = V'(X_t)$.

Instead, we can indirectly derive the IC's for k and g via the Lagrangian of X as given in Equation (4.6.12). Applying the IC of X to $\mathscr{L}$ the ELE's in Equation (4.6.13) we get:

$$\begin{aligned}
\mathscr{L}(0) &= k(0)\left(\dot{X}_0 + V'(X_0) - \xi_0\right) + \frac{1}{2}g(0)^2 + g(0)\left(\dot{\xi}_0 + \alpha\xi_0\right) \\
\implies g(0) &= \pm\sqrt{\frac{2}{3}\mathscr{L}(0)}, \\
\mathscr{L}(T) &= k(T)\left(\dot{X}_T + V'(X_T) - \xi_T\right) + \frac{1}{2}g(T)^2 + g(T)\left(\dot{\xi}_T + \alpha\xi_T\right) \\
\implies g(T) &= \pm\sqrt{\frac{2}{3}\mathscr{L}(T)}.
\end{aligned} \tag{4.6.21}$$

We can also obtain the conditions for k by taking the first derivative of the Lagrangian:

$$\begin{aligned}
\dot{\mathscr{L}}(t) &= \dot{k}(t)\left(\dot{X}_t + V'(X_t) - \xi_t\right) + k(t)\left(\ddot{X}_t + V''(X_t)\dot{X}_t - \dot{\xi}_t\right) + \\
&\quad + g(t)\dot{g}(t) + \dot{g}(t)\left(\dot{\xi}_t + \alpha\xi_t\right) + g(t)\left(\ddot{\xi}_t + \alpha\dot{\xi}_t\right) \\
\dot{\mathscr{L}}(0) &= 3g(0)\left(\alpha g(0) - k(0)\right) \implies k(0) = \alpha g(0) - \frac{\dot{\mathscr{L}}(0)}{3g(0)}, \\
\dot{\mathscr{L}}(T) &= 3g(t)\left(\alpha g(t) - k(t)\right) \implies k(T) = \alpha g(t) - \frac{\dot{\mathscr{L}}(T)}{3g(T)}.
\end{aligned} \tag{4.6.22}$$

Lastly, as we are analyzing the optimal path of the same particle X, we have that the Lagrangians obtained by our results and that of Bray & McKane as in Equation (4.6.20) should be the same,

$\mathscr{L} = \mathscr{L}_{bray}$. Therefore, we can find the IC of k and g by first solving Equation (4.6.14) with suitable initial conditions, finding $\mathscr{L}_{bray}$, and then solving our ELE with initial conditions for X, ξ, g, and k obtained throughout this section. Lastly, we used the IC as part of the **Shooting** method of our numerical computation.

For the Bray & McKane model, the initial conditions are found to be: $X_0 = -1$, $\dot{X}_0 = 0$, $\ddot{X}_0 = 0.000480018$ and $\dddot{X}_0 = -0.00359538$. Interestingly the particle jumping from the bottom well and top well is mainly characterized by the initial condition of its third derivative, also known as *initial jerk*.

By choosing a large time $T = 20$, the result is a perfect fit for instantons X as given in Figure 4.4 below, with the resulting lots for auxiliary instantons k and g given in Figure 4.5.

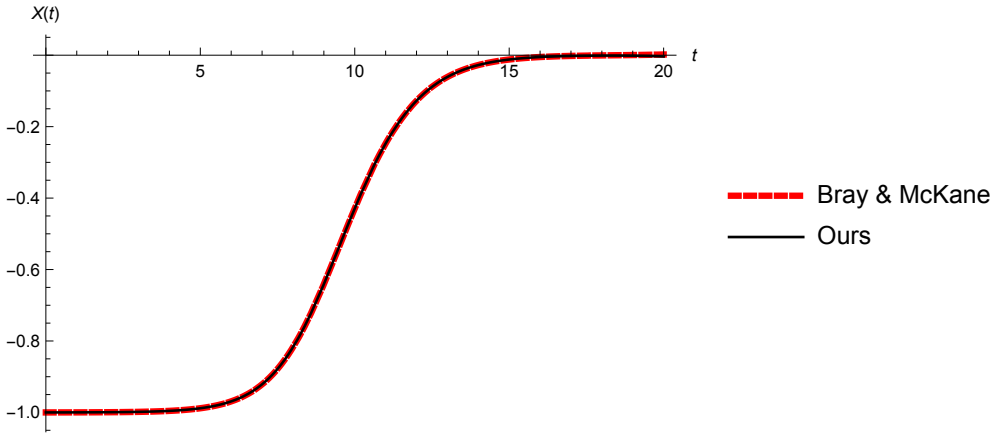

Figure 4.4: Numerical solutions of the instanton path obtained by Bray & McKane's model versus our model, where we computed the path from bottom of the well $d = a$ to the top of the well at $x = b$.

Now that we grasped how the case for exponential decay and Gaussian white noise works, let us extend to the new realm of research by finding optimal paths of X driven by for non-Gaussian colored noise process.

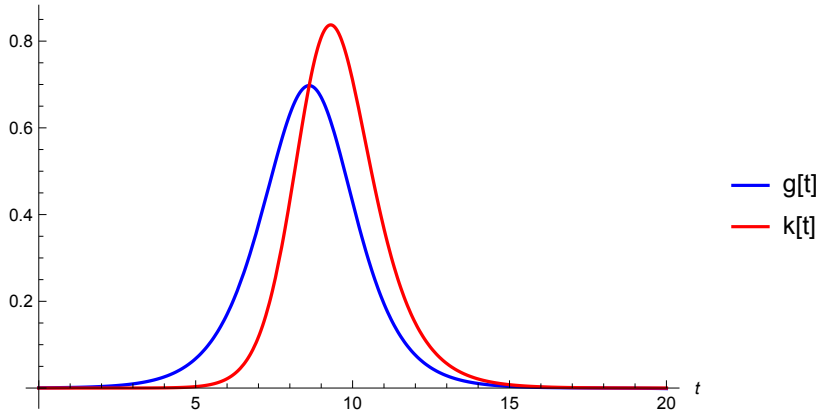

Figure 4.5: Instanton solutions of k and g for longer time range $T = 20$ from top bottom well to top well.

4.6.2 Extension from Literature: CP Noise Process

In this section, we now extend the model proposed by [112] to take into account the CP Noise process ξ formed by the exponentially decaying impulse function $h = \alpha e^{-\alpha x}$. Recall that we already obtained the Lagrangian of a general finite hierarchy system in Equation (4.6.7), followed by the localized ELE's in Equation (4.6.9). In case of our choice of h, the Lagrangian simply becomes:

$$\mathscr{L} = k(t)\left(\dot{X}_t + V'(X_t) - \xi_t\right) + \lambda\left(1 - \phi_{A_1}\left(-ig(t)\right)\right) + g(t)\left(\dot{\xi}_t + \alpha\xi_t\right), \tag{4.6.23}$$

and the local ELE becomes,

$$\begin{aligned} \dot{k}(t) &= V''(X_t)k(t) \\ \dot{\xi}_t &= -\alpha\xi_t + i\lambda\phi'_{A_1}\left(-ig(t)\right) \\ \dot{X}_t &= -V'(X_t) + \xi_t \\ \dot{g}(t) &= \alpha g(t) - k(t). \end{aligned} \tag{4.6.24}$$

As before, the IC's for X and ξ are $X_0 = -1, X_T = 0$ and $\xi_0 = V'(X_0), \xi_T = V'(X_T)$. After trial and errors, we have found instantons for the path X and action S under following jump amplitudes:

- Constant: $\phi_{A_1}(\theta) = \cosh\theta$.
- Gaussian: $\phi_{A_1}(\theta) = e^{\theta^2/2}$,
- Exponential: $\phi_{A_1}(\theta) = 1 + \frac{\theta^2}{2(1-\theta^2)}$,

The candidate variables for g_0 and k_0 are given in the below table, where we fixed g_0 and chose candidate k_0: We then solved this ELE system numerically in Mathematica, where we chose $\lambda = 1, \alpha = 1$

	Constant	Gaussian	Exponential	Gaussian Limits
g_0	0.0004799	0.0004799	0.0004799	0.0004799
$10^8 k_0$	1.552607375	1.456437384	1.337414248	1.59142852

Table 4.1: Candidate initial conditions for instantons of g and k under various jump amplitudes, compared with the case for Gaussian Limits.

and $T = 20$. We next plotted the resulting instantons of X using three jump amplitudes in Figure 4.6. This is followed by Figure 4.7 the instantons of g and k for 3 different jump amplitudes.

Lastly, we have shown in Figure 4.8 the resulting instantons of actions obtained by 3 jump amplitudes plotted against that obtained by Gaussian Limits, all normalized by the escape rate S_∞ via the Bray & McKane model. The results suggest that the stationary action is obtained by the Gaussian Limits, followed by Gaussian, Constant and Exponential jump amplitudes. As our goal is to find the minimum action required for jumping from the bottom well to the top well, we will show in the next section the combination of parameters where one can obtain an even smaller escape rate than that of Gaussian Limits.

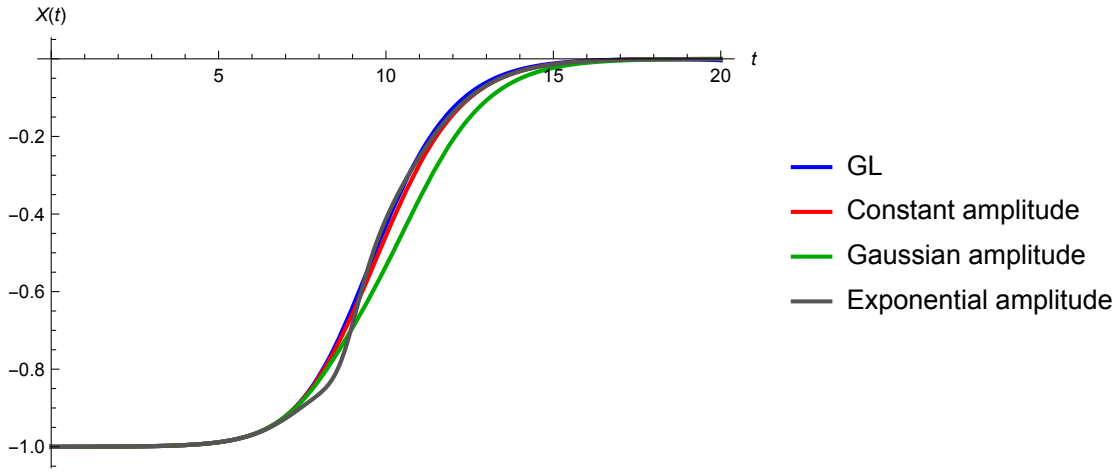

Figure 4.6: Instantons of the paths X obtained from 3 different jump amplitudes (Constant, Gaussian, and Exponential), plotted against the case for Gaussian Limits.

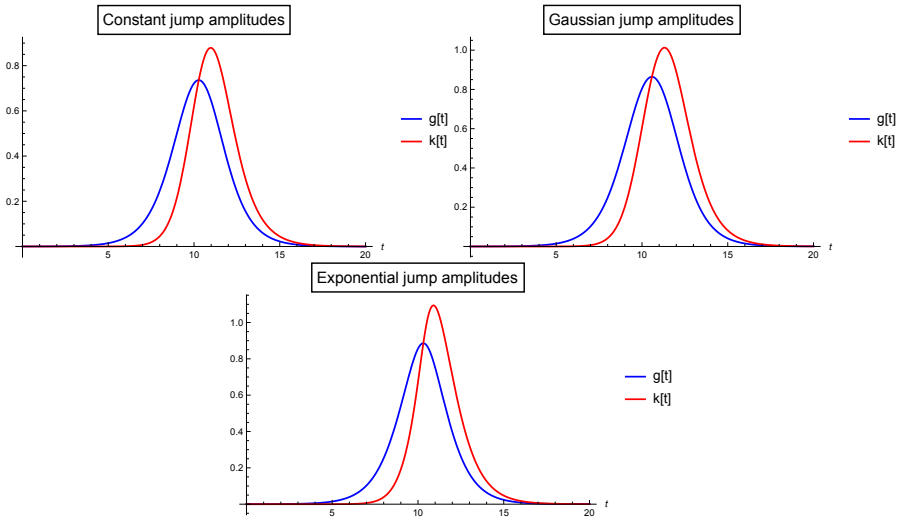

Figure 4.7: Insantons of g and k under 3 different jump amplitudes.

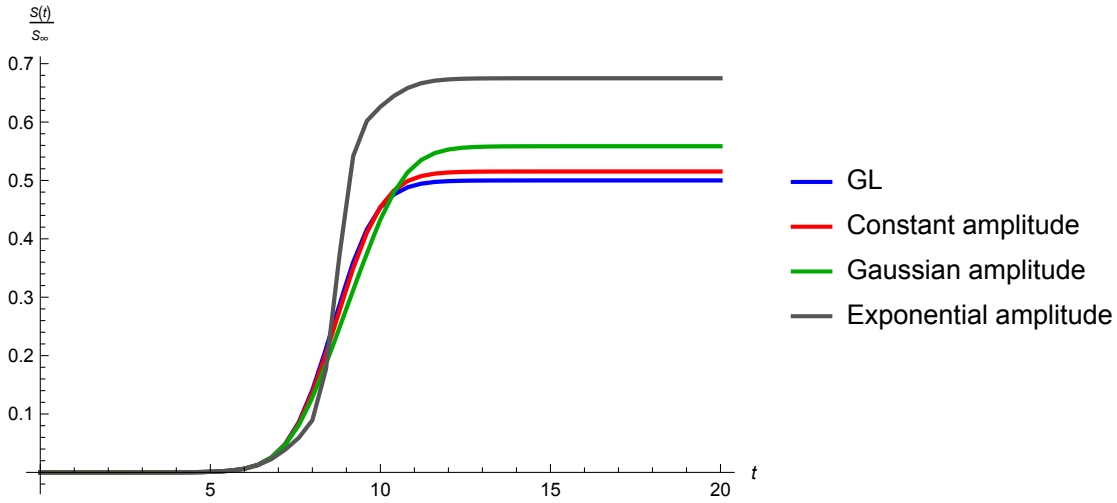

Figure 4.8: Instantons of actions driven by Constant, Gaussian and Exponential jump amplitudes and Gaussian Limits (GL), normalized by escape rate obtained via the Bray & McKane model, S_∞.

4.6.3 Optimal Escape Rates for Different Parameters of the CP Noise ξ

In this section, we now find various combinations of parameters defined by the colored Poisson noise ξ where one can attain smallest escape rate. For more in depth analysis, we will focus on varying parameters of various jump amplitudes, starting with the constant jump amplitude.

Constant Jump Amplitude

Here, the parameters to be varied are the jump intensity λ and amplitude coefficient A_0 such that the CF of the jump amplitudes will be given by $\phi_{A_1}(A_0\theta) = \cosh(A_0\theta)$. As in the previous section, we fixed $g_0 = 0.0004799$ and perturbed k_0 to obtain the escape rates.

Since the derivation of optimal escape calculations for non-Gaussian and non-Markovian processes are new, we will measure the escape rate

$$S = \int_{t_a}^{t_b} \mathrm{d}\tau\, k(\tau)\left(\dot{X}_\tau + V'(X_\tau) - \xi_\tau\right) + \lambda\left(1 - \phi_{A_1}\left(-A_0 i g(\tau)\right)\right) + g(\tau)\left(\dot{\xi}_\tau + \alpha\xi_\tau\right) \quad (4.6.25)$$

by normalizing S with the case for Gaussian Limits on ϕ to see whether one can achieve smaller escape rate (hence normalization is < 1) for different parameters. As in Baule & Sollich paper, the Gaussian Limit is obtained by truncating φ at the quadratic term of its Taylor series of $\cosh$, i.e. $\varphi_{trunc}(\theta) = \sum_{n=0}^{1} \theta^{2n}/(2n)! = 1 + x^2/2$, therefore yielding the Gaussian Limit.

Gaussian Jump Amplitude

We established in the previous subsection that in the case of constant jump amplitudes, the effective escape rate of X driven by colored Poisson noise ξ with Constant jump amplitudes is higher than the Gaussian colored noise.

Now, we outline the case for Gaussian jump amplitudes, where $\phi_{A_1}(A_0\theta) = e^{A_0^2\theta^2/2}$. The Gaussian Limits case will be the same as before: $\phi_{A_1}^{trunc}(A_0\theta) = 1 + A_0^2\theta^2/2$. The IC k_0 of the Gaussian jump amplitudes and the corresponding normalized escape rates are given below Tables, noting that the Gaussian Limit case k_0^{trunc} will be the same as in the constant jump amplitude case. We again started with $g_0 = 0.0004799$.

Furthermore, for $A_0 = 1$, we plotted the escape rates w.r.t. Gaussian and Constant jump amplitudes in Figure 4.9, where we observe that the Gaussian jump amplitude case has more efficient escape rate. Lastly, for various values of A_0 and λ, we plotted heat diagram of S/S_{GL} for Gaussian jump amplitudes in Figure 4.10, where similar decaying behavior is observed for the case in Figure 4.9; however the efficiency of escape rate increases for smaller A_0.

For Various Impulse Function Coefficient α

Now that we established the efficacy of the escape rate of the Gaussian jump amplitude for various λ and A_0, we next show whether perturbing the coefficient α of exponential decaying impulse function $h(x) = \alpha e^{-\alpha x}$ would alter the overall behavior of the normalized escape rate. For simple recall, we note that for $\alpha \to \infty$ the CP noise ξ becomes PWN. This time, we fixed $g_0 = 0.0004799$ for $\alpha = 1.5$ and decreased $g_0 = 10^{-6}$ for $\alpha = 2$.

Now, we showed in this section that relaxation of the TNL ELE yields high order, coupled yet now local ELE's where the tuple of the hierarchies $\left(\xi, {}^{(1)}\xi, \ldots, {}^{(n)}\xi\right)$ together with the position process X jointly become Markovian. We also showed that our hierarchy method matches with the

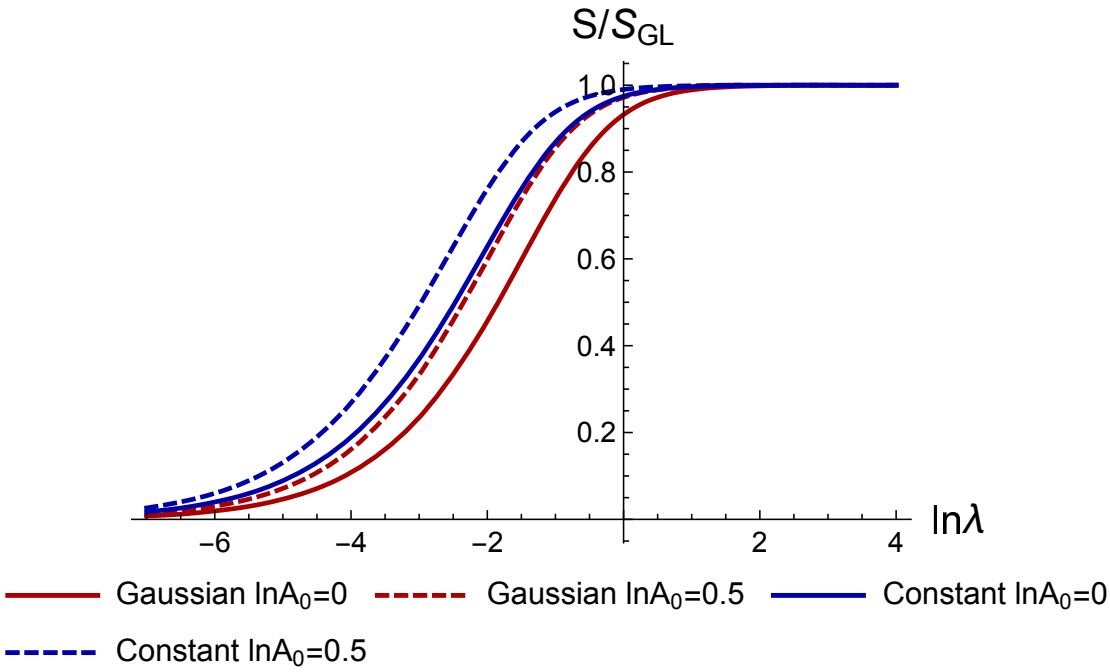

Figure 4.9: Plot of the normalized actions S/S_{GL} with respect to $\ln \lambda$ for Constant and Gaussian jump amplitudes at various A_0.

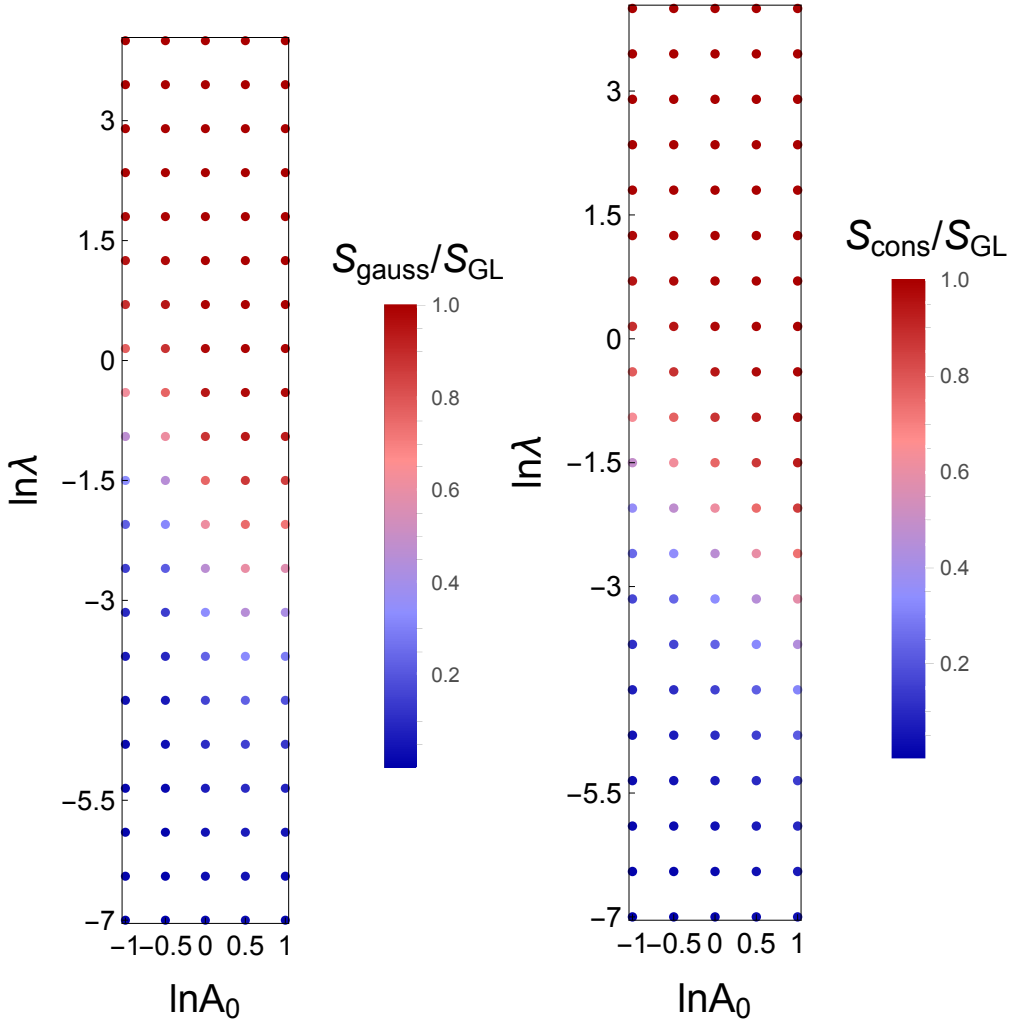

Figure 4.10: Heatmap of normalized escape rates S_{GL} of X driven by Gaussian and Constant jump amplitudes with various λ and A_0.

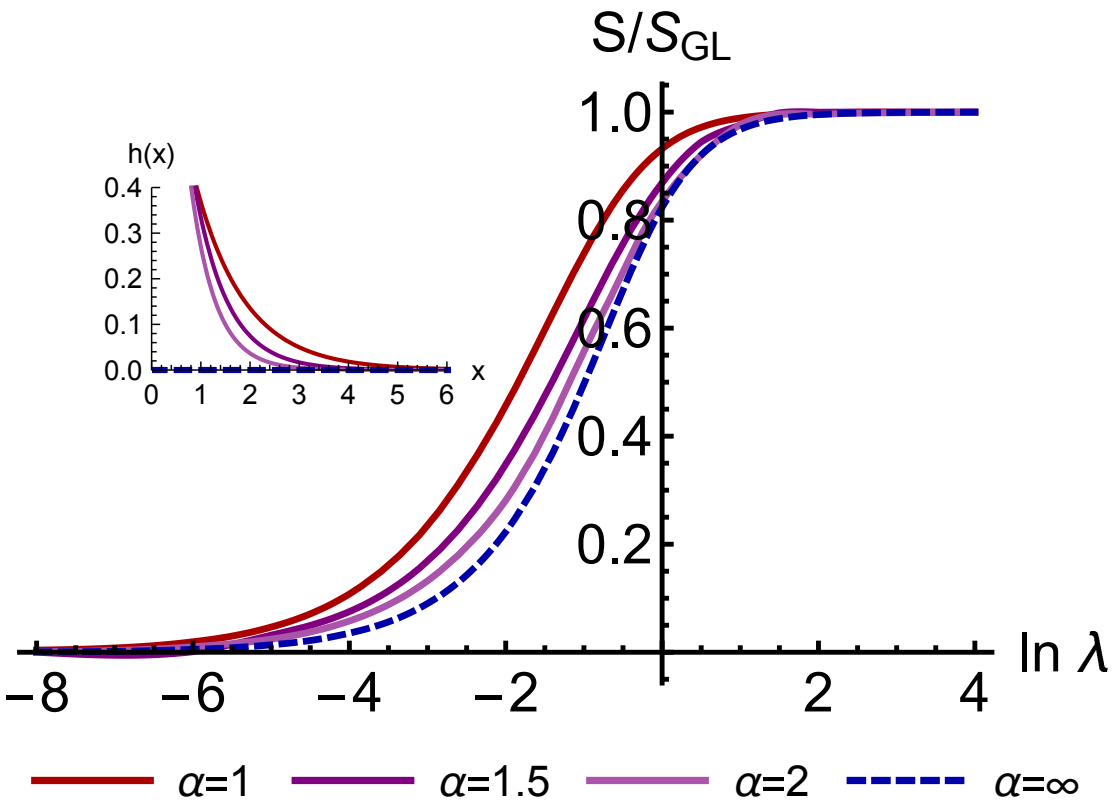

Figure 4.11: Plot of the normalized actions S/S_{GL} with respect to $\ln \lambda$ at $A_0 = 1$ for Gaussian jump amplitudes for various impulse function coefficient α, where $\alpha = \infty$ refers to the Markovian limit $h \to \delta$.

results obtained by[87], where authors solely focused on the CP noise process, the impulse function of which only has unit hierarchy order.

We now expand the impulse functions to higher hierarchy orders and show new methods of computing the localized ELE's by uncoupling them with the *Markov Embedding* principle.

4.7 Uncoupling Time Non Local ELE's By Markov Embedding Technique

So far in the previous section, we have established how the action is calculated using the exponentially decaying impulse function, which is a first hierarchical function. We now extend our method to finding the optimal path of X under a general potential V for higher-order hierarchical functions.

Let us first outline an example for the case of second hierarchical impulse function of the following form:

$$h(x) = \frac{\alpha^2+\beta^2}{\alpha+\beta} e^{-\alpha x} \left(\sin \beta x + \cos \beta x\right). \tag{4.7.1}$$

Recall from Chapter 2 that the impulse function h is now the solution of the second order IVP: $\ddot{h} - 2\alpha\dot{h} + \left(\alpha^2+\beta^2\right) h = 0,\ h(0) = 1,\ \dot{h}(0) = \beta - \alpha$. Therefore, the hierarchy of ξ becomes second order:

$$\begin{aligned} \dot{\xi}_t &= {}^{(1)}\xi_t + \dot{L}_t \\ {}^{(1)}\dot{\xi}_t &= 2\alpha\, {}^{(1)}\xi_t - \left(\alpha^2+\beta^2\right)\xi_t + (\beta-\alpha)\,\dot{L}_t, \end{aligned} \tag{4.7.2}$$

with coefficient vector $\vec{\eta}$ and matrix $\mathbf{A}$ respectively given by $\vec{\eta} = (1, \beta-\alpha)^\top$ and

$$\mathbf{A} = \begin{pmatrix} 0 & 1 \\ -(\alpha^2+\beta^2) & 2\alpha \end{pmatrix}. \tag{4.7.3}$$

Defining $\vec{\Xi}_t = \left(\xi_t, {}^{(1)}\xi_t\right)^\top, \vec{g} = (g_1(t), g_2(t))$ the Lagrangian of as in (4.6.7) is now given by the

following:

$$\begin{aligned}\mathscr{L} = &- ik(t)\left(\dot{X}_t + V'(X_t) - \xi_t\right) + \lambda\left[1 - \phi_{A_1}\left(g_1(t)\right)\right] - ig_1(t)\left(\dot{\xi}_t - {}^{(1)}\xi_t\right) \\ &+ \lambda\left[1 - \phi_{A_1}\left(\left(\beta - \alpha\right)g_2(t)\right)\right] - ig_2(t)\left({}^{(1)}\dot{\xi}_t - \left(\alpha^2 + \beta^2\right)\xi_t + 2\alpha\,{}^{(1)}\xi_t\right).\end{aligned} \tag{4.7.4}$$

Under Wick rotations $k \mapsto -ik, g_1 \mapsto -ig_1$ and $g_2 \mapsto -ig_2$, this yields the following localized ELE as in (4.6.9):

$$\begin{aligned}\dot{k}(t) &= V''(X_t)k(t) \\ \dot{\xi}_t &= {}^{(1)}\xi_t + i\lambda\phi'_{A_1}\left(-ig_1(t)\right) \\ {}^{(1)}\dot{\xi}_t &= -\left(\alpha^2 + \beta^2\right)\xi_t + 2\alpha\,{}^{(1)}\dot{\xi}_t + i\lambda\phi'_{A_1}\left(-i\left(\beta - \alpha\right)g_2(t)\right) \\ \dot{X}_t &= -V'(X_t) + \xi_t \\ \dot{g}_1(t) &= -\left(\alpha^2 + \beta^2\right)g_2(t) + k(t) \\ \dot{g}_2(t) &= g_1(t) + 2\alpha g_2(t).\end{aligned} \tag{4.7.5}$$

Such a system is not only highly coupled, it also results new equations, where we now have to find the *Ansätze* for the initial conditions ${}^{(1)}\xi_0, g_1(0), g_2(0)$ and $k(0)$ and optimize each parameter in order to obtain the optimal path X.

One way to overcome this problem of coupled systems is to approximate the impulse function by simpler functions. In fact, one may approximate any impulse function h by the sum of complex-valued exponential functions. This method of approximating impulse functions is called *Markov Embedding Technique*, which we will introduce in the next section.

Before we progress on this, since the approximate impulse function will be complex-valued, so will the GSN ξ. Therefore, we first need to introduce the concept of *complexifying* stochastic processes.

4.7.1 Complexification of Stochastic Processes

So far throughout this thesis, we considered stochastic processes X on the real line $\mathbb{R}$. In this section, we show that not only one can extend stochastic processes to the complex plane, i.e. *complexify* the stochastic processes, but this extension also preserves the properties and definitions we outlined in Chapter 1.

Let us first begin by explaining the extension for random variables. Complex random variables play an increasingly important role in communications and biomedical signal processing and related fields[38] as well as in condensed matter physics where complex-valued optical scattering indices are observed[39]. Instead of treating random variables as complex-valued, one usually defines a complex random variable as a short-hand notation of defining a pair of real random variables.[40].

In this sense, if we let X and Y be two random variables defined over the probability space $(\Omega, \mathcal{F}, \mathbb{P})$ that need not be independent, then the complex random variable Z can be defined as $Z = X + iY$, where $i = \sqrt{-1}$ is the imaginary number. Indeed, the CDF of Z is a function $F : \mathbb{C} \to [0, 1]$ that is given by the joint CDF of X and Y:

$$F_Z(z) = F_{X,Y}(\Re(z), \Im(z)) = \mathbb{P}(X \leq \Re(z), Y \leq \Im(z)). \tag{4.7.6}$$

If we define $x = \Re(z)$ and $y = \Im(z)$ for easier writing, the PDF of Z, denoted by $f_Z : \mathbb{C} \to [0, 1]$, if it exists, will be given by differentiating the joint CDF of X and Y with respect to x and y:

$$f_Z(z) = \frac{\partial^2}{\partial x \partial y} \mathbb{P}(X \leq x, Y \leq y). \tag{4.7.7}$$

Due to its linear nature, the expectation in complex sense is the same as the expectation of the sum of two random variables: $\langle Z \rangle = \langle X \rangle + i \langle Y \rangle$. However, the variance of complex random variables is not trivial. In literature, the variance in the complex plane is categorized into *absolute variance*

and *pseudo-variance.* The absolute variance is, as hinted in its name, the variance of Z in an absolute sense:

$$\mathrm{var}_{Abs}[Z] = \left\langle |Z|^2 \right\rangle - |\langle Z \rangle|^2 . \tag{4.7.8}$$

By plugging in the definition of Z, we get that $\left\langle |Z|^2 \right\rangle - |\langle Z \rangle|^2 = \left\langle X^2 \right\rangle - \langle X \rangle^2 + \left\langle Y^2 \right\rangle - \langle Y \rangle^2$; therefore, the absolute variance of Z is given by the sum of the variances of X and Y: $\mathrm{var}_{Abs}[Z] = \mathrm{var}[\Re(Z)] + \mathrm{var}[\Im(Z)]$. Therefore, the absolute variance is a positive and real number, just as its real counterpart.

On the other hand, the pseudovariance is the variance of Z that is not in absolute sense: $\mathrm{var}_p[Z] = \left\langle Z^2 \right\rangle - \langle Z \rangle^2$. In this case, the pseudovariance is a generally complex number that is treated the same way as summation of two random variables:

$$\mathrm{var}_p[Z] = \mathrm{var}[\Re(Z)] - \mathrm{var}[\Im(Z)] + 2i\mathrm{cov}[\Re(Z), \Im(Z)] . \tag{4.7.9}$$

Lastly, due to its linear definition, the CF of Z is a function $\phi : \mathbb{C} \to \mathbb{C}$ that is the CF of the sum of two random variables:

$$\phi_Z(\omega) = \left\langle e^{i\Re(\bar{\omega}Z)} \right\rangle = \left\langle e^{i(\Re(\omega)\Re(Z) + \Im(\omega)\Im(Z))} \right\rangle . \tag{4.7.10}$$

Using the case of random variables, one can then extend this notion of complexification to stochastic processes the same way. Complex stochastic processes first arose in a detailed analysis by Hida in 1971 [41] for providing a mathematical model of the complex white noise, i.e. collection of independent complex random variables. This was later brought out extensively to quantum mechanics due to square root dependence of stochastic processes (which is naturally complex-valued) with the solution of Schrodinger's equation [126].

If we let $X = (X_t)_{t \geq 0}$ and $Y = (Y_t)_{t \geq 0}$ be two stochastic processes defined on the probability

spaces $(\Omega, \mathcal{F}, \mathbb{P})$ that also need not be independent, then one can construct a complex stochastic process $Z = (Z_t)_{t\geq 0}$ where each realization is defined by $Z_t = X_t + iY_t$. Since the realization Z_t is a random variable, all the above definitions on expectation, absolute and pseudo-variance, and the CF, are applicable for Z_t.

In addition, by[43], the CFal of Z can also be extended from its CF as follows:

$$\Phi_Z[\omega] = \left\langle \exp i \int_0^\infty \mathrm{d}t\, \Re\left(\overline{\omega(t)} Z_t\right) \right\rangle = \left\langle \exp i \int_0^\infty \mathrm{d}t \left(\Re\left(\omega(t)\right)\Re\left(Z_t\right) + \Im\left(\omega(t)\right)\Im\left(Z_t\right)\right) \right\rangle . \tag{4.7.11}$$

This will be a useful tool in understanding the behavior of the complex-valued GSN process ξ. One way to complexifying ξ is to let the impulse function h be extended to the complex plane, $h : \mathbb{R} \to \mathbb{C}$. Therefore, by definition, the real part (and likewise the imaginary part) of each realization of ξ is given by:

$$\Re\left(\xi_t\right) = \Re\left(\sum_{i=1}^{N_t} A_i h(t - T_i)\right) = \sum_{i=1}^{N_t} A_i \Re\left(h(t - T_i)\right) . \tag{4.7.12}$$

Therefore, if we assume a complex-valued impulse function, we can rewrite CFal of ξ from Equation (2.3.7) as follows:

$$\Phi_\xi[\omega] = \exp\left[\lambda \int_0^\infty \mathrm{d}t \left(\phi_{A_1}\left(\int_t^{t_b} \mathrm{d}s\, \Re\left(\overline{\omega(s)} h(s - t)\right)\right) - 1\right)\right] . \tag{4.7.13}$$

Lastly, we can also define the complex position process X to be the solution of the LE $\dot{X}_t = -V'(X_t) + \xi_t$, where the potential $V : \mathbb{C} \to \mathbb{C}$ is now also complexified.

4.7.2 Path Integral Formulation for Complex Stochastic Processes

From the CFal of the complex GSN process ξ from Equation (4.7.13), we can then extend the path integral formulation X as the LE solution. In the complexified version, the probability amplitude for

the time frame $[t_a, t_b]$ is then given by:

$$\pi(x_b, t_b | x_a, t_a) = \oint_{\mathscr{C}_X} \mathcal{D}[X] \oint_{\mathscr{C}_g} \mathcal{D}\left[\frac{g}{2\pi}\right] \Phi_{\xi}[g] \exp\left(i \int_{t_a}^{t_b} \mathrm{d}t\, g(t) \left(\dot{X}_t + V'(X_t)\right)\right) \cdot \exp\left(\frac{1}{2} \int_{t_a}^{t_b} \mathrm{d}t\, V''(X_t)\right), \tag{4.7.14}$$

where $\Phi_{\xi}[g]$ is the CFal of the complex GSN in Equation (4.7.13) bounded on $[t_a, t_b]$. However, as one refers to the path integral formula, the resulting action and Lagrangian will now also be complex valued.

Complex Lagrangian and action have also been recently studied in analyzing quantum mechanical systems and biochemical dynamics. Complex Lagrangian arises in non-standard cases where there may be hidden properties of a given dynamical system [34], or in general to provide a more accurate approximation of the Master Equation of simple biochemical circuits [35]. Furthermore, complex action has been shown to provide a future-included theory of quantum mechanics, as well as calculating black hole dynamics in general relativity [42].

To approach the principle of stationary action in the complex realm, we complexify the action functional into purely real and purely imaginary values, $S = S_R + iS_I$, hence also the Lagrangian $\mathscr{L} = \mathscr{L}_R + \mathscr{L}_I$. Therefore, by [41] and [42], the probability amplitude for the time frame $[t_a, t_b]$ under weak-noise limit as in (4.2.11) can be rewritten as follows,

$$\pi\left(x_b, t_b | x_a, t_a\right) = \oint_{\mathscr{C}_X} \mathcal{D}[X] \oint_{\mathscr{C}_g} \mathcal{D}\left[\frac{g}{2\pi\varepsilon}\right] \exp\left[-\frac{S_R[X,g]}{\varepsilon} - i\frac{S_I[X,g]}{\varepsilon}\right]. \tag{4.7.15}$$

Therefore, the stationary action will now be taken as the functional expansion on both real and imaginary parts of the action: $\delta S_R = \delta S_I = 0$ and by Equation (4.2.5) the stationary action princi-

ple yields the following TNL ELE:

$$\begin{aligned}\int_{t_a}^{t_b} \mathrm{d}t \left(\delta X_R \sum_{j=0}^{\infty} \left(-\frac{\mathrm{d}}{\mathrm{d}t}\right)^j \frac{\partial S_R}{\partial X_R^{(j)}} + \delta g_R \sum_{j=0}^{\infty} \left(-\frac{\mathrm{d}}{\mathrm{d}t}\right)^j \frac{\partial S_R}{\partial g_R^{(j)}} \right) = 0, \\ \int_{t_a}^{t_b} \mathrm{d}t \left(\delta X_I \sum_{j=0}^{\infty} \left(-\frac{\mathrm{d}}{\mathrm{d}t}\right)^j \frac{\partial S_I}{\partial X_I^{(j)}} + \delta g_I \sum_{j=0}^{\infty} \left(-\frac{\mathrm{d}}{\mathrm{d}t}\right)^j \frac{\partial S_I}{\partial g_I^{(j)}} \right) = 0,\end{aligned} \tag{4.7.16}$$

where we used the same notation $X_R = \Re(X), X_I = \Im(X)$ and $g_R = \Re(g), g_I = \Im(g)$. Thus, the TNL ELE will then be similar to the real-valued counterpart, where the functional derivatives will instead be split to purely real and purely imaginary X and g.

4.7.3 Introduction to Markov Embedding Technique

Markov Embedding is a very useful technique to approximate the behavior of a non-Markovian stochastic process in the Markovian realm. It has been widely applied in theoretical physics to approximate non-Markovian the Schrödinger equation of a quantum particle[88] and modeling complex network dynamics[89].

We first recall that under the [trivial] exponentially decaying impulse function $h(x) = \alpha e^{-\alpha x}$ with $\alpha > 0$, the resulting CP process ξ becomes OU noise, and the tuple process (X, ξ) is Markovian. Here, we will use sum of exponential functions to approximate our impulse function. By[90] and[91], any *continuously differentiable* $h : \mathbb{R} \to \mathbb{C}$ can be approximated by the following sum of exponentials:

$$h(x) \approx h_{appr}(x) = \sum_{j=1}^{K} \beta_j e^{-\alpha_j x}, \tag{4.7.17}$$

where $\alpha_j, \beta_j \in \mathbb{C} \setminus \{0\}$ are complex-valued coefficients with condition $\Re(\alpha_j) > 0$ for all j. Authors in referenced paper neglected the normalization coefficients β_j, however it is essential in our circumstance as we also need set the initial value $h(0) = h_{appr}(0) = \sum_{j=1}^{K} \beta_j$. Therefore, using this

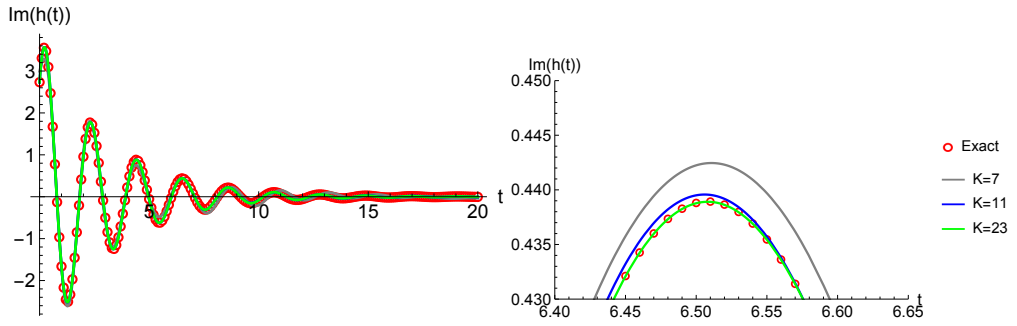

Figure 4.12: Approximating the damped oscillating function $h(t) = \left(\alpha^2 + \beta^2\right) / (\alpha + \beta)\, e^{-\alpha t} (\sin \beta t + \cos \beta t)$ by sum of complex exponentials. We took the Imaginary part $\Im\left(h_{approx}(x)\right)$ in order to plot them in Cartesian coordinates with respect to increasing K. The plot on the right is the closeup version to better see the overlap of approximations with h. We chose $\alpha = 3$ and $\beta = 1/3$ in our calculations.

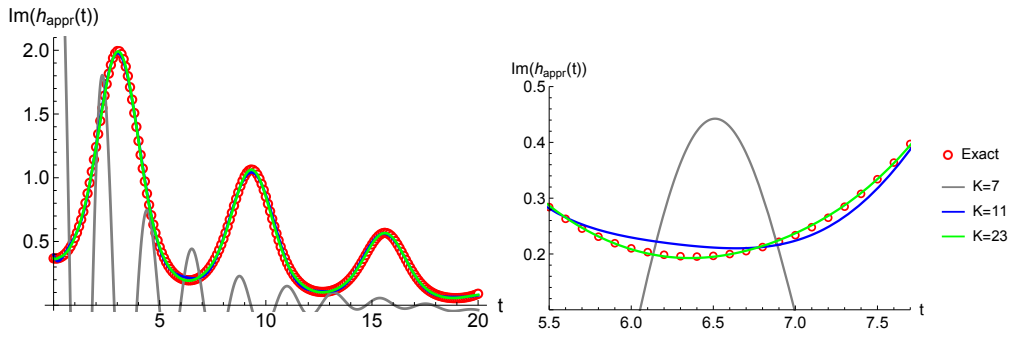

Figure 4.13: Approximating an arbitrary function $h(t) = e^{-(\cos t + t/10)}$ by sum of complex exponentials. We took the Imaginary part $\Im\left(h_{approx}(x)\right)$ in order to plot them in Cartesian coordinates with respect to increasing K. The plot on the right is the closeup version to better see the overlap of approximations with h.

exponential sum term, we can rewrite the realization of the CP process ξ as follows:

$$\xi_t = \sum_{i=1}^{N_t} A_i \sum_{j=1}^{K} \beta^{-\alpha_j (t-T_i)} = \sum_{j=1}^{K} {}^{(j)}\xi_t, \tag{4.7.18}$$

where

$${}^{(j)}\xi_t = \beta_j \sum_{i=1}^{N_t} A_i e^{-\alpha_j (t-T_i)} \tag{4.7.19}$$

has the following time derivative:

$${}^{(j)}\dot{\xi}_t = -\alpha_j {}^{(j)}\xi_t + \beta_j \dot{L}_t, \tag{4.7.20}$$

with $\dot{L}_t$ forming the PWN. Notice that due to α_j and β_j, the GSN ξ becomes complex-valued. Plugging this relation into the LE of X yields a much more simple, [almost] uncoupled, K-th order system of SDE's in derivative form:

$$\begin{aligned}
\dot{X}_t &= -V'(X_t) + \sum_{j=1}^{K} {}^{(j)}\xi_t \\
{}^{(1)}\dot{\xi}_t &= -\alpha_1 {}^{(1)}\xi_t + \beta_1 \dot{L}_t \\
{}^{(2)}\dot{\xi}_t &= -\alpha_2 {}^{(2)}\xi_t + \beta_2 \dot{L}_t \\
&\vdots \\
{}^{(K)}\dot{\xi}_t &= -\alpha_K {}^{(K)}\xi_t + \beta_K \dot{L}_t
\end{aligned} \tag{4.7.21}$$

Note that although the SDE for X is coupled, the rest of the SDE's is uncoupled. Therefore, we first consider the system for ξ. Defining $\vec{\Xi}_t = \left({}^{(1)}\xi_t, {}^{(2)}\xi_t, \ldots, {}^{(K)}\xi_t, \right)^\top$, $\vec{\alpha} = (\alpha_1, \alpha_2, \ldots, \alpha_K)^\top$, and $\vec{\beta} = \left(\beta_1, \beta_2, \ldots, \beta_K\right)^\top$, we can rewrite the ξ system in matrix form:

$$\dot{\vec{\Xi}}_t = -\left(\mathbf{I} \otimes \vec{\alpha}\right) \vec{\Xi}_t + \vec{\beta} \dot{L}_t, \tag{4.7.22}$$

where $\mathbf{I} \otimes \vec{\alpha}$ is the tensor product between the identity matrix and $\vec{\alpha}$ defined by

$$\mathbf{I} \otimes \vec{\alpha} = \begin{pmatrix} \alpha_1 & 0 & 0 & \dots & 0 \\ 0 & \alpha_2 & 0 & \dots & 0 \\ 0 & 0 & \alpha_3 & \dots & 0 \\ \vdots & \vdots & \vdots & \ddots & \vdots \\ 0 & 0 & 0 & \dots & \alpha_K \end{pmatrix}. \tag{4.7.23}$$

We can further define $\vec{Z}_t = \left(X_t, \vec{\Xi}_t\right)^\top$ and find the SDE for $\vec{Z}_t$:

$$\dot{\vec{Z}}_t = F\left(\vec{Z}_t\right) + \vec{Y}_t, \tag{4.7.24}$$

where $F\left(\vec{Z}_t\right) = \left(-V'(X_t) + \left\langle \vec{\Xi}_t, \vec{1} \right\rangle, -\left(\mathbf{I} \otimes \vec{\alpha}\right) \vec{\Xi}_t\right)^\top$ with $\left\langle \vec{\Xi}_t, \vec{1} \right\rangle = \sum_{j=1}^{K} {}^{(j)}\xi_t$ being the inner product of $\vec{\Xi}_t$ and 1-vector, $\vec{1} = (1, 1, \dots, 1)^\top$, and $\vec{Y}_t = \left(0, \vec{\beta}\right) \dot{L}_t = \vec{\eta} \dot{L}_t$. From here, the CFal of $\vec{Y}$ with K-dimensional complex-valued test function $\vec{k}(t) = (k(t), \vec{g}(t))$ is given by:

$$\begin{aligned} \Phi_{\vec{Y}_t}[\vec{k}(t)] &= \left\langle \exp i \int \mathrm{d}t \, \Re\left(\vec{\bar{k}} \cdot \vec{Y}_t\right) \right\rangle = \left\langle \exp i \int \mathrm{d}t \, \Re\left(\vec{\bar{k}} \cdot \vec{\eta}\right) \dot{L}_t \right\rangle \\ &= \exp\left[\lambda \int \mathrm{d}t \, \left(1 - \phi_{A_1}\left(\Re\left(\vec{\bar{k}} \cdot \vec{\eta}\right)\right)\right)\right]. \end{aligned} \tag{4.7.25}$$

Therefore, the real and imaginary parts of the Lagrangian of the system $\vec{Z}$ is now given by:

$$\begin{aligned} \mathscr{L}_R &= \lambda\left[1 - \phi_{A_1}\left(\vec{k}_R\right) \cdot \vec{\eta}_R\right] - i\vec{k}_R(t)\left(\dot{\vec{Z}}_{R;t} - F\left(\vec{Z}_{R;t}\right)\right) \\ &= -ik_R(t)\left(\dot{X}_{R;t} + V'(X_{R;t}) - \left\langle \vec{\Xi}_{R;t}, \vec{1} \right\rangle\right) + \lambda\left[1 - \phi_{A_1}\left(\vec{g}_R \cdot \vec{\beta}_R\right)\right] - i\vec{g}_R\left(\dot{\vec{\Xi}}_{R;t} + \left(\mathbb{I} \otimes \vec{\alpha}_R\right)\vec{\Xi}_{R;t}\right), \\ \mathscr{L}_I &= -ik_I(t)\left(\dot{X}_{I;t} + V'(X_{I;t}) - \left\langle \vec{\Xi}_{I;t}, \vec{1} \right\rangle\right) + \lambda\left[1 - \phi_{A_1}\left(\vec{g}_I \cdot \vec{\beta}_I\right)\right] - i\vec{g}_I\left(\dot{\vec{\Xi}}_{I;t} + \left(\mathbb{I} \otimes \vec{\alpha}_I\right)\vec{\Xi}_{I;t}\right). \end{aligned} \tag{4.7.26}$$

From here, we can find the minimum action of X by minimizing $\mathscr{L}$ with respect to $k, \vec{g}, X, \vec{\Xi}$ as before, yielding the ELE:

$$\begin{aligned}
\dot{X}_{R;t} &= -V'(X_{R;t}) + \left\langle \vec{\Xi}_{R;t}, \vec{1} \right\rangle \\
\dot{X}_{I;t} &= -V'(X_{I;t}) + \left\langle \vec{\Xi}_{I;t}, \vec{1} \right\rangle \\
\dot{k}_R(t) &= V''(X_{R;t}) k_R(t) \\
\dot{k}_I(t) &= V''(X_{I;t}) k_I(t) \\
\dot{\vec{g}}_R(t) &= (\mathbf{I} \otimes \vec{\alpha}_R)\, \vec{g}_R(t) - k_R(t)\vec{1} \\
\dot{\vec{g}}_I(t) &= (\mathbf{I} \otimes \vec{\alpha}_I)\, \vec{g}_I(t) - k_I(t)\vec{1} \\
\dot{\vec{\Xi}}_{R;t} &= -(\mathbf{I} \otimes \vec{\alpha}_R)\, \vec{\Xi}_{R;t} + i\lambda \vec{\beta}_R \phi'_{A_1}\left(\vec{g}_R(t) \cdot \vec{\beta}_R\right) \\
\dot{\vec{\Xi}}_{I;t} &= -(\mathbf{I} \otimes \vec{\alpha}_I)\, \vec{\Xi}_{I;t} + i\lambda \vec{\beta}_I \phi'_{A_1}\left(\vec{g}_I(t) \cdot \vec{\beta}_I\right).
\end{aligned} \tag{4.7.27}$$

Simplifying the Matrix ODE

Although the system is coupled again due to X, the SDE's for both real and imaginary parts of $\dot{X}$ only depends on the sum of the variables ${}^{(j)}\xi_t$, where each of their individual SDE's are uncoupled.

We can actually use the uncoupled property of ${}^{(j)}\xi_t$ to our advantage. Notice that for each j the CP ${}^{(j)}\xi_t$ is a Gen-OU process with initial condition ${}^{(j)}\xi_0 = 0$ a.s., and has the general solution:

$${}^{(j)}\xi_t = \beta_j \int_0^t \mathrm{d}\tau\, \dot{L}_\tau e^{-\alpha_j(t-\tau)}. \tag{4.7.28}$$

Plugging the solution to the LE we get that

$$\dot{X}_t = -V'(X_t) + \sum_{j=1}^{K} \beta_j \int_0^t \mathrm{d}\tau\, \dot{L}_\tau e^{-\alpha_j(t-\tau)} = -V'(X_t) + \int_0^t \mathrm{d}\tau\, \dot{L}_\tau \sum_{j=1}^{K} \beta_j e^{-\alpha_j(t-\tau)}. \tag{4.7.29}$$

Therefore, the Lagrangian of X will now be the integrated Lagrangian of $\dot{L}_t$ as in Equation (4.2.14) of our thesis:

$$\begin{aligned}\mathscr{L}_R &= \lambda\left[1-\phi_{A_1}\left(\int_0^t \mathrm{d}\tau\, g_R(\tau)\sum_{j=1}^{K}\Re\left(\beta_j e^{-\alpha_j(t-\tau)}\right)\right)\right] - ig_R(t)\left(\dot{X}_{R;t}+V'(X_{R;t})\right)\\ \mathscr{L}_I &= \lambda\left[1-\phi_{A_1}\left(\int_0^t \mathrm{d}\tau\, g_I(\tau)\sum_{j=1}^{K}\Im\left(\beta_j e^{-\alpha_j(t-\tau)}\right)\right)\right] - ig_I(t)\left(\dot{X}_{I;t}+V'(X_{I;t})\right).\end{aligned} \tag{4.7.30}$$

Therefore, one can find the ELE for real and imaginary parts as;

$$\begin{aligned}\dot{X}_{R;t} &= -V'(X_{R;t}) + i\lambda\left(\sum_{j=1}^{K}\Re\left(\beta\right)_j\right)\phi'_{A_1}\left(\int_0^t \mathrm{d}\tau\, g_R(\tau)\sum_{j=1}^{K}\Re\left(\beta_j e^{-\alpha_j(t-\tau)}\right)\right)\\ \dot{X}_{I;t} &= -V'(X_{I;t}) + i\lambda\left(\sum_{j=1}^{K}\Im\left(\beta\right)_j\right)\phi'_{A_1}\left(\int_0^t \mathrm{d}\tau\, g_I(\tau)\sum_{j=1}^{K}\Im\left(\beta_j e^{-\alpha_j(t-\tau)}\right)\right)\\ \dot{g}_R(t) &= V''(X_{R;t})g_R(t)\\ \dot{g}_I(t) &= V''(X_{I;t})g_I(t)\end{aligned} \tag{4.7.31}$$

The first two ELE's are a type of Volterra convolution equation[92]. In detail, it is a special type of differo-integral equation that we can transform the second ELE into a second-order ODE.

Let's rewrite the interior of ϕ'_{A_1} as follows:

$$\int_0^t \mathrm{d}\tau\, g(\tau)\sum_{j=1}^{K}\beta_j e^{-\alpha_j(t-\tau)} = \sum_{j=1}^{K}\int_0^t \mathrm{d}\tau\, g(\tau)\beta_j e^{-\alpha_j(t-\tau)} = \sum_{j=1}^{K} k_j(t), \tag{4.7.32}$$

where $k_j(t) = \int_0^t \mathrm{d}\tau\, g(\tau)\beta_j e^{-\alpha_j(t-\tau)}$. We can now conduct the following operations for all $j \in$

$\{1, \ldots, K\}$ to get an equation for g:

$$\begin{aligned}
k_j(t) &= \int_0^t \mathrm{d}\tau\, g(\tau)\beta_j e^{-\alpha_j(t-\tau)} \\
\implies k_j(t)e^{\alpha_j t} &= \beta_j \int_0^t \mathrm{d}\tau\, g(\tau)e^{\alpha_j \tau} \\
\implies \frac{\mathrm{d}}{\mathrm{d}t}\left(k_j(t)e^{\alpha_j t}\right) &= \beta_j \frac{\mathrm{d}}{\mathrm{d}t}\int_0^t \mathrm{d}\tau\, g(\tau)e^{\alpha_j \tau} \\
\implies \left(\dot{k}_j(t) + \alpha_j k_j(t)\right) e^{\alpha_j t} &= \beta_j g(t)e^{\alpha_j t} \\
\implies \frac{\dot{k}_j(t) + \alpha_j k_j(t)}{\beta_j} &= g(t),
\end{aligned} \tag{4.7.33}$$

where the last operation holds as we assumed $\beta_j \neq 0$ for all j. Therefore, since the equation for g above holds for all j, we can take the average of the LHS and equate it to g:

$$\frac{\dot{k}_j(t) + \alpha_j k_j(t)}{\beta_j} = g(t)\ \forall j \implies \frac{1}{K}\sum_{j=1}^{K} \frac{\dot{k}_j(t) + \alpha_j k_j(t)}{\beta_j} = g(t). \tag{4.7.34}$$

Therefore, the ELE for g can now be written as second order ODE:

$$\begin{aligned}
&\frac{1}{K}\sum_{j=1}^{K} \frac{\ddot{k}_j(t) + \alpha_j \dot{k}_j(t)}{\beta_j} = V''(X_t)\frac{1}{K}\sum_{j=1}^{K} \frac{\dot{k}_j(t) + \alpha_j k_j(t)}{\beta_j} \\
\implies &\sum_{j=1}^{K} \frac{\ddot{k}_j(t) - \left(V''(X_t) - \alpha_j\right)\dot{k}_j(t) + \alpha_j V''(X_t)k_j(t)}{\beta_j} = 0 \\
\implies &\ddot{k}_j(t) - \left(V''(X_t) - \alpha_j\right)\dot{k}_j(t) + \alpha_j V''(X_t)k_j(t) = 0,
\end{aligned} \tag{4.7.35}$$

where we can omit the summation in last as k_j forms the basis of g. Thus, we now converted the

ELE into differential form,

$$\begin{aligned}
\dot{X}_{R;t} &= -V'(X_{R;t}) + i\lambda \left(\sum_{j=1}^{K} \Re\beta_j \right) \phi'_{A_1} \left(\sum_{j=1}^{K} \Re k_j(t) \right) \\
\Re\ddot{k}_j(t) &= \left(V''(X_{R;t}) - \Re\alpha_j \right) \Re\dot{k}_j(t) + \Re\alpha_j V''(X_{R;t}) \Re k_j(t) \\
\dot{X}_{I;t} &= -V'(X_{I;t}) + i\lambda \left(\sum_{j=1}^{K} \Im\beta_j \right) \phi'_{A_1} \left(\sum_{j=1}^{K} \Im k_j(t) \right) \\
\Im\ddot{k}_j(t) &= \left(V''(X_{I;t}) - \Im\alpha_j \right) \Im\dot{k}_j(t) + \Im\alpha_j V''(X_{I;t}) \Im k_j(t)
\end{aligned} \tag{4.7.36}$$

Conveniently, we can also find the initial conditions of the system very easily. The first one is the trivial condition for X_R, $X_{R;0} = x_a$, i.e. the starting point of X on the potential in the real line. We also let $X_{I;0} = 0$. As for the rest of the initial conditions, notice first that $\Re k_j(0) = \Im k_j(0) = 0$ due to the definition of k_j and that $\Re\dot{k}_j(0) = \Re\beta_j \Re g(0) = \Re\beta_j \Re g_0$ and similarly $\Im\dot{k}_j(0) = \Im\beta_j \Im g_0$. Therefore, we just have to calibrate g_0 in our numerical calculations in order to find the initial conditions of $\dot{k}_j$ for all j.

4.7.4 Markov Embedding with Exponentially Decaying Impulse Function

Applying our findings we can obtain the optimal path of X in the following figures, where we simulated over $t \in [0, 10]$. We first tested our ELE using the exponentially decaying impulse function $h(t) = \alpha e^{-\alpha x}$, where we chose $\alpha = 1$. We next chose the double-well potential $V(x) = -x^2/2 + x^4/4$, and starting point $X_0 = -1$. We estimated 40th order Markov embedding function, i.e. with $K = 40$.

We found that $g_0 = -0.0000001$, i.e. g_0 is a real number [i]. The complex-valued optimal path, the test function and the Complex Lagrangian are given in the following figures. This results in complex-valued instantons of X_t and $g(t)$ and therefore a complex-valued Lagrangian.

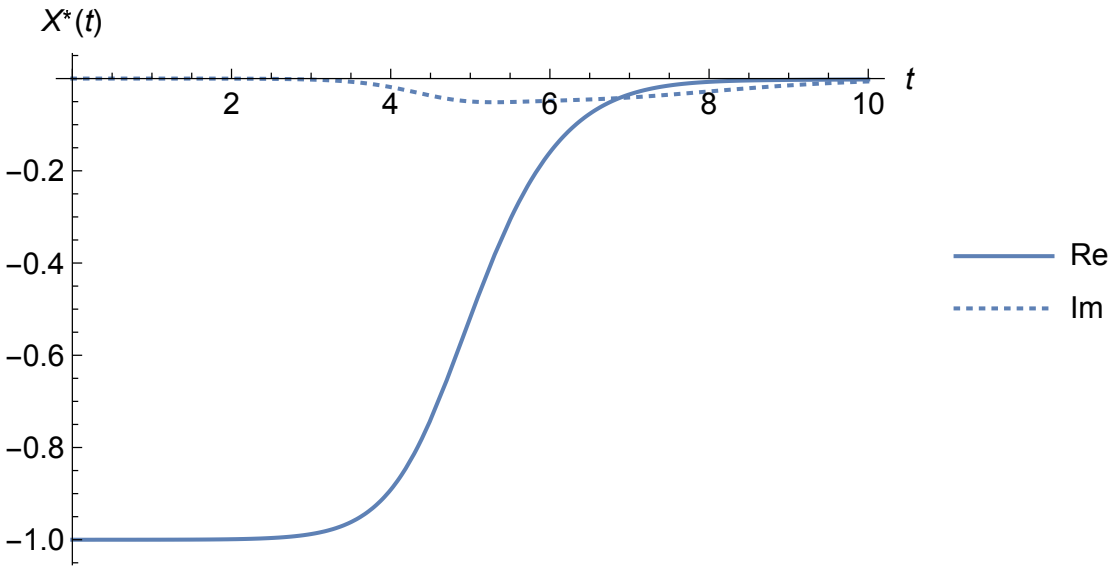

Figure 4.14: Optimal path X_t for Exponential Decay impulse function using Markov Embedding function capped at $K = 40$. Real and Imaginary parts labelled.

[i] The values of Markov embedding kernel α_j will be given in appendix.

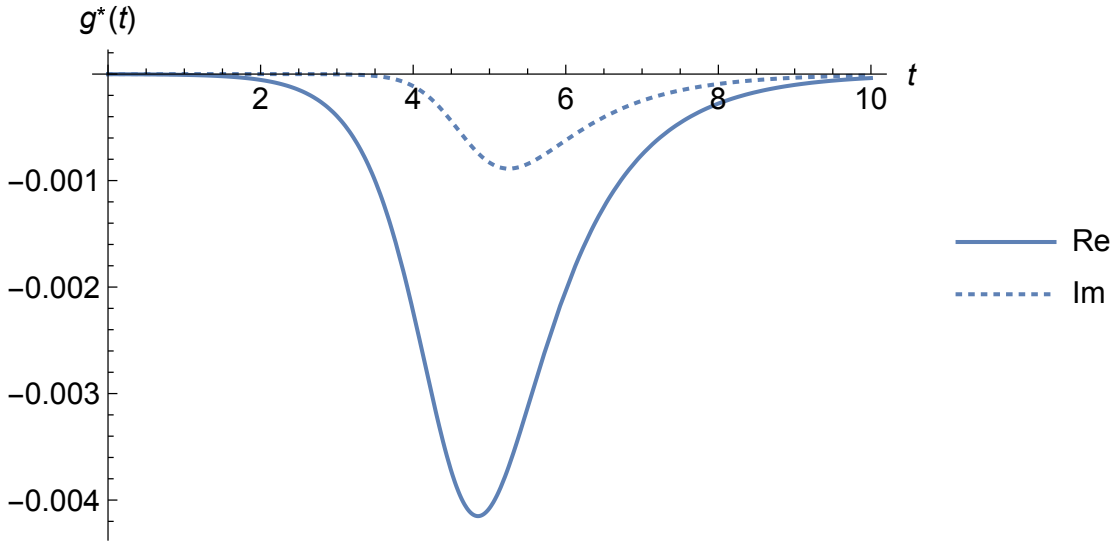

Figure 4.15: Plot of $g(t)$ obtained as the average in (4.18). Real and imaginary parts labelled.

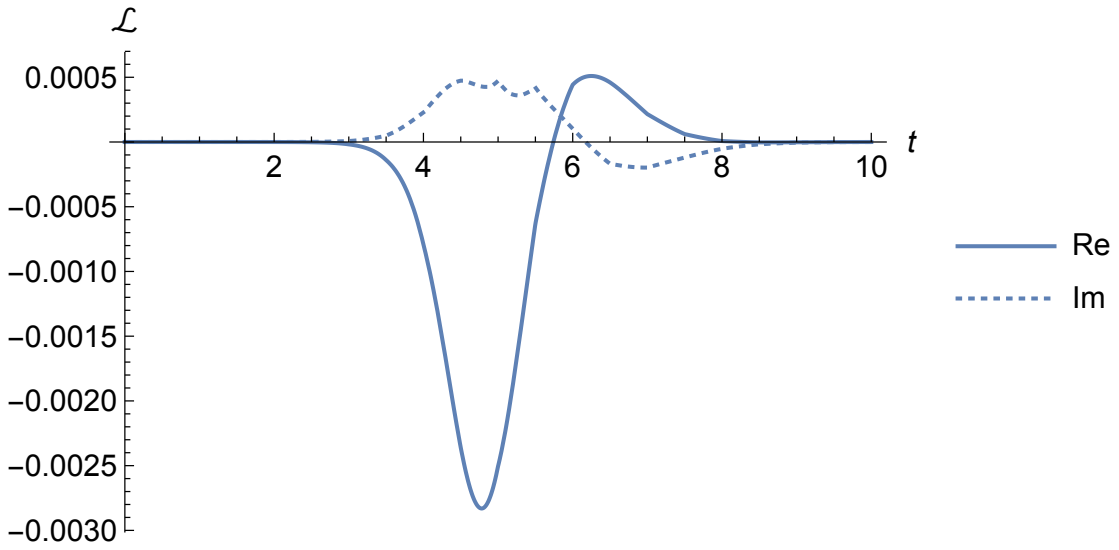

Figure 4.16: The resulting complex-valued Lagrangian. Real and imaginary parts labelled.

4.7.5 Markov Embedding with Power Law Decaying Impulse Function

We can also compare this result with a power-law decaying impulse function, $h(t) = (b-1)/a^{1-b}(t+a)^{-b}$, where $a, b > 0$ are real numbers. This would be an interesting application: firstly one cannot define a hierarchical solution of the power-law decaying impulse function; however, due to the similarity of this impulse function with exponentially decaying case, we should expect similar behaviors in the optimal path and the resulting Lagrangian. We chose the instanton $g_0^{pow} = g_0$, where g_0 is

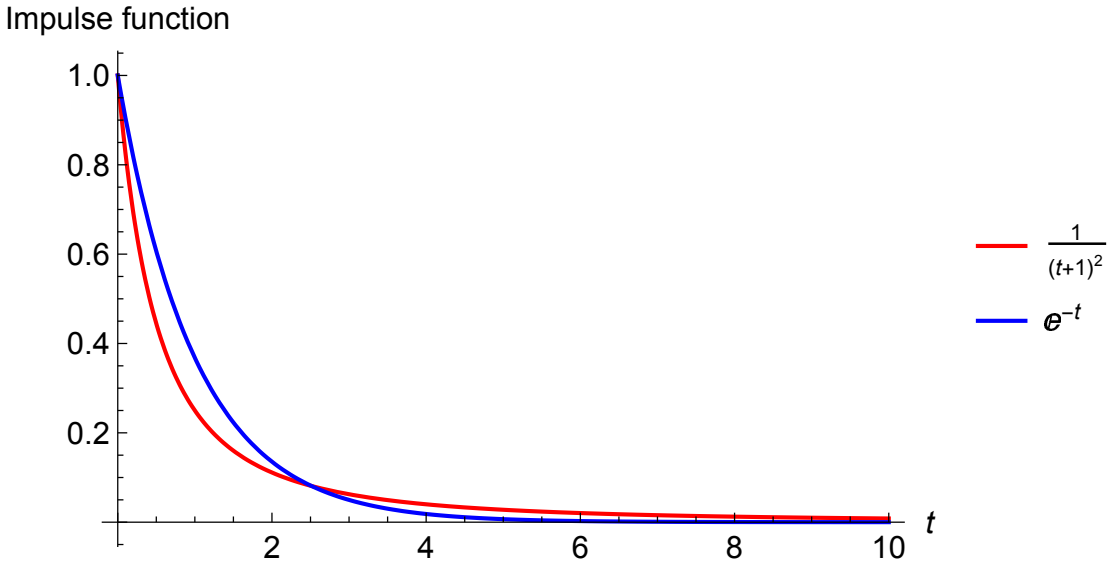

Figure 4.17: Plots of exponential decaying (blue) and power-law decaying (red) impulse functions defined in the legends set. Due to the impulse functions' similarity, we should expect similar optimal path and action.

obtained as in the exponential decay case.

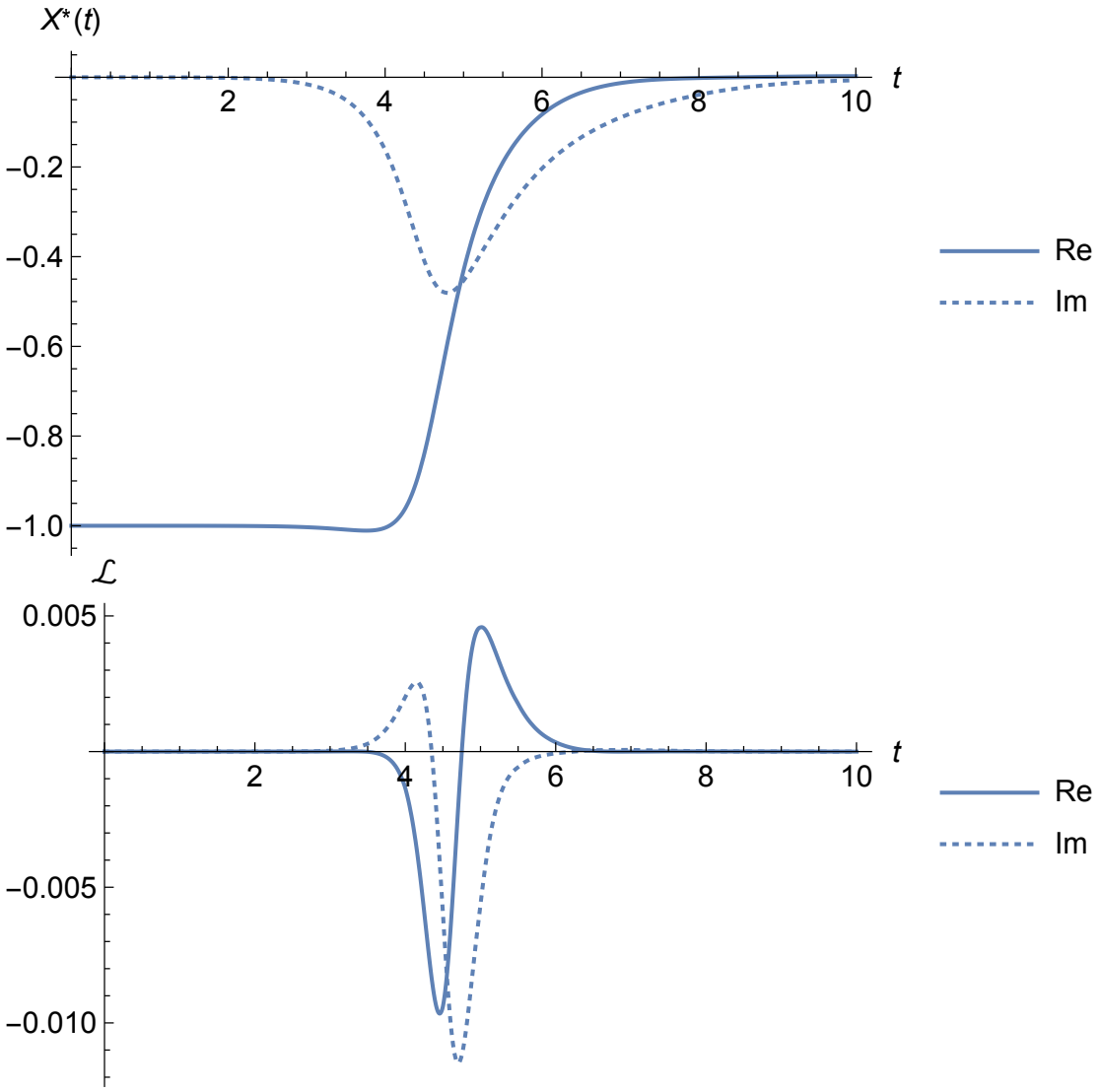

Figure 4.18: Optimal path and Lagrangian of X_t for Power Decay impulse function using Markov Embedding function capped at $K = 40$. Real and Imaginary parts labelled.

4.7.6 Markov Embedding with Damped and Oscillating Impulse Function

We next chose the damped and oscillating impulse function $h(t) = \left(\alpha^2 + \beta^2\right) / (\alpha + \beta)\, e^{-\alpha t} (\sin \beta t + \cos \beta t)$, with $\alpha = 1 = \beta = 2$, where in this case we also simulated over $t \in [0, 10]$. We estimated 40th order Markov embedding function, i.e. with $K = 40$.

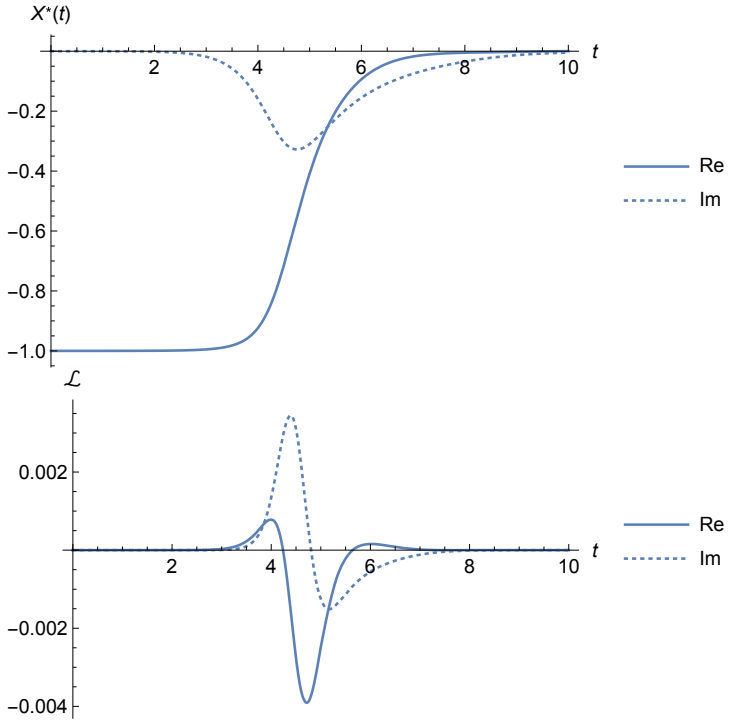

Figure 4.19: Resulting optimal path and Lagrangian of X driven by damped oscillating impulse function decay $h(t) = e^{-t} \cos t$.

4.7.7 Comparison of Actions

Now that we can solve the ELE for 3 different types of impulse functions, we will next compare the actions formed by each impulse function and check which case is more efficient.

Note that we chose impulse functions as in Figure 4.20 to start from same initial value $h(t = 0) = 1$ and that all are decaying as $t = \infty$.

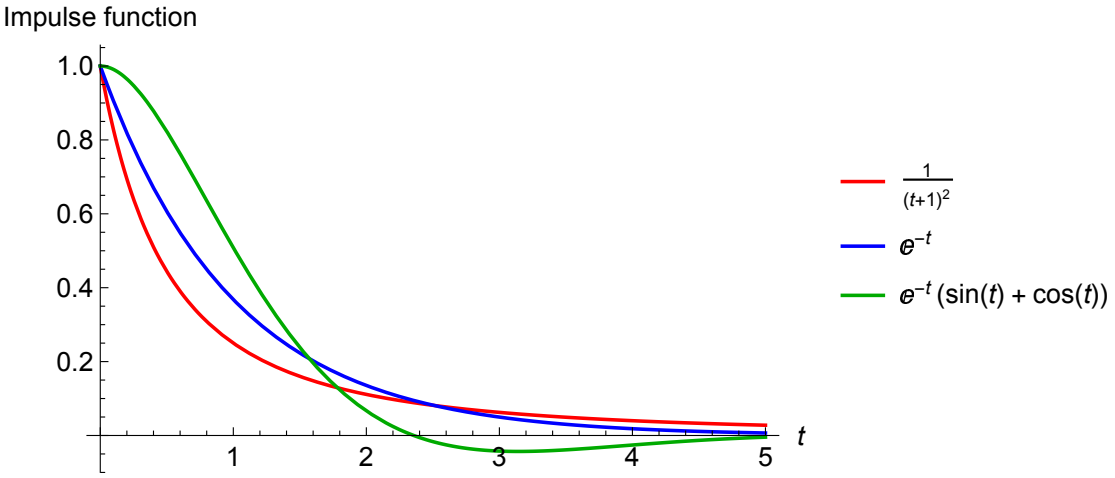

Figure 4.20: Plots of exponential decaying (blue), power-law decaying (red) and damped oscillating (green) impulse functions defined in the legends set with new coefficients.

The optimal paths X^* and the Lagrangian for three types of impulse functions are given in Figure 4.21 below. We can observe from their Lagrangians in Figure 4.21 that damped oscillating impulse function produces more efficient action, as the area of its Lagrangian is smaller. Indeed, in Table 4.2 below we can see the corresponding complex actions and their moduli:

	Exponential	**Power-law**	**Damped Oscillation**
Action (S)	$-0.00499 + 0.00119i$	$-0.009871 + 0.01858i$	$-0.00141 + 0.00101i$
Modulus $(\lvert S\rvert)$	0.005132	0.021041	0.001737

Table 4.2: Action calculation of the Lagrangian for various impulse functions.

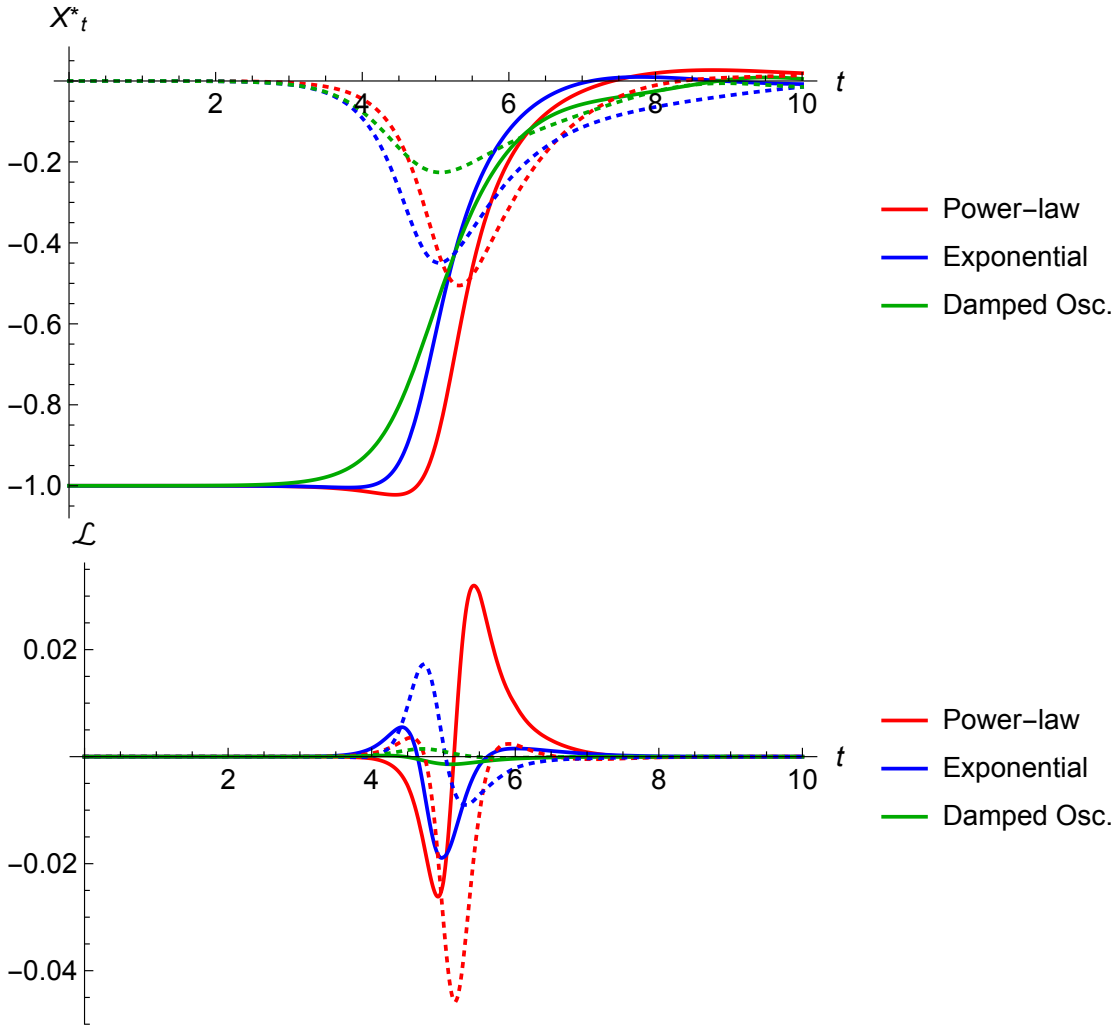

Figure 4.21: Resulting optimal path and Lagrangian of X driven by power-law decay $h(t) = (t+1)^{-2}$, exponential decay, $h(t) = e^{-t}$ and damped oscillating, $h(t) = e^{-t}(\sin t + \cos t)$ impulse functions.

4.8 Chapter Review

This chapter contains important and new findings on the non-Markovian LE's driven by the GSN ξ. We first introduced the concept of path integration, where it was first outlined by Feynman and Hibbs[85] to find a global equation to fully describe the movement of a particle. We defined the Lagrangian function $\mathscr{L}$, the action functional S and the probability amplitude π of such particle's position in time, $X(t)$, from which one can obtain the scope of this thesis: its transition PDF.

These definitions were followed by introducing the Stationary Action Principle, which explains to us that between the time frames $[t_a, t_b]$ the particle *chooses* the path from point $X(t_a)$ to point $X(t_b)$ that has the stationary action. This principle helps us find the probability amplitude of X by minimizing S, where one obtains the *equations of motion* of the particle, also known as the *Euler-Lagrange Equations* (ELE). We also referred to[75] for the probability amplitude of X, paths of which are given the solution of the LE $\dot{X}_t = -V'(X_t) + \xi_t$ such that ξ_t forms the GSN process.

We next embarked on Section 4.1.2, where we outlined the computation ELE's for Markovian and non-Markovian stochastic processes by minimizing S. We showed that due to the impulse function h defined in the GSN ξ, the resulting ELE's for non-Markovian processes are time non-local (TNL ELE's) and hence cannot be defined by their Lagrangian, one instead has to define the TNL ELE's directly from their action functional as in Equation (4.2.13). This is not the case for the Markovian regime, where the ELE's are locally defined on time and one can define the ELE's directly by their Lagrangian. This can be directly visualized by letting $h \to \delta$ in Equation (4.2.8). For simplifying both local and TNL ELE's, we applied the weak noise limit proposed by[113] and continued our further analysis from there.

The introduction to optimal path calculation is then followed by first analyzing the cases of Markovian process and harmonic potential (i.e. the OU process), where we showed that the resulting two dimensional local ELE as in Equation (4.3.1) for X and g can be rewritten solely in form

of X due to the linearity of the ELE for g. However, one cannot fully define the solution X^* analytically unless the Gaussian Limits (GL) are applied. This problem arises due to the implicit equation regarding the initial condition g_0 of the ELE in that is embedded in the CF of jump amplitude, ϕ_{A_1}, and applying GL linearizes the CF as in Equation (4.3.3). The same analysis is then conducted for the non-Markovian regime for the non-Markovian OU process, the TNL ELE is given in Equation 4.2.8.

We next progressed onto Section 4.4, where we assumed a more intricate potential V that need not be harmonic. This implies that the TNL ELE for g and X in Equation (4.4.1) (as well as the Markovian ELE's in Equation (4.4.3)) are not separable, and one has to compute both ODE's simultaneously, which is close to impossible to solve. To overcome this problem, we showed that if the impulse function h is an $n-$hierarchical function as in Section 2.5.3, then, as we outlined in the beginning of Chapter 2, the corresponding $(n+1)-$dimensional tuple $\left(X, \xi, {}^{(1)}\xi, {}^{(2)}\xi, \ldots, {}^{(n)}\xi\right)$, where ${}^{(n)}\xi$ is the GSN process with impulse function $h^{(n)}$, is Markovian. Thus, the corresponding $(n+1)-$dimensional ELE will be local.

We later showed in subsequent sections two main methods of finding the solution of $(n+1)-$dimensional localized ELE. We first showed the method of differentiating X n times and plugging in all the ODE's for hierarchical GSN ${}^{(n)}\xi$ to the ODE of $X^{(n)}$. This method is then independently matched by findings of Bray & McKane [112] in Equation (4.6.16), where the authors used the Gaussian CP process, i.e. the GSN process with exponentially decaying impulse function $h(x) = \alpha e^{-\alpha x}$ under GL. We next extended this to the non-Gaussian CP process in Section 4.6.2 where we analyzed the optimal paths for three different types of jump amplitude A_i distributions: Exponential, Gaussian, and Constant. We followed this by comparing the resulting stationary actions obtained by these three jump amplitudes. We also calculated the optimal path and stationary actions for different parameters of α and showed the results against the case for white noise, i.e. at $\alpha \to \infty$. Differently, the second method of finding the high dimensional localized ELE is by rewrit-

ing the ξ hierarchy in matrix form, $\vec{\Xi}_t = \left(\xi, {}^{(1)}\xi, {}^{(2)}\xi, \ldots, {}^{(n)}\xi\right)$ and deriving the Matrix ODE in Equation (4.6.3) that is the vector form of the GenOU process. We showed that the Lagrangian is local with ELE's and resulting equations of motion given in Equations (4.6.7)-(4.6.9). We apply this method to show the resulting ELE in Section 4.6.2 as well.

The matrix ODE computation is then extended to higher-order impulse functions in Section 4.7, where we first introduced the case for damped and oscillating impulse function, which has hierarchy order 2. The resulting Lagrangian and localized equations of motion are given respectively in Equations 4.7.4-(4.7.5), where we can observe that system of ODE's are coupled and requires the computation of unknown initial conditions.

This caveat leads us to defining the *Markov Embedding Technique* in Section 4.7.3, which we use to localize and simplify TNL ELE's X driven by the GSN ξ such that the impulse functions h *need not* have the $n-$hierarchy property. We show that any integrable h can be approximated by the Markov Embedding function h_{approx} in Equation (6.0.4), where one can define a GSN process with impulse function h_{approx}. Conveniently, plugging this resulting GSN process into our Langevin Equation yields separable and local ELE's with well-defined initial conditions as in Equation (4.7.36). We thus end this chapter by giving examples of various hierarchical (exponential decay, damped oscillation) and non-hierarchical (power-law) impulse functions, where we can solve the equations of motion numerically.

We next move on to the final chapter of our thesis, where we use the properties of the GSN process obtained throughout this thesis to model real-life scenarios.

Mathematical reasoning may be regarded rather schematically as the exercise of a combination of two facilities, which we may call intuition and ingenuity.

Alan Turing

5

Applications of GSN Processes

Throughout the previous chapters, we have focused on detailed analysis of non-Markovian LE's driven by GSN processes, as well as their path integral computation and derivation of equations of motion. We now move on to the last section of our thesis, where we apply the results obtained throughout Chapters 3 and 4 to real-life scenarios.

We provide two applicable scenarios where we will use the Markov Embedding Technique. We first calibrate an impulse function to the clinical data of the Mean Square Displacement of the mi-

tochondria submersed in course-grained medium, where empirical results show the diffusion model is anomalous, suggesting non-Markovianity in nature [33]. We use complex integration in this section and therefore advise our readers to have knowledge of Cauchy's Residue Theorem prior to reading this section. Due to the scope of this thesis, readers are welcome to refer to Chapter 6 of Mitrinovic & Keckic [37] for a more detailed explanation.

In the later section, we apply the GSN process ξ to model the index value of S&P500 obtained from Yahoo Finance [i], and aim to capture its behavior during the Covid-19 pandemic. We expect the reader of this section to be familiar with financial instruments and stochastic calculus. The reader is welcome to refer to [84] for detailed analysis on the stochastic analysis of jump processes, from where we extended our model.

5.1 Application 1: Particle Diffusing in a Coarse-Grained Medium

In this section, we now apply our findings to the MSD of a diffusing particle in coarse-grained medium, published by Höfling & Franosch in 2013 [81] and mathematically modelled by Cairoli & Baule in 2015 [33].

The authors in their paper assert that the MSD of the mitochondria diffusing in mating *S. cerevisiae* cells is given by the following equation in Laplace space:

$$\widetilde{MSD}(\lambda) = \frac{2\sigma}{\lambda\tilde{\Phi}(\lambda)}, \tag{5.1.1}$$

where

$$\tilde{\Phi}(\lambda) := d_1 \left(\frac{\lambda}{d_2}\right)^{\alpha_1} \left(1 + \left(\frac{\lambda}{d_2}\right)^{\frac{1}{\beta}}\right)^{(\alpha_2-\alpha_1)\beta}, \tag{5.1.2}$$

such that the variables are given by $\sigma = 1$, $\alpha_1 = 1$, $\alpha_2 = 0.66$, $\beta = 0.85$, $d_1 = 4.53$, $d_2 = 0.02$.

[i] https://finance.yahoo.com/quote/%5EGSPC/history/

Authors also published the data for the MSD of the subject particle between the time interval $t \in [0.31, 331.608]$, where we will conduct our analysis. Using the MSD fitting with clinical data, the authors next considered a particle X under Harmonic potential $V(x) = \gamma x^2/2$, where $\gamma = 1$ was chosen.

Therefore, the relationship with MSD and the impulse function h for position process X driven by the CP noise ξ under the Harmonic potential $V(x) = x^2/2$ is given in Equation (2.6.7) with $\gamma = 1$, where from there we can define the impulse function h in terms of the MSD by applying change of variables twice:

$$\begin{aligned}
MSD(t) &= \lambda \left\langle A_1^2 \right\rangle e^{-2\gamma t} \int_0^t \mathrm{d}\tau \left(\int_\tau^t \mathrm{d}s\, h(s-\tau) e^{\gamma s} \right)^2 \\
&= \lambda \left\langle A_1^2 \right\rangle e^{-2\gamma t} \int_0^t \mathrm{d}\tau \left(\int_0^{t-\tau} \mathrm{d}u\, h(u) e^{\gamma(u+\tau)} \right)^2 \qquad [u = s - \tau] \\
&= \lambda \left\langle A_1^2 \right\rangle e^{-2\gamma t} \int_0^t \mathrm{d}\tau\, e^{2\gamma\tau} \left(\int_0^{t-\tau} \mathrm{d}u\, h(u) e^{\gamma u} \right)^2 \\
&= \lambda \left\langle A_1^2 \right\rangle e^{-2\gamma t} \int_0^t \mathrm{d}v\, e^{2\gamma(t-v)} \left(\int_0^{v} \mathrm{d}u\, h(u) e^{\gamma u} \right)^2 \qquad [v = t - \tau] \\
&= \lambda \left\langle A_1^2 \right\rangle \int_0^t \mathrm{d}v\, e^{-2\gamma v} \left(\int_0^{v} \mathrm{d}u\, h(u) e^{\gamma u} \right)^2 \\
\implies h(t) &= e^{-\gamma t} \frac{\mathrm{d}}{\mathrm{d}t} \left[\sqrt{\frac{e^{2\gamma t}}{\lambda \left\langle A_1^2 \right\rangle} \frac{\mathrm{d}}{\mathrm{d}t} MSD(t)} \right].
\end{aligned} \tag{5.1.3}$$

Notice from the above equation that due to the non-linear relationship between h and MSD, one cannot apply Laplace transform to define the relationship in Laplace space. Therefore, in order to find h, we first need to convert the MSD data from Laplace space, $\widetilde{MSD}(\lambda)$ to Euclidean space, $MSD(t)$ by Inverse Laplace Transform (ILT), defined by the operator $\mathcal{L}^{-1}$.

The ILT of $\widetilde{MSD}(\lambda)$ is given by *Mellin's Inverse Formula*[58]:

$$MSD(t) := \mathcal{L}^{-1}\left\{ \widetilde{MSD}(\lambda) \right\}(t) = \frac{1}{2\pi i} \lim_{T\to\infty} \int_{-iT}^{+iT} \mathrm{d}\lambda\, e^{\lambda t} \widetilde{MSD}(\lambda), \tag{5.1.4}$$

where we can apply the convolution property to get

$$\mathcal{L}^{-1}\left\{\widetilde{MSD}(\lambda)\right\}(t) = 2\sigma\mathcal{L}^{-1}\left\{\frac{1}{\lambda}\tilde{\Phi}(\lambda)^{-1}\right\}(t) = 2\sigma\int_0^t \mathrm{d}\tau\,\mathcal{L}^{-1}\left\{\Phi(\lambda)^{-1}\right\}(\tau). \tag{5.1.5}$$

Therefore, we need to compute the ILT of $\Phi(\lambda)^{-1}$, which is given by,

$$\begin{aligned}\mathcal{L}^{-1}\left\{\Phi(\lambda)^{-1}\right\}(\tau) :&= \frac{1}{2\pi i}\lim_{T\to\infty}\int_{-iT}^{+iT}\mathrm{d}\lambda\frac{e^{\lambda\tau}}{\Phi(\lambda)}\\ &= \frac{1}{2\pi i}\lim_{T\to\infty}\int_{-iT}^{+iT}\mathrm{d}\lambda\frac{e^{\lambda\tau}}{d_1\left(\frac{\lambda}{d_2}\right)^{\alpha_1}\left(1+\left(\frac{\lambda}{d_2}\right)^{\frac{1}{\beta}}\right)^{(\alpha_2-\alpha_1)\beta}}\\ &= \frac{d_2^{\alpha_2}}{d_1}\frac{1}{2\pi i}\lim_{T\to\infty}\int_{-iT}^{+iT}\mathrm{d}\lambda\frac{e^{\lambda\tau}}{\lambda^{\alpha_1}\left(d_2^{1/\beta}+\lambda^{1/\beta}\right)^{(\alpha_2-\alpha_1)\beta}}.\end{aligned} \tag{5.1.6}$$

Defining the integrand above by $f(\lambda;\tau)$, we can then use Residue Theorem [37] to solve the integral as the sum of the residues over the whole complex plane $\mathbb{C}$ including ∞:

$$\frac{d_2^{\alpha_2}}{d_1}\frac{1}{2\pi i}\lim_{T\to\infty}\int_{-iT}^{+iT}\mathrm{d}\lambda\frac{e^{\lambda\tau}}{\lambda^{\alpha_1}\left(d_2^{1/\beta}+\lambda^{1/\beta}\right)^{(\alpha_2-\alpha_1)\beta}} = \frac{d_2^{\alpha_2}}{d_1}\frac{1}{2\pi i}\oint_{\mathbb{C}^*}\mathrm{d}\lambda\,f(\lambda;\tau) = \frac{d_2^{\alpha_2}}{d_1}\sum_{a_k}\mathrm{Res}(f(\lambda;\tau),a_k), \tag{5.1.7}$$

where $\mathbb{C}^*$ refers to the Complex plane $\mathbb{C}$ with inclusion of infinity, $\mathrm{Res}(f(\lambda;\tau),a_k)$ is the residue of f at singularity $\lambda = a_k$.

By the definition of our coefficients given above, we have the following singularities of f:

- Pole of order α_1 at $\lambda = 0$; and
- Singularity at infinity (behaving like the Riemann zeta function).

The first singularity is obvious; however we can refer to the Figure below to understand the behavior of f at infinity: Therefore, let's identify the residues at each singularity differently.

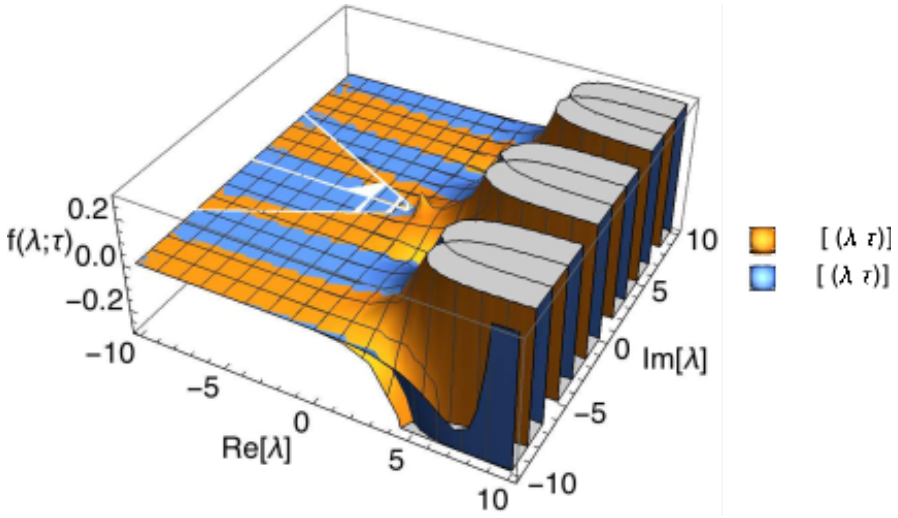

Figure 5.1: Plot of $f(\lambda;\tau=1)$ indicating singularities at infinity and the obvious pole at origin. Blue hue denotes the real part of f and orange its imaginary part.

First Residue The first residue is a α_1-order pole and is directly given by:

$$\begin{aligned}\operatorname{Res}\left(f(\lambda;\tau),0\right) &= \frac{1}{(\alpha_1-1)!}\lim_{\lambda\to 0}\frac{\mathrm{d}^{\,\alpha_1-1}}{\mathrm{d}\lambda^{\alpha_1-1}}\left[\lambda^{\alpha_1}f(\lambda;\tau)\right]\\ &= \frac{1}{(\alpha_1-1)!}\lim_{\lambda\to 0}\frac{\mathrm{d}^{\,\alpha_1-1}}{\mathrm{d}\lambda^{\alpha_1-1}}\left[\frac{e^{\lambda\tau}}{\left(d_2^{1/\beta}+\lambda^{1/\beta}\right)^{(\alpha_2-\alpha_1)\beta}}\right]\end{aligned} \tag{5.1.8}$$

Notice that we can extend this for *any* α_1 [ii].

Second Residue Here, we will use the definition of residue at infinity as:

$$\operatorname{Res}\left(f(\lambda;\tau),\infty\right) = -\operatorname{Res}\left(\frac{1}{\lambda^2}f\left(\frac{1}{\lambda};\tau\right),0\right), \tag{5.1.9}$$

[ii] However, in [33], this coefficient is simply $\alpha_1 = 1$ and hence the above residue simply reduces to $d_2^{\alpha_1-\alpha_2}$.

where we can rewrite $\lambda^{-2}f(\lambda^{-1})$ in terms of series as follows,

$$\begin{aligned}
\frac{1}{\lambda^2}f\left(\frac{1}{\lambda};\tau\right) &= \frac{e^{\tau/\lambda}}{\lambda^{2-\alpha_1}\left(d_2^{1/\beta}+\lambda^{-1/\beta}\right)^{(\alpha_2-\alpha_1)\beta}} \\
&= e^{\tau/\lambda}\lambda^{\alpha_1-2}\left(1+(d_2\lambda)^{1/\beta}\right)^{(\alpha_1-\alpha_2)\beta}\lambda^{\alpha_2-\alpha_1} \\
&= e^{\tau/\lambda}\lambda^{\alpha_2-2}\sum_{k=0}^{\infty}\binom{(\alpha_1-\alpha_2)\beta}{k}(d_2\lambda)^{k/\beta} \\
&= \lambda^{\alpha_2-2}\left(\sum_{n=0}^{\infty}\frac{1}{n!}\frac{\tau^n}{\lambda^n}\right)\left(\sum_{k=0}^{\infty}\binom{(\alpha_1-\alpha_2)\beta}{k}(d_2\lambda)^{k/\beta}\right) \\
&= \sum_{n=0}^{\infty}\sum_{m=0}^{n}\frac{1}{m!}\tau^m\binom{(\alpha_1-\alpha_2)\beta}{n-m}d_2^{\frac{n-m}{\beta}}\lambda^{\frac{n-m}{\beta}-m+\alpha_2-2} \qquad \text{(Cauchy product rule).}
\end{aligned} \tag{5.1.10}$$

Then the corresponding residue will be the coefficient of λ^{-1} satisfying the following equation:

$$\frac{n-m}{\beta}-m+\alpha_2-2=-1 \Longrightarrow m=\frac{n-(1-\alpha_2)\beta}{1+\beta}. \tag{5.1.11}$$

Therefore, the residue at infinity is given by:

$$\begin{aligned}
\operatorname{Res}\left(f(\lambda;\tau),\infty\right) &= -\operatorname{Res}\left(\frac{1}{\lambda^2}f\left(\frac{1}{\lambda}\right);0\right) \\
&= -\sum_{n=0}^{\infty}\frac{1}{\left(\frac{n-(1-\alpha_2)\beta}{1+\beta}\right)!}\binom{(\alpha_1-\alpha_2)\beta}{n-\frac{n-(1-\alpha_2)\beta}{1+\beta}}d_2^{n-\frac{n-(1-\alpha_2)\beta}{1+\beta}}\tau^{\frac{n-(1-\alpha_2)\beta}{1+\beta}}.
\end{aligned} \tag{5.1.12}$$

Thus we have found the ILT of $\tilde{\Phi}(\lambda)^{-1}$ as follows:

$$\begin{aligned}\mathcal{L}^{-1}\left\{\tilde{\Phi}(\lambda)^{-1}\right\}(\tau) &= \frac{d_2^{\alpha_2}}{d_1}\left(\operatorname{Res}(f,0)+\operatorname{Res}(f,\infty)\right)\\ =\frac{d_2^{\alpha_2}}{d_1}\Bigg\{&\frac{1}{(\alpha_1-1)!}\lim_{\lambda\to 0}\frac{\mathrm{d}^{\,\alpha_1-1}}{\mathrm{d}\lambda^{\alpha_1-1}}\left[\frac{e^{\lambda\tau}}{\left(d_2^{1/\beta}+\lambda^{1/\beta}\right)^{(\alpha_2-\alpha_1)\beta}}\right]-\\ &-\sum_{n=0}^{\infty}\frac{1}{\left(\frac{n-(1-\alpha_2)\beta}{1+\beta}\right)!}\binom{(\alpha_1-\alpha_2)\beta}{n-\frac{n-(1-\alpha_2)\beta}{1+\beta}}d_2^{\,n-\frac{n-(1-\alpha_2)\beta}{1+\beta}}\,\tau^{\frac{n-(1-\alpha_2)\beta}{1+\beta}}\Bigg\}.\end{aligned} \tag{5.1.13}$$

Using above, recall that we can simply derive the MSD in Euclidean space as $MSD(t) = 2\sigma\int_0^t \mathrm{d}s\,\mathcal{L}^{-1}\left\{\tilde{\Phi}(\lambda)^{-1}\right\}(s)$.

We have plotted the resulting MSD in Figure 5.2 together with the clinical data below. We next

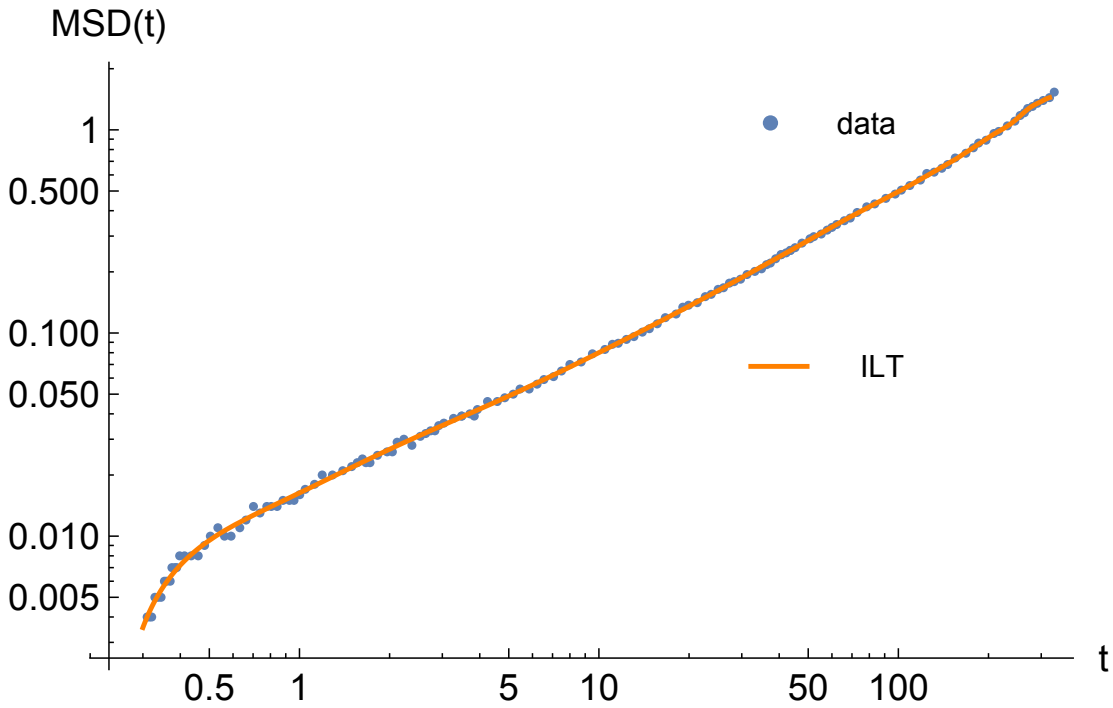

Figure 5.2: Log-log plot of the resulting MSD, $MSD(t) = 2\sigma\int_0^t \mathrm{d}s\,\mathcal{L}^{-1}\left\{\tilde{\Phi}(\lambda)^{-1}\right\}(s)$, where $\mathcal{L}^{-1}\left\{\tilde{\Phi}(\lambda)^{-1}\right\}(s)$ is calculated by the Inverse Laplace Transform (ILT) in Equation (5.1.13). Actual data is obtained from[33].

fitted the MSD to the impulse function using our Markov Embedding technique, where the resulting fit at $K = 15$ is given in Figure 5.3.

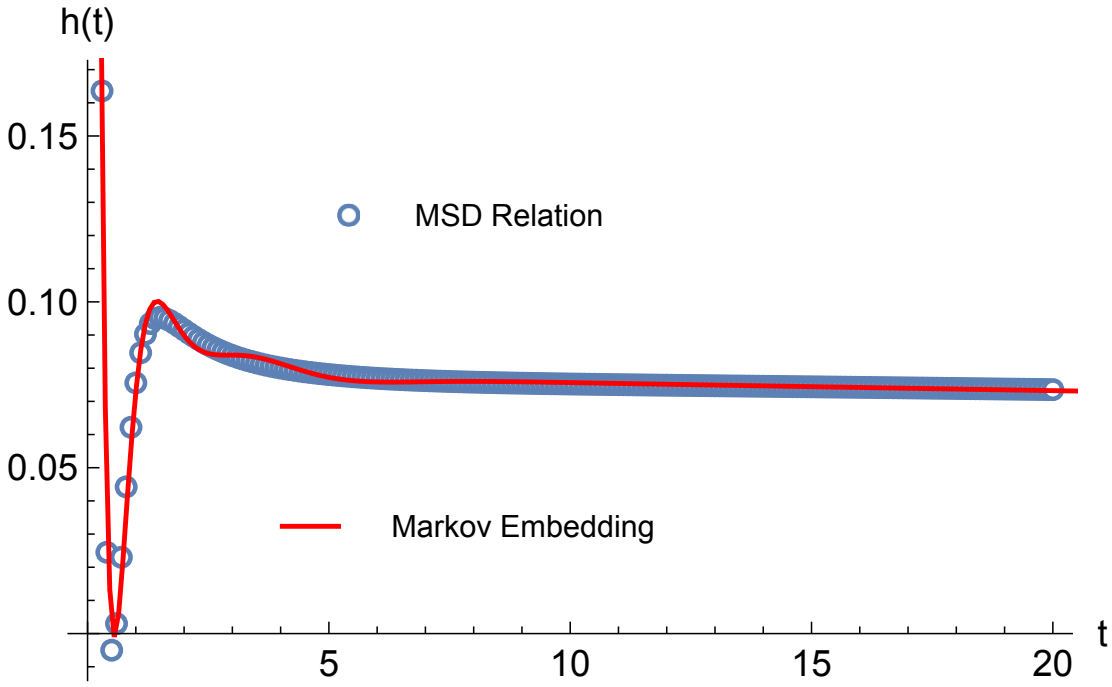

Figure 5.3: Fitting of the impulse function h obtained by MSD relation in Equation (5.1.3) (blue circle) and by fitting with the Markov Embedding function (red line) capped at $K = 15$.

Now that we have successfully retrieved the impulse function of ξ with Markov Embedding Technique, let's now calculate the escape of the particle X driven by ξ if it were under double well potential $V(x) = -x^2/2 + x^4/4$. Using the impulse function in Figure 5.3, we generated the optimal path of X_t from $t \in [0.31, 331.608]$ with instanton $g_0 = 10^{-25}$ in Figure 5.4. The resulting instanton g and complex Lagrangian $\mathcal{L}$ are also plotted in Figures 5.5 and 5.6 respectively.

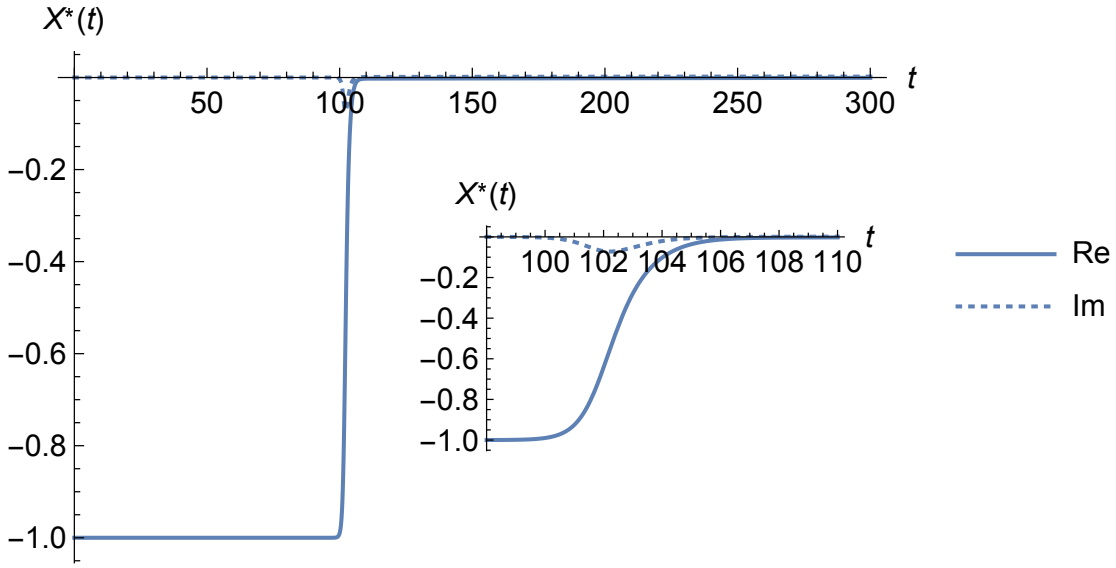

Figure 5.4: Optimal path X formed by the impulse function h in Figure 5.3, with close-up view given in right bottom inset. Real and Imaginary values labelled.

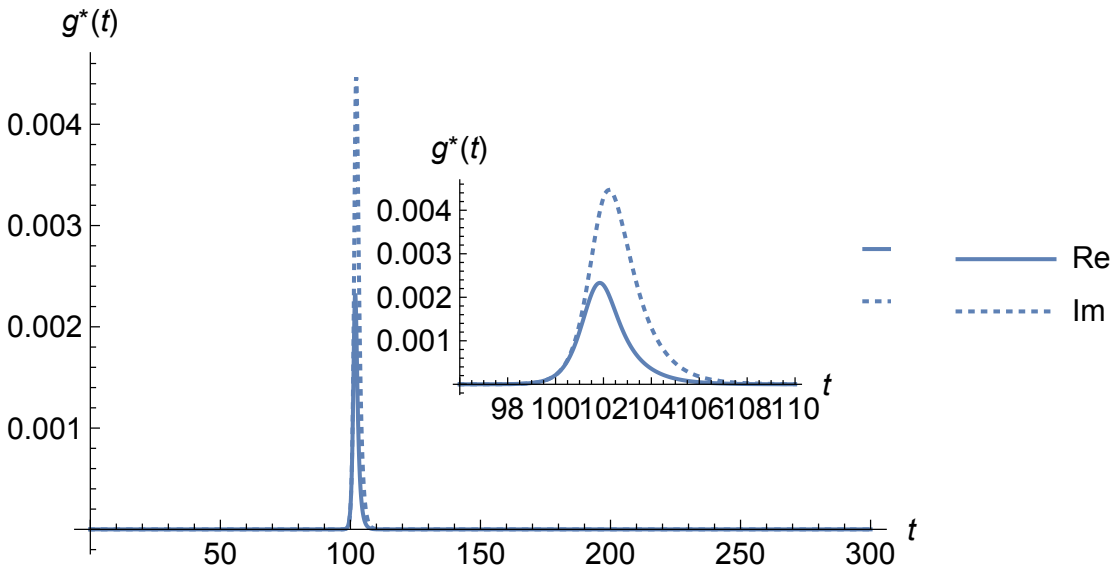

Figure 5.5: Instanton solution g formed by the impulse function h in Figure 5.3, with close-up view given in right bottom inset. Real and Imaginary values labelled.

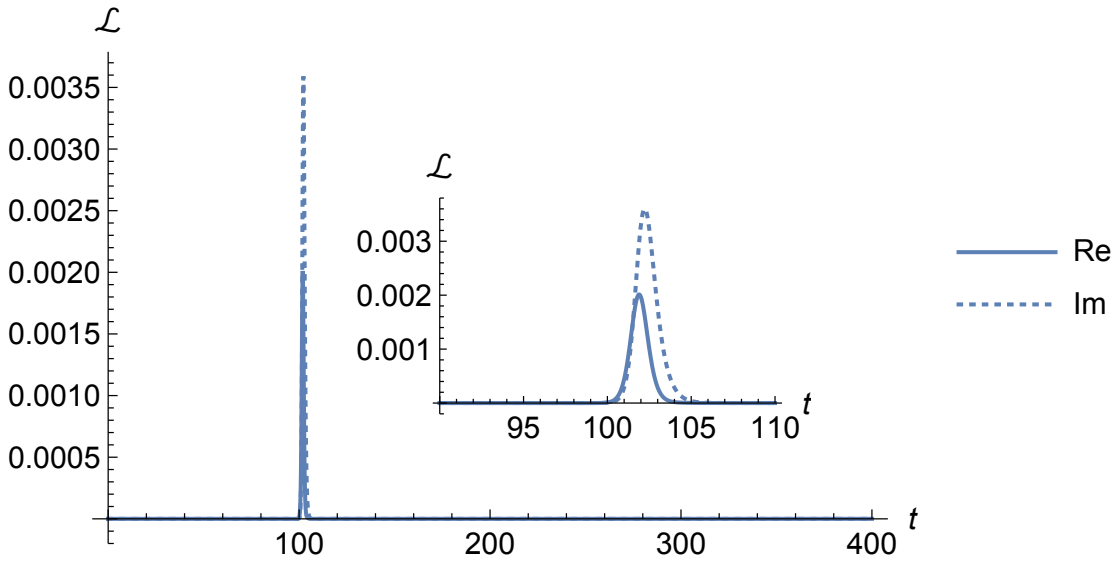

Figure 5.6: Lagrangian of X formed by the impulse function h in Figure 5.3, with close-up view given in right bottom inset. Real and Imaginary values labelled.

5.2 Application 2: Stock Index Behavior During Covid-19 Pandemic

In this example, we now change gears to financial markets, and model the behavior of the S& P 500 Stock Index, which is computed as the weighted average of 500 selected stocks, with the GSN process ξ. We expect the reader of this section to be familiar with financial instruments such as derivatives, stocks, stock indices and bonds, as well as pricing of financial instruments such as the *Fundamental Theorem of Asset Pricing* (FTAP) and quantitative finance. References regarding their definitions can be found in [79], and more mathematical rigour in [135].

5.2.1 Preliminary Definitions

Before we dwell on the realms of financial modeling, we first have to outline some mathematical definitions that will be the essential part of modelling the price of financial instruments.

Martingales and the Equivalent Martingale Measure

In simple terms, a *martingale* is a stochastic process for which at any moment in time, the conditional expectation of its next value is equal to the present value, regardless of all prior values.

A stochastic process $M = (M_t)_{t\geq 0}$ defined on a probability space $(\Omega, \mathcal{F}, \mathbb{Q})$ is called a $\mathbb{Q}$-*martingale* with respect to the *filtration* $\mathcal{F}_s$ if for all $t > s > 0$, the following holds:

$$\langle M_t | \mathcal{F}_s \rangle_{\mathbb{Q}} = M_s. \tag{5.2.1}$$

Here, $\langle\rangle_{\mathbb{Q}}$ refers to the expectation taken with respect to $\mathbb{Q}$ and the filtration is the subset of the event space (cf. Chapter 1), $\mathcal{F}_s \in \mathcal{F}$, that contains all the previous values of M up until time s.

Martingales are very important stochastic processes used in financial modelling, as they ensure that in a *fair market*, if one knows all the past values of the price of a financial instrument, one still cannot predict its future values[135]. Therefore, if one wishes to model the price of a financial instrument in a fair market with a stochastic process, then the stochastic process must be a martingale.

An interesting property of the martingale is that, under necessary conditions[135], one can define another stochastic process as a martingale by changing its probability measure. Given the martingale M with probability measure $\mathbb{Q}$ and another stochastic process X with probability measure $\mathbb{P}$, we say that X is a $\mathbb{Q}$-martingale adapted to the filtration of M if for any $t > s > 0$,

$$X_s = \langle X_t | \mathcal{F}_s \rangle_{\mathbb{Q}} = \langle Z_t X_t | \mathcal{F}_s \rangle_{\mathbb{P}}\,, \tag{5.2.2}$$

where Z_t forms another stochastic process with probability measure $\frac{\mathrm{d}\mathbb{Q}}{\mathrm{d}P}$, commonly referred to as the *Radon-Nikodym derivative* of the *equivalent martingale measure* (EMM) $\mathbb{Q}$ with respect to the original measure $\mathbb{P}$. More properties of the Radon-Nikodym derivative and the EMM can be inferred from Chapter 9 of[105].

Fundamental Theorem of Asset Pricing

We next give a brief introduction to the *Fundamental Theorem of Asset Pricing* (FTAP), which provides necessary and sufficient conditions for a financial market, in which financial instruments (stocks, derivatives, options, etc.) are traded, to be fair. The FTAP asserts that financial models should be *arbitrage-free*, i.e. the models should not give traders a risk-free opportunity. This theorem enables the markets to be efficient and complete, where no traders can gain any risk-free advantage over the other.

Let us show the FTAP condition in a mathematical setting. Let the price of a financial asset A during times $t \in [0, T]$ be modelled by a continuous-time stochastic process $S = (S_t)_{0 \leq t \leq T}$ defined on a probability space $(\Omega, \mathcal{F}, \mathbb{P})$. Let $f(S_t)$ be defined as the price of a financial derivative with A as its underlying. Then, the FTAP suggests that in a fair and arbitrage-free market, the current value of the derivative, $f(S_0)$, is given by the expectation of the *discounted* price of any future value of the derivative under the EMM of $\mathbb{P}$, i.e. for all $T \geq 0$:

$$f(S_0) = \left\langle e^{-rT} f(S_T) \right\rangle_{\mathbb{Q}} = \left\langle e^{-rT} Z_t f(S_t) \right\rangle_{\mathbb{P}} \tag{5.2.3}$$

where r is called the *risk-free interest rate* (e.g. the coupon rate of a government bond), Z_t forms the stochastic process with probability measure as Radon-Nikodym derivative $\mathrm{d}\mathbb{Q}/\,\mathrm{d}\mathbb{P}$ and $\langle\rangle_{\mathbb{Q}}$ denotes the expectation taken with respect to the EMM $\mathbb{Q}$. In most financial settings, $\mathbb{P}$ is traditionally called the *historical PDF* of S as it is obtained by directly modeling the historical values of asset price.

5.2.2 Modeling the Index Value with non-Markovian Geometric Brownian Motion

Modeling the price of financial instruments has been the foundation of stochastic processes ever since its mathematical formulation by Louis Bachelier in 1900[70]. In his paper, Bachelier modelled the price of a stock, X, as the Wiener process, i.e. as the solution of the LE $\dot{X}_t = \sigma \dot{W}_t$, where σ, called the *volatility* of the stock price, measures the strength of the GWN.

Later on, this model was strengthened by Samuel by modeling the natural logarithm of the X as the Wiener process with drift. In this instance, the so-called *geometric Brownian motion* X that models the stock price is defined by the SDE:

$$\frac{\mathrm{d}X_t}{X_t} = \mu\,\mathrm{d}t + \sigma\,\mathrm{d}W_t, \tag{5.2.4}$$

where μ, called the *drift* of the stock price, σ is called its *volatility*, and $\mathrm{d}W_t$ forms the increments of the Wiener process. One can also rewrite this by defining $Y = \ln X$ and applying Ito's lemma on Y_t:

$$\begin{aligned}
\mathrm{d}Y_t &= \frac{1}{X_t}\,\mathrm{d}X_t - \frac{1}{2X_t^2}\,(\mathrm{d}X_t)^2 \\
&= \mu\,\mathrm{d}t + \sigma\,\mathrm{d}W_t - \frac{1}{2}\,(\mu\,\mathrm{d}t + \sigma\,\mathrm{d}W_t)^2 \\
&= \left(\mu - \frac{\sigma^2}{2}\right)\mathrm{d}t + \sigma\,\mathrm{d}W_t.
\end{aligned} \tag{5.2.5}$$

One can rewrite X with respect to Y as $X = \mathcal{E}(Y)$, where $\mathcal{E}$ is called the *stochastic exponential* that is the solution of the SDE for $\mathrm{d}Y_t$ above.

The SDE for Y can also be given in Langevin form below, where $\dot{W}_t$ forms the GWN:

$$\dot{Y}_t = \mu - \sigma^2/2 + \sigma \dot{W}_t. \tag{5.2.6}$$

Although there has been a vast array of candidates for modelling stock prices, by far the most useful model up to date is the geometric Brownian motion as it is the foundation of pricing various financial instruments such as the *Black-Scholes model*.

Without getting into detail, the main idea behind geometric Brownian motion is that the natural logarithm of the derivative of the stock price is a GWN. In a more financial perspective, the model assumes that at any given time, the natural logarithm of the rate of return ("log-return") on investing in a stock is an independent and normally distributed random variable with mean $\mu - \sigma^2/2$ and variance σ^2, i.e. for all t, $\dot{Y}_t \sim \mathcal{N}\left(\mu - \sigma^2/2, \sigma^2\right)$.

Let us now test whether this assumption holds for the S& P 500 index data obtained weekly between 1 January 2020 till 21 October 2021. We specifically chose this region of time as it captures extreme movements in the financial markets due to the implications caused by the Covid-19 pandemic [iii].

In Figure 5.7 below one can see the value of the index, together with the log-return and its MSD. We can directly observe from the MSD that the log-return is not the GWN. By taking the correlation of the LHS and RHS of Equation 5.2.6, we get that

$$\begin{aligned}\left\langle \dot{Y}_t \dot{Y}_s \right\rangle &= \left\langle \left(\mu - \sigma^2/2 + \sigma\dot{W}_t\right)\left(\mu - \sigma^2/2 + \sigma\dot{W}_s\right)\right\rangle = \left(\mu - \sigma^2/2\right)^2 + \sigma^2 \left\langle \dot{W}_t \dot{W}_s \right\rangle \\ &= \left(\mu - \sigma^2/2\right)^2 + \sigma^2 \delta((t-s)).\end{aligned} \tag{5.2.7}$$

The MSD of $\dot{Y}$ hence should be a straight line.

This is the main caveat of using the geometric Brownian motion, as it is an oversimplified pricing model that does not capture movements caused by extreme events, e.g. the Covid-19 pandemic. Although there have been many advancements in further generalizing the geometric Brownian mo-

[iii] Further information can be obtained from the article published by McKinsley & Co. on 10 March 2021: https://www.mckinsey.com/business-functions/strategy-and-corporate-finance/our-insights/the-impact-of-covid-19-on-capital-markets-one-year-in

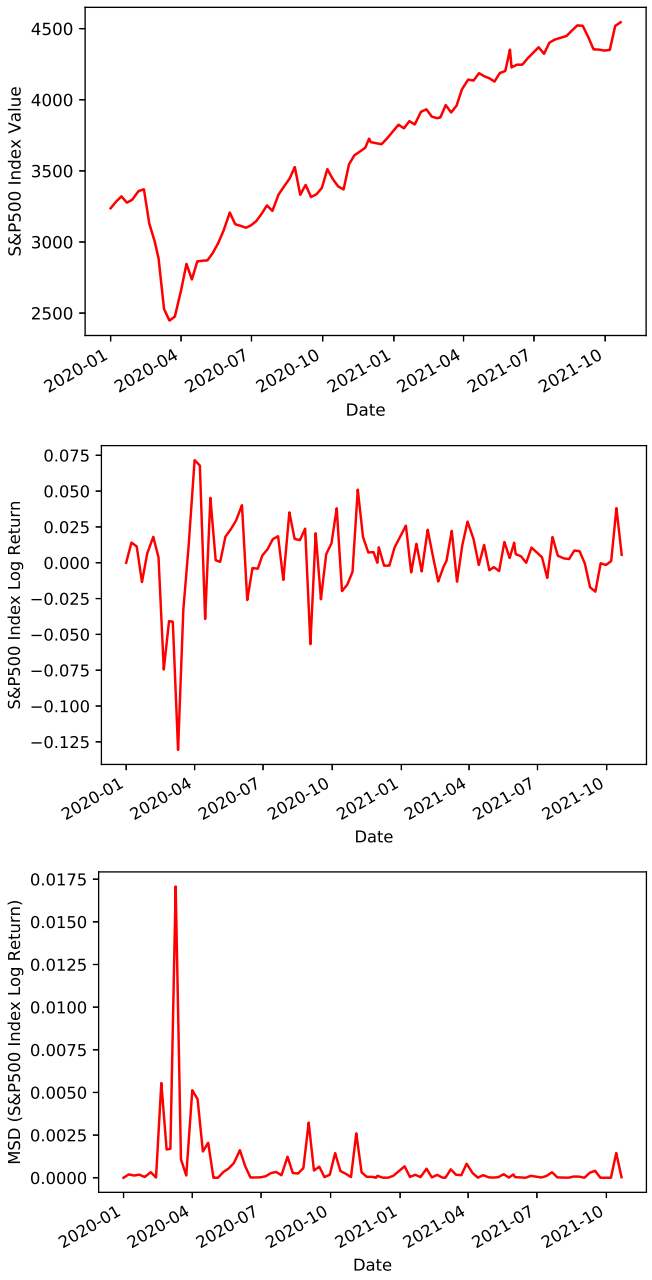

Figure 5.7: Index values of S&P500 (top), the resulting log-returns (middle) and MSD of the log-returns (bottom) obtained between 1 January 2020 until 21 October 2021. Notice the significant drop in index value (and spikes in log-return and MSD log-return) in around March 2020, the beginning of the Covid-19 pandemic.

tion, such as the inclusion of jump processes [118,84], most models assume that the price of a stock (or the value of a stock index) is a Markov process. Here, we assume that it is non-Markovian, where instead of $\dot{W}$, we assume that the log-return is modelled by the derivative of the GSN process $\dot{\xi}$.

Notice first that we cannot fit the impulse function h directly with the MSD of the log-return, as we have conducted in the previous section's application with success. Due to the flip of the MSD as can be observed around October 2020 in Figure 5.7, the impulse function, which is related to the derivative of the square root of the MSD as in Equation (5.1.3), will be complex-valued.

Instead, for this case, we can instead infer the shape of the impulse function directly from S& P 500 log-return as in Figure 5.8 below. If we allow small jump intensity λ and iid jump amplitudes A_i to drive the GSN ξ, then the behavior of ξ will be greatly governed by the impulse function h itself. Therefore, assuming low λ and A_i, we can model S& P500 log-returns with the GSN process by directly fitting the log-returns with the impulse function h.

Indeed, as shown in Figure 5.8, we fitted the log-returns with the impulse function using a polynomial function of degree 20. We then defined the GSN process ξ with the resulting fitted impulse function, $\hat{h}_{SP500}$, and simulated the log-price of the index as $\dot{Y}_t = \mu - \sigma^2/2 + \sigma\dot{\xi}_t$.

The resulting index price process X is then obtained by exponentiating the log-price process Y, given by the following system:

$$\begin{aligned} X_t &= \mathcal{E}\left(Y_t\right) \\ \dot{Y}_t &= \mu - \sigma^2/2 + \sigma\dot{\xi}_t. \end{aligned} \tag{5.2.8}$$

For Monte Carlo simulation, obeying low intensity and iid jump amplitude condition mentioned above, we next fixed the parameters $\lambda = 1, A_i \sim \mathit{Exponential}(\sqrt{\lambda}), \sigma = 1$ and estimated the drift coefficient to be $\mu = \sigma^2/2 + 10^{-4}$. As can be inferred from Figure 5.9 below, the simulation gives a great approximation of the S&P 500 index, and steadily captures the spike occurred during the

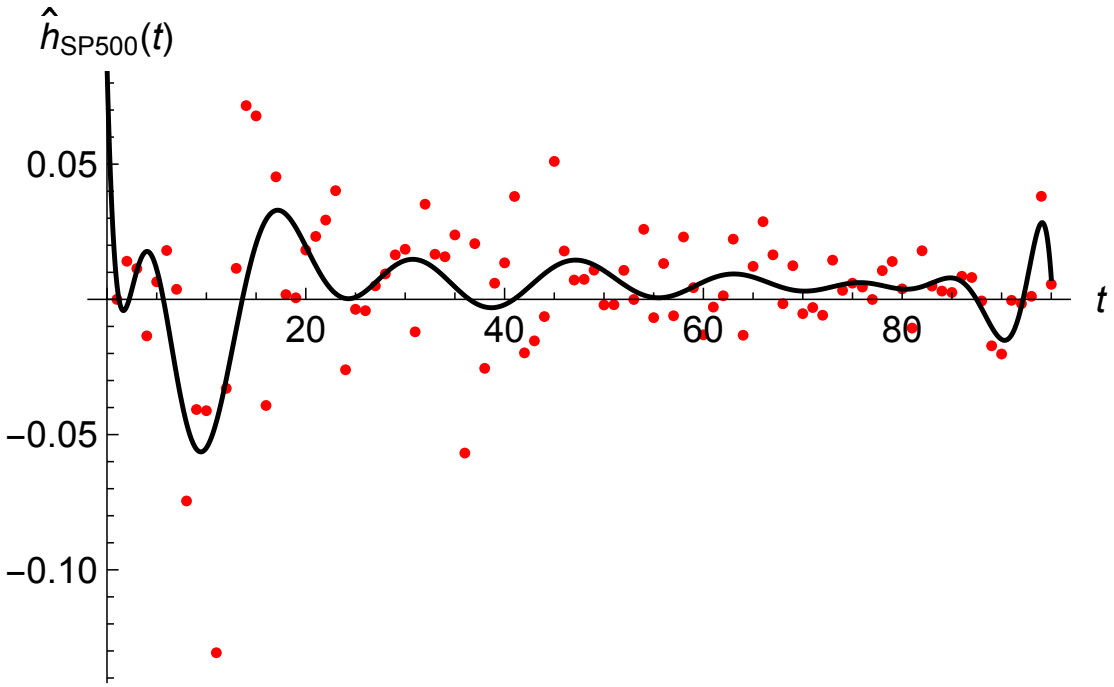

Figure 5.8: Scatter plot of the S&P 500 log-returns with polynomial impulse function fitted directly.

beginning of Covid-19 pandemic.

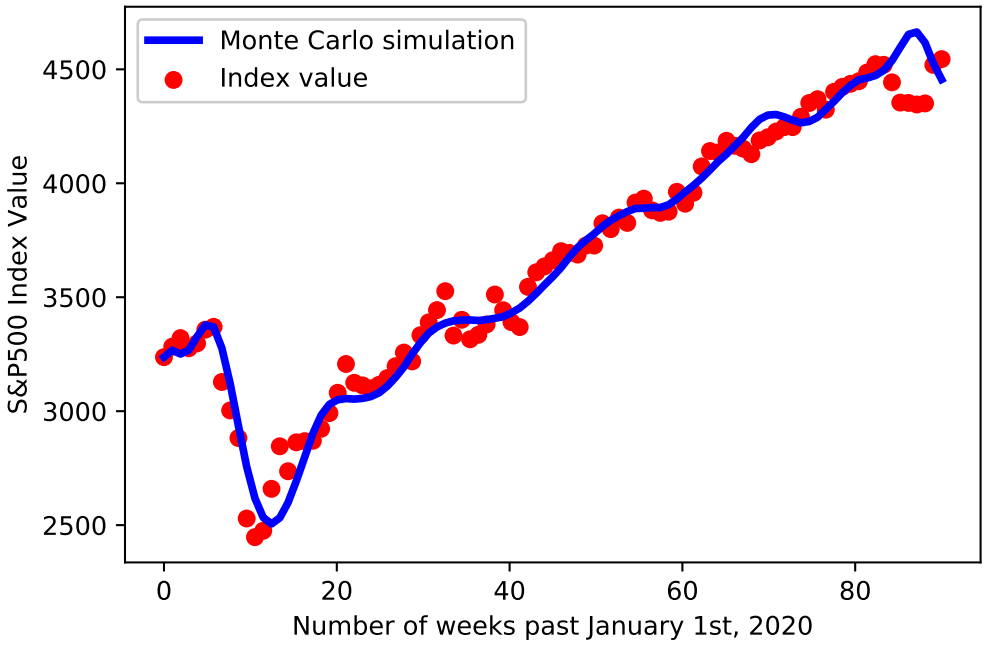

Figure 5.9: Index value (red scatter plot) together with the stochastic process $X = \exp Y$ (blue line) as the solution of the LE $\dot{Y}_t = \mu - \sigma^2/2 + \sigma\dot{\xi}_t$. The GSN process ξ is simulated with Monte Carlo method with 7,000 iterations and using polynomial impulse function $\hat{h}_{SP500}$.

Now that our impulse function is approximated, and the resulting index process X is shown to fit nicely to index data, we can then derive its historical probability measure $\mathbb{P}$. First, notice that the LE of Y and be integrated over $[0, t]$ to give $Y_t = \left(\mu - \sigma^2/2\right) t + \sigma\xi_t$. Then, due to the linearity, we can establish a CFal correspondence between Φ_Y and Φ_ξ as follows:

$$\begin{aligned}\Phi_Y[g(t)] &= \left\langle \exp\left(i \int \mathrm{d}t\, g(t) Y_t\right)\right\rangle = \left\langle \exp\left(i \int \mathrm{d}t\, g(t) \left(\left(\mu - \frac{\sigma^2}{2}\right) t + \sigma\xi_t\right)\right)\right\rangle \\ &= \exp\left(i\left(\mu - \frac{\sigma^2}{2}\right) \int dt\, g(t) t\right) \Phi_\xi[\sigma g(t)].\end{aligned} \tag{5.2.9}$$

Therefore, the probability amplitude of Y can be calculated by using the functional IFT of the

CFal Φ_Y and change the functional space of Y to that of ξ, as outlined in Appendix A:

$$\begin{aligned}
&\pi(y_b, t_b | y_a, t_a) \\
&= \int_{\mathscr{C}_Y} \mathcal{D}[Y] \int_{\mathscr{C}_g} \mathcal{D}\left[\frac{g}{2\pi}\right] \exp\left(i \int \mathrm{d}t\, g(t) Y_t\right) \Phi_Y[g(t)] \\
&= \int_{\mathscr{C}_\xi} \mathcal{D}[\xi] \int_{\mathscr{C}_g} \mathcal{D}\left[\frac{g}{2\pi}\right] \exp\left(2i\left(\mu - \frac{\sigma^2}{2}\right) \int dt\, g(t) t\right) \exp\left(i \int \mathrm{d}t\, g(t) \xi_t\right) \Phi_\xi[\sigma g(t)] \exp\left(-S_J\right),
\end{aligned} \tag{5.2.10}$$

where $\exp(-S_J)$ is the Jacobian obtained from the change of functional space and is given by $S_J = -1/2 \ \ln(\partial Y_t / \delta \xi_0)$. Notice that since the relationship between Y_t and ξ_t is linear, the action will be given by $S_J = -1/2 \ln \sigma$, and hence the Jacobian becomes $\exp(-S_J) = 1/\sqrt{\sigma}$.

From here, one can obtain the historical probability measure of Y by taking the modulus squared of π_Y, after which it remains to find the EMM $\mathbb{Q}$ such that Y becomes a $\mathbb{Q}$-martingale.

Although there are several ways to compute the EMM $\mathbb{Q}$ for Markov processes, such as by Girsanov theorem cited above, as well as the Esscher transform[73], due to the time-dependence on correlations, finding EMM for non-Markovian stochastic processes is not straightforward and is beyond the scope of this thesis. We encourage the readers to check[64] and[65] for a detailed explanation of finding the EMM for specific non-Markovian stochastic processes by means of Esscher transform.

After finding the EMM of $\mathbb{Q}$, we can next use Girsanov theorem[107] to show that since Y is a $\mathbb{Q}-$martingale, the price process X given by the stochastic exponential $X = \mathcal{E}(Y)$ is also a $\mathbb{Q}$-martingale. Establishing an EMM for X will finally enable us to use the FTAP to model the price of a financial derivative $f(X_t)$ at an arbitrage-free market, $f(X_0) = \left\langle e^{-rT} f(X_T) \right\rangle_{\mathbb{Q}} = \left\langle e^{-rT} Z_t f(X_T) \right\rangle_{\mathbb{P}}$, where the probability measure of Z_t can now be calculated by taking the Radon-Nikodym derivative of the EMM $\mathbb{Q}$ with respect to the historical measure $\mathbb{P}$ that can be directly obtained by simulation.

5.3 Chapter Review

In this chapter we applied the properties of the GSN process to real-life scenarios; first on the biophysical diffusion model and second on the financial index.

In first application we found the Markov embedding impulse function of the non-Markovian diffusion data obtained from [33], from where we obtained the optimal path and Lagrangian in Figures 5.4-5.6. This example was relatively straightforward to compute, as we can observe from Figure 5.2 that the MSD of the diffusion model is monotonously increasing, therefore the representation in Equation (5.1.3) the impulse function will always be real-valued.

This is not the case for the second scenario when we apply Markov Embedding Theorem to the value of the S&P500 stock index between January 2020 and October 2021. We used the non-Markovian version of the geometric Brownian motion by switching the GWN process with a GSN process. As we can see in Figure 5.7, the MSD of the log return is not monotonous at around $t = 10$, where we observe a rapid decrease and increase in the index value during the beginning of Covid-19 pandemic. This directly implies that by the MSD relation in Equation (5.1.3) the impulse function will switch from real to a imaginary after around $t = 10$, which is what we observe in Figure 5.7. Nonetheless, this type of reverting MSD has been studied in detail by Großmann et al in 2016 [36], where authors model the anomalous diffusion of a particle in coarse-grained media by a stochastic clock.

Instead of focusing on the reverting MSD, we instead showed that one can directly fit the impulse function with the GSN data as in Figure 5.8. This result naturally arises due to our definition of the price process X, where it directly depends on the stochastic exponential of the GSN process ξ. Using the fitted impulse function, we next showed that the resulting Monte Carlo simulation of X tracks the index data very well as in Figure 5.9. This ultimately means that the LE for the GSN adapted version of the geometric Brownian motion can capture extreme events.

Lastly, we outlined steps to change the historical probability measure of X to the EMM $\mathbb{Q}$, where one can apply the Fundamental Theorem of Asset Pricing to properly model any financial derivative. The methods of finding an EMM for the non-Markovian process X are not as straightforward and require further research that is beyond the scope of this thesis.

As far as the laws of mathematics refer to reality, they are not certain; as far as they are certain, they do not refer to reality.

Albert Einstein

6

Summary and Concluding Remarks

The main goal of this thesis is to find the transition probability of the position process X driven by the non-Markovian GLE, $\dot{X}_t = -V'(X_t) + \xi_t$, where V is the potential of the system and ξ_t forms the GSN process as defined in Definition 2.1.1 by the following realization,

$$\xi_t = \sum_{i=1}^{N_t} A_i h(t - T_i). \tag{6.0.1}$$

By defining the non-Markovian GLE and the GSN process in detail at the beginning of Chapter 2, this thesis provided three main approaches to find the PDF of the non-Markovian position process. The first one was via the CFal of X as shown in Chapter 2, where from the CFal one can obtain the CF of X_t and thus infer the PDF of X via Inverse Fourier Transform (IFT). The strength of this first approach is in its simplicity in finding analytic expressions of the CF for various impulse functions, as well as its numerical efficacy in computing the IFT. However, the downside of the CFal approach is that one can only define the non-Markovian GLE by zero or Harmonic potentials $V(x) = \gamma x^2/2, \gamma \geq 0$. This naturally arises from the fact that under this potential assumption the GLE becomes a linear differential equation, $\dot{X}_t = \gamma X_t + \xi_t$, where finding a functional correspondence between X and ξ is relatively simple. However, if one chooses a potential $V(x) \propto x^\alpha$ for $\alpha > 2$, the resulting GLE is non-linear and becomes impossible to solve. For example, for double-well potential $V(x) = -x^2/2 + x^4/4$ the GLE becomes Abel's equation of the first kind, where the fully analytic solution remains an open question in mathematics.

The second approach to finding the PDF was by obtaining its Master Equation (ME) from Ito's approach as outlined in Section 3.2.1. Ito's approach is simplistic in its own way as it applies Taylor expansion to the differential $\mathrm{d}f(X_t)$ for any continuously differentiable function f; however, due to the non-Markovian nature of X one obtains the average $\langle X_t \xi_t \rangle$ while calculating the ME. Likewise, upon applying Ito's approach for tuple (X_t, ξ_t) one then would be stuck with the average $\left\langle X_t \xi_t {}^{(1)}\xi_t \right\rangle$, recalling that ${}^{(1)}\xi_t$ forms another GSN process with impulse function $\dot{h}$. By induction, one can only obtain the fully described form of the ME by Ito's approach for an infinite-dimensional joint tuple $\left(X_t, \xi_t, {}^{(1)}\xi_t, \ldots, {}^{(n)}\xi_t, \ldots\right)$. Therefore, Ito's approach can only work for Markovian stochastic processes.

The third approach to find the PDF was by obtaining its ME from Hanggi's path integral formulation as in Section 3.2.3. In Hanggi's formulation, instead of applying Taylor expansion on a function of X_t, one obtains the ME by applying the functional Taylor expansion on the CFal of X.

As we show in Equation (3.2.48), the ME can be obtained for the marginal PDF of X for any potential V and impulse function h.

Since Hanggi's formalism captures the non-Markovian nature of X, we then further analyzed it in detail in Chapter 4. We defined Feynman's path integral for calculating the probability amplitude π of the s.p. X between the time $[t_a, t_b]$ as follows:

$$\pi(x_b, t_b | x_a, t_a) = \int_{\mathscr{C}_X} \mathcal{D}[X] \int_{\mathscr{C}_g} \mathcal{D}\left[\frac{g}{2\pi\varepsilon}\right] \exp\left(-S[X,g]/\varepsilon\right), \tag{6.0.2}$$

where the action functional S under the weak noise limit $\varepsilon \to 0$ is given by the integral of the Lagrangian $\mathscr{L}$:

$$\begin{aligned} S[X,g] &= \int_{t_a}^{t_b} \mathscr{L}\left(X_t, \dot{X}_t, g(t)\right) \\ &= \int_{t_a}^{t_b} \mathrm{d}t \left(\lambda\left(1 - \phi_{A_1}\left(\int_t^{t_b} \mathrm{d}s\, h(s-t) g(s)\right)\right) - i g(t)\left(\dot{X}_t + V'(X_t)\right)\right). \end{aligned} \tag{6.0.3}$$

From the probability amplitude, one can simply obtain the transition PDF of X by squaring the modulus of the probability amplitude, $|\pi|^2$.

Due to the non-Markovian nature of X one can only obtain the Euler-Lagrange Equations (ELE's) for X and g from the action functional, which we later showed they are in fact time non-local (TNL) ELE's due to the integration of g in Equation (4.2.13)[2]. Due to the TNL ELE's one has to know the entire value of the function g up to t_b, where it is tricky to compute. We showed that one can circumvent this problem by assuming that h is an $n-$hierarchy impulse function of the form: $\sum_{i=0}^{n} c_i h^{(i)}(t) = 0,\ h^{(i)}(0) = a_i$, where the resulting non-Markovian GLE becomes $(n+1)-$dimensional Markovian GLE as in Equation (4.5.3).

From here, one can either differentiate the first LE for $\dot{X}$ $n-$times and plug the resulting higher-order ODE to the Lagrangian of the PWN to obtain two-dimensional localized ELE's, where the

corresponding $\mathscr{L}$ would then depend on the first n derivatives of X and g, resulting in high-order, coupled and highly nonlinear systems of ODE's. The second option was to solve the $(n+1)-$dimensional Markovian GLE as a matrix ODE, where one would instead obtain $(2n+2)-$dimensional, coupled, localized and first-order ELE's as in Equation (4.6.9). These two methods, although distinct in their own way, share one common caveat, which is the coupling of each component of the localized ELE's.

This let us progress onto defining the Markov Embedding Technique in Section 4.7.3, where we asserted that any continuously differentiable function $h : \mathbb{R} \to \mathbb{C}$ can be approximated by the following sum of complex-exponentials:

$$h(x) \approx h_{appr}(x) = \sum_{j=1}^{K} \beta_j e^{-\alpha_j x}, \tag{6.0.4}$$

where recalling that $\alpha_j, \beta_j \in \mathbb{C} \setminus \{0\}$ such $\Re(\alpha_j) > 0$ for all j. This enabled us to rewrite the GSN process as a sum of independent, complex-valued CP processes (i.e. GSN processes with unit hierarchical order of $n = 1$), which would in turn decouple the localized ELE's. We also outlined in Section 4.7.2 that one can complexify the action and the Lagrangian of complex stochastic processes into a sum of purely real and purely imaginary components. This enabled us to derive twice the amount of localized ELE's from before, now both arising from the real part and purely imaginary parts of the Lagrangian, as in Equation (4.7.27). Therefore, we now showed that one can find the optimal path and action of non-Markovian X for any continuously differentiable impulse function h by the Markov Embedding Technique.

We lastly provided two examples from literature to apply the Markov Embedding Technique in Chapter 5. We first looked at the MSD data of a particle diffusing in coarse-grained medium, where we derived impulse function first, and applied the Markov Embedding Technique to derive localized and uncoupled complex-valued ELE's and outlined the optimal escape problem for the particle un-

der double-well potential, where the optimal path and the Lagrangian are given in Figures 5.4 and 5.6. Due to the monotonic behavior of the MSD, the resulting impulse function was real-valued. On the other hand, our second application on the MSD data of the log-returns of S&P500 stock index values shows that due to the non-monotonic nature of the MSD, the resulting impulse function would fluctuate between purely real to purely imaginary functions. This violates the continuously differentiable condition of the impulse function, where Markov Embedding Techniques could not be applied.

Instead, we fitted the impulse function directly with the log-return, modelled by the derivative of GSN process $\dot{\xi}$, and showed that the resulting SDE for the index process $\mathrm{d}X_t/X_t = \mu\,\mathrm{d}t + \sigma\,\mathrm{d}\xi_t$ fits the index data in Figure 5.9, where it captures extreme changes in index value during Covid-19 pandemic. As we outlined at the end of Section 5.2, by Fundamental Theorem of Asset Pricing, one needs to find the EMM $\mathbb{Q}$ for the index process X to properly price financial derivatives. Due to the colored nature of ξ, X will be non-Markovian, and future work is needed to determine the EMM for this class of non-Markovian processes.

A

Derivation of the Probability Amplitude

Here we show the derivation of the probability amplitude in Equation (4.2.1) and outline the importance of the Jacobian term.

Recall that given the LE $\dot{X}_t = -V'(X_t) + \xi_t$, where ξ_t forms a noise process, and V is the poten-

tial, the probability amplitude for the position process X is given by

$$\pi(x_b, t_b|x_a, t_a) = \int_{\mathscr{C}_X} \mathcal{D}[X] \int_{\mathscr{C}_g} \mathcal{D}\left[\frac{g}{2\pi}\right] \Phi_\xi[g] \exp\left(i \int_{t_a}^{t_b} \mathrm{d}t\, g(t)\left(\dot{X}_t + V'(X_t)\right)\right) \exp\left(\frac{1}{2}\int_{t_a}^{t_b} \mathrm{d}t\, V''(X_t)\right), \tag{A.0.1}$$

recalling that its action S is given by rewriting the integrand as $\exp(-S[X, g])$.

Another way to define π is by taking the *functional* inverse Fourier Transform (IFT), $\mathscr{F}^{-1}$, of the CFal of X, $\Phi_X[g]$, in terms of its angular frequency:

$$\pi_{IFT}(x_b, t_b|x_a, t_a) = \mathscr{F}^{-1}\Phi_X[g] = \int_{\mathscr{C}_X} \mathcal{D}[X] \int_{\mathscr{C}_g} \mathcal{D}\left[\frac{g}{2\pi}\right] \exp\left(i \int_{t_a}^{t_b} \mathrm{d}t\, g(t) X_t\right) \Phi_X[g], \tag{A.0.2}$$

where its action, distinguishing it by S_{IFT}, is also given by rewriting the integrand as mentioned above.

Notice that the probability amplitude given in Equation (4.1.1) depends on the CFal of the noise ξ; whereas the one to be obtained by the functional IFT in Equation (A.0.2) depends on the CFal of X. Thus, our goal is then to rewrite the latter equation in terms of the first equation by change of functional space by the *Fujikawa Method*, proposed by Fujikawa & Suzuki in 2004[78], which is analogous to the change of variables in ordinary integrals. For better understanding, we will first show the case for Harmonic potential $V(x) = \gamma x^2/2.$, where the reader can then easily generalize for general V.

The Fujikawa method posits that the transformation of the action by changing its functional space requires an addition of the correction term called the Jacobian. Defining $\mathscr{C}_g$ as the functional space of action S_g, if we define the change of functional space say $\mathscr{C}_g \to \mathscr{C}_{\tilde{g}}$, then the resulting

action, $S_{\tilde{g}}$ is given by:

$$S_{\tilde{g}} = S_g + S_J, \tag{A.0.3}$$

where correcting term S_J, called the action of the Jacobian, is defined by[80]:

$$S_J = -\frac{1}{2} \ln \left(\frac{\partial \tilde{g}}{\partial g(t_a)} \right). \tag{A.0.4}$$

Now, we can use the Fujikawa method to rewrite π_{IFT}. Under the Harmonic potential, recall from Equation (2.6.1) that one can rewrite the CFal correspondence between X and ξ:

$$\Phi_X[g] = \Phi_\xi \left[e^{\gamma t} \int_t^{t_b} \mathrm{d}s \, g(s) e^{-\gamma s} \right]. \tag{A.0.5}$$

Let us define $\tilde{g}(t) := e^{\gamma t} \int_t^{t_b} \mathrm{d}s \, g(s) e^{-\gamma s}$ such that one can then rewrite the functional correspondence as $\Phi_X[g] = \Phi_\xi[\tilde{g}]$. Furthermore, for $\tilde{g}$ to be a CFal test function, we require $\tilde{g}(t_a) = \tilde{g}(t_b) = 0$.

One can define original functional space $\mathscr{C}_g$ in terms of the transformed space $\mathscr{C}_{\tilde{g}}$ as $g(t) = \gamma \tilde{g}(t) - \dot{\tilde{g}}(t)$. Using these transformations, we can then change the functional space to $\mathscr{C}_{\tilde{g}}$ and rewrite π_{IFT} as:

$$\pi_{IFT}\left(x_b, t_b | x_a, t_a\right) = \int_{\mathscr{C}_X} \mathcal{D}[X] \int_{\mathscr{C}_{\tilde{g}}} \mathcal{D}\left[\frac{\tilde{g}}{2\pi}\right] \exp\left(i \int_{t_a}^{t_b} \mathrm{d}t \, \left(\gamma \tilde{g}(t) - \dot{\tilde{g}}(t) \right) X_t \right) \Phi_\xi[\tilde{g}] \exp\left(-S_J\right). \tag{A.0.6}$$

where S_J is given by:

$$\begin{aligned} S_j &= -\frac{1}{2}\ln\left(\frac{\delta\tilde{g}}{\delta g(t_a)}\right) = -\frac{1}{2}\ln\left(e^{\gamma t}\int_t^{t_b} \mathrm{d}s\, e^{-\gamma s}\delta(s-t_a)\right) \\ &= -\frac{1}{2}\ln\left(e^{\gamma t}e^{-\gamma t_a}\Theta(t_b-t)\right) = -\frac{1}{2}\ln e^{\gamma(t_b-t_a)} \\ &= -\frac{1}{2}\gamma\left(t_b-t_a\right) \\ &= \frac{1}{2}\gamma\int_{t_a}^{t_b}\mathrm{d}t. \end{aligned} \tag{A.0.7}$$

Furthermore, notice that we can simplify the following by integration by parts:

$$\begin{aligned} i\int_{t_a}^{t_b}\mathrm{d}t\ \left(\gamma\tilde{g}(t)-\dot{\tilde{g}}(t)\right)X_t &= i\gamma\int_{t_a}^{t_b}\mathrm{d}t\,\tilde{g}(t)X_t - i\int_{t_a}^{t_b}\dot{\tilde{g}}(t)X_t \\ &= i\gamma\int_{t_a}^{t_b}\mathrm{d}t\,\tilde{g}(t)X_t - i\left(\left[\tilde{g}(t)X_t\right]_{t=t_a}^{t=t_b} - \int_{t_a}^{t_b}\mathrm{d}t\,\tilde{g}(t)\dot{X}_t\right) \\ &= i\gamma\int_{t_a}^{t_b}\mathrm{d}t\,\tilde{g}(t)X_t + i\int_{t_a}^{t_b}\mathrm{d}t\,\tilde{g}(t)\left(-\gamma X_t+\xi_t\right) \\ &= i\int_{t_a}^{t_b}\mathrm{d}t\,\tilde{g}(t)\xi_t \\ &= i\int_{t_a}^{t_b}\mathrm{d}t\,\tilde{g}(t)\left(\dot{X}_t+\gamma X_t\right). \end{aligned} \tag{A.0.8}$$

Gathering all together, the transformed probability amplitude π_{IFT} is given as follows:

$$\pi_{IFT}\left(x_b,t_b|x_a,t_a\right) = \int_{\mathscr{C}_X}\mathcal{D}[X]\int_{\mathscr{C}_{\tilde{g}}}\mathcal{D}\left[\frac{\tilde{g}}{2\pi}\right]\exp\left(i\int_{t_a}^{t_b}\mathrm{d}t\,\tilde{g}(t)\left(\dot{X}_t+\gamma X_t\right)\right)\Phi_{\xi}[\tilde{g}]\ \exp\left(\frac{1}{2}\gamma\int_{t_a}^{t_b}\mathrm{d}t\right), \tag{A.0.9}$$

which directly corresponds to the path integral given in Equation (4.2.1).

References

[1] Bonja F., Shcherbakov, V. (2016) *Lévy Processes with Applications to Option Pricing Models: Theory, Simulation and Calibration*. Royal Holloway, University of London Master's Dissertation.

[2] Twycross J. et al. (2010). *Stochastic and deterministic multiscale models for systems biology: an auxin-transport case study*. BMC Systems Biology **4**:34.

[3] Kanazawa, K., Sano, T.G., Cairoli, A. et al. (2020) *Loopy Lévy flights enhance tracer diffusion in active suspensions*. Nature 579, pp. 364–367.

[4] Needleman, D., Dogic, Z. (2017). *Active matter at the interface between materials science and cell biology.* Nat. Rev. Mat. 2, 17048.

[5] Koch, D. L., Subramanian, G. (2011). *Collective hydrodynamics of swimming microorganisms: Living fluids.* Annu. Rev. Fluid Mech. 43, pp.637-659.

[6] Wu, X.-L., Libchaber, A. (2000). *Particle diffusion in a quasi two-dimensional bacterial bath.* Phys. Rev. Lett. 84, 3017.

[7] Leptos, K. C., Guasto, J. S., Gollub, J. P., Pesci, A. I., Goldstein, R. E. (2009).*Dynamics of enhanced tracer diffusion in suspensions of swimming eukaryotic microorganisms.* Phys. Rev. Lett. 103, 198103.

[8] Miño, G. et al. (2011). *Enhanced diffusion due to active swimmers at a solid surface*. Phys. Rev. Lett. 106, 048102.

[9] Kurtuldu, H., Guasto, J. S., Johnson, K. A., Gollub, J. P. (2011). *Enhancement of biomixing by swimming algal cells in two-dimensional films.* Proc. Natl. Acad. Sci. 108, pp.10391-10395.

[10] Miño G. L., Dunstan J., Rousselet A., Clément E., Soto R. (2013). *Induced diffusion of tracers in a bacterial suspension: theory and experiments*. J. Fluid Mech. 729, pp.423-444.

[11] Jepson A., Martinez V. A., Schwarz-Linek J., Morozov A., Poon W.C.K. (2013). *Enhanced diffusion of non-swimmers in a three-dimensional bath of motile bacteria*. Phys. Rev. E 88, 041002.

[12] Jeanneret, R., Pushkin, D. O., Kantsler, V., Polin, M. (2016). *Entrainment dominates the interaction of microalgae with micron-sized objects.* Nat. Commun. 7, 12518.

[13] Kurihara, T., Aridome, M., Ayade, H., Zaid, I., Mizuno, D. (2017). *Non-Gaussian limit fluctuations in active swimmer suspensions*. Phys. Rev. E 95, 030601.

[14] Almeira N., Gusman S. R. (2017). *Role of transcriptional bursts in cellular oscillations*. Journal of Theoretical Biology **426**:49-56.

[15] Malik Z. MD. et al. (2015). *Fluctuations in network dynamics: SMAR1 can trigger apoptosis*. arXiv:1510.02718 [q-bio.MN]

[16] Kosiol Carolin, Goldman Nick (2011) *Markovian and Non-Markovian Protein Sequence Evolution: Aggregated Markov Process Models*. J Mol Biol. 2011 Aug 26; 411(4-6), pp.910–923.

[17] Cartwright Reed A., Lartillot Nicolas, Thorne Jeffrey L. (2011). *History Can Matter: Non-Markovian Behavior of Ancestral Lineages*. Systematic Biology, Volume 60, Issue 3, pp.276–290.

[18] Bénichou O. et al. (2011). *Intermittent search strategies*. Reviews of Modern Physics **83**:81.

[19] Harris T. H. et al. (2012). *Generalized Lévy walks and the role of chemokines in migration of effector CD81 T cells*. Nature **486**:545–548.

[20] Chiarugi D. et al. (2015). *Modelling non-Markovian dynamics in biochemical reactions*. BMC Systems Biology **9(Suppl 3)**:S8.

[21] Giaquinta Mariano, Hildebrandt Stefan (1996). *Calculus of Variations 1. The Lagrangian Formalism*. Grundlehren der Mathematischen Wissenschaften, 310 (1st ed.), Berlin: Springer-Verlag.

[22] Hand Louis N., Finch D. Janet (2008). *Analytical Mechanics*. Cambridge University Press.

[23] Zoli, Marco (2013). *Modeling DNA Dynamics by Path Integrals*. Journal of Physics Conference Series. 410. 10.1088/1742-6596/410/1/012038.

[24] Mikhail I Katsnelson et al (2018). *Towards physical principles of biological evolution*. Phys. Scr. 93 043001.

[25] L. Ferialdi and A. Bassi (2012). "*Functional Lagrange formalism for time-non-local Lagrangians*". EPL, 98 (2012) 30009.

[26] Ashok K. Das, Sudhakar Panda and J. R. L. Santos (2015). *A path integral approach to the Langevin equation*. International Journal of Modern Physics A Vol. 30, No. 07, 1550028

[27] Fox Ronald Forrest (1978). *Gaussian Stochastic Processes in Phystics*. Physics Reports (Review Section of Physics Letters) 48, No. 3. pp. 179-283.

[28] Önalan Ömer (2009). *Financial Modelling with Ornstein–Uhlenbeck Processes Driven by Lévy Process*. Proceedings of the World Congress on Engineering 2009 Vol II

[29] Kac M. and Siegert A. J. F. (1947). *An Explicit Representation of a Stationary Gaussian Process*. Ann. Math. Statist. 18:3. pp.438-442.

[30] Baule A., Friedrich R. (2008). *Two-point correlation function of the fractional Ornstein-Uhlenbeck process*. Europhysics Letters 79:6, p.60004.

[31] Polyanin Andrei D. (2020). *Functional Separation of Variables in Nonlinear PDEs: General Approach, New Solutions of Diffusion-Type Equations*. Mathematics, 8(1), p.90.

[32] Schiesser W. E. (1991). *The Numerical Method of Lines: Integration of Partial Differential Equations*. Academic Press, Inc. Lehigh University, Bethlehem, Pennsylvania.

[33] Cairoli A., Klaiges R., Baule A. (2015). *Weak Galilean invariance as a selection principle for coarse-grained diffusive models*. PNAS May 2018, 115 (22), pp. 5714-5719;

[34] El-Nabulsi Ahmad Rami, Tirdad Soulati, Hamidreza Rezazadeh (2013). . Journal of Advanced Research in Dynamical and Control Systems Vol. 5, Issue. 1, 2013, pp. 50-62.

[35] Schnoerr David Schnoerr, Sanguinetti Guido, Grima Ramon (2014). *The complex chemical Langevin equation*. J. Chem. Phys. 141, 024103.

[36] Großmann R et al (2016). *Diffusion properties of active particles with directional reversal*. New J. Phys. 18 043009.

[37] Dragoslav S. Mitrinovic, J.D. Keckic (1984). *The Cauchy Method of Residues: Theory and Applications*. Springer Netherlands, Ed. 2. (Edited By Hazewinkel M.) ISBN: 0-7923-2311-4.

[38] Eriksson Jan, Ollila Esa, and Koivunen Visa (2009). *Statistics for Complex Random Variables Revisited.* Proceedings of the IEEE International Conference on Acoustics, Speech, and Signal Processing, ICASSP 2009.

[39] R.Piazza, V.Degiorgio (2005). *Rayleigh Scattering*. Encyclopedia of Condensed Matter Physics pp. 234-242.

[40] Miller Scott L., Childers Donald (2004). *Probability and Random Processes*. Elsevier. ISBN: 978-0-12-172651-5.

[41] Hida T (1971). *Complex white noise and infinite dimensional unitary group*, Lecture Note, Nagoya University (1971).

[42] Keiichi Nagao, Holger Bech Nielsen (2017). *Complex action suggests future-included theory*. Prog. Theor. Exp. Phys. 2017, 111B01

[43] Jondral F. (1981). *Some Remarks about Generalized Functionals of Complex White Noise*. Nagoya Math. J . Vol. 81 (1981), pp. 113-122.

[44] Bäuerle N., Rieder U. (2011). *Markov Decision Processes with Applications to Finance*. Springer 2011. DOI:10.1007/987-3-642-18324-9.

[45] Kehinde S. James (2012). *Share Price Movement and the White-noise Hypothesis: the Algebraic Approach*. Int. J Busi. Inf. Tech. Vol: 2 No. 1, pp. 10-15.

[46] van Kampen N.G. (1998). *Remarks on Non-Markov Processes*. Brazilian Journal of Physics, Vol: 28 No. 2, pp. 90-96.

[47] Stirzaker David (2000). *Advice to Hedgehogs, or, Constants Can Vary*. The Mathematical Gazette Vol. 84, No. 500, pp. 197-210.

[48] Guidolin M. (2011). *Markov Switching Models in Empirical Finance*. Advances in Econometrics, Vol. 27 Part 2 pp.1-86.

[49] Bassler Kevin E., Gunaratne G. H., McCauley J. L. (2006). *Markov processes, Hurst exponents, and nonlinear diffusion equations: With application to finance*. Physica A 369:2 pp.343-353.

[50] Ross, Sheldon M. (2014). *Introduction to Probability Models* Academic Press, 11th Edition. ISBN: 9780124079489.

[51] Guttorp Peter, Thorarinsdottir Thordis L. (2012). *What Happened to Discrete Chaos, the Quenouille Process, and the Sharp Markov Property? Some History of Stochastic Point Processes*. International Statistical Review. 80 (2): pp. 253–268.

[52] Dias J. G., Vermunt J. K., Ramos S. (2009). *Mixture Hidden Markov Models in Finance Research*. Advances in Data Analysis, Data Handling and Business Intelligence pp. 451-459.

[53] Baldovin F., Bovina D., Camana F., Stella A. L. (2009). *Modeling the non-Markovian, non-stationary scaling dynamics of financial markets*. Econophysics of Order-driven Markets, New Economic Windows. pp 239-252.

[54] Frank T. D. (2007). *Kramers–Moyal expansion for stochastic differential equations with single and multiple delays: Applications to financial physics and neurophysics*. Phys. Let. A 360 pp.552-562.

[55] Bender Carl M; Orszag Steven A (1999). *Advanced mathematical methods for scientists and engineers I : asymptotic methods and perturbation theory*. New York, NY : Springer, 1999.

[56] Risken H. (1984). *Solutions of the Kramers Equation - The Fokker-Planck Equation*. Springer Series in Synergetics, vol 18. Springer, Berlin, Heidelberg.

[57] Risken Hannes, Frank Till *The Fokker-Planck Equation: Methods of Solution and Applications*. Springer-Verlag New York, 2nd Edition.

[58] Kwok Sau Fa (2012). *Generalized Klein-Kramers equations*. J. Chem. Phys. 137, 234102.

[59] Bray A. J., McKane A. J., Newman T. J. (1990). *Path integrals and non-Markov processes. II. Escape rates and stationary distributions in the weak-noise limit.* Physical Review A 41:2. pp. 657-667.

[60] Cortés Emilio (1996). *First integral of the Euler-Lagrange equation and boundary conditions for stochastic processes: Bistable potential driven by colored noise*. Physics Letters A. 223:4. pp.251-254.

[61] Giaquinta Mariano; Hildebrandt Stefan (1996). *Calculus of Variations 1. The Lagrangian Formalism*. Grundlehren der Mathematischen Wissenschaften, 310 (1st ed.), Berlin: Springer-Verlag.

[62] Ali Hirsa, Salih N. Neftci (2014). *An Introduction to the Mathematics of Financial Derivatives (Third Edition)*. Chapter 7 - Differentiation in Stochastic Environments. Academic Press pp.111-122, ISBN 9780123846822.

[63] Rudin Walter (1991). *Functional Analysis*. International Series in Pure and Applied Mathematics. 8 (Second ed.). New York, NY: McGraw-Hill Science/Engineering/Math.

[64] Monoyios Michael (2005). *Esscher transforms and martingale measures in incomplete diffusion models*.

[65] Siu Tak Kuen, Shen Yang (2017). *Risk-minimizing pricing and Esscher transform in a general non-Markovian regime-switching jump-diffusion model*. Discrete & Continuous Dynamical Systems - B, 22 (7). pp. 2595-2626.

[66] Giuggioli L, Neu Z. (2019). *Fokker–Planck representations of non-Markov Langevin equations: application to delayed systems.* Phil. Trans. R. Soc. A 377: 20180131. http://dx.doi.org/10.1098/rsta.2018.0131

[67] Das A. K., Panda S., Santos J. R. L. (2015). *A path integral approach to the Langevin equation*. arXiv:1411.0256v2

[68] Kyprianou A. E. (2006). *Introductory Lectures on Fluctuations of Lévy Processes with Applications*. Springer Science+Business Media.

[69] Bettenbuhl Mario, Rusconi Marko, Engbert Ralf, Holschneider Matthias (2012). *Bayesian Selection of Markov Models for Symbol Sequences: Application to Microsaccadic Eye Movements*. PLoS ONE 7(9): e43388.

[70] Bachelier Louis (1900). *The Theory of Speculation*. Translated by D. May from *Annales scientifiques de l'École Normale Supérieure* Séries 3. pp.21-86

[71] Williams, D. (1991). *Probability with Martingales*. Cambridge University Press

[72] Liu J. (1998). *A Generalized Girsanov Theorem and its Applications*. Acta Mathematica Scientia **18S**:51-57.

[73] Gerber H. U. and Shiu E. S. W. (1994). *Option Pricing by Esscher Transforms*. Transactions of Society of Actuaries **46**.

[74] Hänggi P. (1978). *Correlation Functions and Masterequations of Generalized (Non-Markovian) Langevin Equations*. Z. Physik B 31 pp.407-416.

[75] Hänggi P. (1989). *Path integral solutions for non-Markovian processes*. Z. Phys. B - Condensed Matter 75, pp.275-281.

[76] Piscitelli Antonio, Ciamarra Massimo Pica (2017). *Escape rate and diffusion of a Stochastically Driven particle*. Sci Rep 7, 41442.

[77] Grabert H., Olschowski P., Weiss U. (1987). *Calculation of quantum escape rates from a metastable well*. Zeitschrift für Physik B. Condensed Matter volume 68, pp. 193–199.

[78] Fujikawa K., Suzuki H. (2004). *Path Integrals and Quantum Anomalies*. Clarendon Press, May 2004.

[79] Parameswaran Sunil (2011). *Fundamentals of Financial Instruments: An Introduction to Stocks, Bonds, Foreign Exchange, and Derivatives*. Wiley Finace. ISBN: 978-0-470-82490-0.

[80] Karyn M. Apfeldorf, Horacio E. Camblong, and Carlos R. Ordóñez (2001). *Field Redefinition Invariance in Quantum Field Theory*. Modern Physics Letters A, Vol. 16, No. 03, pp. 103-112.

[81] Höfling F., Franosch T. (2013). *Anomalous Transport in the Crowded World of Biological Cells*. Rep Prog Phys 76:046602.

[82] Chupeau Marie, Gladrow Jannes, Chepelianskii Alexei, Keyser Ulrich F., Trizac Emmanuel (2020). *Optimizing Brownian escape rates by potential shaping*. PNAS January 21, 2020 117 (3), pp. 1383-1388.

[83] Hertz John A et al. (2017). *Path integral methods for the dynamics of stochastic and disordered systems*. J. Phys. A: Math. Theor. 50 033001.

[84] Cont Rama, Tankov Peter (2004). *Financial Modelling with Jump Processes*. Chapman & Hall/CRC Financial Mathematics Series 1st Edition.

[85] Feynman, R.P., Hibbs, A.R. (1965). *Quantum mechanics and path integrals*. New York: McGraw Hill Book Comp.

[86] Cecile Morrette DeWitt (1972). *Feynman's Path Integral Definition Without Limiting Procedure*. Commun. Math. Phys. 28, pp. 47-67. Springer-Verlag

[87] Bray A. J., McKane A. J. (1989). *Instanton Calculation of the Escape Rate for Activation over a Potential Barrier Driven by Colored Noise*. Phys.Rev.Lett. 62:5. pp.493-496.

[88] Xiantiao Li (2021). *Markovian embedding procedures for non-Markovian stochastic Schrödinger equations*. X. LiPhysics Letters A 387, 127036.

[89] Lacasa Lucas et al. (2018). *Multiplex Decomposition of Non-Markovian Dynamics and the Hidden Layer Reconstruction Problem*. Physical Review X 8, 031038

[90] Gregory Beylkin, Lucas Monzón (2010). *Approximation by exponential sums revisited* . Appl. Comput. Harmon. Anal. 28, 131–149.

[91] Fredrik Andersson, Marcus Carlsson, Maarten V. de Hoop (2010). *Nonlinear approximation of functions in two dimensions by sums of exponential functions*. Appl. Comput. Harmon. Anal. 29, 156–181.

[92] Arcadii Z. Grinshpan (2012). "*Volterra convolution equations: solution–kernel connection*". Integral Transforms and Special Functions, 23:4, 263-275, DOI:

[93] Bass R. (2011). *Infinitesimal generators. In Stochastic Processes* Cambridge Series in Statistical and Probabilistic Mathematics, pp. 286-301. Cambridge University Press.

[94] Plyukhin A. V. (2005). *On the higher order corrections to the Fokker-Planck equation*. Physica A 351:2–4. pp. 198-210.

[95] Kyurkchiev Nikolay, Markov Svetoslav (2015). *Sigmoid Functions: Some Approximation and Modelling Aspects*. Lambert Academic Publishing, 1st Edition.

[96] Campos L.M.B.C. (2001). *On some solutions of the extended confluent hypergeometric differential equation*. Journal of Computational and Applied Mathematics 137:1, pp.177-200.

[97] McKane A. J., Luckock H. C., Bray A. J.(1990). *Path integrals and non-Markov processes. I. General formalism*. Physical Review A 41:2. pp. 644-656.

[98] Panayotounakos Dimitrios E., Zarmpoutis Theodoros I. (2011). *Construction of Exact Parametric or Closed Form Solutions of Some Unsolvable Classes of Nonlinear ODEs (Abel's Nonlinear ODEs of the First Kind and Relative Degenerate Equations)*. International Journal of Mathematics and Mathematical Sciences, Volume 2011, Article ID 387429.

[99] C´aceres Manuel O., Budini Adri´an A. (1997). *The generalized Ornstein–Uhlenbeck process*. J. Phys. A: Math. Gen. 30 pp.8427–8444.

[100] Suweis Samir, Porporato Amilcare, Rinaldo Andrea, Maritan Amos (2011). *Prescription-induced jump distributions in multiplicative Poisson processes*. Phys. Rev. E 83, 061119.

[101] Zhu You-xin, Chen Li-hua (1991). *Dynamical Properties of Systems Driven by Colored Poisson Noise*. Commun. Theor. Phys. Vol:15 No.1, pp. 19-26.

[102] J-Q. Liang, H.J.W. Müller-Kirsten (1992) *Periodic instantons and quantum-mechanical tunneling at high energy*. Phys.Rev.D 46. pp.4685–4690.

[103] Sandrič Nikola (2018). *Stability of the overdamped Langevin equation in double-well potential*. Journal of Mathematical Analysis and Applications 467:1. pp.734-750.

[104] Lima L.S., Miranda L.L.B. (2018). *Price dynamics of the financial markets using the stochastic differential equation for a potential double well*. Physica A 490. pp.828-833.

[105] Schreve Steven E. (2000). *Stochastic CalcuIus for Finance II: Continuous-Time Models*. Springer Finance Series. ISBN 0-387-40101-6.

[106] Wolfgang Bock, Jinky B. Bornales, Cresente O. Cabahug, Torben Fattler, and Ludwig Streit (2020). *Fractional Brownian motion - Some recent results and generalizations*. AIP Conference Proceedings 2286, 020001.

[107] Jinfu Lui (1998). *A Generalized Girsanov's Theorem and its Applications*. Acta Mathematica Scientia Vol. 18 (Supp.) pp. 51-57.

[108] von Smoluchowski, M. (1906). *Zurkinetischen Theorie der Brownschen Molekularbewegung und der Suspensionen*. Analen der Physik 326:14.

[109] Chen Li-hua (1998). *Systems Driven by Colored Poisson Noise: Unified Colored Noise Approximation*. Commun. Theor. Phys. Vol:30 No.1. pp.45-49.

[110] Courant, R; Hilbert, D (1953). "*Methods of Mathematical Physics*". Vol. I (First English ed.). New York: Interscience Publishers, Inc. ISBN 978-0471504474.

[111] Villarroel Javier, Vega Juan A., Montero Miquel (2019). *Escape probabilities of compound renewal processes with drift*. arXiv:1907.11894 [math.PR]

[112] Bray A. J. , McKane A. J. (1989). *"Instanton Calculation of the Escape Rate for Activation over a Potential Barrier Driven by Colored Noise"*. Phys. Rev. Lett. 62: 493.

[113] Baule A. and Sollich P. (2015). "*Optimal escape from metastable states driven by non-Gaussian noise*". arXiv:1501.00374 [cond-mat.stat-mech].

[114] A. Iserles (1994). "*On Nonlinear Delay Differential Equations*". Transactions of the American Mathematical Society 4:31, pp.441-477.

[115] N. Nass Aminu (2019). "*Lie symmetry analysis and exact solutions of fractional ordinary differential equations with neutral delay*". Applied Mathematics and Computation 347, pp.370–380.

[116] Goudenège Ludovic, Molent Andrea, Zannette Antonino (2020). *Machine Learning for Pricing American Options in High-Dimensional Markovian and non-Markovian models*. Quantitative Finance Vol 4. pp. 573-591.

[117] Zhu Chinwen et al (2021). *Markovian Approximation of the Rough Bergomi Model for Monte Carlo Option Pricing*. Mathematics 2021, 9, 528.

[118] Merton Robert C. (1976). *Option pricing when underlying stock returns are discontinuous.* Journal of Financial Economics 3 pp.125-144.

[119] Ayensa-Jiménez Jacobo et al. (2019). "On the Simulation of Organ-on-Chip Cell Processes: Application to an In Vitro Model of Glioblastoma Evolution". Advances in Biomechanics and Tissue Regeneration, 2019, pp. 313-341.

[120] Debath L (2016). "*The Double Laplace Transforms and Their Properties with Applications to Functional, Integral and Partial Differential Equations*". Int. J. Appl. Comput. Math. 2 pp.223–241.

[121] Fazli A., Allahviranloo T., Javadi Sh. (2016). "*Numerical solution of nonlinear two-dimensional Volterra integral equation of the second kind in the reproducing kernel space*". Math Sci 11 pp.139–144.

[122] Øksendal Brent (1998). *Stochastic Differential Equations: An Introduction with Applications*. Fifth Edition. Springer-Verlag Heidelberg New York.

[123] Hasegawa Y. and Arita M. (2011). *Noise-intensity fluctuation in Langevin model and its higher-order Fokker–Planck equation* . Physica A **390-6** pp.1051-1063.

[124] Hölzel, M., Bovier, A. and Tüting, T. (2013). *Plasticity of tumour and immune cells: a source of heterogeneity and a cause for therapy resistance*> Nat. Rev. Cancer **13**:365–376.

[125] Łuczka J. (2005). *Non-Markovian stochastic processes: Colored noise*. Chaos 15, 026107.

[126] Frasca Marco (2012). *Quantum mechanics is the square root of a stochastic process.* arXiv:1201.5091

[127] Gillepsie Daniel T. (200). *Non-Markovian stochastic processes*. AIP Conference Proceedings 511:49.

[128] Barcons F.X., Garrido L. (1983). *Systems under the Influence of White and Colored Poisson Noise*. Physica 117A pp.212-226.

[129] Yulmetyev R.M., Gafarov F. (1999). *Markov and non-Markov processes in complex systems by the dynamical information entropy*. Physica A 274:1–2 pp.381-384.

[130] Baar M. et al. (2016). *A stochastic model for immunotherapy of cancer*. Scientific Reports **6**, Article number: 24169.

[131] Srivastava S., Chen L. (2010). *A two-parameter generalized Poisson model to improve the analysis of RNA-seq data*. Nucleic Acids Research 38:17 e170.

[132] Balvodin F. et al. (2010). *Modeling the non-Markovian, non-stationary scaling dynamics of financial markets*. arXiv:0909.3244v2 [q-fin.ST].

[133] McDonald M. et al. (2008). *Impact of Unexpected Events, Shocking News and Rumours on Foreign Exchange Market Dynamics*. Physical Review E **77**:4-046110.

[134] Jondeau E. et al. (2007). *Financial Modeling Under Non-Gaussian Distributions*. Springer Finance, Springer-Verlag London.

[135] Wilmott Paul (2013). *Paul Wilmott Introduces Quantitative Finance*, 2nd Edition. Wiley Finance.

[136] Meerschaert M. M., Scalas E. (2006). *Coupled continuous time random walks in finance*. Physica A, vol. 370, pp.114-118.